DTNH22-95-H-07002

TWO ACTIVE SYSTEMS FOR ENHANCING DYNAMIC STABILITY IN HEAVY TRUCK OPERATIONS

Final Report

UMTRI-98-39

July, 1998

Prepared by:
The University of Michigan
Transportation Research Institute
2901 Baxter Road, Ann Arbor, MI 48109-2150
under Cooperative Agreement: DTNH22-95-H-07002

for:
National Highway Traffic Safety Administration
U.S. Department of Transportation
400 7th Street S.W.
Washington, D.C. 20590

UMTRI The University of Michigan Transportation Research Institute

Technical Report Documentation Page

1. Report No.	2. Government Accession No.	3. Recipient's Catalog No.

4. Title and Subtitle

TWO ACTIVE SYSTEMS FOR ENHANCING DYNAMIC STABILITY IN HEAVY TRUCK OPERATIONS

5. Report Date	July 1998
6. Performing Organization Code	032914
8. Performing Organization Report No.	UMTRI-98-39

7. Author(s) Ervin, R., Winkler, C., Fancher, P., Hagan, M., Krishnaswami, V., Zhang, H., Bogard, S.

9. Performing Organization Name and Address

The University of Michigan
Transportation Research Institute
2901 Baxter Road, Ann Arbor, MI 48109-2150

10. Work Unit No. (TRAIS)	
11. Contract or Grant No.	DTNH22-95-H-07002
13. Type of Report and Period Covered	Final Report
14. Sponsoring Agency Code	

12. Sponsoring Agency Name and Address

National Highway Traffic Safety Administration
U.S. Department of Transportation
400 7th Street S.W.
Washington, D.C. 20590

15. Supplementary Notes

16. Abstract

Two types of intelligent subsystems were developed to enhance a truck driver's ability to obtain stable operations with an articulated heavy-duty vehicle. The systems in question address the potential instabilities of 1) quasi-steady-state rollover and 2) rearward amplification of lateral acceleration in multiply articulated trailer combinations. Both system types were designed, constructed, and evaluated through full-scale testing.

The system addressing the rollover issue employed a parameter-identification technique to automatically determine the as-loaded rollover limit of a tractor semitrailer, while normal driving was underway. Obtaining accuracies in the range of +/-10% of actual rollover limits, the system was able to present a driver's display of the stability level within a few minutes of having changed either the payload or the attached semitrailer. Data that would show a given driver's accumulated "roll stability margin" is also discussed in terms of its value for fleet safety management. The "rollover stability advisor" system employs force and moment sensing at the tractor and/or semitrailer units, supporting discrete tractor-based and trailer-based approaches for marketing this safety feature, commercially.

The system addressing rearward amplification constituted a control system that applies right-left braking pulses at trailer and dolly axles to automatically suppress the tendency for exaggerated motions at rearmost trailers in reponse to abrupt steering by the driver. The system concept utilizes electronically controlled braking systems (EBS) at trailer and dolly axles, reducing rearward amplification of a common doubles combination to approximately that of a tractor-and-short-semitrailer configuration.

The results show that both system types are viable, from a technical point of view.

17. Key Words	18. Distribution Statement
Trucks, Stability, Intelligent Systems, Parameter Identification, Control	Unrestricted

19. Security Classif. (of this report)	20. Security Classif. (of this page)	21. No. of Pages	22. Price
None	None	206	

TABLE OF CONTENTS

LIST OF FIGURES

LIST OF TABLES

EXECUTIVE SUMMARY

INTRODUCTION

Physical prototypes for two forms of intelligent subsystems that would enhance a truck driver's ability to obtain stable operations with an articulated heavy-duty vehicle have been designed, constructed, and demonstrated. The two systems deal, respectively, with (1) quasi-steady-state rollover and (2) rearward amplification of lateral acceleration (especially in multiply articulated trailer combinations). Both forms of instability have been broadly documented through prior research and both are known to directly influence the crash record.

The project was conducted by University of Michigan Transportation Research Institute (UMTRI), with in-kind participation by six commercial partners: Freightliner Corporation, Hendrickson-Turner, Holland Hitch Company, Haldex Brake Systems, Rockwell Autonetics Division, and TRW's Commercial Steering Division.

THE ROLL STABILITY ADVISOR

The first of the two stability-enhancement systems is called the roll-stability advisor, or RSA system.

The basic roll stability of a heavy-duty vehicle combination (tractor and semitrailer) is largely determined by the vehicle's payload; and, of course, that payload changes every day for the typical driver. The purpose of the RSA system is to determine the basic roll-stability level of the vehicle as it travels down the road and to display that stability level to the driver in a way that enables him to appraise rollover risks while underway in normal service.

Application of this concept requires the use of sensing devices whose electronic output signals are processed to determine the *rollover threshold* of the vehicle as it is currently loaded. To be most effective, this estimate must be obtained within a few minutes of driving following any significant change in load condition—coupling to a new semitrailer, adding or removing payload, or the inadvertent shifting of payload while under way. Also, the thresholds for rollover to the left and to the right must be determined separately to account for the possibility of off-center loads in the trailer.

The estimated rollover thresholds are presented as one aspect of the display to the driver. The other element of the display is the *roll-stability demand*—the instantaneous value of lateral acceleration—which is placed on the vehicle by virtue of the current driving situation. Thus, as the vehicle is driven during the ensuing trip, the level of demand for roll stability is continuously presented to the driver with immediate visual reference to the vehicle's rollover threshold. Because the driver is probably not able to pay much attention to a display during the rare dramatic maneuver, the system also allows display of recent peak values of demand after the fact. Further, the full records of demand and capability for an entire trip can be retained for later processing and review by company managers.

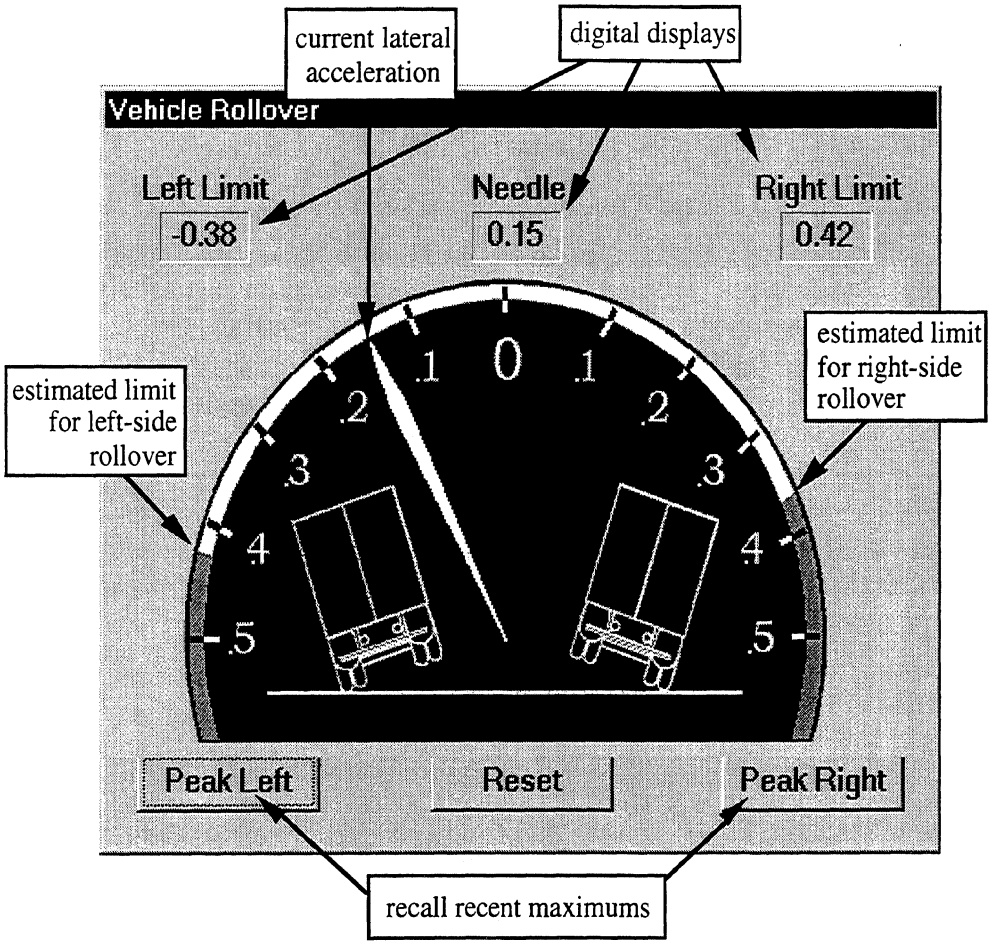

The RSA display used in the cab of the test vehicle

The RSA concept outlined here implies a *training instrument* in contrast to either a rollover warning device or an automatic rollover-avoidance system. The collaborators in this project have tended toward the views that (1) warning of an imminent rollover is likely to have minimal safety benefit because rollover-precipitating conditions, once established, avail little opportunity for driver correction, and (2) systems of the automatic intervention type are not commercially feasible for the foreseeable future.

The prototype RSA demonstrated in this project had two subsystems that estimated the respective lateral accelerations at which (1) the tires of the tractor's drive axles and (2) the tires of the trailer's axles would lift from the road surface. The primary sensor for the system on the tractor was a high-quality, fifth-wheel load transducer which measures the vertical and lateral forces and the overturning moment applied to the tractor by the trailer. Signals from this transducer plus a lateral accelerometer mounted on the front axle of the tractor were used to determine the acceleration for liftoff of the tractor tires. (The signal from this accelerometer was also used to indicate the current lateral acceleration on the driver's display.) The RSA system on the trailer used an air-pressure transducer to measure internal pressure in air-springs of the trailer suspension, thus allowing estimation of the suspension load. Strain gages applied to the axle of the trailer suspension were used to measure overturning moment on the suspension. A second lateral accelerometer was

mounted on the trailer axle. The signals from all these sensors were processed according to vehicle-rollover models, special filtering and gating routines, and recursive statistical regressions, all of which are described in the full report. It was found that good estimates (generally within 0.02 g) of the rollover thresholds of the test vehicle could be obtained within about one minute of driving above 40 miles per hour.

Limitations of this first prototype RSA are (1) in the case of the tractor, the dependence on an expensive, specialized, load transducer, and (2) in the case of the trailer (which uses considerably cheaper transducers) a need for special system calibration. It is believed that further development can likely overcome these problems and possibly lead to a successful, tractor-only RSA.

REARWARD AMPLIFICATION SUPPRESSION

The second stability-enhancement system is an automatic-intervention system for rearward amplification suppression (RAMS) in multi-trailer combinations. The RAMS concept involves measurement of steering input and forward speed, followed by computations that determine whether a significant rearward amplification event is pending. The control algorithm then establishes a sequence of carefully phased brake applications at selected trailer wheels so as to induce yaw moments that oppose the rearward-amplifying motions of trailers and dollies. The concept requires electronically controlled brake systems (EBS) at trailer axle positions and requires placement of and communications with yaw-rate sensors in individual trailer and dolly units.

In concert with industrial progress in electronic braking systems and all-axle antilock systems, the RAMS function could enhance the obstacle-avoidance capabilities of doubles and truck-full-trailer combinations and enable the wider use of triple-trailer combinations.

The report explains the creation and evaluation of a prototype RAMS system. The design process involved specifying the desired behavior of the system; envisioning how an assembly of sensors, control-system components and brake actuators could be used to reduce rearward amplification; developing suitable control objective functions (algorithms); selecting and engineering components that can perform the subfunctions needed for the RAMS functionality; and installing the RAMS components into a doubles combination, thereby creating a prototype system suitable for testing and demonstration.

The functional purpose of the RAMS is to allow drivers of multi-trailer combinations to successfully steer around a vehicle that has suddenly stopped or pulled in front of the truck. In technical terms the design objective is specified as follows:

With the driver steering to follow a path defined by an 8 foot lateral translation over a down-range distance of 200 feet, kinematically corresponding to a peak lateral acceleration of 0.25 g at 55 mph (80 ft/sec), the lateral acceleration of the center of the floor of the rear trailer should not exceed 0.3 g.

The testing and demonstration activities showed that the prototype RAMS system met this objective and the system was capable of achieving its functional purpose. Even with a heavy load with a very high center of gravity, the system achieved its rearward-amplification objective, thereby preventing the last trailer from rolling over. (Demonstration

test runs without the RAMS in operation showed that the last trailer would have rolled over if it were not for the outriggers used in the demonstration.)

The testing and demonstration runs confirmed that the functional purpose for the RAMS was achievable using particular design configurations employed in this project. In addition the work in this project has clarified how the design of future RAMS systems could be improved to make them more attractive for deployment.

Without RAMS—
the last trailer of
the test vehicle
would rollover
if not for the
outriggers

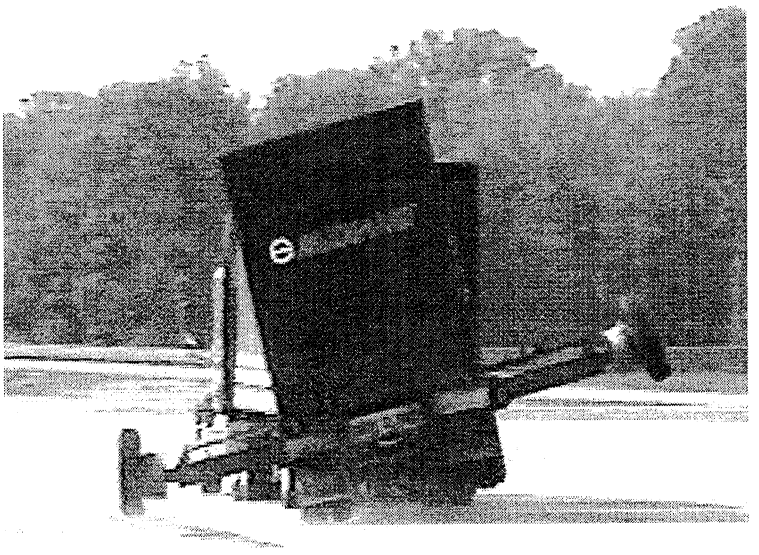

With RAMS—
the test vehicle
completes the
maneuver without
lifting any tires
from the road

Demonstration of the RAMS system in a rapid evasive maneuver

1.0 INTRODUCTION

This document is the final report on a Cooperative Agreement to Foster the Deployment of a Heavy Vehicle Intelligent Dynamic Stability Enhancement System. This project has designed, constructed, and demonstrated physical prototypes for two forms of intelligent subsystems that would enhance a truck driver's ability to obtain stable operations with an articulated heavy-duty vehicle. The systems in question address the potential instabilities of A) quasi-steady-state rollover and B) rearward amplification of lateral acceleration (especially in multiply articulated trailer combinations.) Both forms of instability have been broadly documented through prior research and both are known to directly influence the crash record.

Funding was provided through cooperative agreement number DTNH22-95-H-07002 by the sponsor, the National Highway Traffic Safety Administration (NHTSA) to the University of Michigan Transportation Research Institute (UMTRI), with in-kind participation by six industrial companies that have interests in the commercial potential for dynamic stability-enhancement products. The commercial partners and their respective interests in this work are the following:

- Freightliner Corporation, North America's highest-volume manufacturer of heavy-duty trucks and tractors in the United States, which is interested in tractor-based stability enhancements as a further area of improvement in the safety performance of its vehicles
- Hendrickson-Turner, the leading U.S. manufacturer of truck suspensions, which is interested in augmenting its air-spring suspension products with sensory features that will enable rollover proximity assessments
- Holland Hitch Company, the major supplier of fifth-wheel hitches and other coupling components to the trucking industry, which is interested in instrumented fifth-wheel products that may support an active stability enhancement function
- Haldex Brake Systems, a major supplier of brake components to U.S. and European markets, which seeks to find value-added improvements in the functionality of electronic braking systems for heavy-duty vehicle
- Rockwell Autonetics Division, a U.S. developer of micromachined inertial sensing instruments for automotive applications, which is interested in intelligent truck applications for such products
- TRW's Commercial Steering Division, the largest seller of integral steering gears for the North American truck market, which is interested in enhanced features that may add value to steering systems

This report presents each of the two stability-enhancement systems in terms of its underlying functional concept, design approach, physical implementation, and performance measurement. Physical prototypes of both system types are described, as they have each been implemented and demonstrated on a heavy-duty vehicle combination. Results from the preliminary testing of each system are also presented and discussed. While there is clearly room for both performance improvements and configurational alternatives with each of the developed systems, the results obtained from this study show that both system types are, indeed, viable from a technical point of view.

The report presents the development and evaluation of each system type in sections 2 and 3, comprising the main body of the document. Section 2 addresses the system pertaining to rollover stability and section 3 addresses the system pertaining to rearward amplification. Section 4 presents conclusions that are drawn from the initial experience with these two system types and section 5 presents recommendations. Appendix A provides a compilation of all parametric measurements that were conducted on the suspensions of the tested vehicle combination provided to the project by Freightliner Corporation and Haldex Brake Systems. Appendix B presents road maps documenting the routes taken during normal-driving trips within which the rollover-stability assessments were computed on board the test vehicle. Appendix C presents an overview of the analysis by which a complete system identification for roll-stability assessment is to be determined. Appendix D is a users' guide for the UMTRI fifth-wheel.

2.0 THE ROLLOVER STABILITY ADVISOR SYSTEM

The first of the two stability enhancement systems is called the roll-stability advisor, or RSA system. In section 2.1, below, the concept of the system as a safety countermeasure is discussed as is the background rationale for selecting this function as a high-priority enhancement for modern trucks.

Given a statement of the RSA concept and rationale, the remainder of section 2 deals with the system implementations that were developed and tested here. In section 2.2, the mathematical formulation of basic modeling approaches to the on-board computation of the rollover threshold estimate are presented. The overall approach is introduced in section 2.2.1 and is then presented in the specific form of tractor-based (in section 2.2.2) and trailer-based (in section 2.2.3) schemes. Each of these two respective approaches toward the RSA system model identify respective design parameters of the platform vehicle which are incorporated as known information within the system function. For a tractor-based function, it is assumed that mechanical parameters relating to tractor suspension geometry and stiffnesses, plus unsprung mass values and track width are known. Correspondingly, a trailer-based RSA computation requires prior knowledge of certain similar properties of the trailer suspension and track, including a calibrated conversion from air-spring pressure

to static axle load (assuming air-suspended trailer axles). Section 2.3 presents measurement methods and data samples from which these design parameters were quantified. A complete set of these measurements covering the Freightliner tractor suspensions and the Hendrickson trailer suspension are presented in appendix A of this report.

Each of the tractor-based and trailer-based approaches for obtaining RSA roll-stability estimates requires that the vehicle be equipped with specialized sensors for deducing force and/or moment reactions. Section 2.4 presents the sensors that were developed for each approach, together with sample data showing each sensor's performance as a force/moment transducer, per se. Section 2.4.1 describes the fifth-wheel sensor that supports the tractor-based RSA system and section 2.4.2 describes the instrumented trailer axle that supports the trailer-based system.

Section 2.5 presents the means by which data from the sensor devices were processed within an on-board computer for deriving the RSA estimations of rollover limits on the test vehicle. Sample data are presented in this section revealing the significance of a "gating velocity" above which new sensory data would be admitted for updating the computation of wheel liftoff limits.

Section 2.6 describes a set of tilt-table tests that were performed to obtain precise reference values for the wheel-lift and rollover threshold limits of the tractor semitrailer vehicle loaded in differing conditions of payload weight and payload center-of-gravity height. These data are compared with RSA predictions in section 2.7 as a means of expressing the accuracy of RSA-derived estimates.

Section 2.7 presents test data obtained from normal driving trips for which the RSA system was active in computing an estimate of the vehicle's rollover limit. Section 2.7.1 provides a summary of such test conditions and the resulting data for the tractor-based version of the system. Section 2.7.2 presents the corresponding information for the trailer-based version.

The basic concept of the RSA function is embodied in an in-cab display to the driver. Section 2.8 presents the data display configuration that was developed and employed in the test vehicle during this study. Section 2.9 discusses broader consideration of the RSA application that go beyond the approach of a driver display of the information. This discussion deals primarily with how recorded data from RSA measurements of rollover limits and maneuvering demand might be used to support the practice of fleet-safety management.

2.1 CONCEPT AND RATIONALE FOR ROLL STABILITY ADVISOR

By way of introduction and background to the RSA system, we present below the underlying concept as well as the rationale linking such a system function to the potential for actually improving the safety record through the use of such systems.

2.1.1 RSA Concept

The RSA concept involves a real-time computation of the roll-stability level of a heavy-duty vehicle combination, as it travels down the road. The computed result is then employed in a display, which enables the truck driver is to appraise rollover risks while underway in normal service. The concept requires the operation of sensing devices whose electronic output signals are processed through some form of *system-identification* algorithm in order to derive the display information. The algorithms will first automatically estimate the as-loaded roll stability limit of the vehicle, termed the "rollover threshold." This stability estimate must be obtained within a few minutes of driving following any significant change in roll stability due to adding or removing payload or attaching a new semitrailer to the tractor. The estimated rollover threshold of the vehicle is then presented and sustained as one aspect of the display.

As the vehicle is driven during the ensuing trip, the level of maneuver severity—or the *demand* that is being imposed for roll stability—is captured and presented on the driver's display, with perhaps supplemental audio or steering-torque cues to attract the driver's attention to unusual demand worth noting. Assuming that the driver is unable to pay much attention to any visual display during the rare dramatic maneuver, the advisory system display is made to be inherently retentive such that an after-the-fact review of the rollover proximity that prevailed in the prior maneuver is available at a glance.

Clearly, the RSA concept as outlined here implies a training, or conditioning, instrument in contrast to, say, an automatic-rollover-avoidance system that can actually intervene to circumvent a rollover crash. The collaborators in this project have tended toward the view that systems of the automatic intervention type are commercially infeasible as rollover countermeasures for the foreseeable future. Further, it should be noted that the described RSA function goes well beyond that of *rollover warning,* which is invoked only when an instability is pending. In fact, it is felt that warning of an imminent rollover is likely to have minimal safety benefit because rollover-precipitating conditions, once established, tend to avail little opportunity for driver correction.

Accordingly, the RSA concept has been targeted to address the classical problem of the driver's failure to perceive (a) the as-loaded stability level of the vehicle in relation to (b) the roll-inducing demands actually imposed while underway. This approach recognizes that the driver has a general need to appreciate the rollover margin, especially with each new load that is carried. While this *appreciation* must eventually become intuitive, it is

hypothesized that an intelligent advisory system can cultivate an accurate intuitive grasp of the essential rollover-conflict issue within a reasonable term of system usage. After a few months of exposure to the RSA system just described, it is expected that the typical driver would cease to consult the rollover-proximity display with any frequency and would, instead, simply note the as-loaded stability level as a sort of "calibration" before beginning a trip with a new load. At this stage, the driver would be making it a point to observe the as-loaded stability indicator as a regular in-trip supplement to the walk-around, pretrip inspection of the rig.

Alternative applications of the same on-board sensing and computational function would include various fleet-management or safety-auditing practices, perhaps having special value in fleets carrying hazardous materials or those having an otherwise exaggerated concern for minimizing rollover risk. By this approach, one might histogram each driver's compiled data showing the margin between maneuver severity while driving to the extant levels of rollover threshold that prevailed. As fleet knowledge on rollover occurrence grows, such histograms would gradually support a policy of managing rollover risk—with explicit evidence relating the objective on-board measurements to the empirically validated likelihood of rollover. More detailed consideration of the management considerations is presented also in section 2.9.

Moreover, the concept was seen as offering a fundamental capability for influencing the rate of rollover accidents with heavy vehicles. While various end-use applications can be envisioned, they all trace back to the ability to estimate rollover thresholds and the associated demands thereon that accrue during normal driving.

2.1.2 Rationale underlying selection of the RSA concept for study

The RSA rationale was based upon the fundamental observation that the low level of roll stability in heavy-duty trucks constitutes the principal manifestation of dynamic limitations in this vehicle class. Further, the compelling size of the safety problem that is posed by truck rollover crashes is recognized as the principal argument suggesting a potential market for an RSA product. On the other hand, as stated earlier, the development of a product for automatically *controlling* the vehicle to avoid a pending rollover calls for too large a technological stretch (especially for the historically conservative commercial truck market) and thus was seen as posing a commercially unrealistic goal. Further, a simple system that would warn only when rollover is imminent—based upon the immediate dynamic state of motion—would probably offer little value as a countermeasure. A further assumption was that any system requiring a *cooperative infrastructure* or even a roadway database having micro geometric data on road curvature and superelevation in order to give anticipatory rollover warning is too futuristic to qualify as a state-of-the-art implementation.

The primary fact arguing that the RSA approach would offer value as a strategic sort of countermeasure to rollover-risky driving arises from the probabilistic nature of the demand for rollover resistance, from one maneuver to the next. The probability density of roll-stability demands is known to be distributed in a manner very much like that which has been documented in many other domains of driver control behavior.[1] Thus, for every steering maneuver that demands 0.3 g of lateral acceleration, for example, there are approximately 20 that have demanded 0.25 g, 200 that demanded 0.2 g, and 2,000 that demanded 0.15 g. [e.g. 2] Accordingly, the very high incidence of sub-limit demand events offers a great opportunity within which to train, or at least acquaint, the driver with an accurate and current illustration of proximity to rollover.

In an era when there is a high rate of entry of inexperienced drivers into the trucking industry, the value of an RSA system is greater. Thus, while it is suspected that even very experienced truck drivers could benefit from RSA advice, there is no question that a special market stimulus derives from the high state of flux in the truck-driving population.

One can imagine that many fleets might wish to equip at least a few of their tractors with RSA systems simply for upgrading their drivers, or introducing new ones, to a high state of rollover-proximity awareness. At the same time, it is assumed that the RSA concept is not devalued significantly by the background risk of rollover that will prevail while the "training phase" of a driver's first use of an RSA system is underway. It is noted, for example, that the absolute risk of rollover averages around six per 100 million miles of tractor-semitrailer operation.[3] In, say, the first month of RSA-assisted training on rollover-proximity awareness, a driver covering 5,000 miles would have otherwise had only a 1-in-3,000 chance of rollover. Thus, such a system which gives on-the-job safety-training is not significantly reduced in value by the fact that the safety risk prevails (as with all on-the-job exposures) throughout the training period, itself.

On the matter of rationalizing the configuration of an RSA system product for maximum sales appeal, it is useful to reflect on the vehicular platform upon which differing portions of the system investment might be made. Firstly, one should note that tractors are replaced in the larger fleets every 3 to 5 years while semitrailers are removed from fleet inventory every 15 to 20 years. Thus, if one is to create a marketing strategy for introducing a new stability-enhancement package, the commercial opportunity for rolling out a stand-alone, tractor-based system is much greater than for a system requiring matched tractors and trailers in cooperation.

Further, the tractor manufacturers have engineering groups that are growing in technical sophistication and are moving inexorably to play major roles in the integration of chassis and drivetrain controls. Thus, this project recognized the value in developing an RSA system based upon a tractor-only implementation, as a priority goal. At the same time, the project also included a provision for considering trailer-based measurements in deriving the

roll-proximity information. This latter approach is more straightforward in terms of the mechanics of the problem but it poses a marketing strategy that will be difficult to realize except in fleets with "married combinations", having the opportunity to optimally equip both the tractor and the semitrailer as a complementary system. In any case, the project was set up to address alternative approaches for implementing the rollover-proximity concept.

2.2 Models for RSA Stability Estimations

2.2.1 Overview of the system approach

The overall approach of the RSA that was developed and demonstrated in actual hardware in this project is shown in figure 1. The system is configured for use on a tractor semitrailer combination. Using sensors installed on both the tractor and the trailer, it produces independent estimates of the lateral accelerations at which the tires of the tractor drive suspension and the trailer suspension, respectively, would lift from the road surface. These two estimates are combined by weighted averaging, and the result is projected as the estimate of the static rollover limit of the vehicle. To account for off-center loads, the process is accomplished for rollover in left and right turns, respectively. The display to the driver also includes the current lateral acceleration such that he may be aware of the performance *demands* that his driving places on the system relative to the performance *capability* of the system represented by the RSA estimates.

The individual estimates of tire liftoff derive from straightforward linear extrapolation of the relationships between lateral acceleration and the relevant suspension loads that the RSA is able to observe in ordinary driving. This approach, and the rationale for averaging these results, is illustrated in figure 2.

Figure 2 is a highly simplified plot of various roll moments of the truck system as a function of lateral acceleration. The total overturning moment acting on the vehicle results from (1) the D'Alembert force acting laterally through the center of gravity as a direct result of lateral acceleration and (2) the outboard lateral translation of the cg relative to the track due to roll motions of the vehicle. This moment is opposed by the roll moments developed at the individual suspension by side-to-side transfer of vertical tire loads. At equilibrium, the sum of the stabilizing suspension moments equals the destabilizing overturning moment. Prior to any tire lift, the relative strength of the various suspension moments is determined by the relative roll stiffnesses of the suspensions as well as by certain other properties such as roll-center height. The figure illustrates the typical situation in which the trailer suspension is the stiffest and both the trailer-axle and drive-axle suspensions are much stiffer than the tractor steer-axle suspension

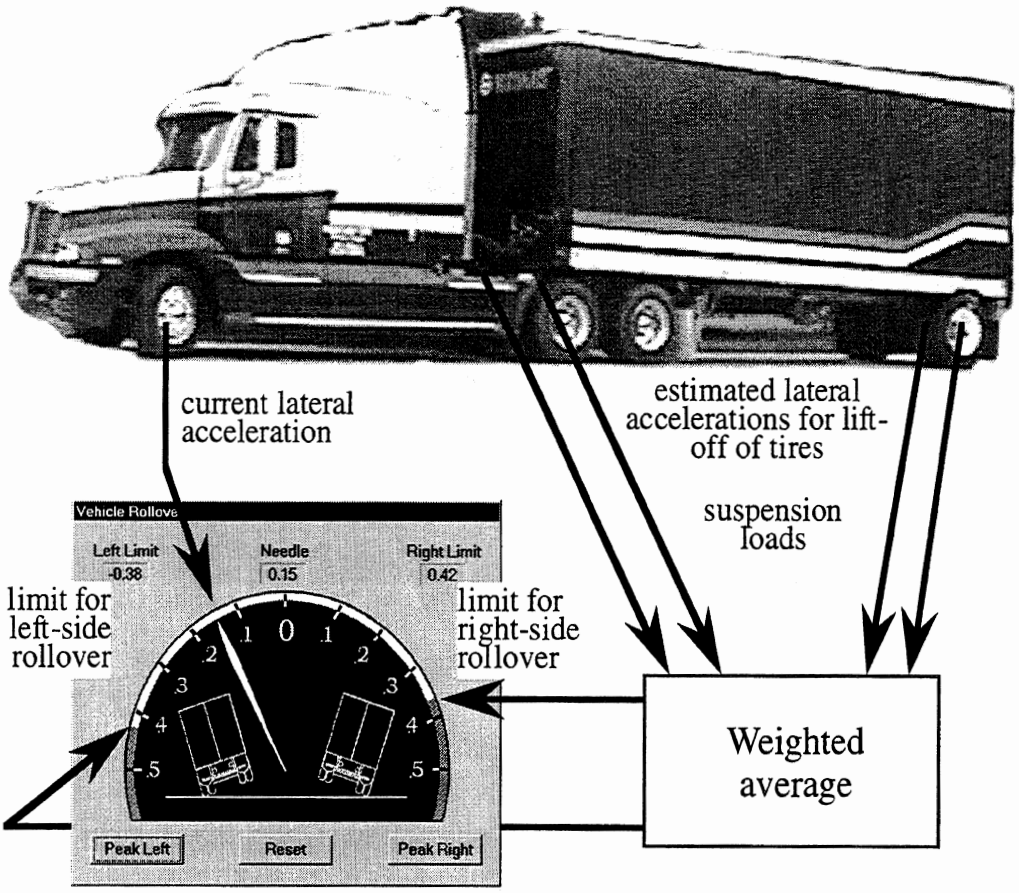

Figure 1. The roll stability advisor (RSA) system

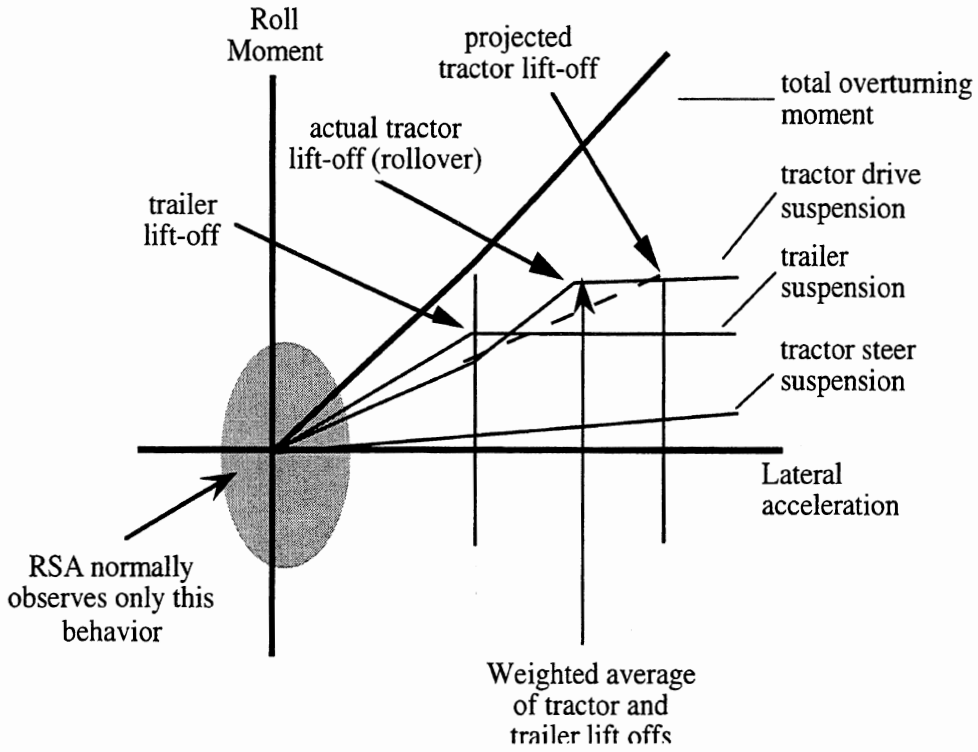

Figure 2. Roll moments in the tractor semitrailer system

Tire liftoff occurs when all of the load on a particular suspension is transferred to one side. In the figure, this occurs first (i.e., at the lowest lateral acceleration) for the trailer suspension. Above its liftoff point, the trailer suspension can produce no more stabilizing moment, so its trace on the graph becomes horizontal. The liftoff of the tires of the trailer also causes (1) the overturning moment to increase more rapidly with lateral acceleration (since the vehicle will roll more rapidly with increasing lateral acceleration) and (2) the tractor suspension moment to increase more rapidly (since it now bears a much larger portion of the increase in overturning moment). At some greater level of lateral acceleration, the tractor drive-axle tires will liftoff. Only the steer axle remains to provide a stabilizing roll moment, but the stiffness of this axle is typically much too low to stabilize the entire vehicle. Therefore the stability limit is identified by the liftoff of the drive-axle tires. (For cases in which the drive-axle tires liftoff first, liftoff of the trailer-axle tires would indicate the stability limit.)

While figure 2 represents the behavior of the tractor semitrailer system as it proceeds all the way to rollover, it also shows that the RSA can base its estimates of stability only on observations made of the very first stages of this process–the regime of normal driving. It is only from this very limited range of data that the system must extrapolate to predict rollover. This is not a serious penalty with respect to predicting the first point of tire liftoff. However, it is extremely unlikely that the RSA could ever observe the inflection in the response of the tractor suspension which occurs as the trailer tires lift. Thus, a linear extrapolation of data from the normal driving range would overestimate the acceleration needed for liftoff of the tractor axles. The solution is to calculate a weighted average (i.e., weighted by the vertical loads carried by the suspensions) of the two accelerations projected for the respective trailer and tractor liftoffs, and to report this value as the final estimate for the liftoff of the tractor drive-axles and, therefore, of rollover. (In the event that the base projection for tractor liftoff was lower than that for trailer liftoff, this weighted average would be the prediction for trailer axle liftoff and also for rollover of the vehicle.)

2.2.2 The model for estimating the liftoff of tractor drive-axle tires

The lateral acceleration required for liftoff of tractor drive-axle tires is estimated using the simple model shown in figure 3. The figure shows a freebody diagram of the aft section of the tractor including the lower fifth-wheel coupling, the aft section of the tractor frame, and the drive-axle suspension and unsprung masses. The model assumes that 1) the roll torque passed along the tractor frame from the front of the tractor to the rear is negligible; 2) the relevant fraction of the tractor sprung mass (i.e., the fraction supported by the drive-axle suspension) is small and can be lumped with the unsprung mass; 3) roll motions are small (such that linearity can be assumed); and 4) the system is in steady state. The model also assumes that the relevant tire, suspension, and mass properties of the tractor are known and are constant. Known constants include:

h_{5t} the height of the fifth-wheel load transducer above the ground

h_{rc} the height of the suspension roll center above the ground

h_u the height of the center of gravity of the unsprung mass above the ground

K_s the total roll stiffness of the suspension (i.e., between unsprung and sprung masses) about the roll center

K_t the total roll stiffness of the tires (i.e., between ground and unsprung mass) about the mid-track point at the ground

T_{eff} the effective track width

W_u tare weight of the drive-axle suspension (i.e., the unsprung mass plus the relevant fraction of the tractor sprung mass)

It is also assumed that lateral acceleration, a_y,and the loads applied by the trailer at the fifth-wheel, F_{y5}, F_{z5}, and M_{x5}, are available as measured variables.

Figure 3 shows the freebody diagram of interest on level ground with gravity acting perpendicular to the ground and lateral acceleration parallel to the ground. While we will not demonstrate the fact explicitly here, it is true that the model and the resulting analysis properly–and automatically–account for the influence of the cross slope of the road (within

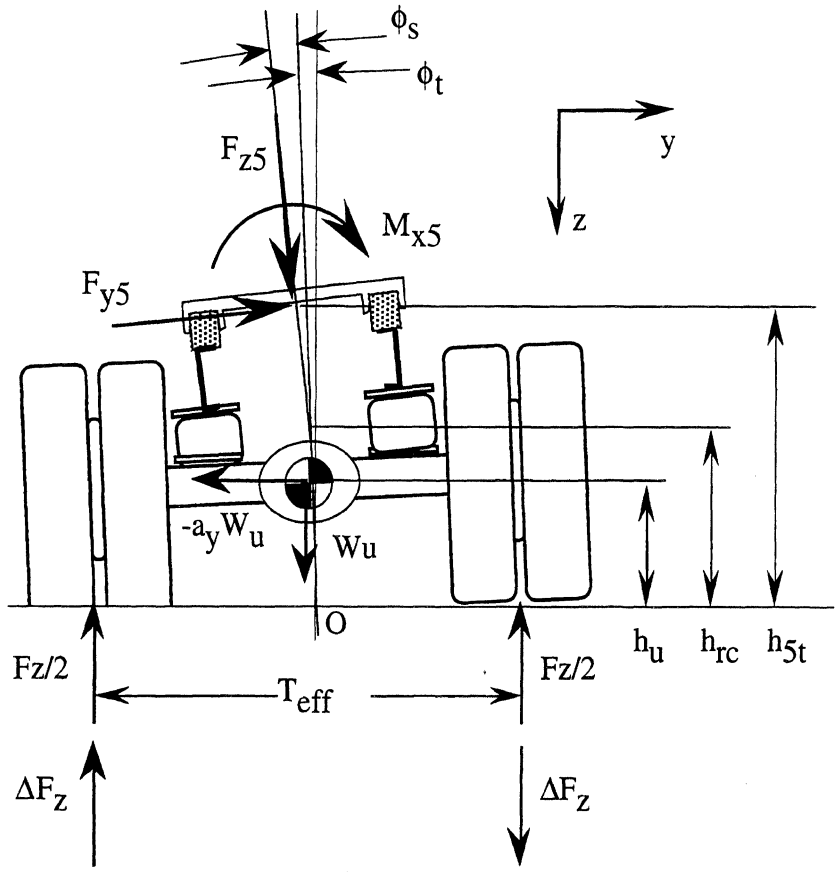

Figure 3. A roll-plane model of the rear of the tractor

the relatively small range of slopes typical of roadways) on rollover if the "lateral" acceleration is actually that component that is parallel to the road surface and includes the component of gravity parallel to the road.

In this study, lateral acceleration of the tractor was measured by an accelerometer mounted on the steer axle of the tractor. Since the steer axle of the typical truck is subject to rather small roll moments, this mounting position ensures that the accelerometer signal is a good approximation of the desired variable.

Also, as the RSA was implemented in this study, F_{y5}, F_{z5}, and M_{x5}, were measured directly using a high-quality, fifth-wheel load transducer developed by UMTRI for this project. In practice, such a transducer may be too costly as a commercial product, and alternative means to measure these loads may be required. For this first-level feasibility study, however, the ability to develop the data-processing algorithms using high-quality signals was desirable. The discussion in the next section dealing with the estimation of liftoff of the trailer tires will indicate an alternative method that can be used to measure similar quantities.

Assuming that the relationships between roll angles and roll moments are linear, that is, that K_t/ϕ_t = roll moment at the ground and that K_s/ϕ_s = roll moment at the roll center, it can be shown that, for the model of figure 3,

$$a_{ylift} = b_0 + b_1\left(\frac{\pm F_{zsus}\left(\frac{T}{2}\right) + b_1c_1 - a_0\left(1 - F_{z5}c_4\right)}{h_{rc} - b_1c_1 + \left(a_1 + c_3\right)\left(1 - F_{z5}c_4\right)}\right) \quad (1)$$

where:

$$M_{x5} = a_0 + a_1F_{y51}, \quad (2)$$

$$a_y = b_0 + b_1 F_{y5}, \quad (3)$$

$$F_{zsus} = W_u + F_{z5}, \quad (4)$$

$$c_1 = h_uW_u, \quad (5)$$

$$c_2 = 1 - c_1/K_t, \quad (6)$$

$$c_3 = h_{5t} - h_{rc}, \quad (7)$$

$$c_4 = h_{rc}/K_s. \quad (8)$$

The parameters c_1 through c_4 are known constants. The parameters a_0, a_1, b_0, and b_1 are all obtained on board the operating vehicle by the appropriate recursive linear regressions of the measured variables a_y, F_{y5}, and M_{x5} as implied by equations 2 and 3. The load carried

by the drive axles, F_{zsus} is determined by simply adding the known tare weight, W_u to the measured value of F_{z5}.

2.2.3 The model for estimating the liftoff of trailer tires

Figure 4 shows a simplified, steady-state model for predicting liftoff of the tires of the trailer axle. Freebody diagrams of the sprung and unsprung masses are shown separately. The sprung mass represents only that portion of the trailer supported by the trailer suspension. The unsprung mass is the trailer axle assembly. These two bodies are connected at a pivot joint, the so-called roll center. The total effective weight of these elements (i.e., the weight carried by the trailer suspension, W_s) is lumped in the sprung mass. Other nomenclature in the figure is as follows.

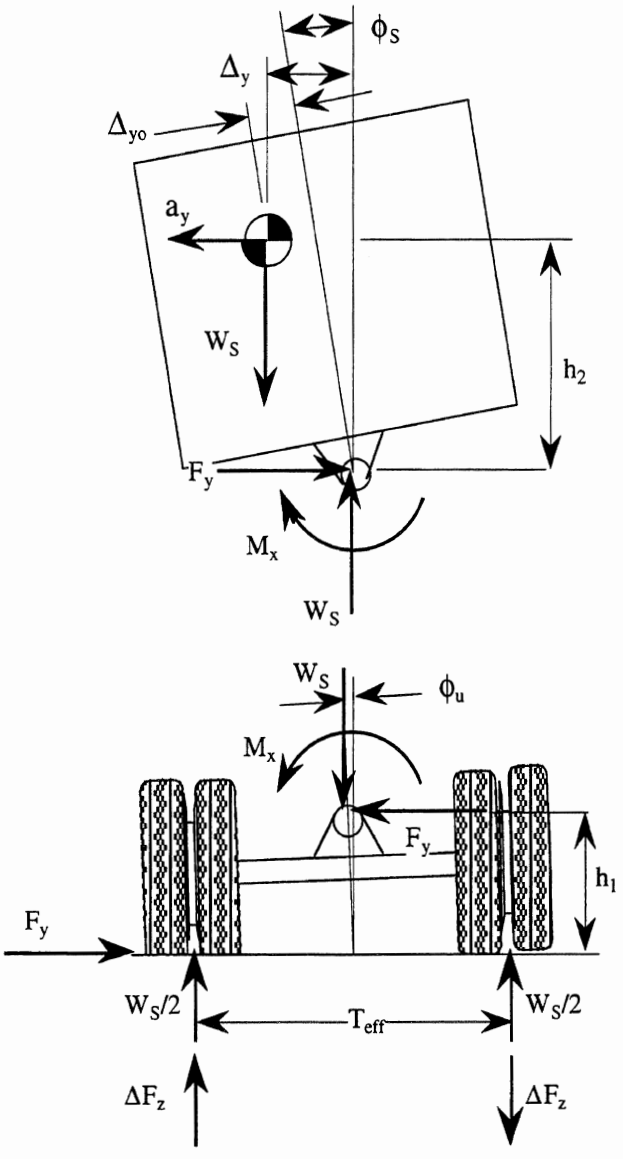

Figure 4. A roll-plane model of the trailer sprung and unsprung masses

a_y	is lateral acceleration
F_y	is the total side force acting on the axle
h_1	is the effective height of the roll center
h_2	is the height of the center of gravity of the mass above the roll center
M_x	is the suspension roll moment about the roll center
T_{eff}	is the effective track width
ΔF_y	is the vertical load transferred from right-side to left-side tires
Δy	is the lateral offset of the sprung mass from the center of the track at the ground
Δy_o	is the lateral offset of the sprung mass from the centerline of the trailer (i.e., at the zero-roll condition)
ϕ_S	is the roll angle of the sprung mass
ϕ_U	is the roll angle of the unsprung mass

The condition of static equilibrium applied to the sprung mass requires that

$$F_y = a_y W_S , \tag{9}$$

$$M_x = a_y h_2 W_S + \Delta y W_S . \tag{10}$$

(Note that the discussion associated with figure 3 in the previous section essentially showed that equation 9 is only approximate in the context of the dynamic experience of driving. Nevertheless, this analysis will use this equation, recognizing that correcting for the approximation will be part of the "calibration" process required for the trailer axle system which uses equation 9 and the measurement of a_y essentially as an approximate means of determining F_y.)

By the geometry of the figure, and assuming linear roll behavior,

$$\Delta y = \Delta y_o + \phi_S h_2 = \Delta y_o + a_y k_{\phi S} h_2 , \tag{11}$$

where $k_{\phi S}$ is the effective roll rate of the sprung mass with respect to lateral acceleration.

By combining these three equations, it can be shown that

$$M_x = a_0 + a_1 a_y , \tag{12}$$

where $$a_0 = (\Delta y_o W_S)/(1 - k_{\phi S} h_2 W_S) , \qquad a_1 = (h_2 W_S)/(1 - k_{\phi S} h_2 W_S) . \tag{13}$$

Static equilibrium of the unsprung mass of figure 4 requires

$$\Delta F_z T_{eff} = M_x + h_1 F_y + W_S \phi_U h_1 , \tag{14}$$

which, by using equation 9, can be restated as

$$\Delta F_z T_{eff} = M_x + h_1 W_S a_y + W_S \phi_U h_1 . \tag{15}$$

In equation 15, the third term on the right side is generally small and can be neglected. This can be shown by further substituting equation 10 and factoring W_S to obtain

$$\Delta F_z T_{eff} = W_S[a_y (h_1 + h_2) + \Delta y + \phi_U h_1] . \quad (16)$$

Near-tire liftoff, the value of $[a_y (h_1 + h_2)]$ is typically at least 20 inches and Δy may be large or small. However, the value of $[\phi_U h_1]$ is always small–on the order of 0.5 inch. Thus, the following approximation of equation 15 is justified.

$$\Delta F_z = b_1 M_x + b_2 W_S a_y , \quad (17)$$

where $$b_1 = 1/ T_{eff} , \qquad b_2 = h_1/T_{eff} . \quad (18)$$

By definition, at tire liftoff:

$$\Delta F_z = \pm W_S/2 . \quad (19)$$

Equations 12, 18, and 19 can be solved for a_y at liftoff as follows:

$$a_{ylift} = \frac{\pm W_S/2 - a_0 b_1}{a_1 b_1 + b_2 W_S} . \quad (20)$$

Equation 20 is the basis on which the RSA predicts the lateral acceleration at which trailer tires will liftoff the road surface. The parameters b_1 and b_2 are obtained from preliminary "calibration" of the suspension. They become permanent constants of the RSA routine for a given trailer. The values of W_S, a_0, and a_1 are obtained on board the operating vehicle in real time. The prediction process goes on continuously, and the resulting value of a_{ylift} is continuously updated. (Note that in this process, the values of a_0, a_1, b_1, and b_2 are all found directly. That is, there is no need to determine all the individual components that appear on the right-hand sides of equations 13 and 18.)

2.3 SPECIALIZED SENSORS FOR THE RSA

2.3.1 Sensor for the tractor-based RSA

Implementation of the model for predicting liftoff of the drive-axle tires, which was described in the preceding section, requires measurement of the loads applied to the tractor by the trailer through the fifth-wheel. To meet this requirement, UMTRI designed and fabricated a fifth-wheel load transducer, or sensor, which measures all the major loads at the fifth-wheel. These loads, diagrammed in figure 5, are:

F_x longitudinal (fore/aft) force
F_y lateral (sideways) force
F_z vertical force

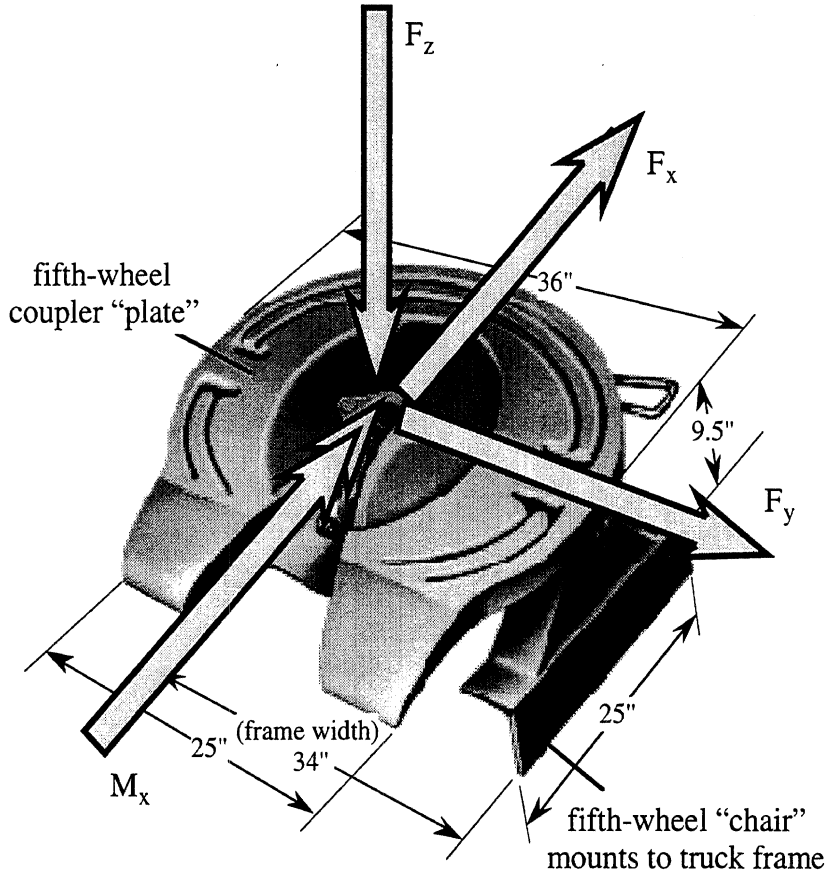

Figure 5. A standard fifth-wheel with loads and nomenclature

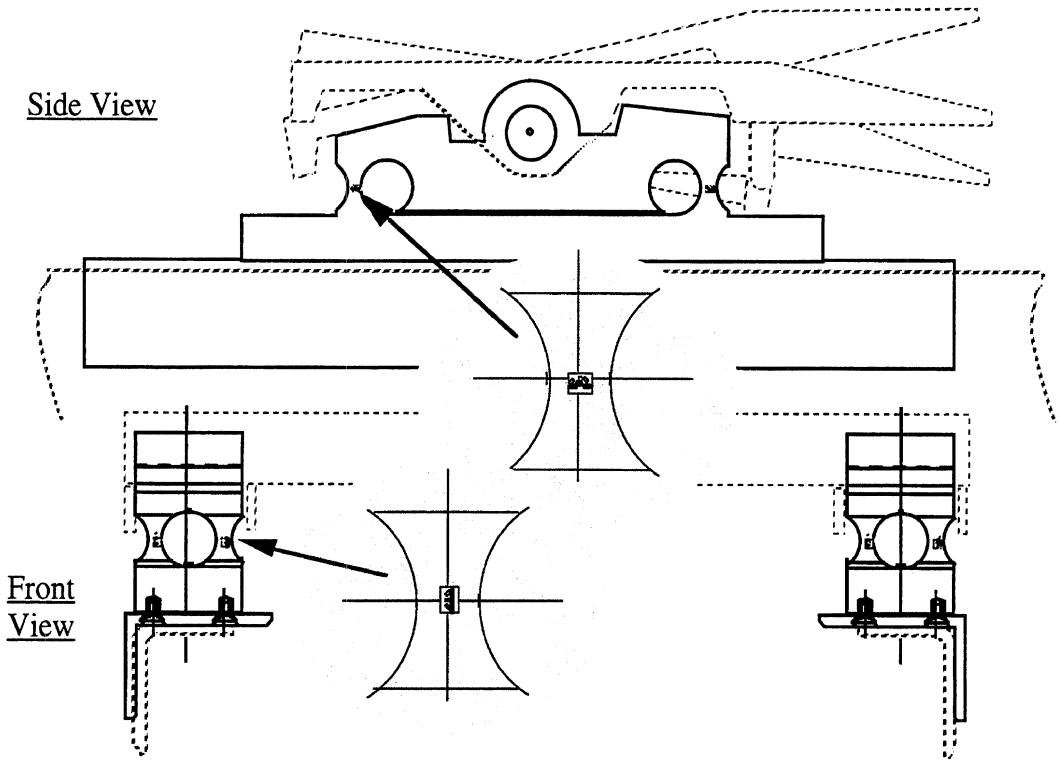

Figure 6. General design of the UMTRI fifth-wheel load transducer

M_x overturning (roll) moment

UMTRI's approach to measuring these loads was to replace the standard fifth-wheel chairs with specially made chairs, which each transduce four similar loads. Total fifth-wheel loads are obtained through the appropriate adding and/or subtracting of the signals from left- and right-side transducers.

Figure 6 is a sketch that shows the general design of the transducer system. The transducer has approximately the same overall dimensions as the standard chair shown in figure 5. However, this chair is cut from a solid block of high-strength steel in a manner such that all loads applied to it by the fifth-wheel plate flow down into the truck frame through four precisely machined posts. Each post has twelve strain gages applied to it, three on each face. On each post, these gages are wired into three resistive bridges sensitive to longitudinal shear, lateral shear, and vertical tension/compression, respectively. In turn, the twelve bridges are wired in parallel in a manner to obtain four signals from each chair. Two of these signals represent longitudinal and lateral load on the chair, respectively. The other two represent vertical load in the left-side and right-side posts, respectively. These may be summed to obtain total vertical load and subtracted to obtain a signal proportional to overturning moment. Finally, the signals from the two chairs may be combined appropriately to obtain the total values of longitudinal, lateral, and vertical force, and overturning moment applied through the fifth-wheel.

The calibration process showed the nominal accuracy of these cells to be in the range of 1 to 2 percent. Additional test have shown the cells to be rather insensitive to twisting and bending loads applied through their base. (This is an especially important issue for a fifth-wheel load cell since it is normal for the typical commercial truck frame to flex substantially during use). Calibration loading is depicted in figure 7 and results are reviewed in tables 1 and 2. The loads for the base-distortion sensitivity tests are depicted in figure 8 with results presented in table 3.

Appendix D is a users' guide for the UMTRI fifth-wheel transducer.

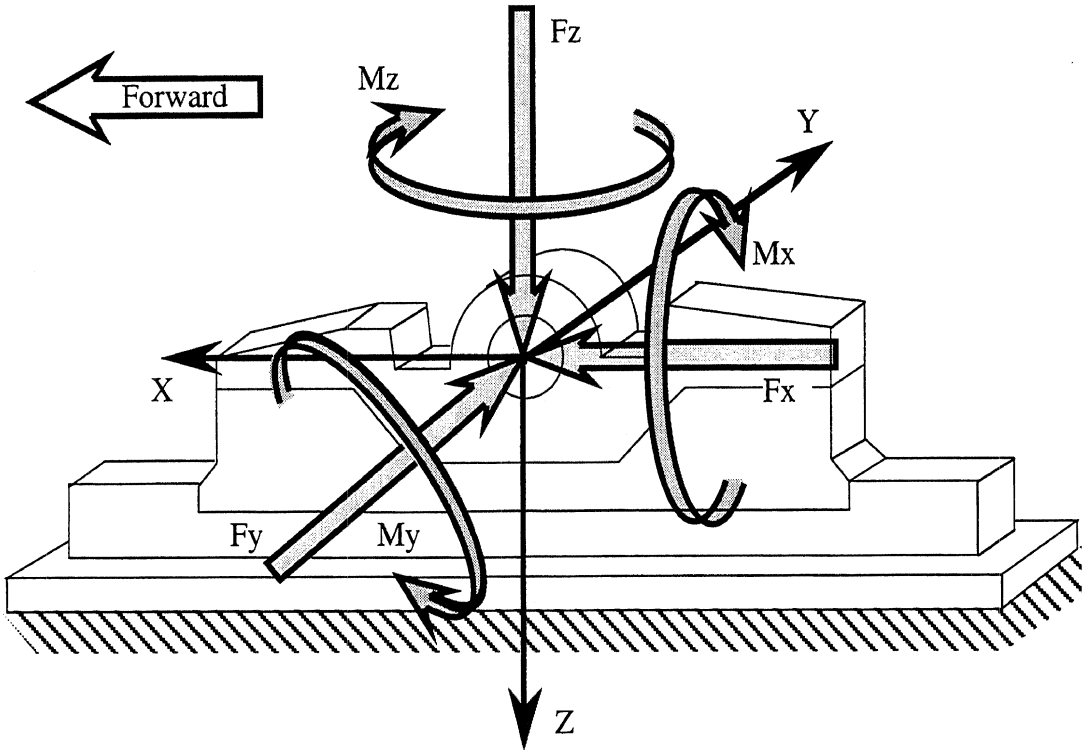

Fx, Fy, Fz, Mx, My, and Mz loads are applied through the load cell to ground.
Load cell transduces only Fx, Fy, Fz, and Mx.

Figure 7. Load-cell calibration tests

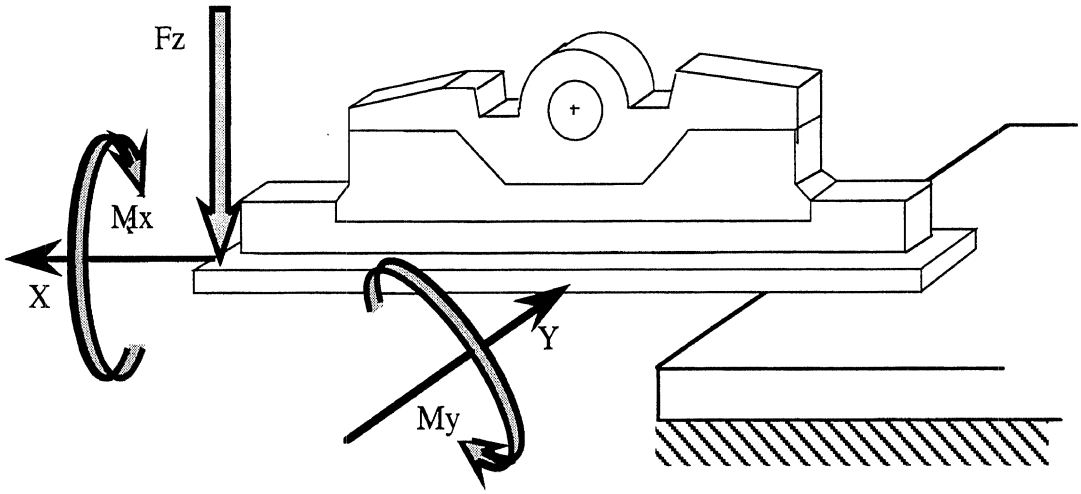

Loads are applied through base to ground.
NO loads are applied through the load cell.

Figure 8. Base distortion tests

Table 1. Calibration results—UMTRI 5th-wheel Load Cell #1

Test Conditions*

Peak values of applied loads

Test	Fx	Fy	Fz	Mx	My	Mz
	[kilo lb]			[kilo in-lb]		
1	20.3					
2	21.1					
3	20.2					40.3
4	21.2					42.5
5	20.5					-41.1
6	-20.4					40.9
7	-20.9					41.8
8	-20.8					-41.5
9	-20.4					-40.8
10	-22.6					
11	-22.6					
12	-22.6					
13	22.9					
14	23.4					
15		22.3				
16		22.5				
17		20.0				-40.0
18		19.9				-39.8
19		20.0				-40.0
20		19.0				38.0
21		19.0				38.0
22		20.0		-40.0		
23		20.0		-40.0		
24		21.2		42.4		
25		20.7		41.4		
26		-21.2				
27		-20.6				
28		-21.0				42.0
29		-20.5				41.1
30		-20.8				-41.7
31		-20.9				-41.8
32		-21.0		-42.0		
33		-21.0		-41.9		
34		-21.0		42.1		
35		-21.1		42.2		
36			20.8			
37			22.4			
38			22.9	45.7		
39			22.8	45.7		
40			17.1	-34.1		
41			16.7	-33.3		
42			23.7			
43			24.0			
44			10.3		-20.5	
45			10.5		-21.0	
46			10.5		21.0	
47			-20.8			
48			-20.8			

Load Cell Evaluation

Correlation coefficients (r^2)

Test	Fx	Fy	Fz	Mx
All**	0.999998	0.999996	0.999786	0.999880

Errors in measured loads

Test	Fx [lb]		Fy [lb]		Fz [lb]		Mx [in-lb]	
	Peak to peak	RMS	Peak to peak	RMS	Peak to peak	RMS	Peak to peak	RMS
All**	69	12	132	15	545	80	599	118
***	0.5%	0.1%	0.6%	0.1%	2.3%	0.3%	2.1%	1.3%
1	68	14	22	12	120	43	37	7
2	91	43	25	15	122	54	49	18
3	75	29	28	10	126	45	82	19
4	96	13	29	10	141	45	95	26
5	59	14	31	12	131	51	53	10
6	55	30	28	10	111	42	213	103
7	50	14	31	15	103	35	194	85
8	45	12	8	1	155	63	166	69
9	51	13	7	2	155	69	172	72
10	67	13	18	7	149	72	57	24
11	59	14	20	7	142	54	55	13
12	78	13	16	5	142	57	56	21
13	95	36	25	12	152	71	43	11
14	58	16	22	12	147	68	45	10
15	12	5	68	16	316	130	163	89
16	9	3	59	16	320	139	218	61
17	12	2	66	19	261	88	541	212
18	15	4	64	16	269	109	469	251
19	15	5	59	19	266	120	571	250
20	12	5	104	13	273	113	614	288
21	14	5	105	12	277	100	672	313
22	10	4	67	12	171	67	235	76
23	9	3	74	16	171	72	286	91
24	11	5	54	12	562	235	620	252
25	10	2	61	12	513	228	632	217
26	7	1	161	48	298	126	313	144
27	6	1	54	9	280	133	237	130
28	16	5	94	11	295	128	370	142
29	17	8	43	13	287	139	281	141
30	9	2	46	12	282	141	391	184
31	11	5	66	12	280	141	386	178
32	6	1	49	14	188	82	236	65
33	8	1	57	11	175	77	226	59
34	9	3	50	17	525	259	891	303
35	11	5	49	18	529	258	833	255
36	16	7	46	13	217	114	380	167
37	8	4	57	22	257	146	323	118
38	14	6	17	6	286	133	401	146
39	14	5	18	4	266	121	376	120
40	10	2	55	18	211	100	408	97
41	9	3	51	17	198	100	387	102
42	20	10	69	25	262	138	407	137
43	21	7	71	26	260	133	450	144
44	14	6	11	3	47	22	113	28
45	13	5	10	2	42	17	111	32
46	9	3	19	5	63	33	148	41
47	20	9	94	41	86	42	245	95
48	16	7	95	47	90	43	281	136

*Loads smoothly applied from zero to maximum to zero over approximately 30 seconds.

**Results for all tests combined are after digital filtering at 5 hz. (Results for Individual tests from unfiltered data.)

*** Percent of maximum applied.

Table 2. Calibration results—UMTRI 5th-wheel Load Cell #2

Test Conditions*

Peak values of applied loads

Test	Fx	Fy	Fz	Mx	My	Mz
	[kilo lb]			[kilo in-lb]		
1			-20.9			
2			-20.8			
3			-20.8	-41.6		
4			-20.7	-41.3		
5			-20.5	-41.0		
6			-20.4	-40.9		
7			-20.4			
8			-20.5			
9			-20.2	40.5		
10			-20.3	40.7		
11			20.5	-41.0		
12			20.4	-40.8		
13			20.4	40.9		
14			20.5	41.0		
15			20.5			
16			22.4			
17			13.6		27.2	
18			19.3		38.7	
20			20.4		-40.7	
21		21.2				
22		21.3				
23		21.0		-42.0		
24		20.7		-41.4		
25		20.8		41.7		
26		20.9		41.8		
27		20.7				41.5
28		21.3				42.5
29		20.6				-41.2
30		20.5				-41.1
31		-20.5				
32		-20.7				
33		-20.6		-41.2		
34		-20.8		-41.5		
35		-20.4		40.8		
36		-20.6		41.2		
37		-20.6				41.2
38		-20.5				41.0
39		-20.5				-41.0
40		-20.5				-41.1
41	-20.6					
42	-20.7					
43	-20.6					41.2
44	-20.6					41.3
45	-20.6					-41.2
46	-20.5					-41.1
47	20.7					41.5
48	20.7					41.3
49	20.6					
50	20.7					
51	20.5					-41.1
52	20.5					-41.1

Load Cell Evaluation**

Correlation coefficients (r^2)				
Test	Fx	Fy	Fz	Mx
All	0.999994	0.999989	0.999874	0.999895

Errors in measured loads								
Test	Fx [lb]		Fy [lb]		Fz [lb]		Mx [in-lb]	
	Peak to peak	RMS	Peak to peak	RMS	Peak to peak	RMS	Peak to peak	RMS
All	101	14	139	25	522	86	729	150
***	0.5%	0.1%	0.7%	0.1%	2.3%	0.4%	1.7%	0.4%
1	12	86	86	195	67	36	195	115
2	12	83	83	184	70	41	184	87
3	14	19	19	462	108	7	462	237
4	13	18	18	482	117	8	482	260
5	13	19	19	391	166	8	391	204
6	11	19	19	367	142	9	367	179
7	10	76	76	423	97	32	423	201
8	10	78	78	411	95	34	411	246
9	13	139	139	611	115	62	611	270
10	14	138	138	633	104	65	633	195
11	18	108	108	512	152	20	512	102
12	17	79	79	481	167	16	481	100
13	16	124	124	662	155	59	662	184
14	15	127	127	683	163	61	683	204
15	12	81	81	295	105	38	295	123
16	13	91	91	360	138	49	360	171
17	5	37	37	73	64	16	73	20
18	11	68	68	165	95	30	165	45
20	27	86	86	620	112	43	620	328
21	6	50	50	179	295	19	179	50
22	6	54	54	184	286	14	184	63
23	5	61	61	430	166	14	430	254
24	4	55	55	418	159	12	418	192
25	6	52	52	646	500	12	646	247
26	8	60	60	729	503	16	729	296
27	11	55	55	206	284	13	206	85
28	13	51	51	181	296	13	181	71
29	15	51	51	143	305	13	143	58
30	13	43	43	182	305	10	182	54
31	4	65	65	147	287	40	147	50
32	5	47	47	214	291	11	214	67
33	5	52	52	288	196	21	288	107
34	5	33	33	253	200	9	253	119
35	6	58	58	473	490	17	473	178
36	6	43	43	540	522	8	540	216
37	8	41	41	343	290	13	343	166
38	8	50	50	355	292	14	355	205
39	9	43	43	522	270	9	522	258
40	9	39	39	504	274	9	504	259
41	90	20	20	93	130	12	93	50
42	82	15	15	101	126	7	101	52
43	75	10	10	43	134	5	43	25
44	101	6	6	35	145	2	35	18
45	71	7	7	144	129	3	144	67
46	68	7	7	148	124	2	148	76
47	84	2	2	100	111	0	100	54
48	64	6	6	96	106	3	96	48
49	59	11	11	94	113	5	94	45
50	61	11	11	97	112	5	97	43
51	54	13	13	269	180	8	269	144
52	55	15	15	258	167	9	258	132

*Loads smoothly applied from zero to maximum to zero over approximately 30 seconds.
**Evaluations performed following digital filtering at 5 hz.
*** Percent of maximum applied.

Table 3. Base-deformation tests of the UMTRI fifth-wheel load cells

Load Cell #1

Test	Loads applied to base			False Load Cell Signals F_x, lb	F_y, lb	F_z, lb	M_x, in-lb
49	F_z, lb	609	Max	32	7	21	293
	M_x, in-lb	50,522	Min	-6	-18	-125	-56
	M_y, in-lb	8,522	Range	37	25	146	349
50	F_z, lb	612	Max	31	8	21	253
	M_x, in-lb	50,834	Min	-9	-17	-126	-62
	M_y, in-lb	8,574	Range	40	25	147	315
51	F_z, lb	593	Max	5	6	12	155
	M_x, in-lb	1,779	Min	-39	-56	-109	-31
	M_y, in-lb	55,155	Range	44	62	120	185
52,53	F_z, lb	618	Max	14	14	33	188
	M_x, in-lb	1,853	Min	-42	-67	-127	-56
	M_y, in-lb	57,457	Range	56	82	160	244

Load Cell #2

Test	Loads applied to base			False Load Cell Signals F_x, lb	F_y, lb	F_z, lb	M_x, in-lb
53	F_z, lb	588	Max	-24	-29	11	526
	M_x, in-lb	48,816	Min	-141	-52	-112	47
	M_y, in-lb	8,234	Range	99	40	123	479
54	F_z, lb	663	Max	-22	-28	5	568
	M_x, in-lb	55,047	Min	-142	-51	-114	52
	M_y, in-lb	9,285	Range	85	42	119	516
55	F_z, lb	616	Max	-12	-29	-66	147
	M_x, in-lb	1,849	Min	-38	-53	-353	-836
	M_y, in-lb	57,305	Range	26	45	288	983
56	F_z, lb	666	Max	-13	-36	-33	144
	M_x, in-lb	1,999	Min	-38	-59	-366	-772
	M_y, in-lb	61,970	Range	26	49	333	916

2.3.2 Sensors for the trailer-based RSA

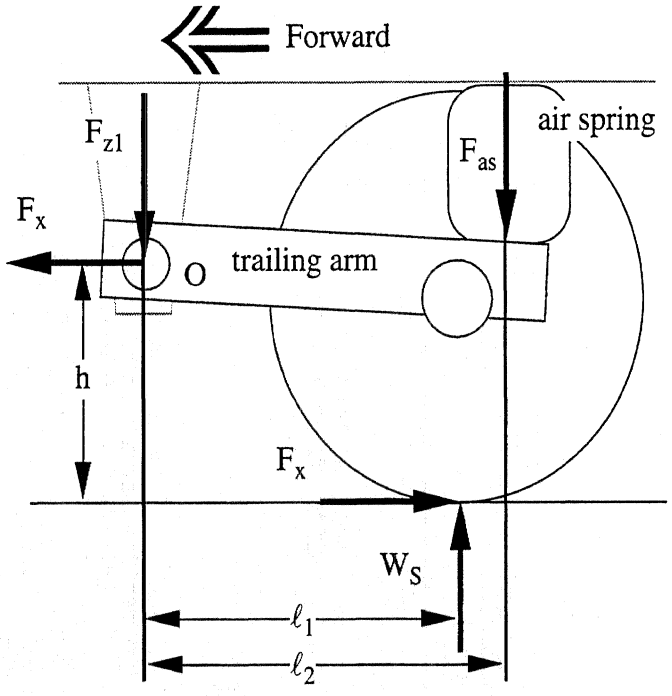

Figure 9. Freebody of a typical air suspension

The sensor for determining vertical load on the trailer axle, W_S, is a pressure transducer that continually measures the internal pressure of the air-springs. Figure 9 is a freebody diagram of a typical air-suspension axle in the side view. Summing moments about the trailing-arm pivot reveals that the force applied by the air-spring is a function of the vertical load supported by the axle and that axle's longitudinal (braking/driving) force. F_{as} is obviously also a function of the internal pressure of the air-spring (P_{as}). That is,

$$F_{as} = \ell_1/\ell_2\, W_S + h/\ell_2\, F_x = f(P_{as}). \qquad (21)$$

If F_x is known to be nearly zero, then equation 23 can be written as

$$W_S = \ell_1/\ell_2\ f(P_{as}) = g(P_{as})\,. \qquad (22)$$

The function g can be found directly from calibration experiments, and W_S can be determined in real operation using air-spring pressure measured when F_x is known to be small.

Laboratory measurements used to determine the function g were accomplished using the UMTRI heavy-vehicle suspension-measurement facility shown in figure 10. (A full complement of suspension properties, including vertical spring rate, total and auxiliary roll rates, roll-center height, and lateral compliance, were measured for both tractor and trailer

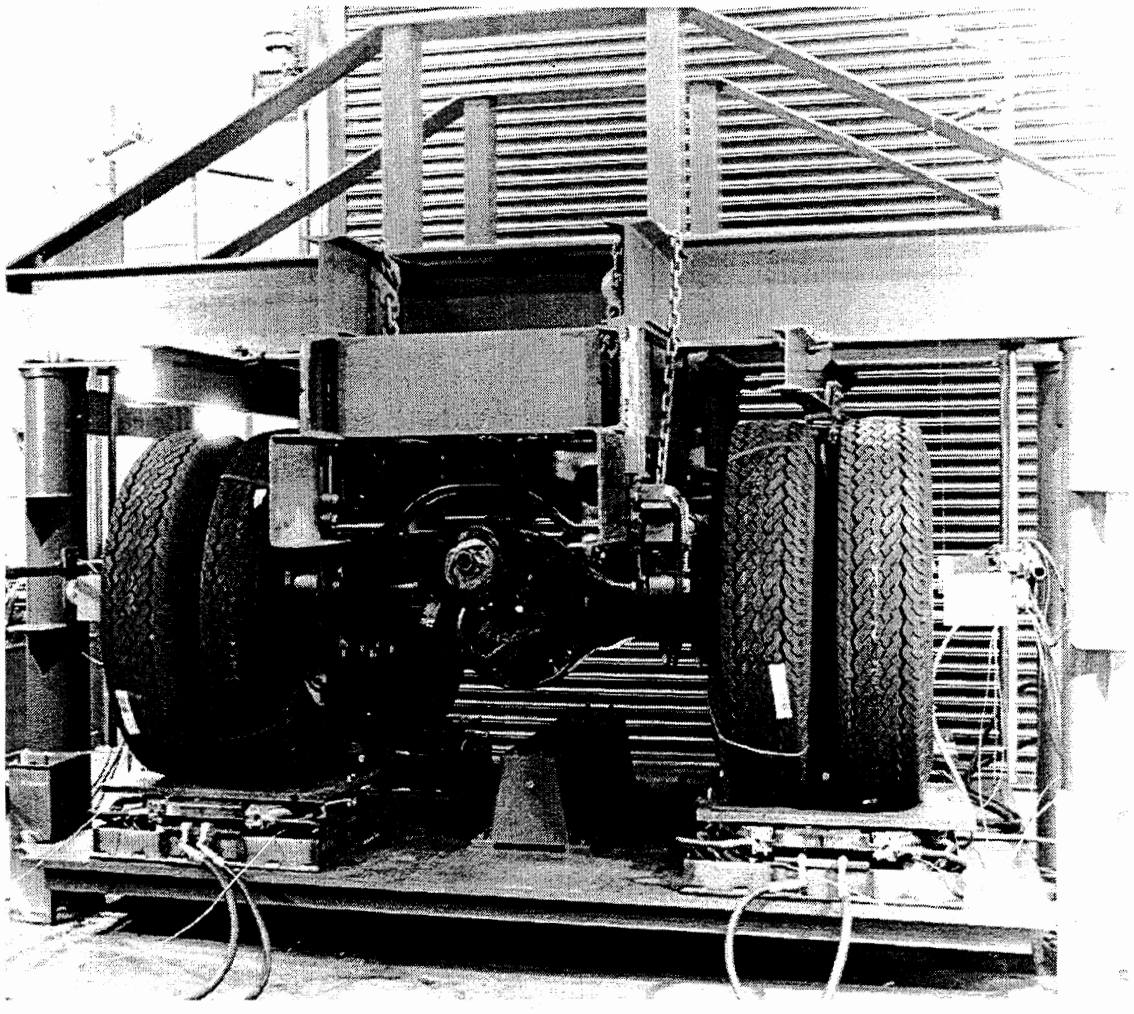

Figure 10. UMTRI heavy-vehicle suspension-measurement facility

suspensions using this facility. Graphical presentations of test data and reduced numerics associated with these properties are presented in appendix A.)

Figure 11 presents data from five separate tests of the trailer suspension, which show the relationship between vertical load and air-spring pressure. In each test, a nominal load condition was established by setting the suspension at its specified ride height and inflating the air-springs to the pressure required to obtain a desired, static, axle load. The air system was then sealed and the suspension exercised vertically. (Axle load internal air-spring pressure were measured and were plotted against one another.) This procedure was repeated for five different static conditions. All five plots of load versus pressure are superimposed in figure 11. Additionally, the five open-square data points indicate the five static test conditions.

The data of the figure show that the relationships between load and pressure, which apply to dynamic load changes operating on the "sealed" air-springs, is substantially nonlinear and changes with the static condition. The relationship between load and pressure in the static conditions is very orderly, but different from any of the individual dynamic

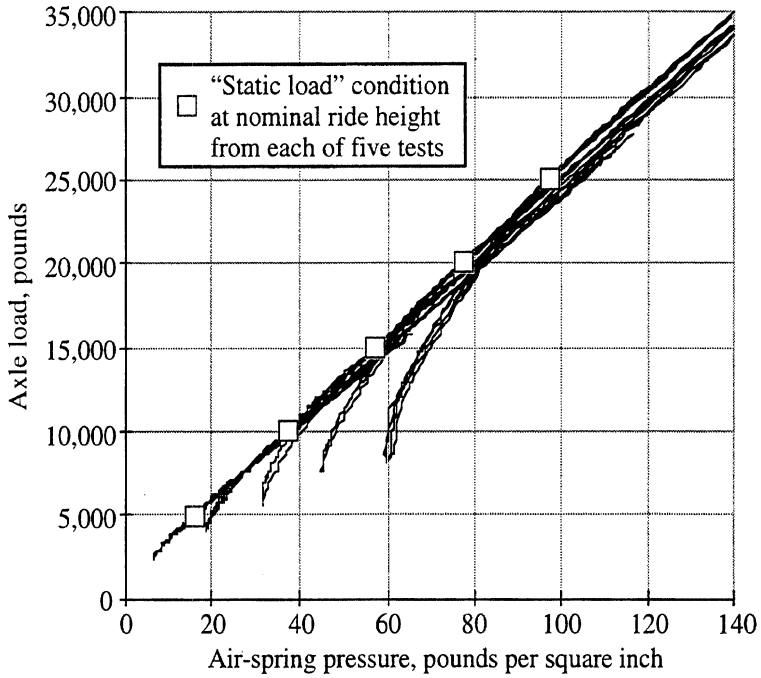

Figure 11. Axle load versus air-spring pressure for the trailer suspension

relationships. Regression analysis of the five static data points yields the following relationship for the trailer suspension.

$$W_S = 1290 + 230.2\, P_s + 0.144\, P_s^2, \qquad (23)$$

where W_S is the static axle load in pounds and P_s is the static air-spring pressure in pounds per square inch. This relationship is used by the RSA—within a statistical context and with certain constraints—to determine vertical load on the trailer suspension in operational conditions. The resulting value of W_S is then used to estimate the lateral acceleration for liftoff of the trailer tires according to equation 20.

The parameters a_0 and a_1 of equation 20 are determined using data from continuous measurements of a_y and M_x in a regression analysis as implied by equation 12. A conventional accelerometer, mounted on the trailer axle, is used to determine a_y. (The accelerometer is mounted on the axle to maintain its sensitive axis as nearly parallel to the road surface as practical.) Strain gages applied to the trailer axle are used to obtain a signal representing M_x.

Figure 12 is a sketch of a typical air suspension showing the conventional components as well as the location of the strain gages. In air suspensions, the air-springs themselves are so compliant that they provide very little resistance to rolling. Consequently, roll stability must be derived mostly from an *auxiliary roll stiffness* mechanism. Use of auxiliary roll stiffness is common in automotive suspensions where it is embodied in the so-called antisway bar. In the modern truck air suspension, the assembly composed of the right-side trailing arm, axle tube, and left-side trailing arm acts as a very stiff antisway bar and

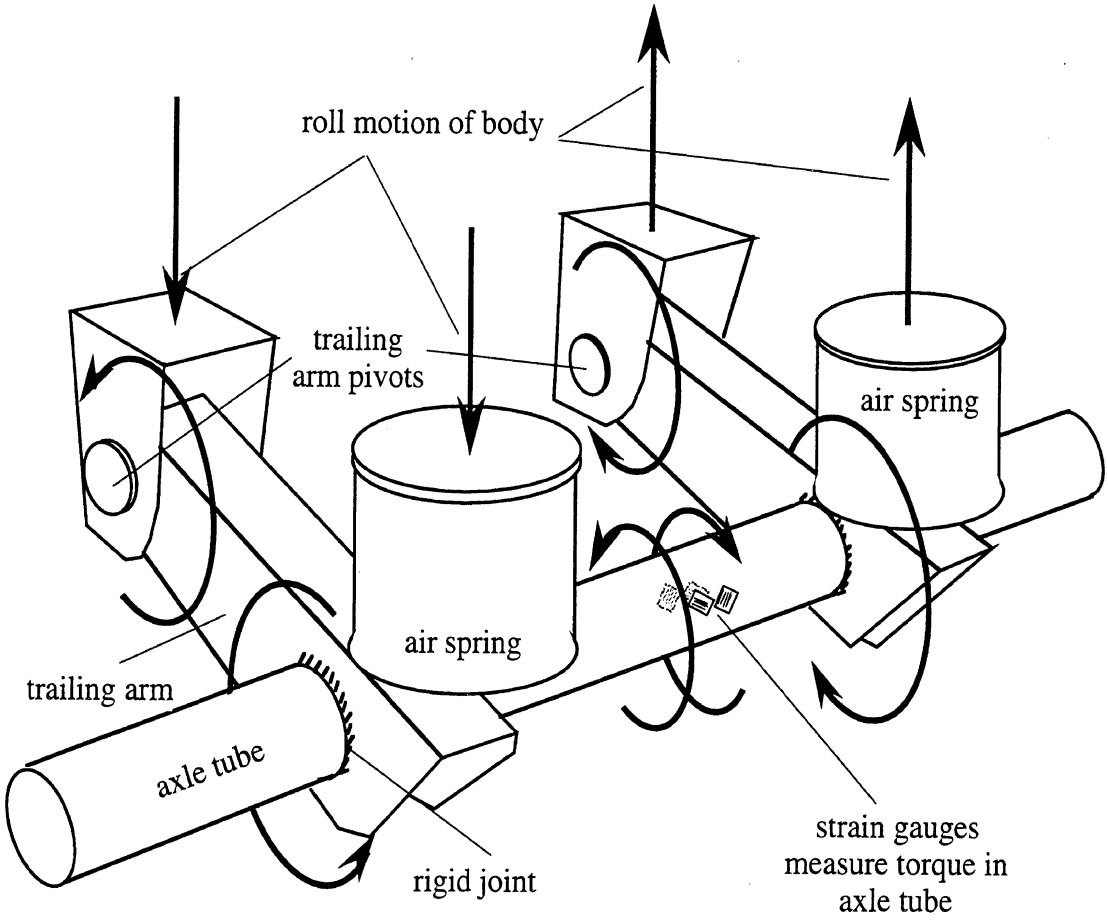

Figure 12. The axle tube of a trailing-arm air suspension experiences torsional stress during roll motion

provides most of the roll stability of the suspension. As the vehicle rolls, the left and right trailing arms must rotate in opposite directions about their forward pivot. For this to happen, the axle tube between the trailing arms must "wrap up" and suffer a resulting torsional load. Strain gages can be applied to the axle to sense this torsion. This measured torsion is *not*, itself, suspension roll moment. However, because this signal is expected to be proportional to suspension roll moment, it can be used as a roll-moment sensor in the same sense that the air-pressure transducer discussed above can be considered a vertical load sensor.

The trailer-based RSA sensor was fashioned by strain-gauging the axle as shown in figure 12. This transducer's output signal, S_s, is assumed to be proportional to the previously defined trailer axle roll moment about a roll center, M_x, such that equation 14, from section 2.2.3, can be rewritten as

$$S_s k_S = M_x = \Delta F_z T_{eff} + W_S \phi_U h_1 + h_1 F_y , \qquad (24)$$

where k_S is the transducer gain, that is, the constant of proportionality.

Laboratory measurements on this instrumented suspension included a series of tests to verify equation 24. Tests included 1) rolling the suspension such that ΔF_z varied while F_y remained essentially zero; 2) applying F_y while ΔF_z was held equal to zero; and 3) simultaneously altering F_y and ΔF_z. In each case, W_S was held constant during the test, but each test was repeated for five values of W_S from 6,000 to 24,000 lbs.

Data from all of these tests are superimposed in figure 13. In this figure, M_x has been calculated based on h_1 = 20 inches (as determined by trial and error) and has been plotted on the horizontal axis. The strain-gage signal is plotted on the vertical axis. (This signal is shown in arbitrary calibration; one calibration unit equals the level obtained with the calibration shunt resistor placed across one arm of the strain-gage bridge.) The rather consistent proportionality between signal and moment (as indicated by the equally constant slope of the plot) implies that the gages constitute a reasonable transducer of roll moment about a center 20 inches above the ground. Two deviations from the RSA model are, however, apparent in these data 1) The spread in the data at large roll moments (all series-1 data) indicates that the transducer has some sensitivity to vertical load; 2) Other elements of the suspension measurement program show the roll center of the suspension to be nominally 25 inches above the ground, implying that the "center" of the transducer and the roll center are not superimposed.

Using the same test data as the figure (and interpreting M_x in transducer calibration units), regression analysis yields values of 1850 and 0.2763 for the parameters b_1 and b_2 of

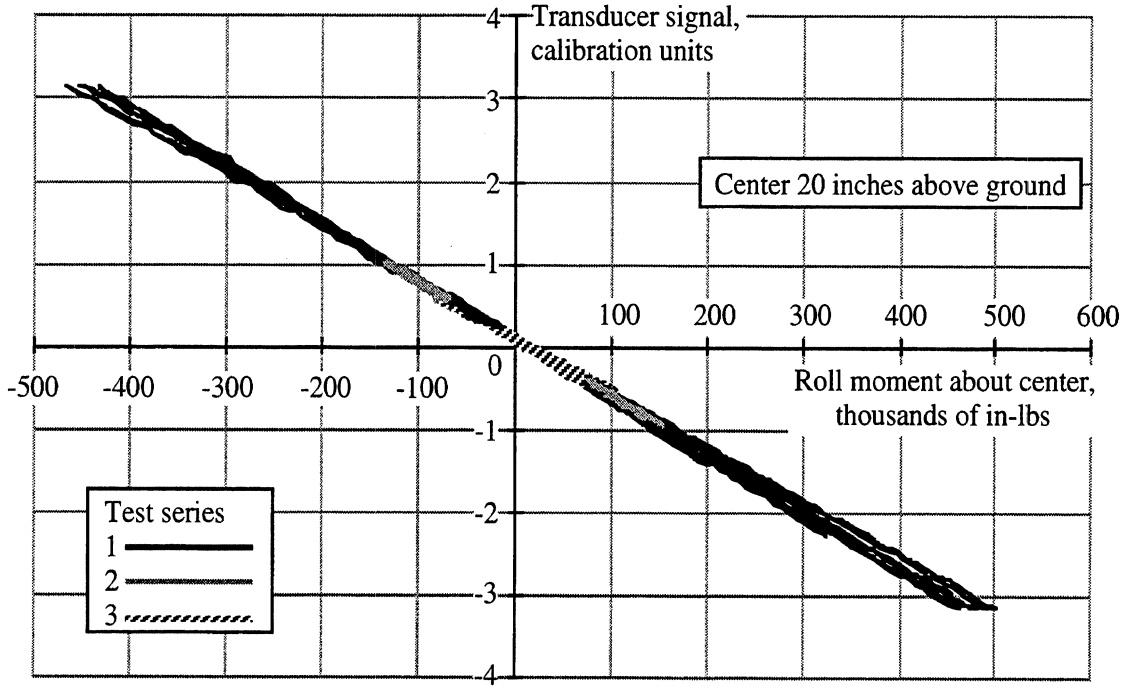

Figure 13. Strain gage signal versus roll moment; suspension loads from 6,000 to 25,000 pounds

equation 20, respectively. These values and the measured roll moment (i.e., S) and side force (F_y) can be used in equation 17 to estimate ΔF_z. Figure 14 shows the rather good agreement between this estimated value and the measured value of ΔF_z in the three test series. This result indicates that the strain-gaged trailer axle, in this air-spring suspension configuration, yields a reasonable sensor for the RSA prediction of trailer axle liftoff.

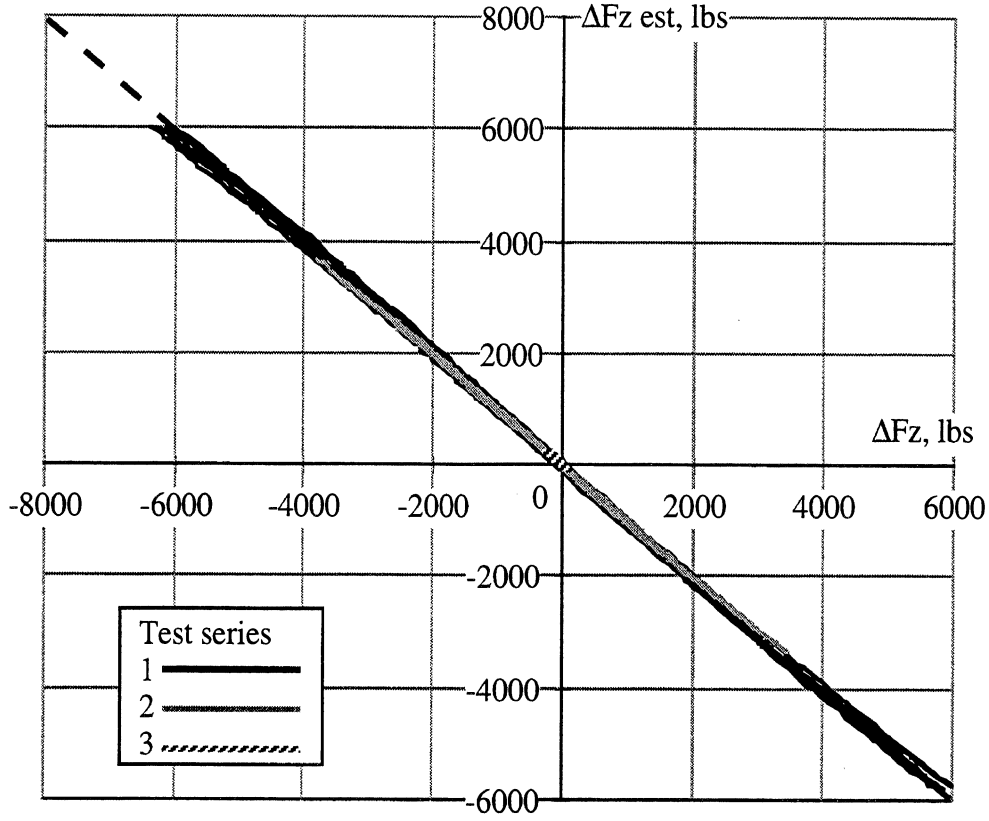

Figure 14. Measured and estimated ΔF_z from suspension measurements

2.4 TILT-TABLE TESTS SUPPORTING DEVELOPMENT OF THE RSA

The test vehicle was subject to a series of tilt-table tests in order to provide the necessary "truth data" for evaluating the RSA estimations of the lateral accelerations required for tire liftoff and for rollover. Tilt-table experiments were conducted with several different loading configurations.

Figure 15 presents a simplified diagram of the tilt-table experiment. The tilt-table methodology is a physical simulation of the roll-plane experience of a vehicle in a steady turn. The vehicle is placed on a tilt table and is very gradually tilted over in roll. As shown in the figure, the component of gravitational forces parallel to the table surface provides a simulation of the centrifugal forces experienced by a vehicle in turning maneuvers. The progressive application of these forces by slowly tilting the table serves to simulate the effects of quasi-statically increasing lateral acceleration in steady turning maneuvers. The

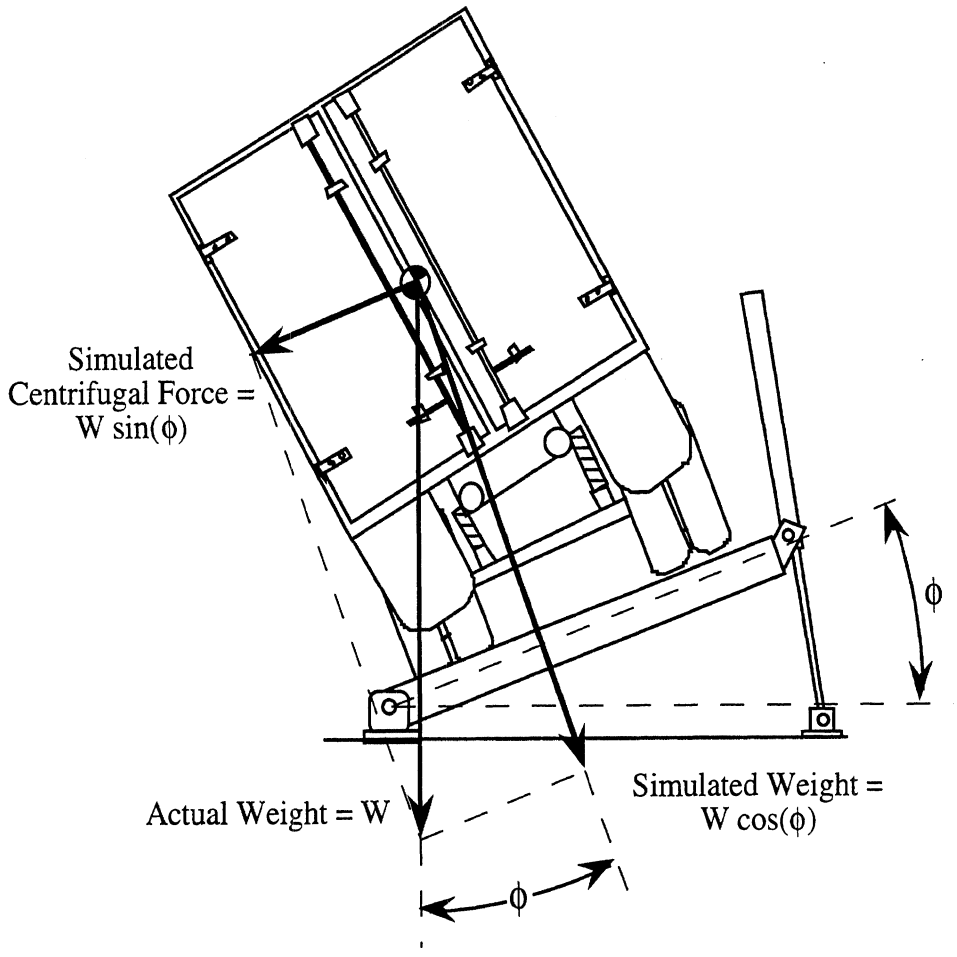

Figure 15. The tilt-table experiment

tilting process continues until the vehicle reaches the point of roll instability and "rolls over." Tilt angle at which special "events" (in this case, the liftoff of tires on the trailer axle) occur are also noted.

When the table is tilted, the component of gravitational forces parallel to the table surface, $W \bullet \sin(\phi)$, simulates lateral forces, and the weight of the vehicle itself is simulated by the component of gravitational forces that are perpendicular to the table (i.e., $W \bullet \cos(\phi)$, where W is the actual weight of the vehicle and ϕ is the roll angle of the table relative to the true gravitational vector). Thus, the forces acting during the tilt-table test are scaled down by a factor of $\cos(\phi)$. Since the most fundamental mechanisms of actual rollover depend on the ratio of the centrifugal forces to the vertical, gravitational forces, it is appropriate to take the ratio of the simulated lateral acceleration forces to the simulated weight to represent lateral acceleration when interpreting the results of a tilt-table experiment. That is:

$$a_{ys} \equiv \tan(\phi) = W \bullet \sin(\phi) / W \bullet \cos(\phi) , \qquad (25)$$

where:

a_{ys} is the simulated lateral acceleration (expressed in gravitational units)

ϕ is the roll angle of the tilt table

W is the actual weight of the vehicle

The test trailer (including the actual suspension whose properties had been measured in the laboratory) was equipped with a load rack, which allowed adjustment of both the weight and the height of the center of gravity of a ballast load. Tests were conducted with two different gross loads, each at three different center-of-gravity heights. Two tests were conducted in each of these six conditions. Results are reviewed in figure 16.

Note that in all tests, the trailer tires liftoff first (at lower values of simulated lateral acceleration) and that the vehicle remains stable after this occurs. At a somewhat high simulated lateral acceleration, the tractor drive-axle tires liftoff and the vehicle becomes unstable in roll. Thus, "rollover" and "tractor liftoff" are synonymous in these data.

As was done with the suspension measurement data, the tilt-table results can be used to obtain values for the trailer-axle parameters b_1 and b_2 of equation 17. Analysis of the trailer-axle data yields values of 5468 and 0.4683 for b_1 and b_2, respectively. Surprisingly, these values of b_1 and b_2 are substantially different from those obtained from the suspension measurements. An interpretation of these new values is that the strain-gage transducer now appears to measure roll moment about a center that is 39 inches above the ground as opposed to the height observed in the suspension measurements which is 20 inches for the transducer's measurement center and 25 inches for the suspension roll center.

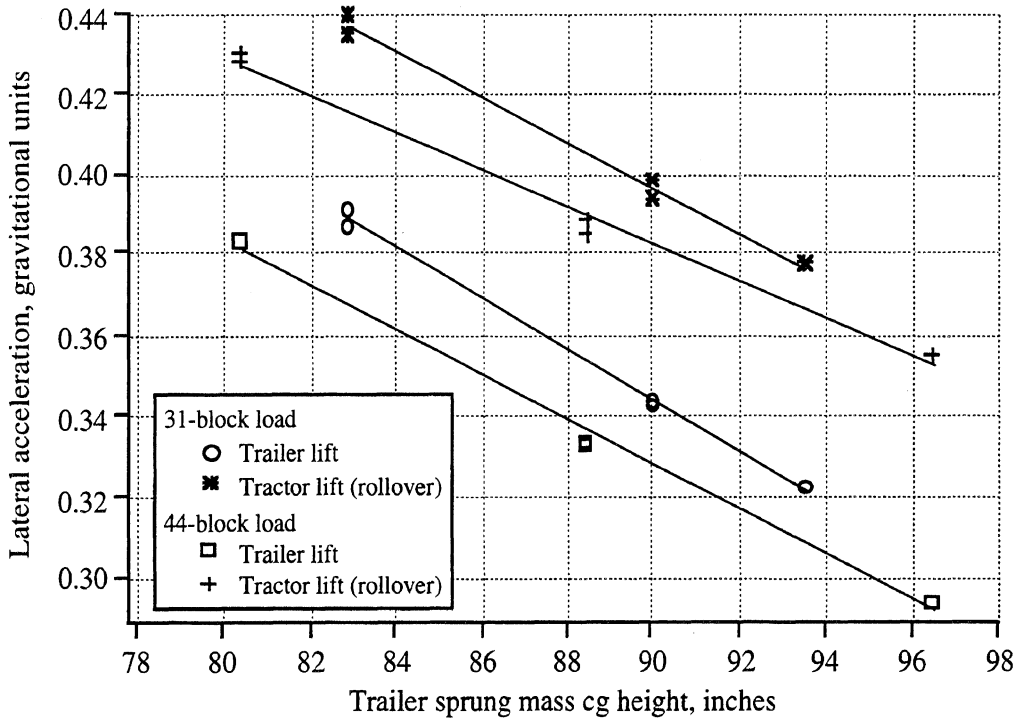

Figure 16. Review of the results of tilt-table testing

The discrepancy between suspension measurements and tilt-table results is not understood at this time. One possible explanation involves the suspension mounting. On the suspension facility, the suspension components are mounted directly to the very stiff superstructure of the facility. On the vehicle, the suspension is mounted to the (probably) more compliant subframe and floor structure of the trailer. Compliance in these elements may very well result in a change in height of the effective roll center and/or measurement center of the suspension.

Regardless of the reason the RSA system appears capable of rather good, on-road prediction of the liftoff of trailer tires when the b_1 and b_2 values from the tilt table tests are used (as will be seen in following sections).

2.5 On-Board Processing of Data for RSA

Measurements made with transducers on board the test tractor are used to (1) determine the vertical load on the drive axles per equation 4, (2) deduce the parameters a_o, a_1, b_o, and b_1 of equations 2 and 3 by linear regression, and (3) use these results according to equation 1 to estimate the lateral acceleration that would result in liftoff of the tractor drive-axle tires. The transducers on the trailer are used to (4) determine the vertical load on the trailer suspension according to equation 23, (5) deduce the parameters a_0 and a_1 of equation 12 by linear regression, and (6) use these results in equation 20 to estimate the lateral acceleration required for liftoff of the trailer tires. Finally, according to the discussion associated with figure 2, the weighted average of the two estimated liftoff accelerations is determined and is then presented to the driver as the final estimate of the rollover threshold for the vehicle. (Separate projections for left and right turns are made and presented.)

Each of processes 1, 2, 4, and 5 requires some filtering and gating of the measured data. Figure 17 is a flow diagram for the calculations associated with the estimates of vertical loads and lateral accelerations for liftoff of tires (steps 1, 2, and 3 for the tractor drive axles or steps 4, 5, and 6 for the trailer axles).

As shown in the figure, the analog data signals are filtered appropriately for anti aliasing and sampled at 50 hz. The first specialized processing is to discard all data taken when the truck is stationary or when the brakes are applied. The assumption here is that a parked vehicle may be in an unrepresentative configuration (e.g., with one wheel in a hole or up on a curb) for a long period of time. Measurement taken in such conditions could result in the "averaging" processes arriving at erroneous conclusions. Further, all the algorithms used are based on simplified roll-plane models whose validity depends in part on the absence of large longitudinal acceleration. Additionally, the algorithm for determining vertical load at the trailer suspension is based on the predetermined relationship between air-spring pressure and suspension load which is only valid in the absence of significant longitudinal loading, thus, the requirement for no braking.

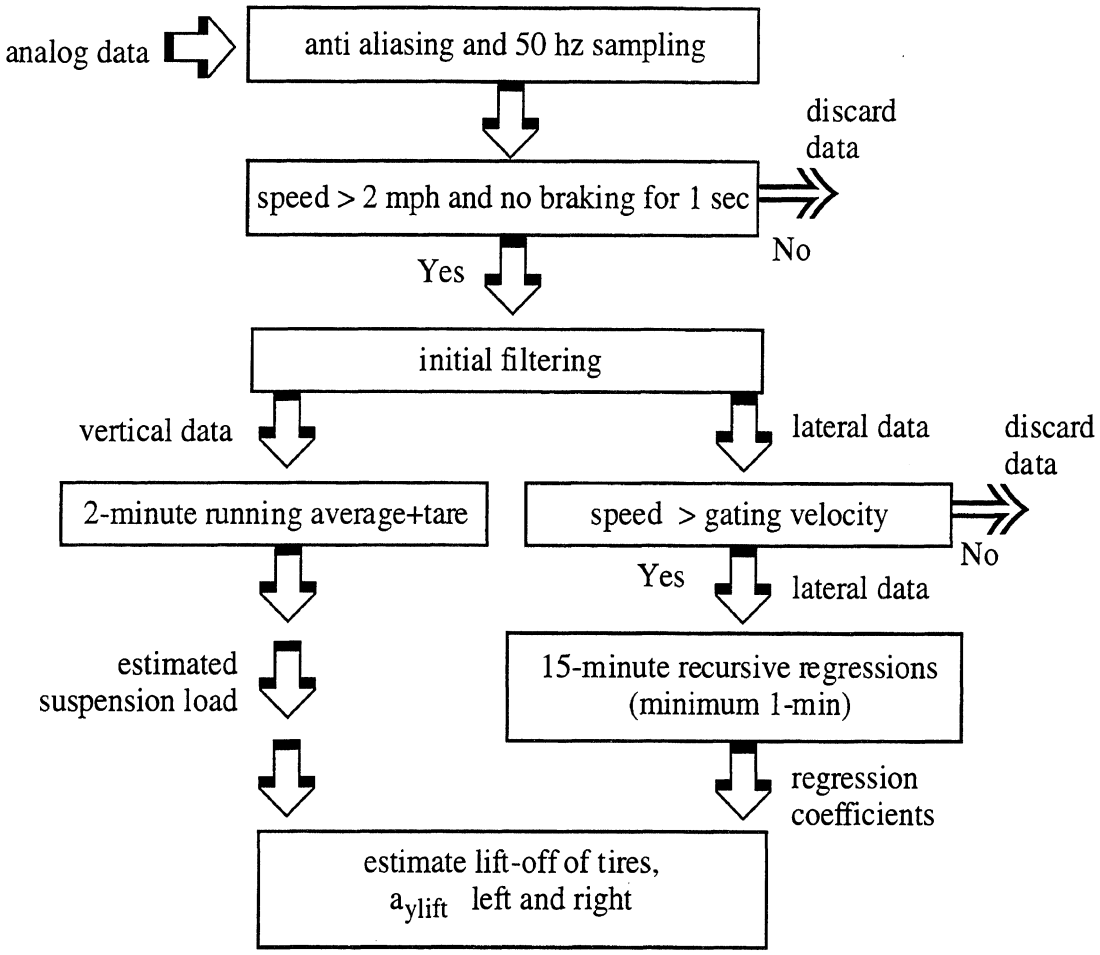

Figure 17. Filtering and statistical processing of the data from the tractor

The surviving data are filtered digitally with an algorithm providing a low-pass bandwidth of 0.1 hz. The data for vertical load (vertical load at the fifth-wheel and air-spring pressure from the trailer) are then used in a 2-minute running average to calculate the vertical load on the suspensions. In the second branch of the analysis, the lateral data (lateral accelerations from both units, lateral force and overturning moment at the fifth-wheel and suspension moment from the trailer) are further segregated by velocity. The gating velocities are 30 mph for the tractor and 40 mph for the trailer. Below these speeds, it appears as if the development of lateral acceleration at different points along the length of the vehicle is sufficiently out of phase to make the simple suspension-by-suspension analysis undertaken here inappropriate. However, the data remaining after this final gating are used in the three recursive regression analyses to determine the necessary coefficients. The resulting coefficients plus the estimated suspension loads are then used to calculate the estimated rollover limits in both left and right turns.

It has been found that one full minute of data gathered above the gating velocity is generally adequate to produce reasonably stationary predictions for liftoff. Thus the algorithms output their first result when the vehicle has been traveling 40 mph or faster for

1 minute. The recursive routines continue to add data to the regression problems until the data in use spans 15 minutes of travel above the gating velocity. Thereafter, the regressions use only the data from the latest 15 minutes of such travel. Thus, the influence of shifting cargo, for example, would be fully discerned within 15 minutes of the shift.

The regressions of equations 2, 3, and 12 are, of course, the heart of this calculation process, and the business of filtering and gating of data for use in these regressions is key to the accuracy of predicting the basic static stability of the vehicle from the low-level data gathered in normal driving. Figure 18 shows the influence of the filtering and gating on the regression problem of equation 3 (i.e., the fit between lateral acceleration of the tractor and lateral force at the fifth-wheel). Figure 19 shows the influence of various choices for gating velocity on the regression problem of equation 12 (i.e., the fit between lateral acceleration of the trailer and overturning-moment signal of the trailer suspension).

The graphs in figure 18 are based on data collected during a test run of approximately one hour. The figure includes three graphs of the a_y versus F_{y5} data, and the line representing the linear regression fit to the data, at various stages in the processing. Note that, for the very simple, static roll-plane model of figure 3, it would be expected that the slope of this fit should be $-1/F_{z5}$. The actual value of F_{z5} in this test run was 14,200 lb. The top graph of figure 18 shows the unfiltered data and the regression fit for a_y and F_{y5} following the first gating for 2 mph and no braking. The data are fairly noisy and the slope of the fitted line is -1/18,100. The second graph shows the same data after it is filtered at 0.1 hz. A great deal of the scatter is removed from the data, and the phasing of the data has been affected such that the slope of the fitted line is now -1/16,100. The final graph shows the data after discarding the data taken at less than 30 mph. The data are now quite clean, and the slope of the fit is -1/15,900. This processing, then, has caused the regression fit to come closer and closer to the result that would be expected from a truly steady-state situation (but raising the velocity gate higher than 30 mph has been found to have little additional effect). Nevertheless, there remains about a 12 percent discrepancy between the slope of the processed, dynamic data and the expectations for a truly static model. It is likely that the discrepancy is associated with the superposition of yaw dynamics on the simple roll model in use. That is, some portion of the observed F_{y5} is associated with rotational acceleration of the yaw inertia of the trailer, and is likely accompanied by an out-of-phase F_y component at the trailer suspension. Given that good-quality measures of both vertical and lateral force are directly available from the fifth-wheel load cell, this is of little consequence with respect to predicting the liftoff of the tractor drive-axle tires. However, effects like this will likely be more important in the future when and if surrogate measures are used to eliminate the need for the expensive fifth-wheel transducer.

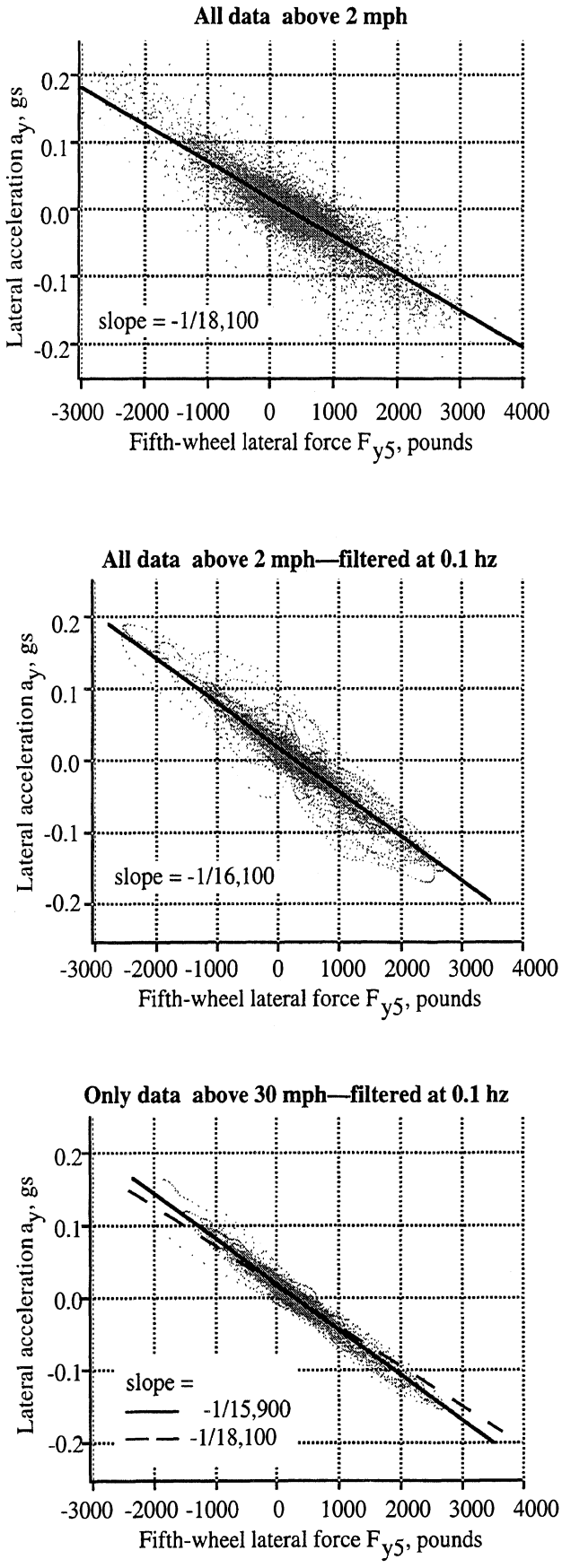

Figure 18. The influence of filtering and gating on the tractor regression problem

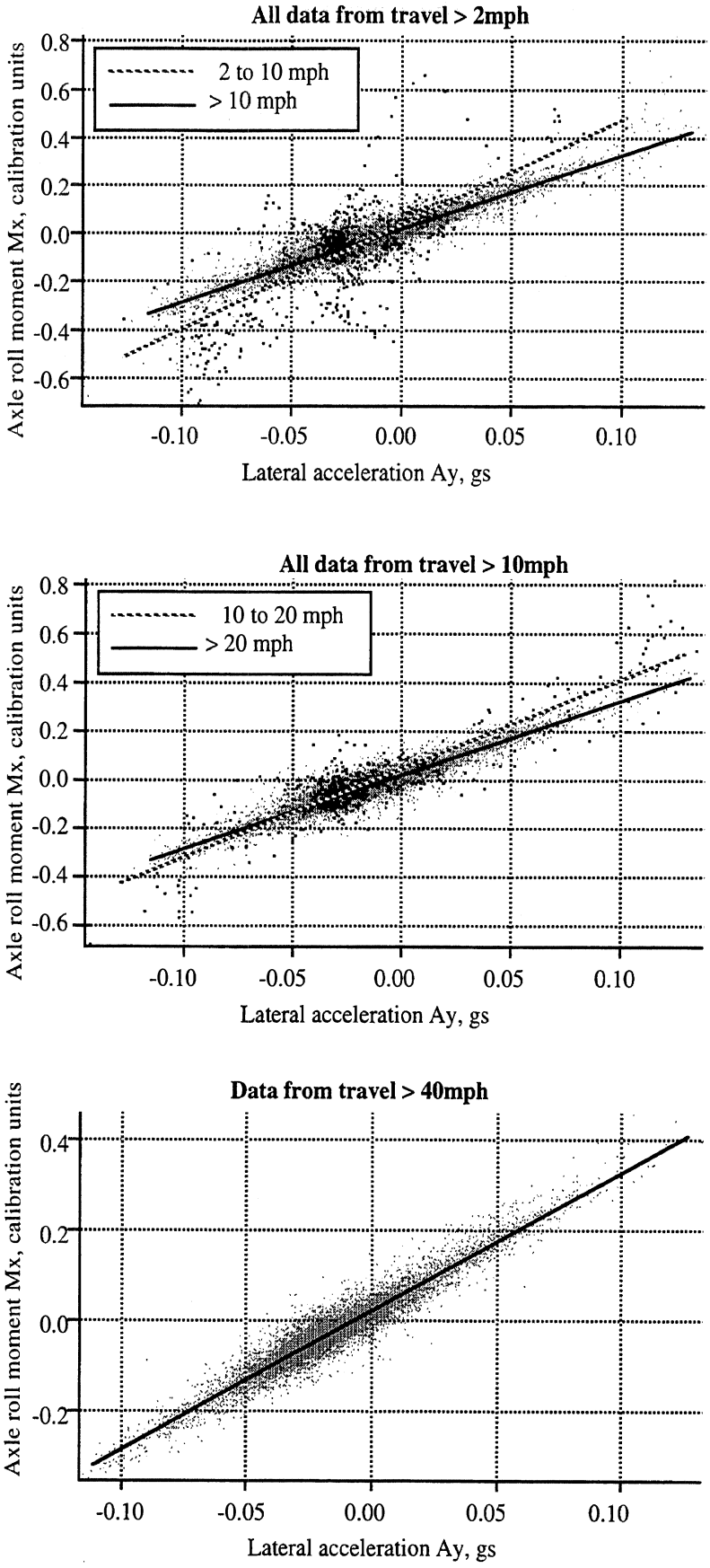

Figure 19. The influence of velocity on the trailer regression problem

Figure 19 presents more evidence of the influence of velocity by showing results of the regression analysis for equation 12 as a function of the velocity range of the data. The figure presents filtered axle-moment and lateral-acceleration data for the trailer from a test run of approximately 1 hour. The first graph shows all of the data for travel above 2 mph with no braking. Lines indicating separate regression fits for the data above and below 10 mph are shown. In the second graph, data collected below 10 mph have been discarded and the two lines are the best fits for the remaining data above and below 20 mph. The third graph shows only data gathered above 40 mph and the best fit to that data. In general, the data become progressively more orderly as data from lower speeds are eliminated. Also, the best-fit lines rotate in more-or-less asymptotic fashion toward a final slope as the effective gating velocity is increased.

2.6 Experimental Operation of the RSA

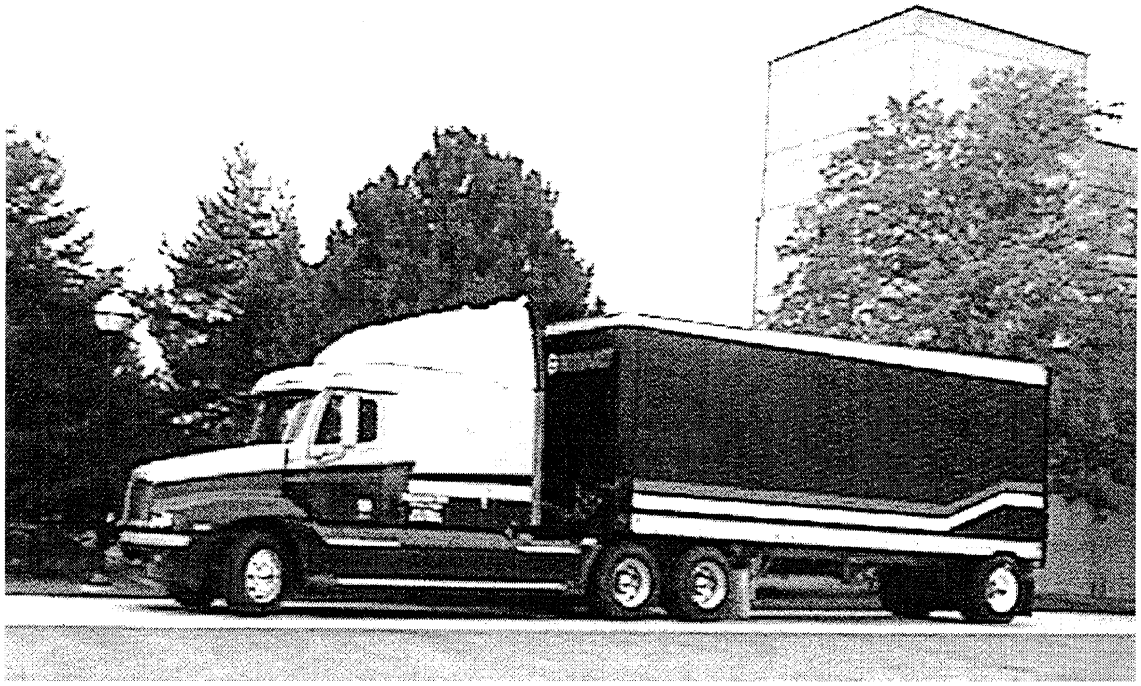

Figure 20. Photograph of the RSA test vehicle

The RSA was implemented on the test vehicle shown in figure 20. The vehicle consists of a long-wheelbase, Freightliner four-by-six tractor and single-axle, 28-foot van trailer. The tractor, provided for the project by Freightliner, was equipped with tandem drive axles with Freightliner's proprietary air suspension. The trailer, provided for the project by Haldex Brake systems (Midland Grau, at the time) was equipped with an air suspension provided by Hendrickson-Turner. The tractor was instrumented with an accelerometer mounted laterally on the steer axle, and with the UMTRI fifth-wheel load transducer described in section 2.3.1. The trailer also had an accelerometer mounted laterally on its

axle plus strain gages for measuring torque in the axle tube and a pressure transducer to sense air-spring pressure, as described in section 2.3.2.

The details of the calculation routines described were developed using data gathered during several trips around public roads in and about Ann Arbor, Michigan. The typical trip course started in the parking lot at the UMTRI facility and proceeded through several blocks of suburban streets, including multiple stops and turns at intersections. The course then proceeded onto the four-lane, restricted-access highway system in the Ann Arbor area. Some trips went east to Dearborn via US-23 north, M-14 east and I-96 east (test route 1). Others went north to Howell via US-23 north and I-96 west (test route 2). Still others went west to Chelsea via US-23 north, M-14 west and I-94 west (test route 3). The outbound leg of travel on the four-lane highway was followed by several miles of travel on secondary roads and then a return to UMTRI via essentially the same four-lane route. The three routes are presented on local maps in appendix B.

RSA test trips were conducted on these routes under a variety of loading conditions. Data from the tilt-table tests were used (either directly or by interpolation or extrapolation) to provide the "true" reference lateral acceleration values for tire liftoff and rollover against which RSA estimates are compared. Section 2.6.1 and 2.6.2, which follow, present results obtained from these tests for the tractor- and trailer-based systems, respectively.

2.6.1 Test results for the tractor-based portion of the RSA

Some thirteen trips on test routes 2 and 3 were used to develop the calculations for liftoff of the tractor drive-axle tires. The various loading conditions for these trips, and the reference lateral accelerations for liftoff of the drive-axle tires and, therefore, for rollover are given in table 4. Payloads in the first five runs were deliberately offset from the centerline to the right resulting in substantially lower rollover thresholds in left than in right turns. In the other runs, payload is nominally on center, although individual wheel weights showed small biases to the left or right, which are reflected in small differences in the left- and right-turn reference lateral accelerations.

(Note that the averages of the reference lateral acceleration for left and right turns come directly from the results of the tilt-table tests. The differences in the reference values for left and right turns, however, are calculated based on the observed left-to-right differences of static wheel weights. Note also that the reference lateral accelerations are for the actual liftoff of the drive axle tires, i.e., for the rollover threshold. As per the discussion associated with figure 2, since the drive-axle tires liftoff at a higher lateral acceleration than do the trailer tires, the on-board estimation procedure for liftoff of the drive-axle tires is *expected* to result in estimates that are too high and which are then corrected by weighted averaging with the estimates for liftoff of the trailer tires. Accordingly, in the following discussion, *the estimates for the lateral accelerations for liftoff of the tractor drive-axle tires*

Table 4. Trailer mass properties and reference lateral accelerations for road tests of the tractor-based RSA

Test	Total trailer		Trailer sprung mass		Nominal payload	Reference a_{ylift}, g	
No	GVW, lb	GAW, lb	Wt, lb	Est height, in	offset, in	Left turn	Right turn
1	36,200	18,300	34,450	91.7	6.1	0.335	0.402
2	36,200	18,300	34,450	91.7	6.1	0.335	0.402
3	36,200	18,300	34,450	91.7	6.1	0.335	0.402
4	36,200	18,300	34,450	84.8	6.1	0.357	0.429
5	36,200	18,300	34,450	84.8	6.1	0.357	0.429
6	36,200	18,800	34,450	80.9	0	0.417	0.403
7	36,200	18,800	34,450	80.9	0	0.417	0.403
8	36,200	18,800	34,450	97.4	0	0.354	0.343
9	36,200	18,800	34,450	97.4	0	0.354	0.343
10	29,800	15,600	28,050	83.6	0	0.415	0.429
11	29,800	15,600	28,050	83.6	0	0.415	0.429
12	29,800	15,600	28,050	94.6	0	0.364	0.376
13	29,800	15,600	28,050	94.6	0	0.364	0.376

are the corrected (weighted average) values. Further, since trailer-axle data was not collected in these runs, the lateral accelerations for liftoff the trailer tires that are used in the averaging process are the reference values obtained from the tilt-table tests.)

Figure 21 is a typical example of the estimate of the lateral acceleration for liftoff of tractor drive-axle tires during a test run of about 60 minutes on test route 3. The overall accuracy of the estimates are within about 0.02 g. Further, the initial estimates, made after only a minute of travel above 30 mph, are reasonably accurate. There does appear to be a tendency for the difference in left- and right-turn estimates from the RSA to be greater than the difference of left- and right-turn reference values from the tilt table. (This might just as well be a result of the treatment of the tilt-table data as it is of the RSA estimates.) All of these observations are fairly typical for all of the runs of table 4.

Figure 22 reviews the overall accuracy of RSA estimates for rollover from all of the runs of table 4. This figure plots the average estimated lateral acceleration for rollover in left and right turns for each of the test runs (e.g., the time averages of the two solid lines of figure 21), against the reference lateral-acceleration values for those runs. Each test run, then, appears as two data points on the graph. "Perfect" estimates (relative to the references) would appear as data points lying on the center of the three, 45-degree reference lines on the plot. The other two lines show the range of estimates accurate to within ± 0.02 g. The graph indicates that the majority of the RSA estimates lie within this accuracy range. The worst-case average estimate has an error of 0.034 g.

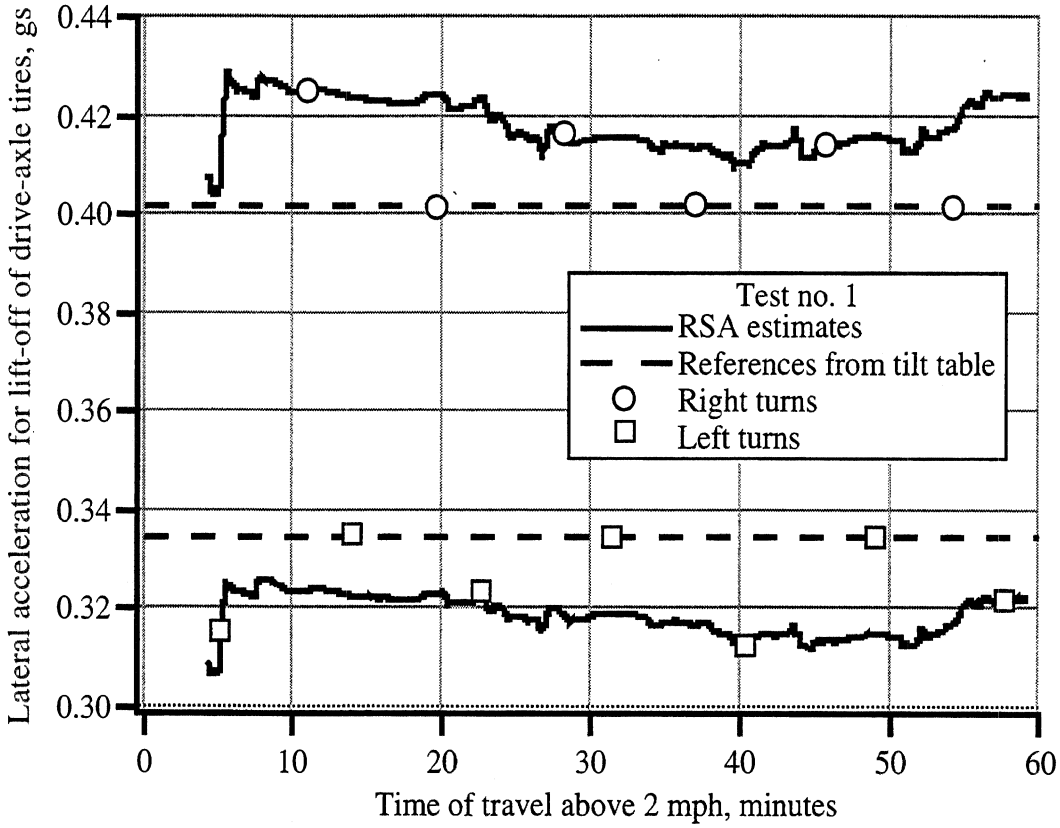

Figure 21. Example of the RSA estimates of the rollover limit (the lateral accelerations required for liftoff of the tractor drive-axle tires)

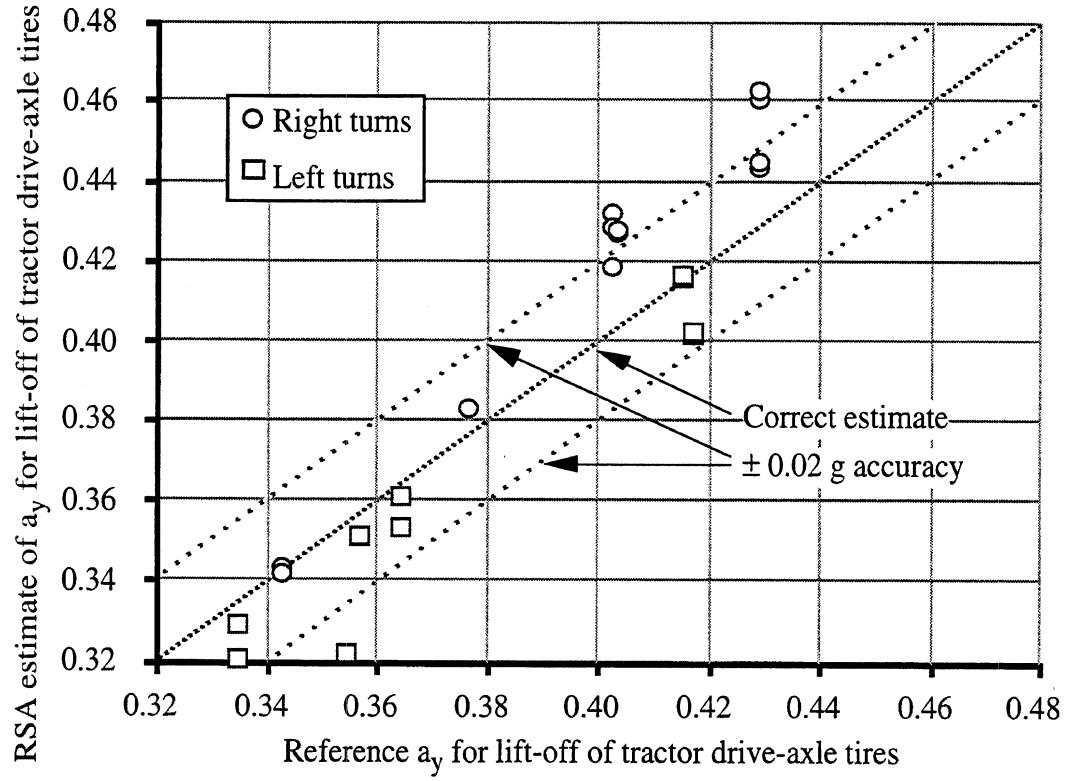

Figure 22. Review of the average estimate of the rollover threshold for the test runs of table 4

2.6.2 Test results for the trailer-based portion of the RSA

Eleven trips on route 1 were used to develop the calculations for liftoff of the trailer tires. On these trips, the center of gravity of the trailer payload was on the left-right centerline. Two additional trips with off-center loading were used as check runs. The loading conditions and the known (from tilt-table tests) reference values of the lateral acceleration required for liftoff of trailer tires for each of these trips appears in table 5.

Figure 23 presents a time history of the lateral acceleration required for liftoff of the trailer tires as estimated by the RSA in trip number 7. The reference lateral acceleration is also shown. The first estimates appear after about 8 minutes of driving above 2 mph. This would have coincided with the time in this particular run at which 1 full minute of travel above 40 mph had occurred. Based on only a minute's data, the estimate is changing rapidly but settles down to a rather consistent estimate when sufficient data for the moving, 15-minute average becomes available. At about 40 to 50 minutes into the test, the vehicle reaches the end of the out-bound highway run and spends 10 minutes or so at less than 40 mph. As a result, the estimate stays virtually constant during this time.

Figure 24 is a composite presentation of all eleven development test runs. In order to show all runs on the same scale, the vertical axis is not the estimated acceleration itself, but the error in the estimate relative to the reference for the loading condition. The figure shows that the RSA typically homes in on an estimate within +0.02 to -0.04 g of the reference. In fact, we believe that part of the reason for this range of error is associated with insufficient

Table 5. Trailer mass properties and reference lateral accelerations for road tests of the trailer-based RSA

	Trailer Properties				Reference a_{ylift}, g	
Test No	GVW, lb	GAW, lb	Est. sprung mass cg height., in	Equiv lateral offset trailer axle load, in	Right turn	Left turn
1	21,350	11,710	71.9	0	0.489	0.489
2	21,350	11,710	82.1	0	0.420	0.420
3	29,460	15,660	72.2	0	0.452	0.452
4	35,920	18,840	80.4	0	0.357	0.357
5	35,920	18,840	96.5	0	0.285	0.285
6	29,460	15,660	82.9	0	0.391	0.391
7	29,460	15,660	93.5	0	0.323	0.323
8	29,460	15,660	86.4	0	0.365	0.365
9	29,460	15,660	79.3	0	0.397	0.397
10	35,920	18,840	72.4	0	0.434	0.434
11	35,920	18,840	88.5	0	0.307	0.307
12	35,940	18,700	90.8	8.74	0.360	0.279
13	35,940	18,700	84.1	8.74	0.398	0.309

attention to "zeroing" of instrumentation signals prior to some test runs, and that a range of ±0.02 g is likely a more appropriate description of the quality of the RSA routine.

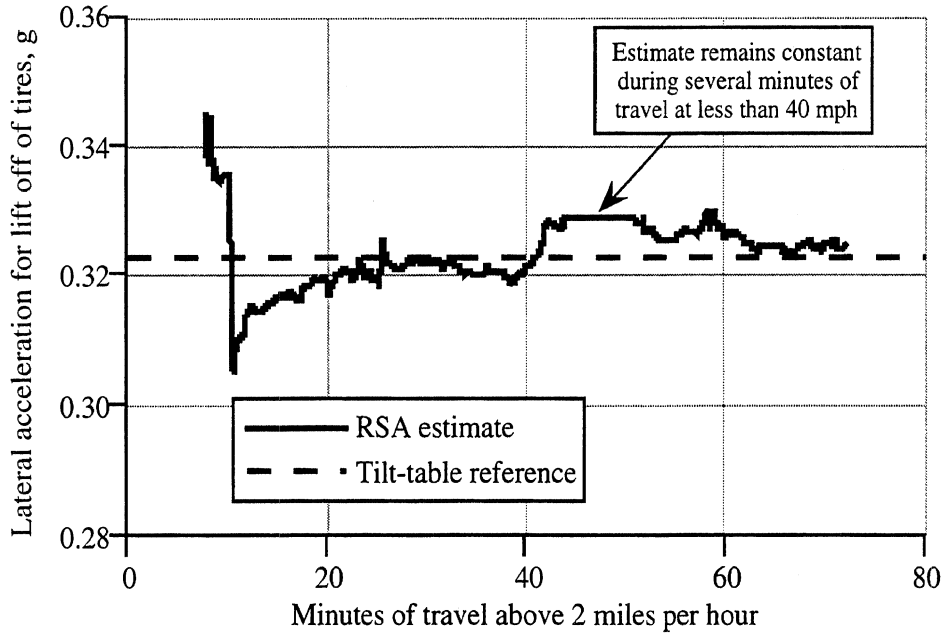

Figure 23. RSA estimate of lateral acceleration for liftoff of trailer wheels

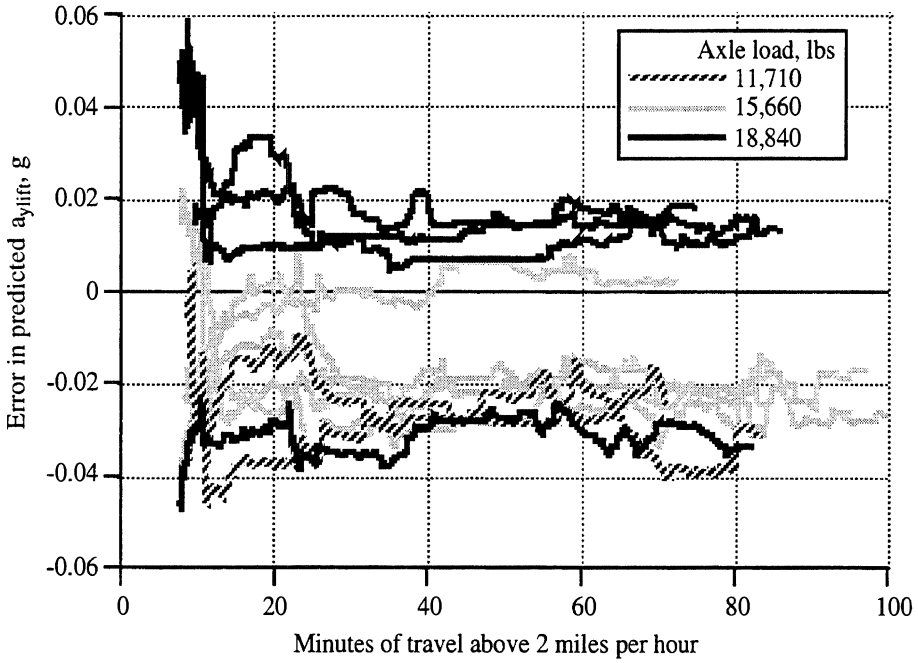

Figure 24. Estimation error of the RSA in eleven development runs

Results for the two additional runs with off-center loading appear in figure 25. The figure shows that the RSA estimates different liftoff thresholds for left- and right-going turns in these additional runs. Estimates for lifting the right wheels are nominally within 0.02 g, and estimates for the more stable, right-hand turns (lifting the left wheel) are seen

to be even more accurate. (Closer attention was given to proper zero calibrations prior to these two final test runs.)

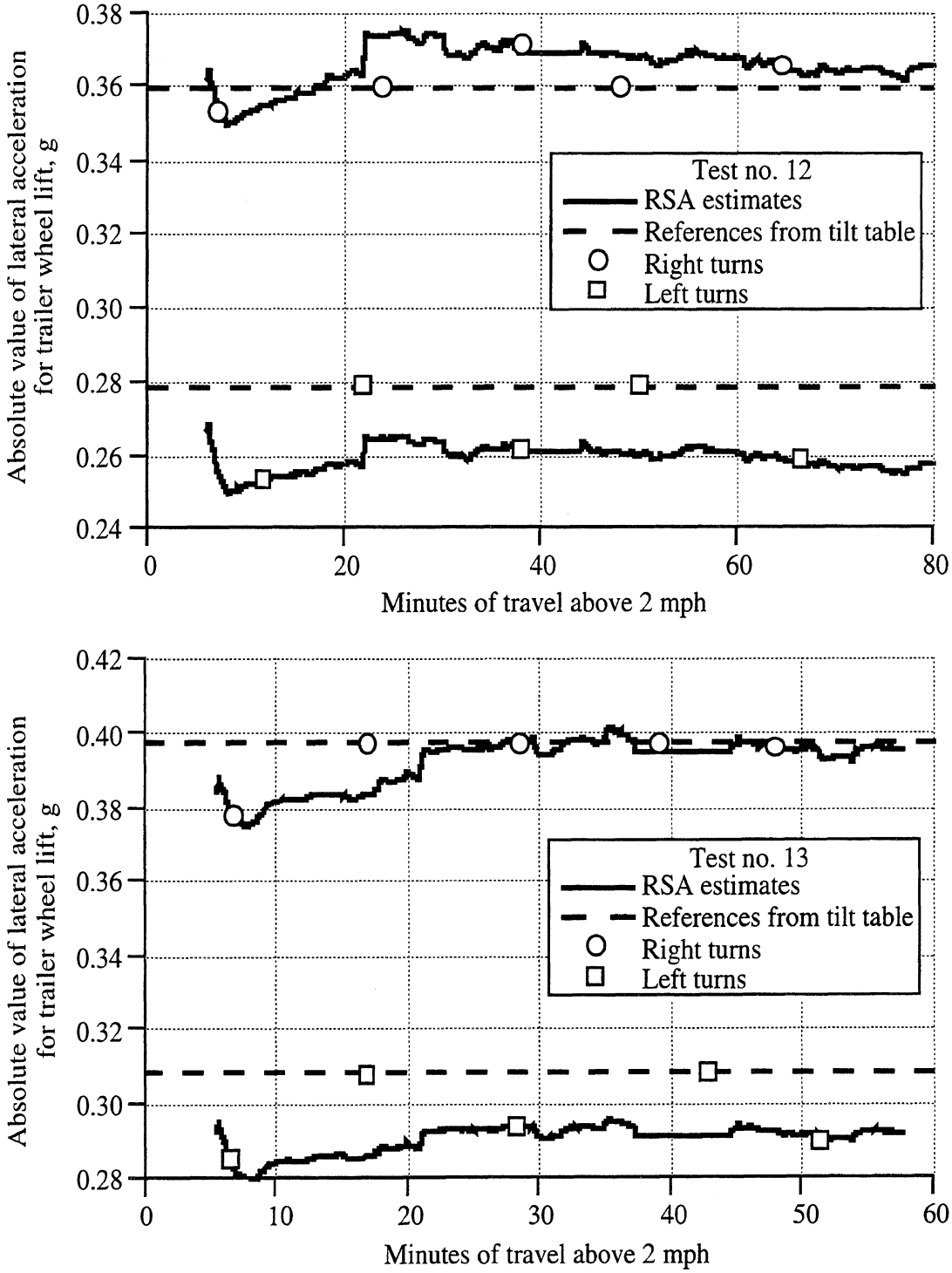

Figure 25. RSA time-histories for test runs with asymmetric loading

2.7 RSA Display for the Driver

The RSA display used in the cab of the test vehicle in this study is shown in figure 26. The display presents both the estimated roll-stability limits and the current lateral acceleration of the vehicle. With such a display, the driver can see and understand the relationship between the ultimate capability of his vehicle as presently loaded and the demand placed on that capability by his driving. Additional features of this particular display are the digital presentations of the data above the analog dial, plus the ability to recall the recent peaks of lateral acceleration experience in left and right turns.

As discussed earlier in this document, such a display is intended as a driver-education aid more so than as an immediate warning of pending rollover. The aim is that, over time, the driver will learn the relationship between the appearance of the load in the trailer, the resulting stability of the vehicle, and the stability demands that are being made on the vehicle. The goal is that the driver will soon learn to recognize those loading conditions that require special care while driving.

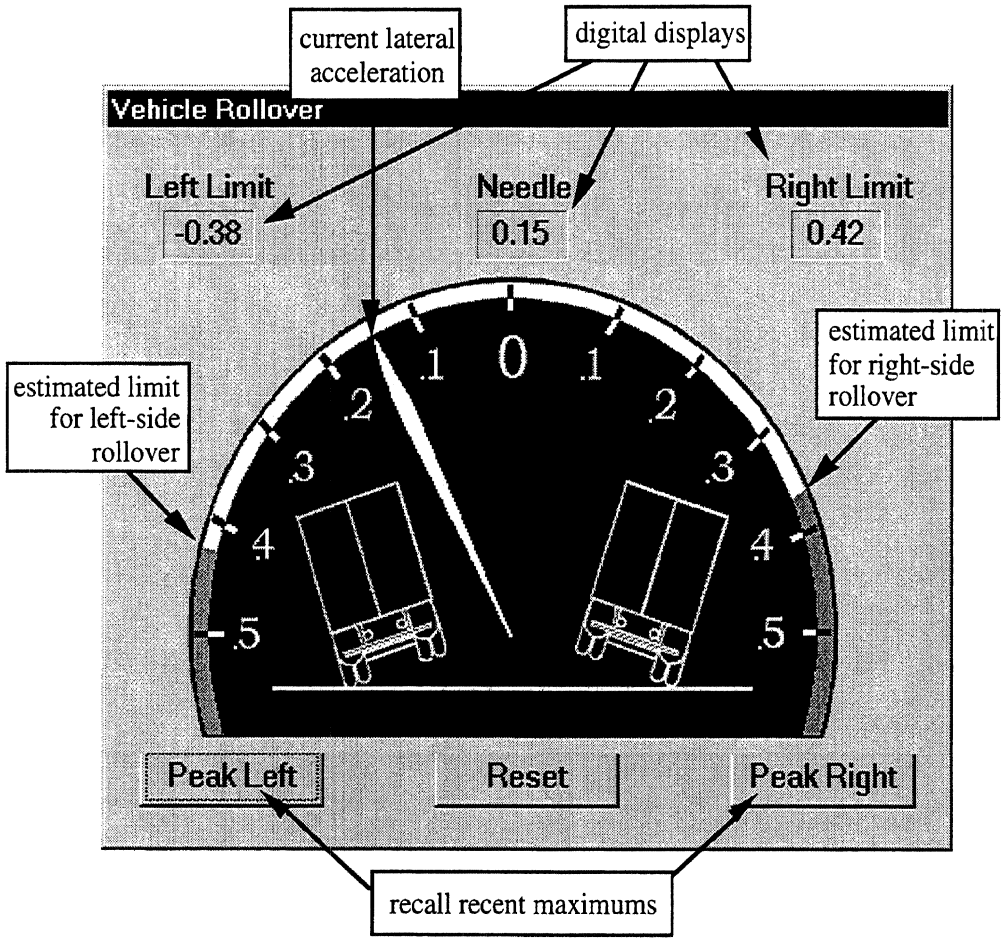

Figure 26. The RSA display used in the cab of the test vehicle

2.8 Broader Consideration of RSA Data Applications

Beyond the issue of in-cab display, there are, of course, other potential uses of the RSA data for reaching the same general goal of minimizing rollover risk. In particular, the RSA system could be configured to store both the stability estimates and the actual lateral-acceleration history—probably in condensed form—for later review and evaluation by a fleet safety supervisor.

Firstly, the operating lateral acceleration data alone is of interest. For example, figure 27 presents a histogram of the lateral acceleration experience of the test vehicle during one of the test runs. The solid line presents the histogram for all travel above 40 mph. The dash line isolates that portion of the travel that took place on secondary roads. It is obvious that lateral acceleration is close to zero for the great majority of travel time. And, of course, the concentration at low accelerations is not so great for travel on secondary roads alone. Interestingly, the peak of either distribution does not fall right at zero, but rather at about -0.005 g. This probably corresponds to the influence of the average cross slope of the road (dominated by travel in the right-hand lane on all roads). The "ripple" in the distribution, which is apparent at small, positive lateral accelerations for travel on all roads, but which is

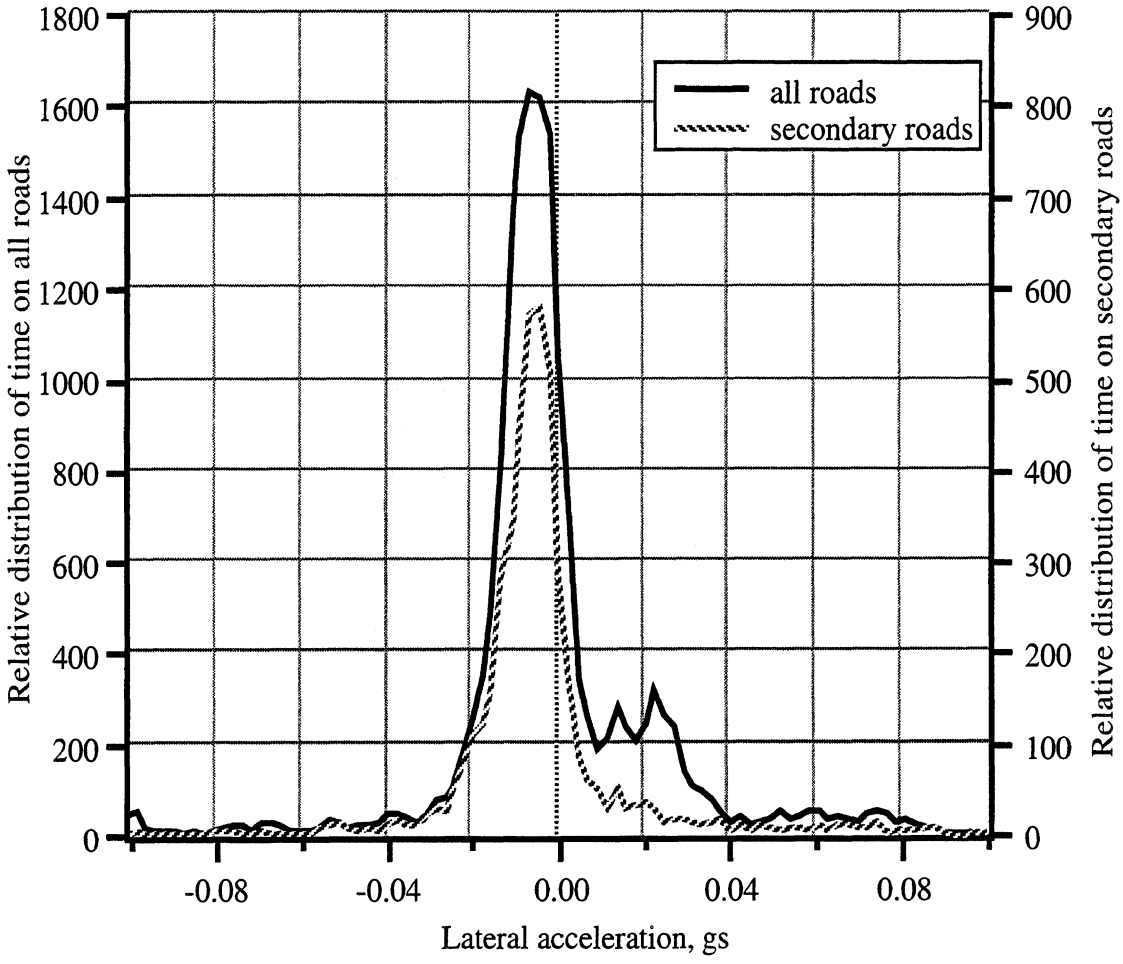

Figure 27. A lateral acceleration time history for a test run of one hour

not present on only secondary roads, may be associated with the cross slope experienced during travel in the left lane on four-lane highways.

Figure 28 reviews similar lateral-acceleration experience in a different format and with regards to the rollover limit. This figure shows a cumulative histogram constructed for the lateral-acceleration data from another l-hour trip. The data has been treated in two ways. First, only the magnitude of acceleration is considered so that we are analyzing the severity of experience without regard to whether the turn is to the left or to the right. Also, the operating lateral-acceleration data has been normalized by the estimate of the rollover threshold, so that lateral acceleration is now expressed as a fraction of the rollover limit.

Starting from the left-hand edge of the plot, we see that, of course, that the vehicle spent virtually 100 percent of the time at lateral accelerations above zero. Just a bit more than 10 percent of travel time was spent at lateral accelerations exceeding 10 percent of the rollover threshold. And only about two percent of travel time was spent above 20 percent of the rollover threshold. Below this level, this presentation becomes difficult to read.

Figure 29 presents the same data of figure 28, but on a log-linear graph. This allows much closer examination of the low-value range of the data. We can now see that 0.1 percent of time was spent at lateral accelerations exceeding 0.4 of the rollover threshold.

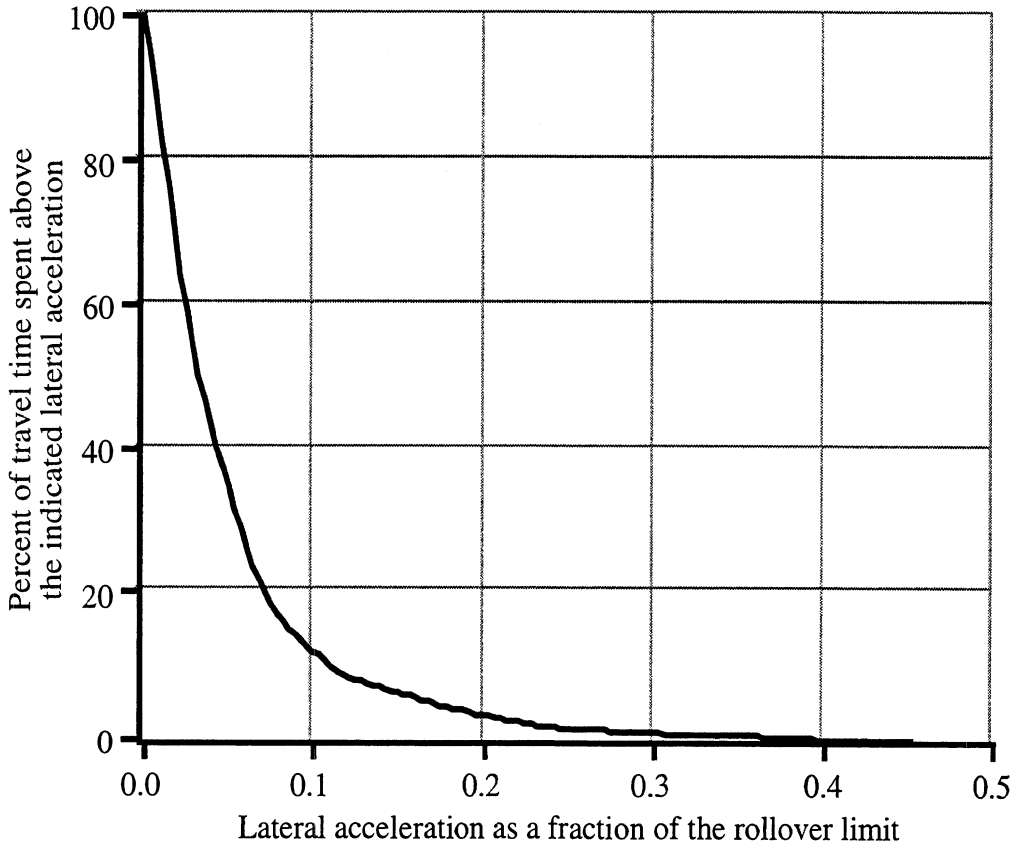

Figure 28. Cumulative histogram of normalized lateral acceleration

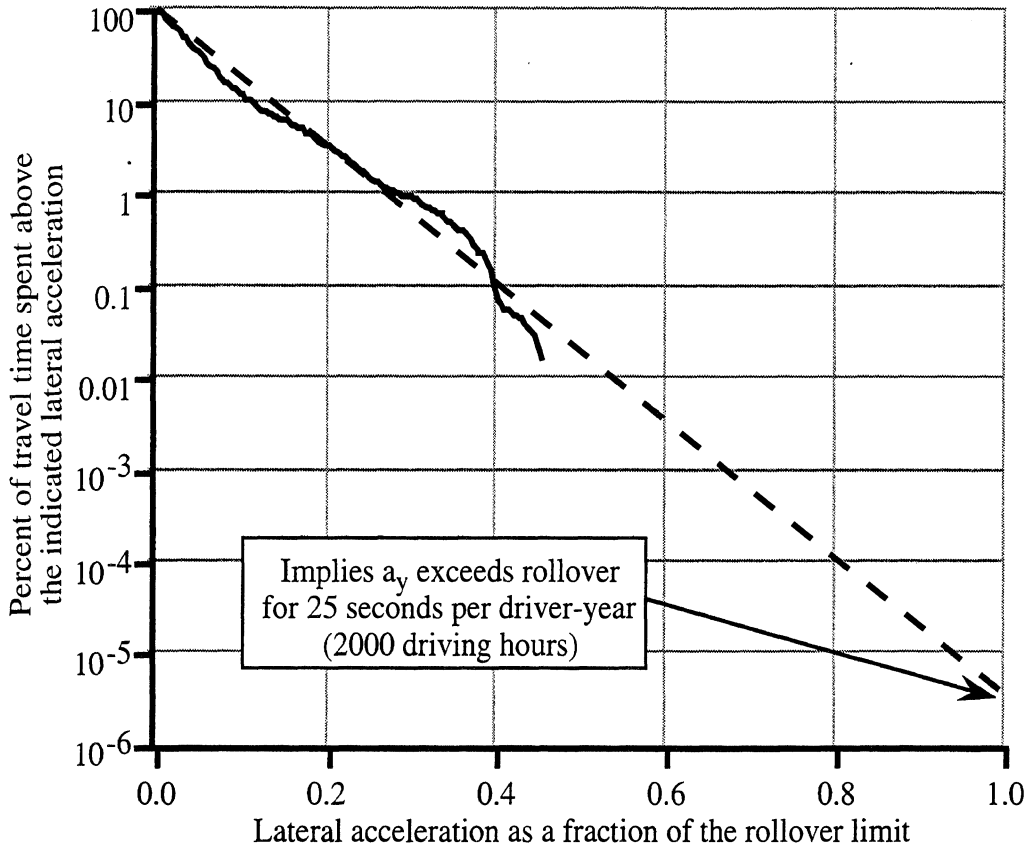

Figure 29. Cumulative histogram of normalized lateral acceleration in log-linear form

Figure 29 also reveals that the data plot is nearly linear in this log-linear format, thus suggesting the possibility of extrapolation. If the apparent linear quality of the data were to hold, the extrapolation would suggest that, under similar conditions, the lateral acceleration of this vehicle might exceed the rollover threshold for a total of about 25 seconds in 2,000 hours. Note, however, that this data display contains no information on frequency content of the data. Thus, this 25 seconds might be composed of anything from many, many very brief excursions above the limit (i.e., little more than road noise in the data) to a single sustained event (or attempt at an event) which would result in rollover.

Regardless of the specific implications of the projection suggested in figure 29, such a data presentation would certainly be useful to management when taken in the context of similar data for an entire fleet. That is, the cumulative histogram of many runs of many drivers on many routes with many loads would provide a performance reference for a given trucking company. Managers could then compare similar histograms for a specific driver, a specific route, a specific class of cargo, or for any other operating condition of interest, in order to evaluate the relative risk of rollover associated for such factors and to counsel drivers accordingly.

3.0 REARWARD AMPLIFICATION SUPPRESSION SYSTEM

In addition to the RSA system, the project has developed an automatic intervention system for rearward amplification suppression (RAMS) in multitrailer combinations. The RAMS concept involves measurement of steering input and forward speed at the tractor, followed by computations that determine whether a significant rearward amplification event is pending. The control algorithm then establishes a sequence of carefully phased brake applications at selected trailer wheels so as to induce yaw moments that oppose the rearward-amplifying motions of trailers and dollies. The concept requires electronically controlled brake systems (EBS) at trailer-axle positions and requires placement of and communications with yaw-rate sensors in individual trailer and dolly units. If successful, the system would obviate the need for innovative dollies or other countermeasures for taming the rearward amplification behavior of, for example, triples combinations.

3.1 RATIONALE FOR SUPPRESSING REARWARD AMPLIFICATION

While it is known that rearward amplification is a very real response problem occurring with commonly employed doubles and triples equipment, NHTSA's crash data show that the total scope of the safety issue does not compare with that of rollover, per se. Nevertheless, the rearward-amplification problem is serious and it is seen as one of the major deficiencies preventing the nationwide allowance of triple-trailer combinations.

As a technical backdrop to the RAMS application, it has been known for fifteen years that rearward amplification does not simply derive from low levels of yaw damping, as is the case with many other modal oscillations of trailers (for example, in the case of rhythmic yaw motions of recreational trailers having negligible tongue load). Rather, the motion of concern constitutes a forced vibration of the last trailer that is stimulated peculiarly by steering inputs that lie in the frequency zone near 0.5 Hz.[e.g., 4] This technical detail is highly fortuitous because 0.5Hz steer inputs, of any significant amplitude, are exceedingly rare. Thus the prospect of "false alarms," in terms of unneeded and perhaps disruptive brake applications from a RAMS controller, is made inherently improbable by the rare-but-pronounced nature of the critical input conditions. The RAMS system can look for those conditions, and only those, with little concern that the condition can be mistaken for some other nonthreatening type of steering input.

Further, it is highly significant that the RAMS function might enable widespread triples usage—by a scheme that may involve a modest cost increment beyond that of an all-axle antilock system. Such aspirations are in concert with industrial progress in EBS hardware, and other developments as mentioned below.

EBS products are moving into European-manufactured trucks currently and efforts are well underway to market corresponding products for U.S. vehicles. As with so many

other electronic-control advances involving powertrain or chassis functions, EBS technology powerfully elevates the potential for integrating braking with other vehicular functions in behalf of new, whole-vehicle, performance goals such as stability and tracking enhancements. In the passenger car market, for example, both foreign and domestic manufacturers offer automatic yaw control systems in certain luxury models based upon inertial motion sensing and EBS braking. And, of course, a number of vehicles across the passenger vehicle and truck spectrum have already implemented automatic traction control. In the heavy vehicle application involving multiply articulated trailer combinations, the addition of a RAMS functionality may help in tilting the balance of value versus cost in favor of upgrading to EBS equipment.

The possibility of taming rearward amplification without replacing the conventional dolly is also expected to provoke a substantial interest from the large commercial operators of doubles and triples. Especially in the case of the major LTL carriers who wish dearly to operate triples nationwide, the chance to "do it all" for the ballpark price of an EBS system may be attractive, indeed. Thus one can imagine an outcome in which a convincing demonstration of the RAMS concept would underpin a legislative initiative to allow triples on, say, the designated highway system if they were required to implement the RAMS package—perhaps pending confirmation of the commercial readiness of the concept by means of a field operational test.

3.2 Development of a RAMS Controller

This section describes the system-design process employed in developing the initial design of this RAMS system. The next section (3.3) presents results used to provide an initial evaluation of the design. The ideas involved in the creation of the design (section 3.2) and the evaluation of the design (section 3.3) are unified by considering five levels of abstraction ranging from a statement of functional purpose (at the level of objectives) to a description of the physical form of the design (its appearance, the location of the parts, etc.). These levels of abstraction and their relationships with regard to creating a design and then evaluating it are presented in figure 30.

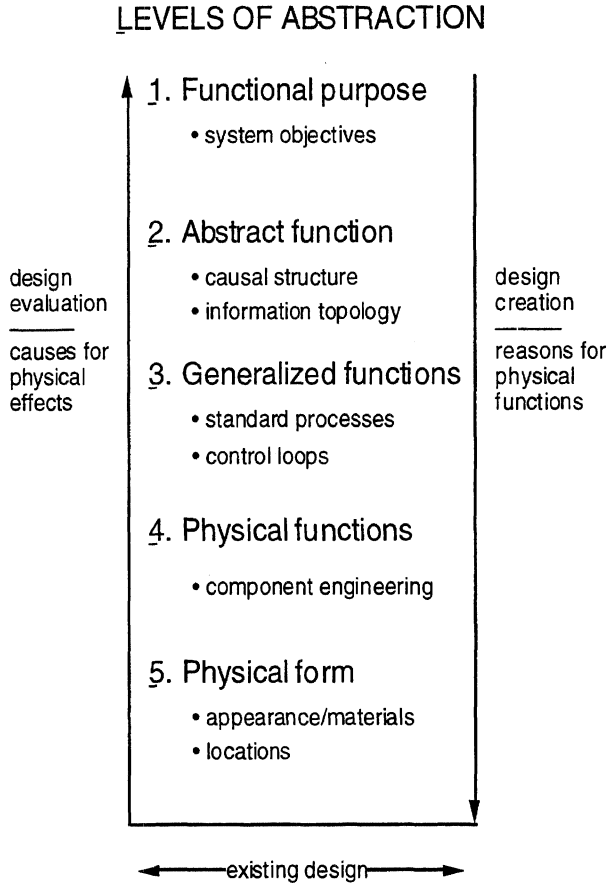

Figure 30. Creating and evaluating the design of the RAMS system

The right side of figure 30 pertains to the design process. The design process involves decisions that are based primarily on reasons for physical functions. According to this portrayal of the design process, one goes from an abstract idea of what the system is to do to a real physical system that is expected to perform the desired function. Although there could be many different systems that will perform the desired function with some degree of fidelity and satisfaction, the selected design consists of only one particular system out of the multitude of possible systems.

In order to explain the RAMS system that has been developed in this project, the following subsections discuss matters associated with each of the five levels of abstraction listed in figure 30. In general, the design process has proceeded from objectives on the top to a system on the bottom as illustrated by the top/down arrow at the right side of figure 30. However, in actual practice the time sequence of design events tends to jump back and forth from one level of abstraction to another as the physical form of the design becomes clearer. The initial form of the design is arrived at when enough "reasons" (choices, constraints, etc.) have been specified to allow the assembly of one specific system.

3.2.1 Functional purpose

The purpose of the RAMS design is to create a system that will reduce rearward amplification of multiply articulated heavy trucks, thereby reducing the tendency for these vehicles to roll over and/or sweep out a large path in a severe obstacle-avoidance maneuver.

Figure 31 illustrates the concept of rearward amplification.

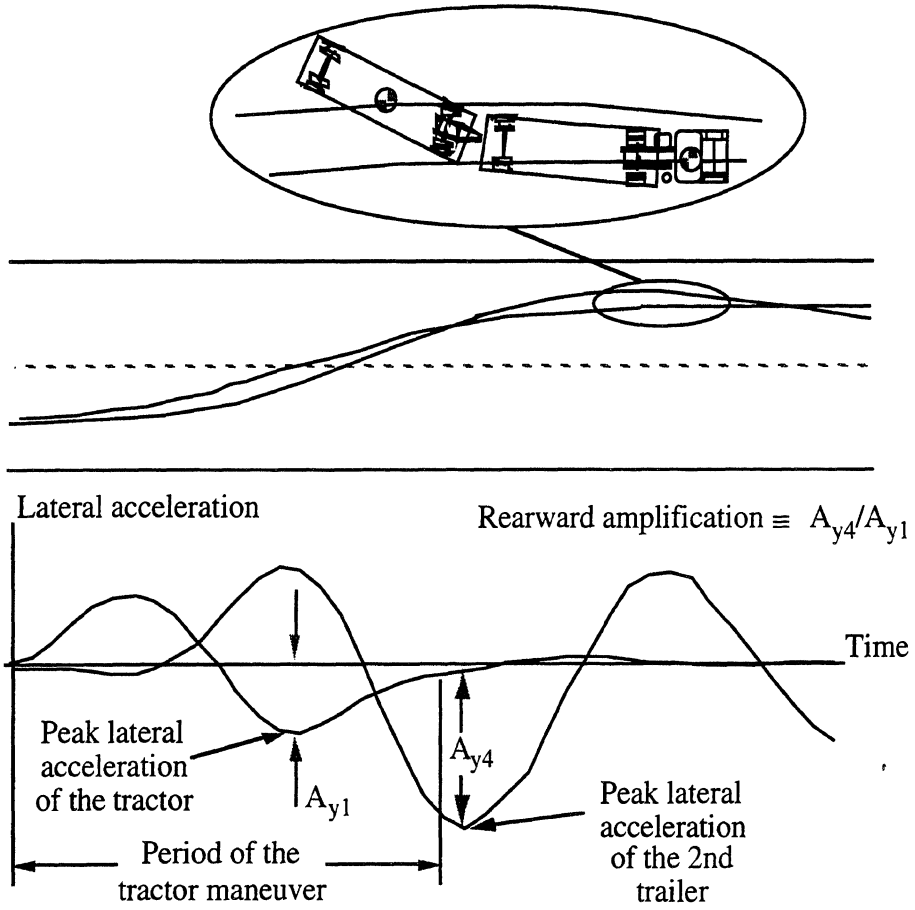

Figure 31. Rearward amplification is the ratio of the maximum lateral acceleration of the last trailer to the maximum lateral acceleration of the tractor.

Currently the design goal may be stated in terms of bounds on distinct levels of lateral acceleration occurring in prescribed maneuvers. Specifically, the current objective is as follows:

With the driver steering to follow a path defined by an 8 ft lateral translation over a down-range distance of 200 ft, kinematically corresponding to a peak lateral acceleration of 0.25 g at 55 mph (80 ft/sec), the lateral acceleration at the center of the floor of the rear trailer should not exceed 0.3 g.

A statement of this type has been found to be reasonable given experience with testing a prototype system. In a sense, the process of describing and developing the system is circular in that new ideas and findings feed back to put more specificity into the design concept.

3.2.2 Abstract function

The RAMS system may be envisioned as an assembly of sensors, control system components, and brake actuators that modify vehicle behavior in a manner that reduces rearward amplification. Figure 32 provides a very simplified overview of the causal structure and information flow for this system. At this level of abstraction there could be many systems that could be represented by figure 32. The figure itself illustrates how abstraction can be viewed as a means of simplification. Nevertheless, even though the figure is very simple, it conveys a great amount of information concerning the basic form of the system being created.

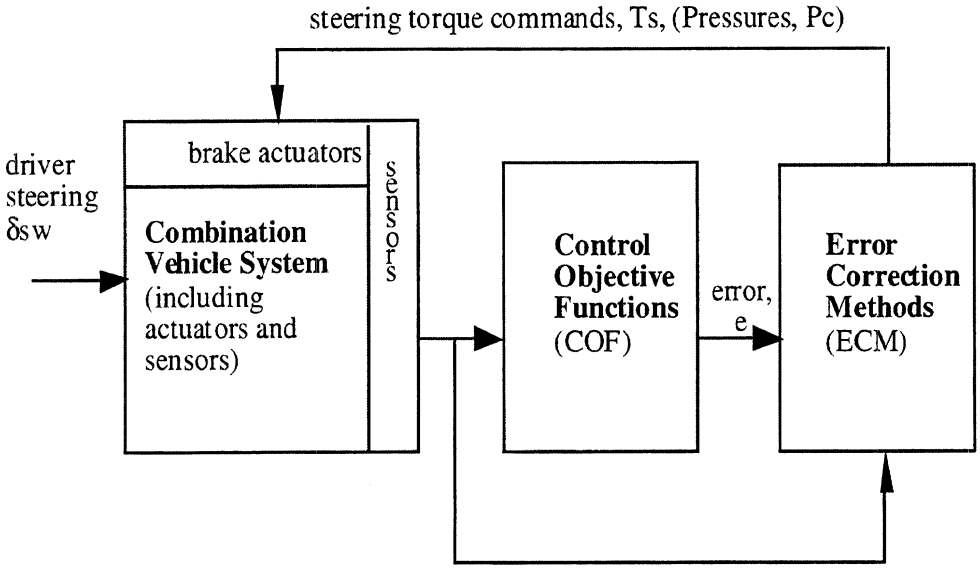

Figure 32. Overview of RAMS structure

The system consists of a battery of sensors whose outputs provide the information needed to compute corrective commands to brake actuators that produce braking forces tending to steer (rotate) the units of the combination vehicle in a manner that reduces rearward amplification. The control-objective functions (included in figure 32) represent the rules used by the RAMS system to achieve its functional purpose. The formulations of these control-objective functions are the primary inventive steps in the process of designing the RAMS. Their formulation represents a jump in insight that unifies physical form with functional meaning. They are at the heart of this invention of a RAMS system. The functional quality of the RAMS depends upon the quality of the control-objective functions employed in the system.

3.2.3 Generalized functions

The actual RAMS system uses a number of standard subfunctions to achieve its purpose. There is a wide variety of devices that could be suitable for performing these subfunctions. In this project the choices of equipment are influenced by the availability of standard equipment from the partners in the program. For example, the brake actuation process employs electronic brake system (EBS) components developed by Haldex Brake Systems. Although not immediately apparent to the vehicle dynamist, the development of a working system depends upon the process of communicating information to its point of application. The tractor supplied by Freightliner has a communication bus that conforms to SAE Standard J1708/J1587. In addition, standard commercially available sensors have been employed to measure the other vehicle dynamics variables used in the control loops that will be discussed next.

The inventive part of the RAMS design involves the development of suitable control loops. In this project, a vehicle simulation was developed and utilized to try out various control schemes. See references 5 and 6. Linear analyses were also used to study the rearward amplification problem further. Furthermore, there exists a substantial literature on rearward amplification. (See references 7 though 11.) Reference 10 in particular provides test and analytical results indicating the proficiency of various mechanical linkage and constraint systems in reducing rearward amplification. All of this knowledge and understanding was used to envision and try a number of control objective functions. After a considerable amount of effort, it was predicted by evaluating simulation results that a RAMS system using EBS control systems on the axle of the first semitrailer, the dolly axle, and the axle of the last semitrailer in a doubles combination could be used to reduce rearward amplification to less than a factor of 1.2 as compared with approximately 2.0 for a typical western-doubles combination without a RAMS.

Of the many control-objective functions that were tried, an arrangement that provided articulation-rate damping to the axles of the first and last semitrailers plus "steering" torque to the dolly axle was selected. These control-objective functions could be evaluated using information from yaw-rate sensors for each unit with a yaw degree of freedom (tractor, first semitrailer, dolly, and last semitrailer) plus measurement of the driver's steering input and the forward velocity of the vehicle. Attempts to apply control-objective functions using measurements of lateral acceleration directly did not succeed. While this outcome does not prove that such an arrangement cannot work, it does indicate that the selected application of lateral-acceleration measurements does not yield a workable system.

Two ideas providing the basis for the jumps of insight leading to the control loops employed in the RAMS are:

- Rearward amplification is a crack-the-whip phenomenon that can be reduced by damping the articulation motion occurring at the hitching joints at the front of each semitrailer.
- The motion of the full trailer can be controlled so as to mimic that of the tractor by applying steering torque to the dolly axle.

There does not seem to be any method short of simulation and testing to show that a RAMS system based upon these ideas will work well. We do not know of any way to guarantee success prior to experimenting with the real thing or experimenting with models (simulation). Since simulation and initial testing indicate that this RAMS will work satisfactorily, we will describe the control loops for manifesting this concept of the RAMS system.

There is a separate control loop for each of the axle sets on the trailing units of the combination. In figure 33 these axle sets are identified by the numbers 3, 4, and 5. (Although the tractor used in the demonstration had a tandem rear-axle set, this distinction is not important here because those axles were not engaged as part of the RAMS control function.) The nomenclature used in this report is based on the numbering system shown in figure 33. Thus, the yaw-rate of the tractor is designated as r1, for example and yaw-rates for the first semi, the dolly, and the second semi are designated as r2, r3, and r4 respectively. Of particular importance to the discussion of the control systems, Γ_C represents the articulation angle between the dolly and the second semi. Also, the symbol Pb is used to indicate brake pressures, and L and R are used to indicate right or left side wheels. For example, the symbol PbL3 represents the desired brake pressure on the left side of axle set number 3 at the rear of the first semi.

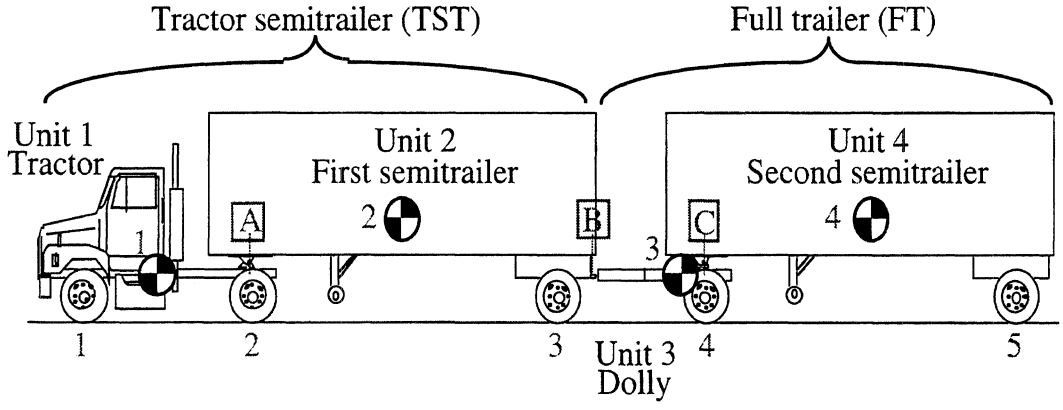

Figure 33. Vehicle sketch identifying mass units, axle sets, and articulation joints

Each control loop has its own control-objective function. However, the control-objective functions for the axles on the semitrailers only differ in the yaw-rates they use in evaluating the rate of change of the pertinent articulation angle. The purpose of these

control loops is to damp the articulation rates of the semis with respect to the unit ahead in the multiply articulated vehicle. This purpose is implemented by the choice of the functional form of the control-objective function. The chosen functional forms are listed in figure 34.

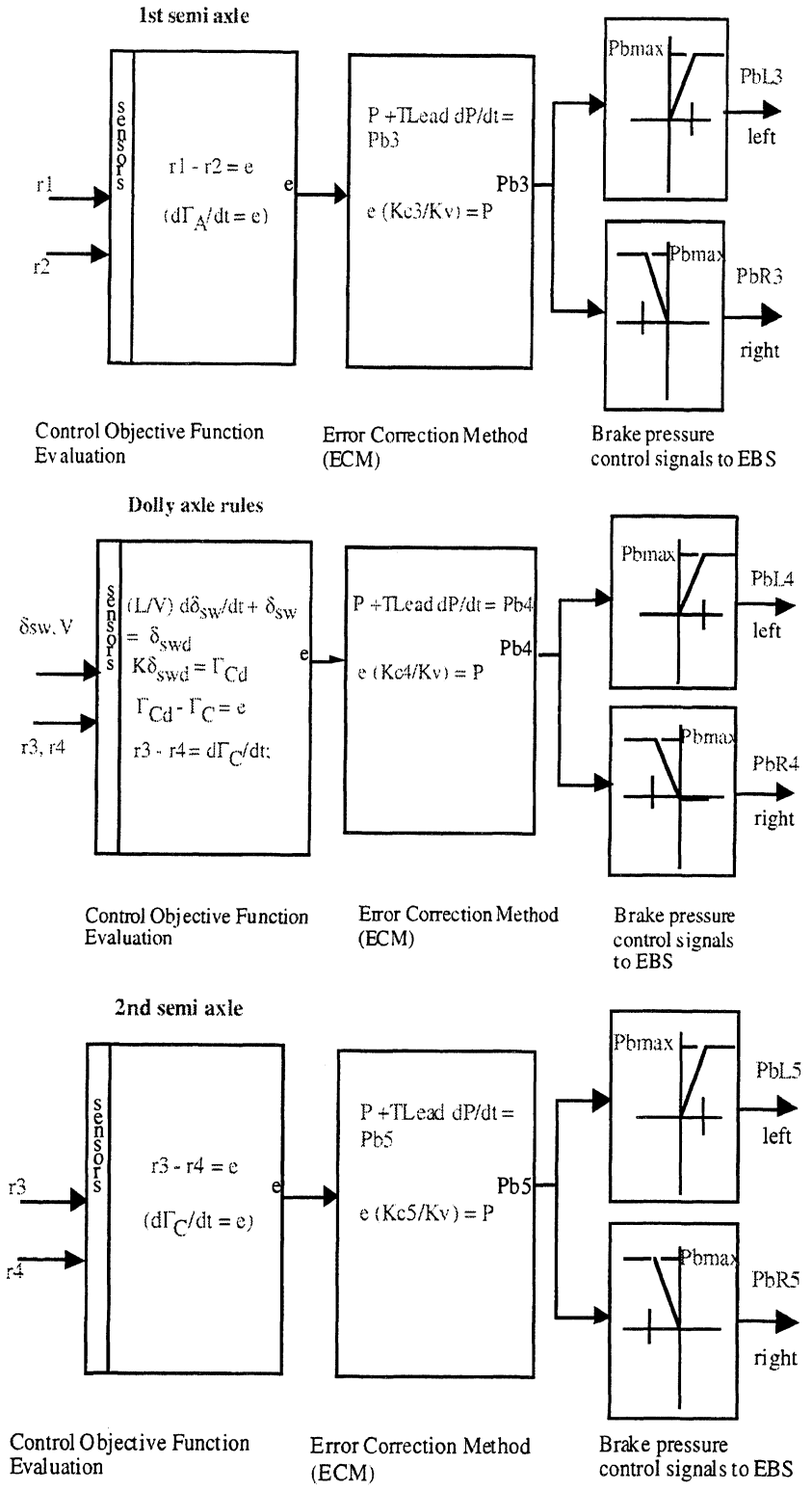

Figure 34. Commanders and equations for the loops controlling braking in the RAMS

The control-objective function for the dolly axle is more complicated in that its purpose is to steer the dolly axle in a manner that will cause the full trailer to follow the path of the tractor. In order to explain this, it is convenient to think of the unit that evaluates the control-objective function as a "commander" because it performs the first step in executing the control plan. The plan involves determining a desired articulation angle between the dolly and the last semi (Γ_{Cd}). The difference between the desired angle and the actual articulation angle (Γ_C) is the difference between what we want and what we have; that is, the error. Because it is believed to be difficult to measure articulation angle satisfactorily and because we already plan to measure the yaw-rates r3 and r4, the articulation angle is computed using a high-pass-filtered integral of the difference in yaw-rates. The desired articulation angle depends upon how the driver steers the tractor as expressed by the steering-wheel angle δ_{SW}. There are two parameters used in the equations for desired articulation angle as given in figure 34. One is the distance, L, from the front axle of the tractor to the dolly axle. The other is K, the ratio of the wheel base of the full trailer to that of the tractor. The purpose of these parameters is to cause the full trailer to maneuver at the place on the road where the tractor maneuvered and to control the amount of lateral motion to be approximately equal to that of the tractor. These parameters directly address the meaning and functional purpose of the RAMS.

Each of the control-evaluation units (constituting part of a central processor) develops a control signal, e, that is used in an error-correction method specially tailored to the RAMS application. See figure 34. In general, each error-correction unit employs a gain factor as needed to perform a proportional control function. Studies were made trying more sophisticated control methods including a modified sliding-surface control methodology but the results showed that the sophisticated control methods produce very little improvement in suppressing rearward amplification at the expense of a great deal of control activity that could be detrimental to the control valves and air-reserve capacities in the braking system.

In addition, each of the error-correction units employs compensation for the gain of the brake and the time needed to pressurize the brake chambers. This compensation provides the means for applying "steering" (yawing torque) of the desired magnitude at the desired time for performing the RAMS function. Since the polarity of the torque depends upon which brake (left or right side of an axle) is actuated, there is need for a logical operation called a "splitter" that splits the pressure commands to provide the proper polarity of steering torque throughout a period of RAMS activity. Furthermore there is a limiter that limits the maximum braking command so that the RAMS system will not tend to lockup the wheels on lightly loaded axles. These features of the error correction method are illustrated by the graphs included in figure 34.

Although there are three separate control loops (one for each axle), they work together and do not tend to fight each other. The arrangement of damping and steering works much

better than using one or the other alone. Fortunately, the simulations show a synergy such that the combination of damping and steering works better than might be expected based upon results for damping or steering, individually.

3.2.4 Physical functions

The components of the RAMS system have been implemented in a truck combination. This means that certain properties of these components are known in detail. One overall system aspect of the engineering properties of the components has to do with communication of information. The informational properties of this RAMS system are summarized by saying that the system operates at an update rate of once every 0.01 seconds (100 samples per second). The signals generally have 8 bits for resolving values over their range of interest. Simulation experiments were used in choosing these levels. The results showed that the system would work, but with some degradation at 50 samples per second. On the other hand, 16-bit resolution did not provide much improvement over 8-bit resolution. This appears to mean that timing is more important than resolution in the context of the levels of timing and resolution studied.

Given that this is a prototype, the actual mechanical, electrical, and environmental toughness of the components is not as important as it would be if this were a finished product. Nevertheless, the components used in the RAMS prototype appear to be strong enough and sufficiently resistant to extraneous influences to survive and perform in the truck environment encountered at a proving grounds.

A good way to summarize the description of the physical functions performed within this RAMS system is to provide a block diagram of the communication system. See figure 35.

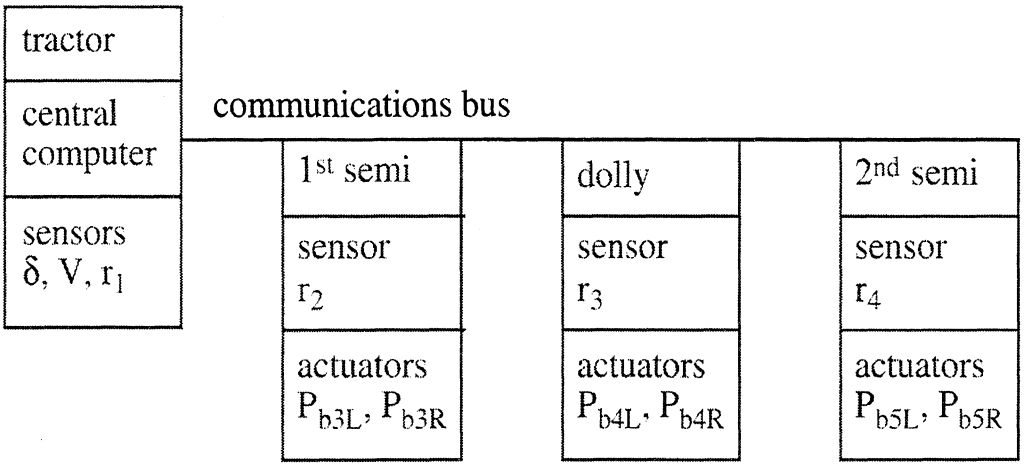

In addition, lateral accelerations A_{y1} and A_{y4} are also measured to evaluate the system.

Figure 35. Communication diagram

The actuators shown in figure 35 involve the EBS system, including compensation for the properties of the brake system as in the manner illustrated in figure 36.

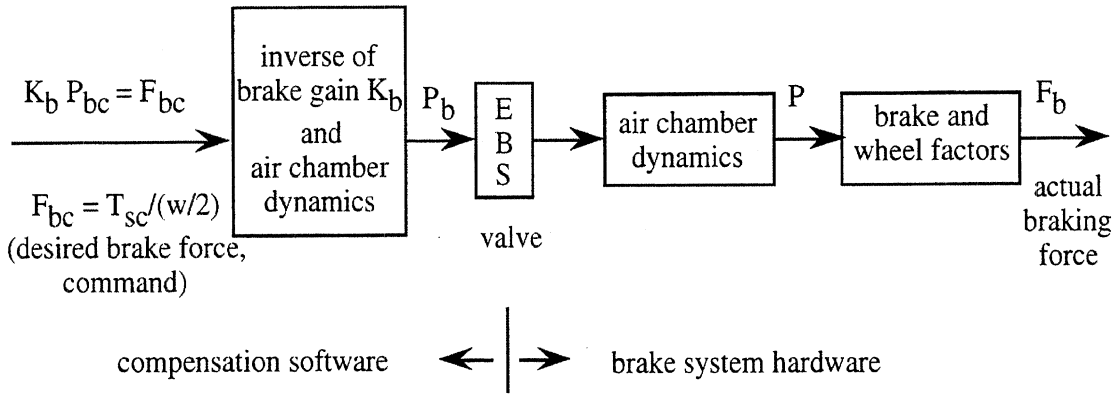

Figure 36. Compensation for brake properties

3.2.5 Physical form

The locations and appearance of the RAMS components as observed in the demonstration were not intended to represent a finished product. The actual dimensions and mounting are issues to be considered in later development if the concept is carried forward to deployable systems. At this time in the development of the system, the important things are to know where to mount the sensors and how to obtain information to use in evaluating the system. To the extent that many of the components are already products or near-production versions of products, their physical properties have been checked for operation in service. In general, many practical and pragmatic aspects of the final form of a deployable RAMS system are beyond the scope of this project.

3.3 Experimental Results from Initial Testing of the RAMS

This section presents a first evaluation of the design of the RAMS system using results from an initial set of vehicle tests. The form of the evaluation refers back to figure 30 on the levels of abstraction. However the emphasis here is on causes for physical effects rather than on reasons for physical functions. In a sense, analysis of the test results is like troubleshooting the system to see how it works and to compare measured performance with what the system is intended to do. At the higher levels of abstraction, the discussion of the comparison between actual function and desired function need not be very complicated since the data show that this RAMS system satisfies its functional purpose. Nevertheless, there are aspects of component engineering and system development that need attention. After introducing the test procedure, there are subsections addressing each of the levels of abstraction but not strictly in the bottom-up sequence implied by the upward arrow shown at the left in figure 30.

The process for examining the performance of the RAMS system involves a modified version of SAE recommended practice J2179 entitled "A Test for Evaluating the Rearward Amplification of Multi-Articulated Vehicles." This test procedure specifies the layout of a test course (path) for the driver to follow. The design of the course is based upon a lateral-acceleration function of time corresponding to one cycle of a sine wave. The path obtained from this type of lateral acceleration is a lateral-displacement maneuver. If the time period of the maneuver is short, the path is representative of an emergency obstacle-avoidance maneuver. A kinematic analysis of this maneuver indicates that the time period of the maneuver T, the amount of lateral displacement Y, and the maximum value of lateral acceleration A (expressed in consistent units) are related by the following equation:

$$Y = A\,T^2/2\pi \tag{25}$$

The J2179 procedure is based upon a lateral acceleration of 0.15 g and a time period of 2.5 seconds when driven at a speed of 55 mph (80 ft/sec). This yields a lateral displacement of 4.8 ft in a course that is 200 ft long. Although there were some tests done at 0.15 g and 4.8 ft, the procedure was modified to do a more aggressive maneuver. The course was widened to 8 ft yielding a lateral acceleration of 0.25 g. This elevated level of lateral acceleration provides a more demanding test for challenging the capabilities of the RAMS system.

The results presented here are for the 8 ft and 0.25 g course. (This corresponds to the maneuver used in the simulation runs since we wanted to challenge the RAMS design in the simulation runs.) Note that drivers may be able to follow the 0.25 g course with minimal errors in position and only employ a maximum of approximately 0.2 g at the tractor. However this is not a problem here because the results are interpreted in terms of the lateral acceleration actually achieved and furthermore the purpose of this initial testing is to evaluate the viability of the design concept regardless of the test procedure.

For these tests the trailers were loaded to provide a doubles combination vehicle that weighed approximately 80,000 pounds. The weights in the last trailer were placed in a special load rack such that the center of mass could be raised and lowered. The test conditions were the same for tests with and without the RAMS in operation. The vehicle could be and was tested with higher-placed loads without the danger of rolling over the last trailer, since outriggers were used on the last trailer.

3.3.1 Functional purpose

The ultimate test of performance is to look at the lateral-acceleration time histories for the tractor and the last semitrailer. Figure 37 shows results from a test run without the RAMS system in action. Since these data are for a test with a low cg position, the outriggers did not touch the ground. Examination of the time history for the tractor shows that the driver did employ approximately 0.2 g in steering the tractor to follow the course

with an 8 ft translation in lateral position. Examination of the time history of lateral acceleration for the last trailer shows clearly that the last trailer did not make the goal of no more than 0.3 g of lateral acceleration. The last trailer has a peak lateral acceleration that is greater than 0.45 g.

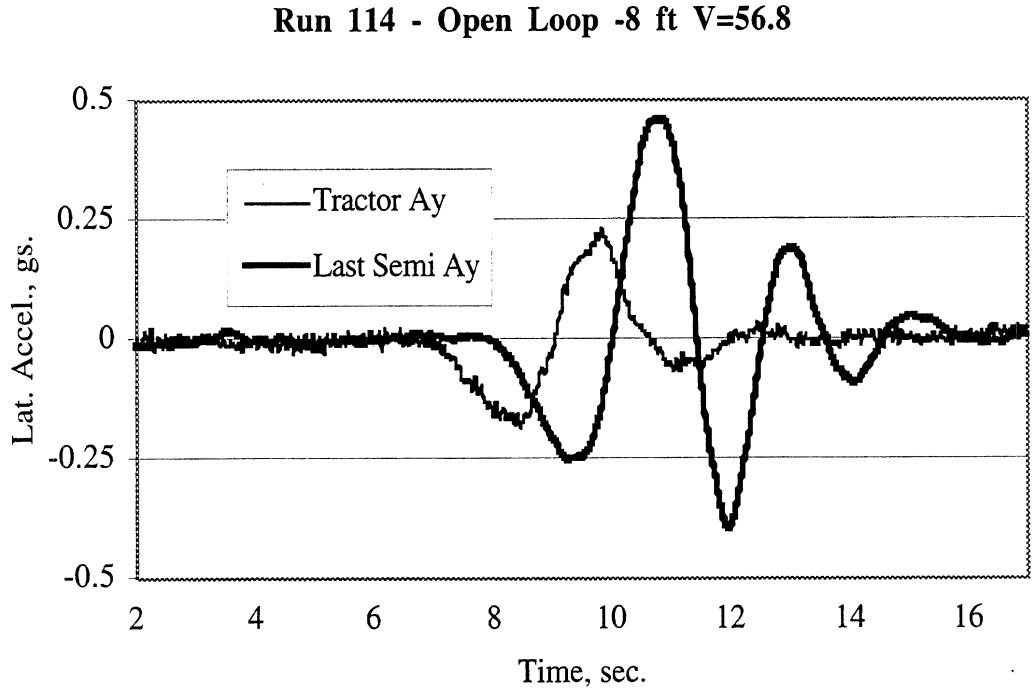

Figure 37. Lateral acceleration without RAMS

If the last trailer were to have been in a "cubed-out-maxed-out" (high cg) condition, it would have rolled over (up onto the outriggers). For typical doubles combinations, one might expect a steady-turn rollover threshold at or above 0.3 g when the vehicle is fully laden with a moderate density cargo. This observation is part of the rationale for using 0.3 g as an objective for assessing the ability of the RAMS system to satisfy its functional purpose.

Figure 38 shows an example of the performance of the vehicle in the 8 ft maneuver with the RAMS system functioning. In this run, the tractor again achieved approximately 0.2 g but the lateral acceleration of the last trailer was reduced to a peak value of 0.3 g due to the RAMS control.

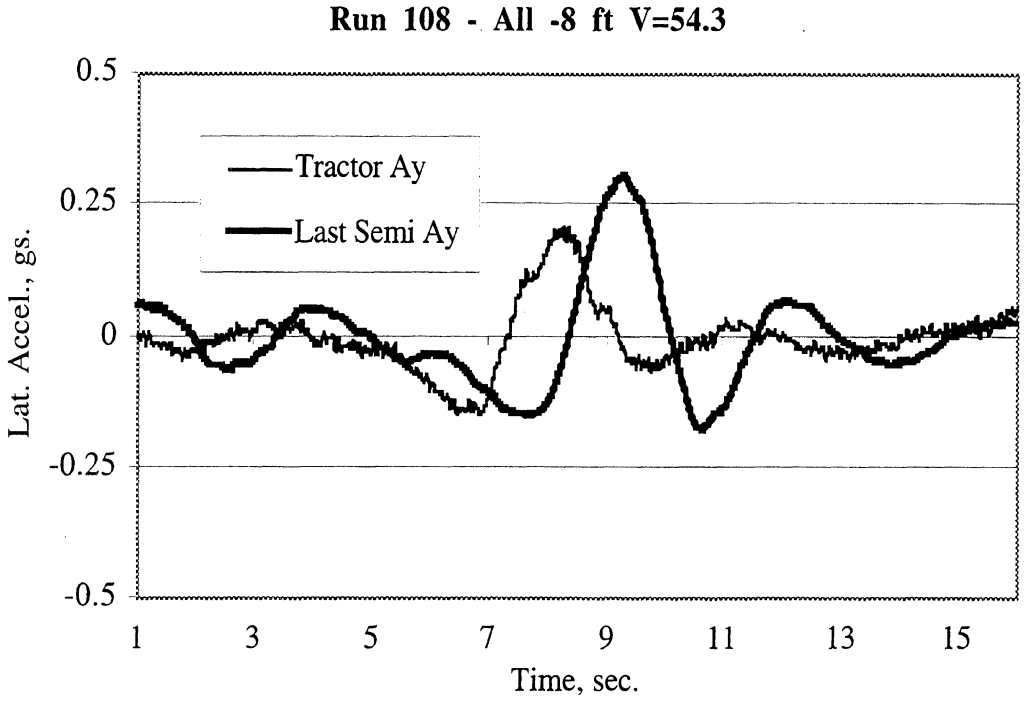

Figure 38. Lateral acceleration with RAMS

In summary, these results alone indicate that this design of the RAMS system appears to be a viable approach for suppressing rearward amplification.

3.3.2 Physical form

In going from functional purpose (section 3.3.1) to physical form (this section), the discussion skips from the most abstract to the least abstract. The reason for putting the evaluation of functional purpose first is to set the tone for viewing further details of the test results knowing that the system works. Once functionality is established, it seems reasonable to address ways to improve the performance of the system.

With regard to physical form there is not much to infer from the test results directly. The fact that the vehicle could be run and tested represents evidence that the location of the parts did not interfere with normal operation of the truck. At the simplest level, the ability to operate the system in a dynamic environment shows at least a minimal level of practicality for the physical form of the system. Based upon our experience exercising the vehicle with the RAMS in action, we have no suggestions for changing the physical layout of the equipment or its appearance.

3.3.3 Physical functions

The ability to operate at 100 samples per second did not come easily. Laboratory testing, troubleshooting, and evaluation were needed to get the sensor and actuator data on and off of the communications bus in a timely manner. However, once these problems

were corrected in the laboratory, intravehicle communications were not a problem during the initial testing exercise.

The electronic braking equipment did show some temperature sensitivity in the beginning of the installation of the equipment on the vehicle. These difficulties were resolved insofar as the system was tested without incident in cold weather (December) and hot summer days (July) at TRC in Ohio.

Clearly, the initial testing did not constitute an endurance test nor did it involve checking out electrical or mechanical specifications for the equipment. Rather the initial testing showed that the components worked as a system and their basic physical functions did not need to be investigated to solve operational problems that would cause the system to malfunction.

3.3.4 Generalized functions

Once the basic functional performance was established, the primary value of the initial testing was the opportunity to observe how the control loops and associated standard process performed in an obstacle-avoidance maneuver.

Even when the RAMS was not engaged, performance of the sensors could be checked and results could be obtained to aid in understanding the differences between driving with and without the RAMS. Figure 39 shows the yaw-rate signals from the transducers mounted on each of the articulating units of the doubles combination. These data are for the same test as the data presented in figure 37 (run 114). A notable feature of these time histories is that the yaw-rates of the dolly and the last semi are much larger than those of the tractor and the first semi. There is also an amplification of rotational motion of the last semi compared to that of the tractor. Also the yawing motion of the last semi takes several seconds to damp out. As indicated in the figure, the amplitude of the first half cycle of oscillation is less than that occurring during the second half cycle. This is typical behavior indicating that the heading correction required to return to the original direction of travel is more severe than that used to initiate the maneuver.

With regard to the components and processes of the RAMS system, these data indicate that the yaw-rate transducers work, their signals are communicated properly to the central processing unit, and the vehicle behaves as expected.

Figure 40 shows the same yaw-rate signals but with the RAMS in operation. (The lateral acceleration signals for this run were presented in figure 38.) One can see by comparing the time histories in figures 39 and 40 that the RAMS suppresses and damps the yaw-rates, particularly for the full trailer consisting of the dolly and the last semi. This is an indication that the control loops are having the intended effect on the yaw motion of the vehicle.

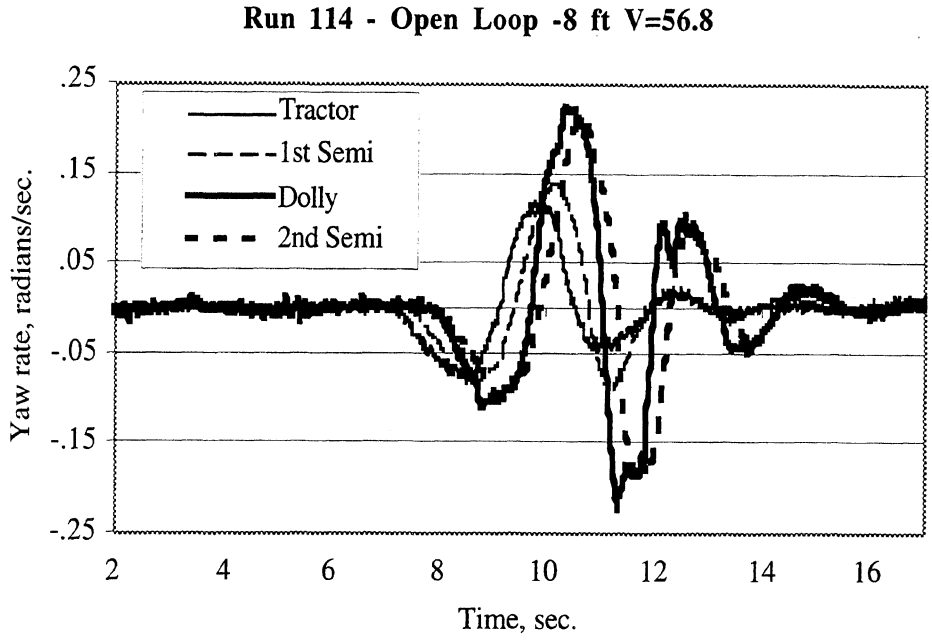

Figure 39. Yaw-rate signals without RAMS

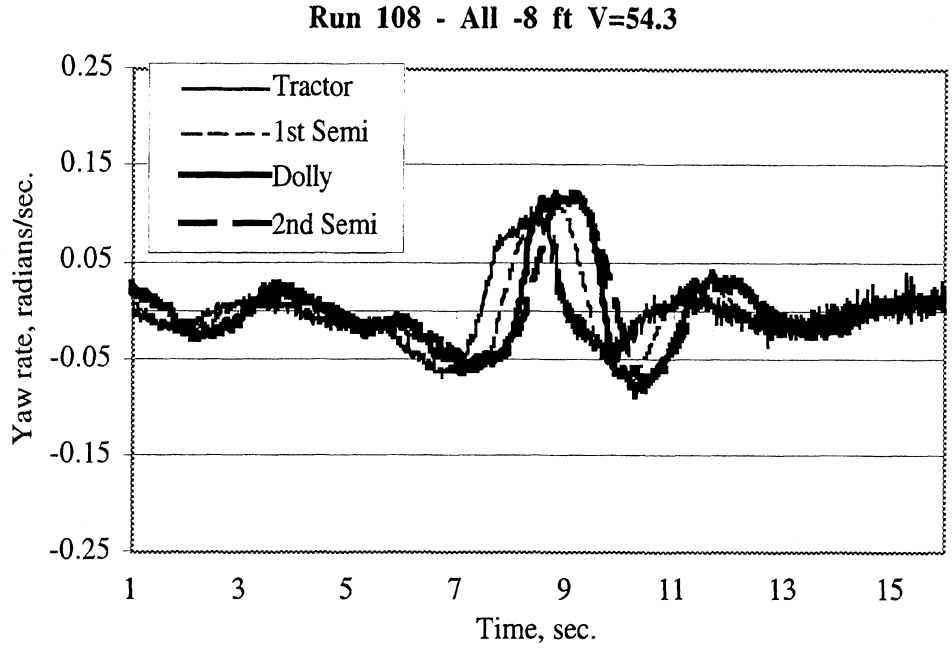

Figure 40. Yaw-rate signals with RAMS

Insight into the operations of the control-objective function for the dolly can be obtained by examining figure 41. These data show the steering of the front wheels of the tractor as well as the delayed (lagged) steering signal and the computed articulation angle. The reason why the signals for the lagged steer angle and the dolly angle start and end where they do is that the RAMS system does not operate all of the time. If it were continuously active, it could overheat and wear the brakes. RAMS operation is triggered by a sudden

steering action in which the change in steering wheel angle exceeds a preset threshold in a preset period of time. Once the RAMS is engaged it stays on for 10 seconds and then disengages.

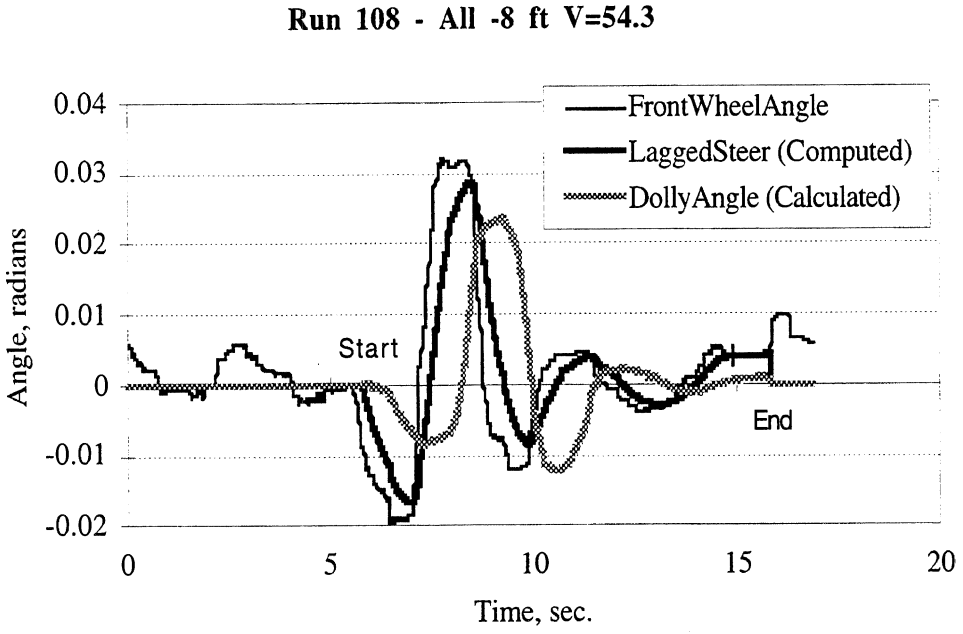

Figure 41. Signals pertaining to the dolly's control objective function

These data look qualitatively reasonable except that there is a difference between the lagged steer and the calculated dolly-articulation angle. Fortunately, the control loop is fairly robust in the sense that it will still work even if the gains and delays are not perfect. Nevertheless we anticipate that adjusting the delay and the gain could result in some improvement in rearward-amplification suppression.

For this run (run 108), the rearward amplification is approximately 1.4 to 1.5. The computer simulations predicted that the RAMS system would be capable of a rearward amplification of 1.2 or less in this maneuver. This leads us to believe that improvement in the steering control for the dolly could help to reduce rearward amplification.

Insight into the performance of the error correction and EBS systems has been gained by examining figures 42 through 44. These figures show the pressure obtained in the left and right brake chambers of the axles on the first semi, the dolly, and the last semi, respectively. The pressures are going on and off at roughly the intended times. They are switching between the right and left brakes as expected. This means that the splitters are functioning properly. In hindsight we see (although it is not obvious) that the value of lead used in compensating for the lag in pressure involved with filling the brake chambers may have been too long.

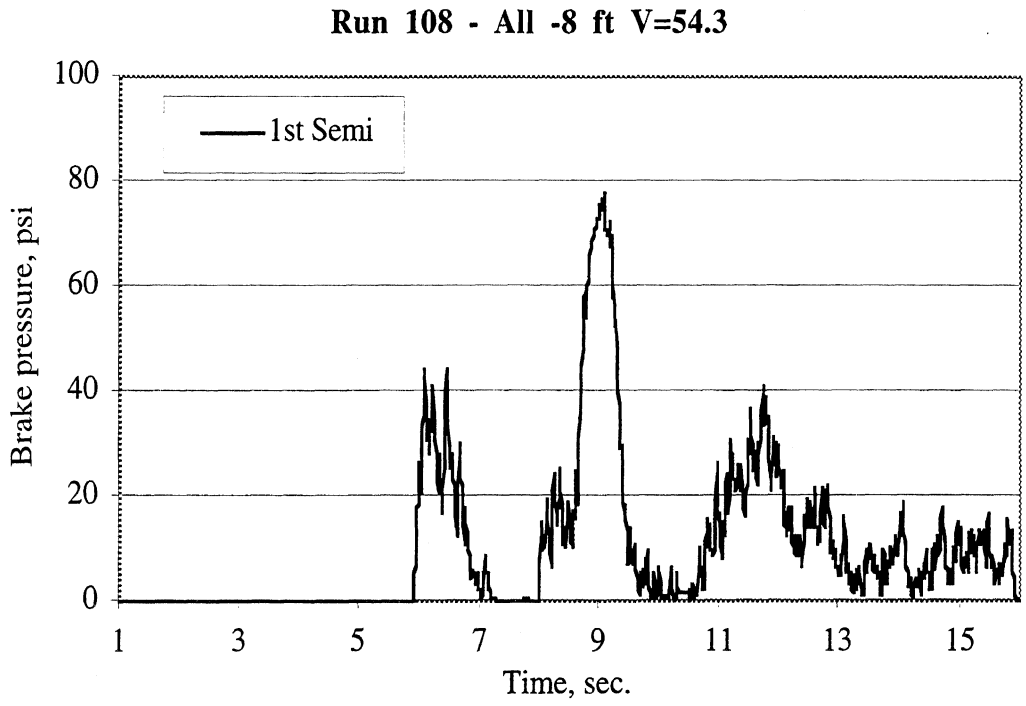

Figure 42a. RAMS–controlled brake pressure at the left wheels of the axle on the first semitrailer

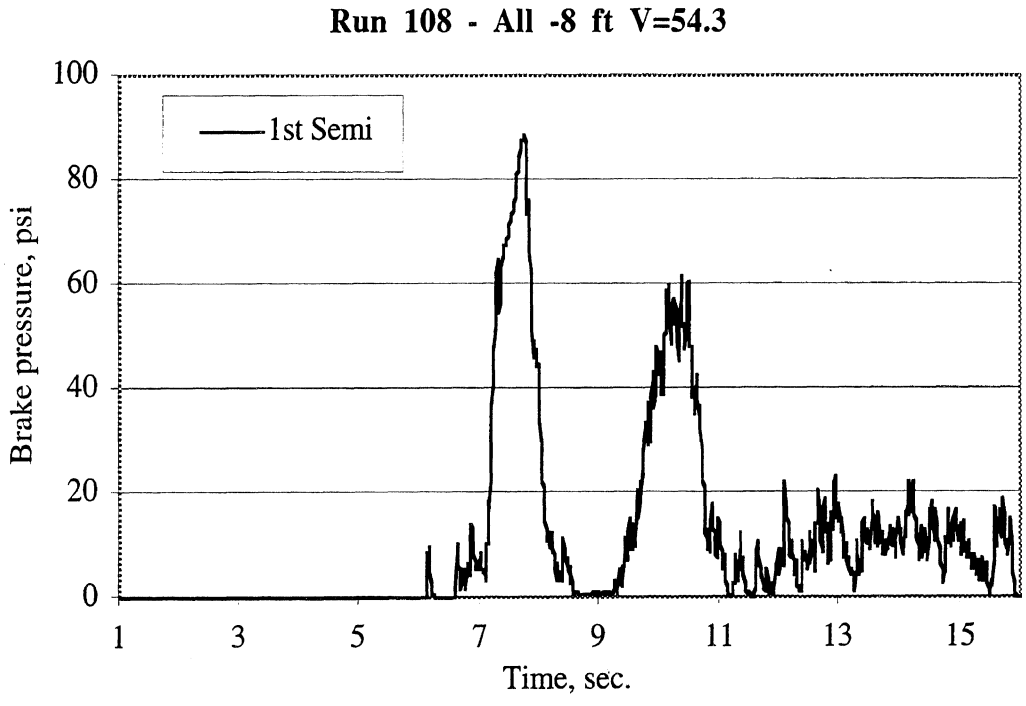

Figure 42b. RAMS–controlled brake pressure at the right wheels of the axle on the first semitrailer

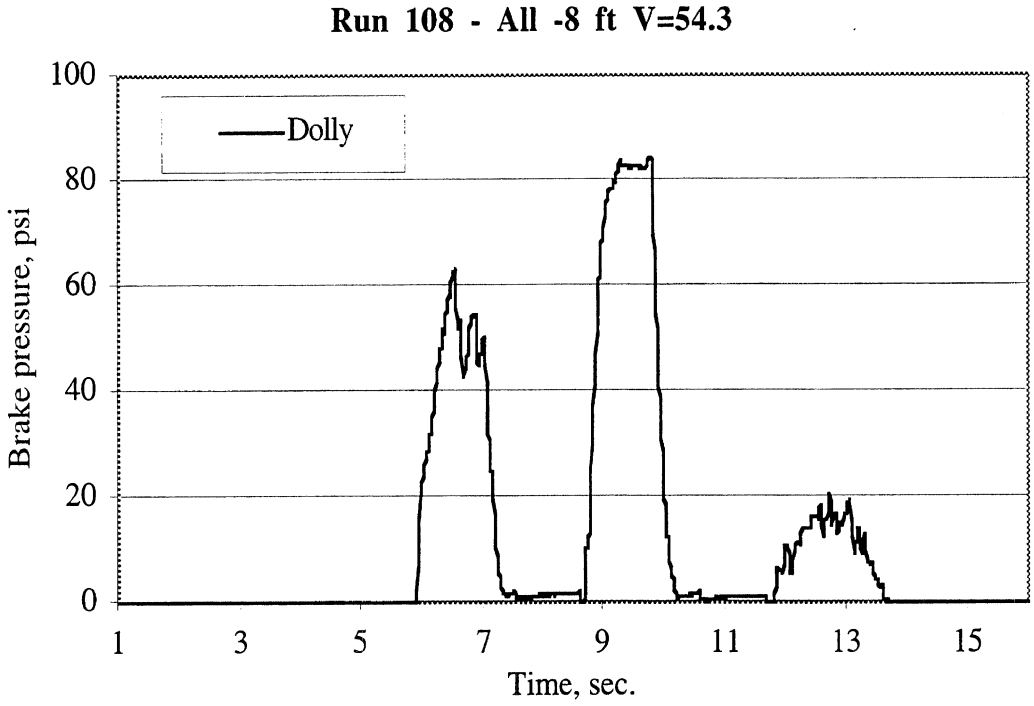

Figure 43a. RAMS–controlled brake pressure at the left wheels of the axle on the dolly

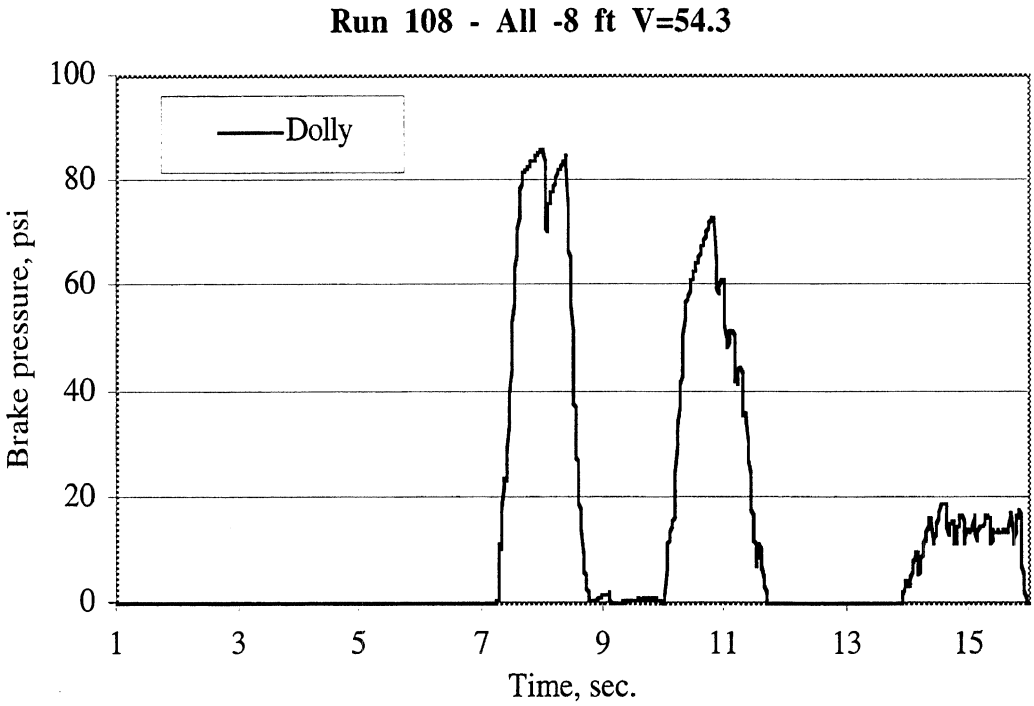

Figure 43b. RAMS–controlled brake pressure at the right wheels of the axle on the dolly

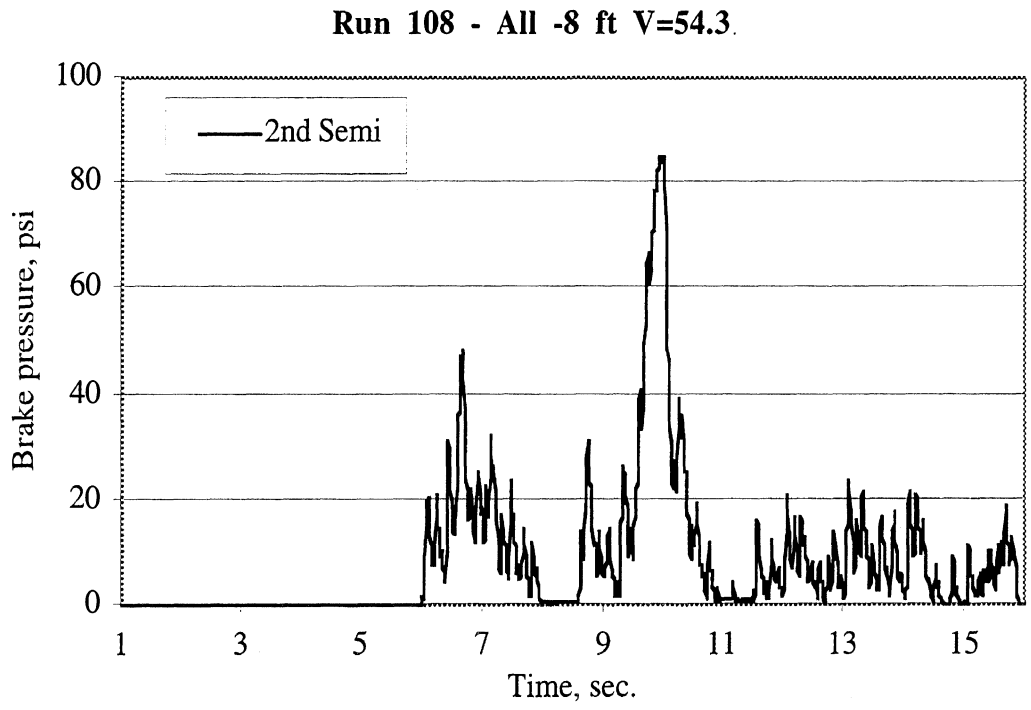

Figure 44a. RAMS–controlled brake pressure at the left wheels of the axle on the last semitrailer

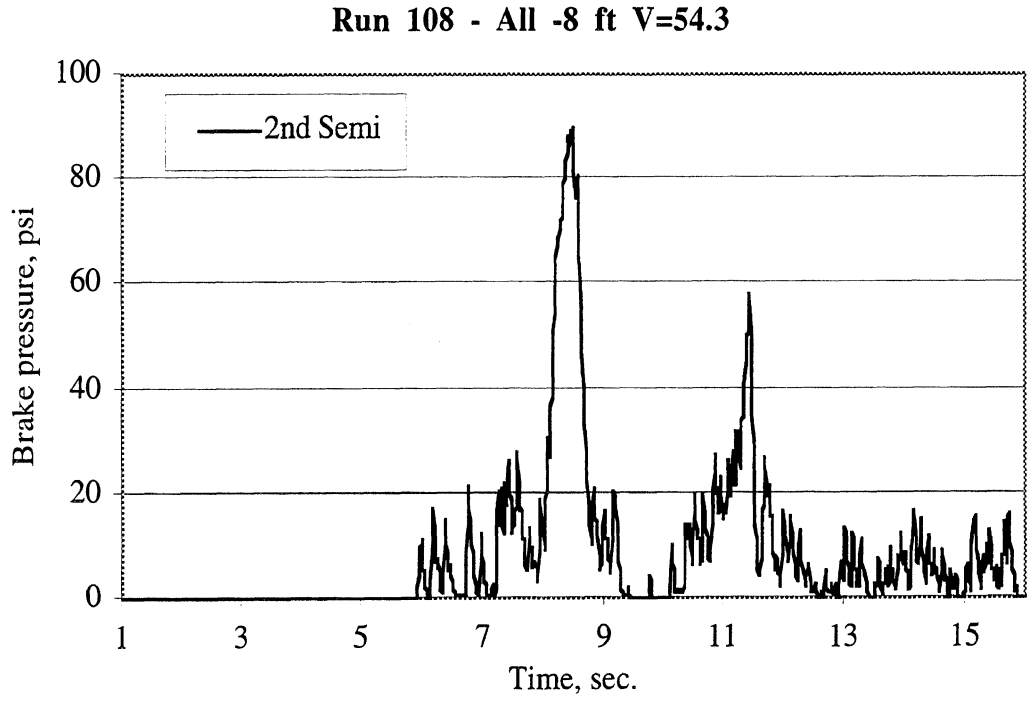

Figure 44b. RAMS–controlled brake pressure at the right wheels of the axle on the last semitrailer

An eye-catching feature of the braking action is the magnitude and steepness of the pulses of braking pressure shown in figures 42 through 44. Magnitudes over 70 psi are surprising because 70 psi was intended to be the limiting value of brake pressure in the tests conducted during December 1997. Computer simulation had shown that pressures up to the limit were to be expected, but obviously pressures over the limit are not to be expected. Troubleshooting this symptom indicated an improper interaction of the limiter circuit and our use of suspension airbag pressure as a direct indicator of axle load. It was subsequently noted that we had neglected to consider that braking torque is reacted in the suspension in a manner that increases the airbag pressure suddenly. The original intention of using the airbag-pressure signal to adjust the brake gain was as an aid in preventing wheel lockup on an axle with a light static load. In the tests and demonstration runs performed in July 1998 the brake pressure was limited to 90 psi without any adjustment for the pressure in the suspension airbags. (Operation on slippery surfaces or at light axle loads would be controlled by the ABS thereby preventing wheel lock.)

The steepness of the braking pulses indicates that the system in effect is nearly a bang-bang system. This means that the timing of the onset and fall of each pulse is more important than the magnitude as long as the magnitude is large enough. Clearly when the pulse is limited to a maximum amplitude, an increase in gain will not change the control action. Because of this, it may be that changing the value of the limit on braking pressure could be as important as a change in gain. However, even a little improvement to a rearward amplification of 1.3 or 1.2 would be important.

Another test run also illustrates important considerations for correcting and improving the system. In particular, the data shown from run 106, shows that the RAMS system did not trigger on the first half cycle of steering activity. In this case the driver did not initiate the maneuver as aggressively as in run 108.

However, examination of figure 46 shows that the RAMS still did very well in suppressing rearward amplification well below 0.3 g in this maneuver. This is further indication of the robustness of the control system, but it also indicates the need to reexamine the triggering criteria to better understand its influence on RAMS performance. It could be that there is something to be gained by a more accommodating arrangement of the triggering system.

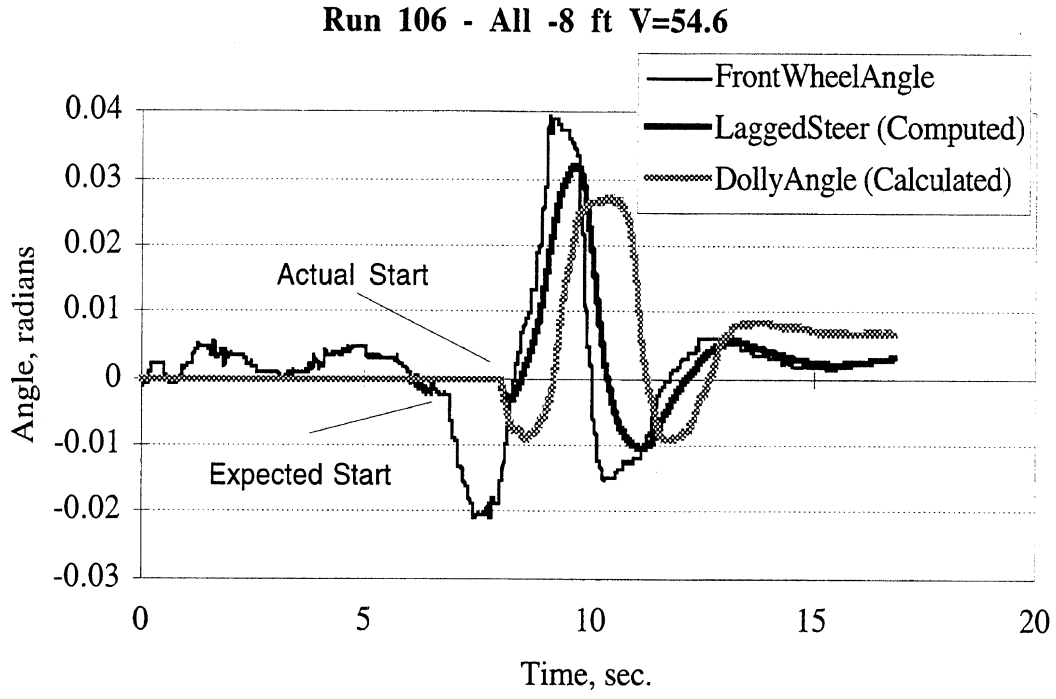

Figure 45. Example of late triggering of RAMS

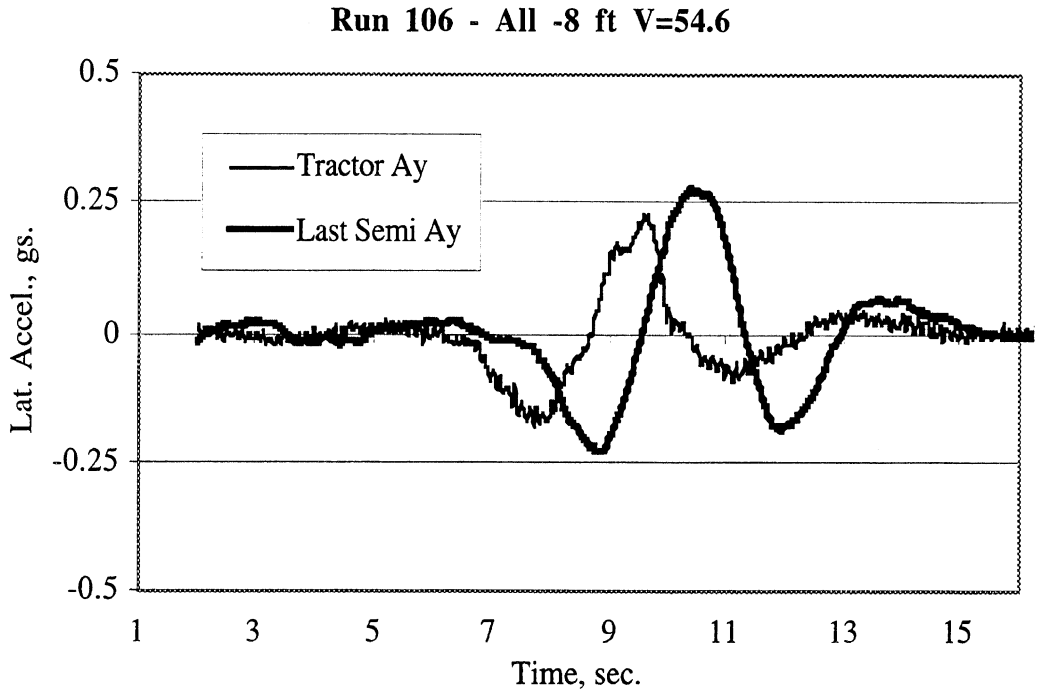

Figure 46. Rearward amplification for the second half cycle of run 106

Given that the RAMS performed acceptably with a low center-of-gravity load in the testing done in December 1997, it was decided to examine performance of the RAMS system as the center of gravity of the load was raised in the last trailer.

A sequence of tests was performed while gradually raising the height of the center of gravity of the payload in the last semitrailer. The RAMS system performed well at each higher load position. However, when operated without the RAMS functionality available, the vehicle rolled more and more as the center of gravity height increased. At the highest level tested with a payload of 28,400 lb (including the outriggers) and a payload center of gravity of 101 inches off the ground, the vehicle without RAMS experienced extraordinarily hard contact of the outriggers. It would have rolled over without RAMS. This high load position was used in the demonstration to exhibit the benefits of the RAMS system in reducing the likelihood of last trailer rollover in obstacle avoidance situations.

A replay of the complete video recording taken at the demonstration provides the best visual impression for comparing roll motion with and without the RAMS system in operation. Figures 47 and 48, show video frames that do portray the maximum roll motions observed in the demonstration. These figures illustrate the differences in roll motion occurring with and without RAMS in operation.

The pictures in figure 47, without RAMS in operation, show the outriggers preventing the last trailer from rolling over. The inside trailer wheels are well off the ground. If it were not for the outriggers, the last trailer would have rolled over in the 8-foot obstacle-avoidance maneuver.

The pictures in figure 48, with RAMS in operation, show that the outriggers did not touch down in these runs. The trailer wheels are still on the ground even though the trailer has rolled substantially.

In the demonstration there were 6 runs without RAMS and 6 runs with RAMS.

In all the runs without RAMS, dramatic roll motions that would have resulted in rollover occurred during the obstacle avoidance maneuver. In all cases the outside outrigger crashed down on the ground in the correction (second) half of the maneuver. (The impact was usually hard enough that the outrigger on the other side hit when the vehicle rebounded in response to the impulse generated by the first hard touchdown. Clearly vehicle motion after an outrigger has hit is artificial. Only the motion up to the point of touchdown is valid.)

When the RAMS was in operation there was only one case in which it appeared that an outrigger may have momentarily touched down. In the other five cases the outriggers did not touch down and cleared the ground by an appreciable margin. The rear wheels on the last trailer did not liftoff in these five cases. These results indicate that this version of the RAMS is able to prevent rollover in an extreme obstacle-avoidance maneuver for a vehicle with an extremely high payload. However, the situation of load and maneuver as tested is close to the limit of performance for this system. Nevertheless this is a major improvement over the performance of the same vehicle operating under the same conditions without RAMS.

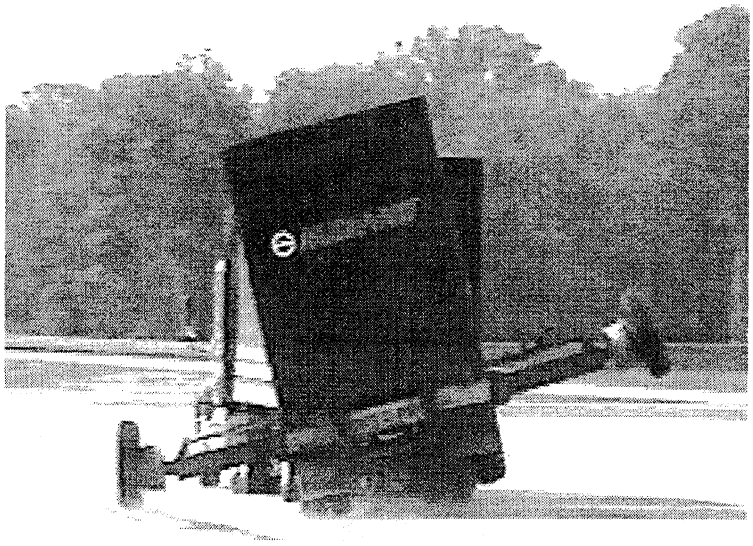

Run 3

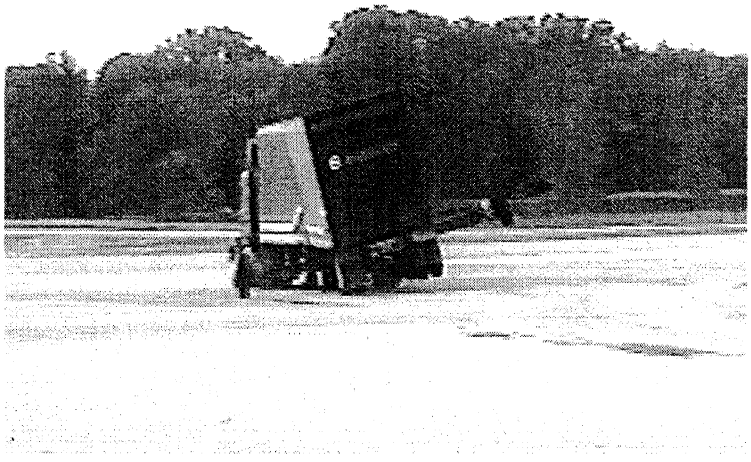

Run 11

Figure 47 Without RAMS, example video frames at maximum roll angle

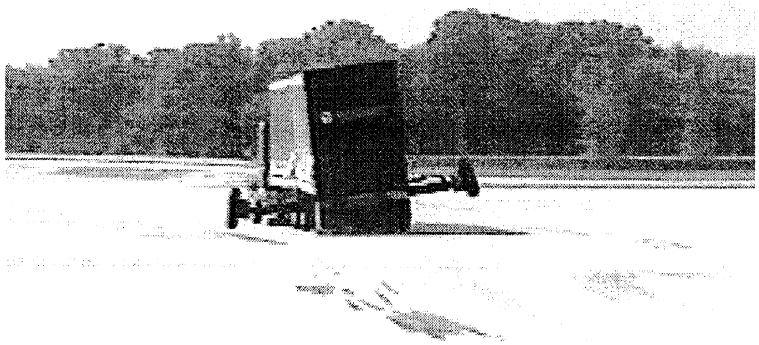

Run 4

Run 12

Figure 48 With RAMS, example video frames at maximum roll angle

The time history results for tests with a high center of gravity are more difficult to interpret than those with a low center of gravity. This is because the results are meaningless after an outrigger has touched down and because this RAMS system was approaching the limit of its effectiveness in a severe maneuver with a high center of gravity load. Nevertheless, data for lateral accelerations and yaw-rates are useful to compare during the first part of the obstacle avoidance maneuver.

As shown in figures 49 and 50, during the initial swerving part of the maneuver, the RAMS system (figure 50a) holds rearward amplification to nearly 1.0 and the yaw-rates (figure 50b) are roughly equal in magnitude. While figures 49a and 49b show that this does not happen for the vehicle without RAMS. The rearward amplification during the first half cycle in figure 49a and 49b without RAMS, before the outrigger has touched down is approximately 1.6, and it would have been over 2.0 in the second half cycle if the outrigger had not prevented the vehicle's dynamics from continuing to roll over. Similar results were obtained later in the demonstration as shown in figures 51 and 52. The results also indicate that the driver does not need to steer as drastically when the RAMS is operating. This is believed to be because the vehicle is slowing down and is easier to control with RAMS in operation. Although there are interesting facets of the driver control that could be investigated further, the basic finding is that, even though the steering feel was different with RAMS in operation, the driver did not experience difficulty in controlling the path of the vehicle.

3.3.5 Abstract Function

After having performed the initial tests it seems appropriate to offer another view of the RAMS structure in contrast to the communications-systems perspective provided by figure 35. This view is provided by figure 53. Figure 53 situates the activation rules as the enabler of the RAMS control and shows the information flow to each of the articulating units of the vehicle. Since the initial design has now been evaluated for the first time, there now exists a better feel for what is important and how to portray the system. In particular, the work has progressed through the hierarchy of abstractions in the context of design considerations and back through that same hierarchy in the context of evaluating the performance of the RAMS system. This process has confirmed that the functional purpose and the abstract function need not be changed in any significant manner. In addition, they have clarified how future iterations of this cycle of design and evaluation can be aimed at improving and optimizing the design of this RAMS system.

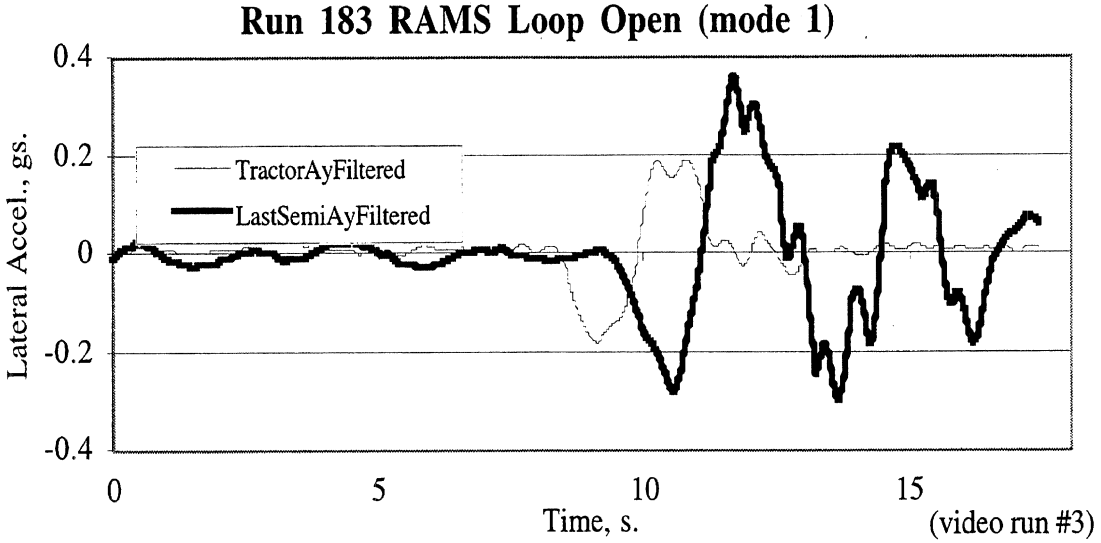

Figure 49a. Without RAMS, lateral acceleration, high cg load

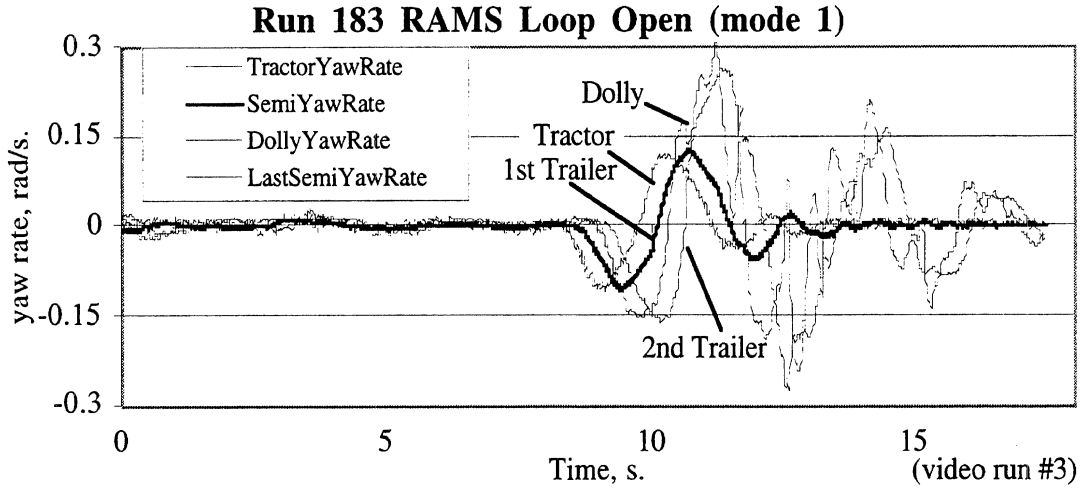

Figure 49b. Without RAMS, yaw-rates, high cg load

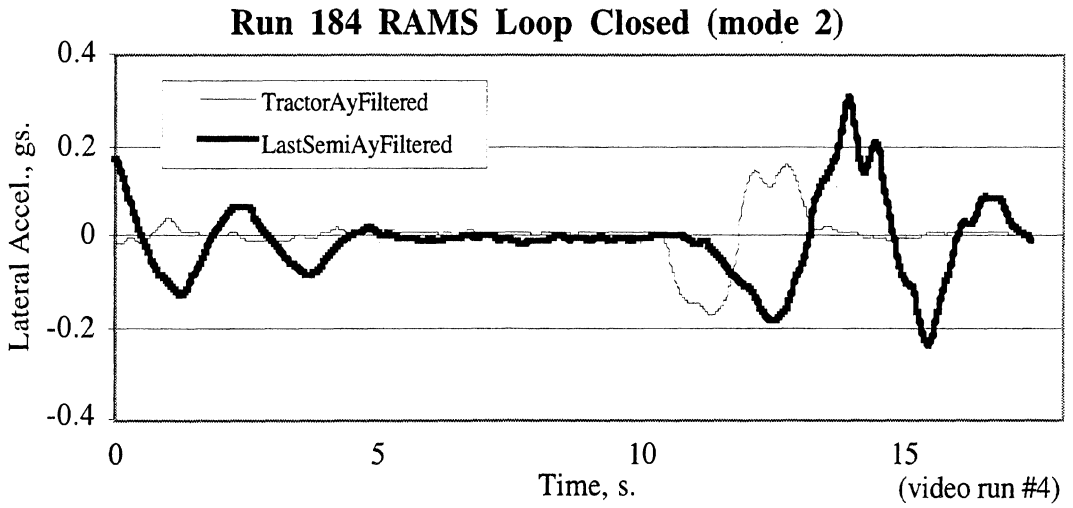

Figure 50a. With RAMS, lateral acceleration, high cg load

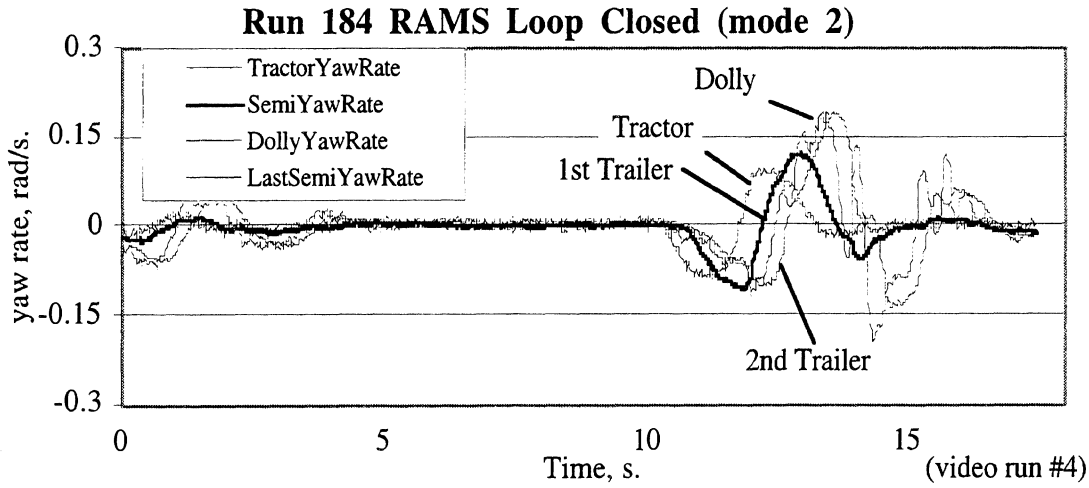

Figure 50b. With RAMS, yaw-rates, high cg load

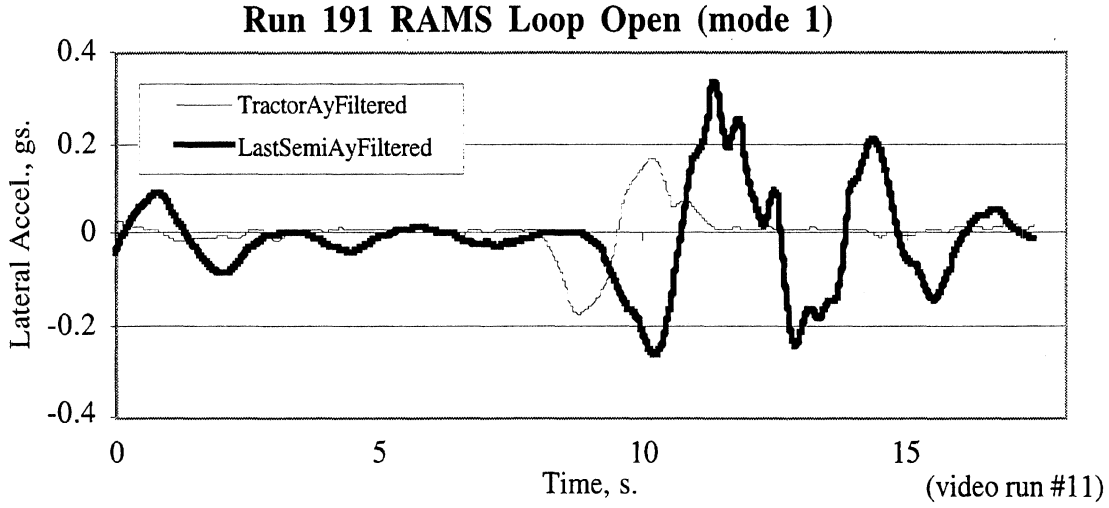

Figure 51a. Without RAMS, lateral acceleration, high cg load

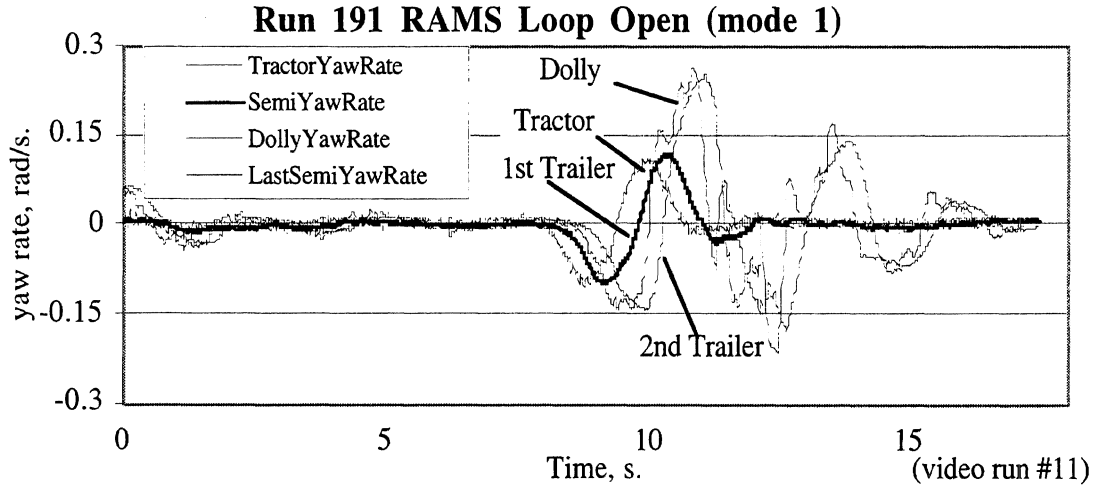

Figure 51b. Without RAMS, yaw-rates, high cg load

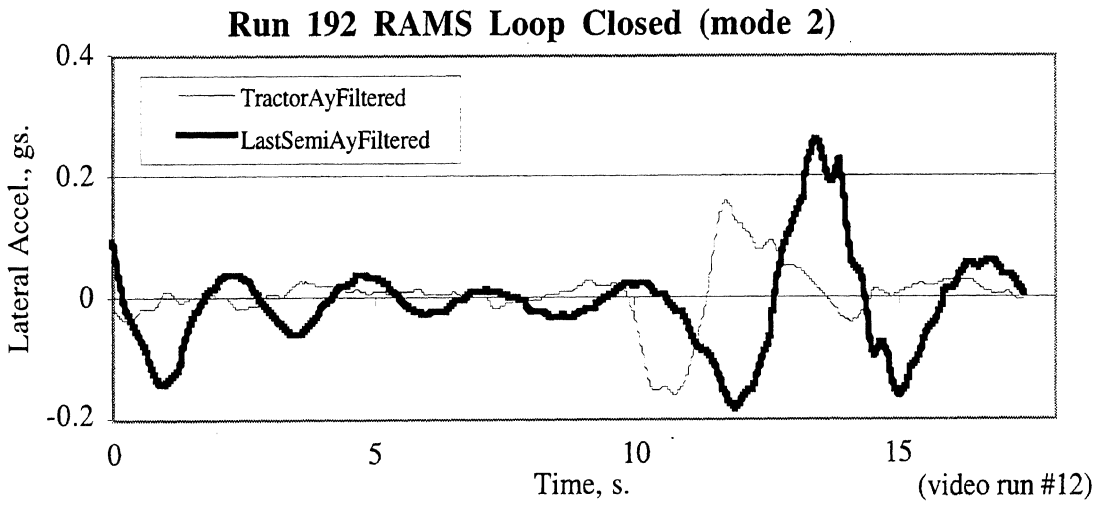

Figure 52a. With RAMS, lateral acceleration, high cg load

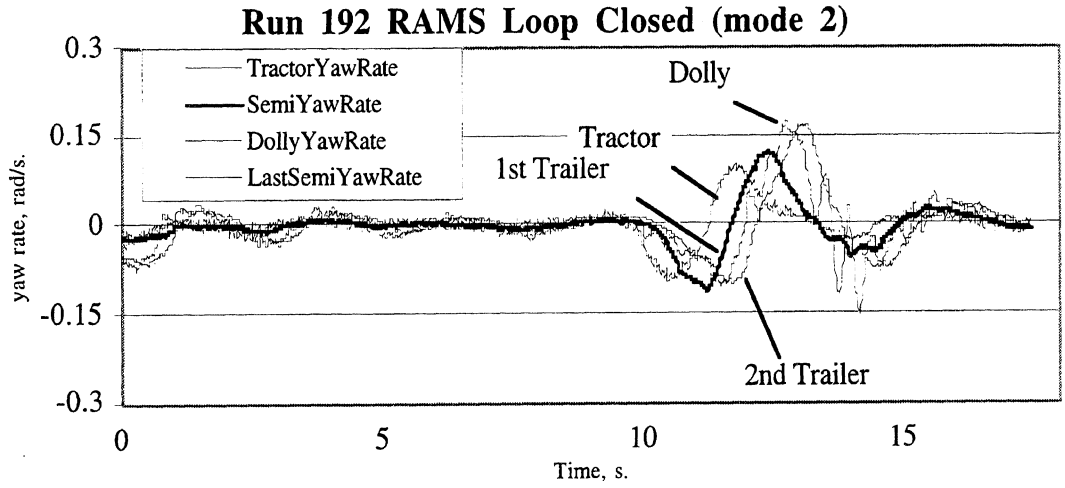

Figure 52b. With RAMS, yaw-rates, high cg load

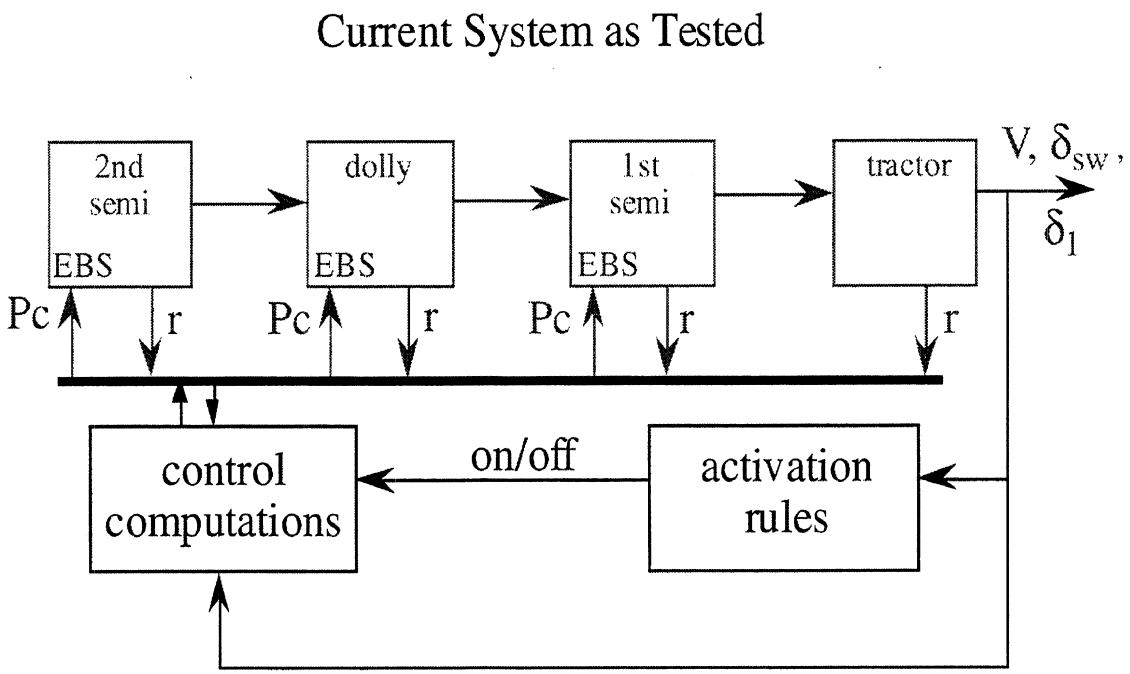

Figure 53. Connectivity diagram of the RAMS system currently being tested

4.0 CONCLUSIONS

The foregoing presentation has shown that the two intended forms of truck-stability enhancement represent viable technical concepts, and that specific prototype systems built during this project have been largely successful in achieving the desired performance objectives. In this section, the experience of this research is summarized in terms of concluding observations that should help in guiding follow-on efforts to develop commercial products.

4.1 CONCLUSIONS RELATING TO THE RSA SYSTEM

1. Two basic approaches for estimating axle-liftoff limits were examined in this study, as follows:

    - The first, which was demonstrated in both tractor-based and semitrailer-based versions of on-board RSA computation, involved regression operations using a 15-minute-long moving window of sensory data. This tractor-based system was successful in estimating the tractor-axle liftoff limit within approximately 10 percent but had no basis for estimating semitrailer liftoff. Conversely, the semitrailer-based system could estimate semitrailer-axle liftoff within a comparable accuracy band, but could not address tractor liftoff.

- A second approach for predicting the semitrailer-liftoff limit using tractor-only sensory measurements was not demonstrated as an on-board computation but was examined by processing measured data in an off-line environment. This approach used a parameter-identification technique to resolve the values of several semitrailer parameters so as to predict semitrailer-axle liftoff. The resolution of semitrailer parameter values, L and h_{cg}, using this method was found to be very difficult due to the small signal-to-noise ratios appearing in the response mechanisms governed by these parameters. Thus, a tractor-only RSA algorithm that can predict not only the tractor-axle liftoff but also the semitrailer liftoff limit must presently incorporate the "blind assumption" of at least one key semitrailer parameter. In appendix C, example data were shown based upon a good assumption for the semitrailer suspension roll stiffness, yielding approximately +/- 10 percent accuracy in estimating the semitrailer-liftoff limit from tractor-mounted sensors. An alternative assumption that would apply well to many trucking fleets whose semitrailers lie only in the popular 48-ft and 53-ft overall length configurations might involve the assumption of a 40- or 41-ft value for semitrailer wheelbase. In any case, the parameter identification method for RSA prediction of rollover limits is very attractive and opens a variety of application avenues, albeit with some further work for their detailed development.

2. The trailer-based RSA system shown here is remarkably simple and presumably inexpensive. Although its derived answer—the lateral acceleration level at which the trailer axle(s) liftoff the ground—rarely marks the rollover threshold of the whole vehicle combination, it does represent a conservative estimate of roll stability that might offer an attractive application for fleets having "married units"—that is, tractors and semitrailers that stay coupled together for long periods of time. In such a scenario, tractors equipped with the RSA display would be consistently coupled to a semitrailer outfitted with an instrumented axle assembly, with suitable interconnecting communications.

3. Either of the tractor- or trailer-based versions of the RSA system that were demonstrated on-board the test vehicle was shown capable of computing its corresponding axle-liftoff limit within less than 5 minutes of normal driving above 40 mph. Computations were rendered inactive at speeds below 40 mph because the tight curve radii that accompany slower-speed travel induce large phase lags in the response of the semitrailer relative to the tractor (i.e., dynamic effects that would violate the steady-state assumptions that underly RSA algorithm design).

4. It is straightforward to estimate a right/left bias in roll stability arising from a payload offset with either the tractor- or semitrailer-based RSA system—to the

same nominal accuracy (for right and left limits) as is achieved when the payload is placed on-center.

5. A force and moment transducer has been developed for sensing fifth wheel loads within an accuracy of 1 to 2 percent of full scale, in support of a tractor-based RSA functional prototype. While this device provides for rather precise estimation of the loads contributing to tractor drive-axle liftoff, it does not represent a design candidate for a high-volume, low-cost product. Nevertheless, the developed load cell should serve as the benchmark device for qualifying simpler sensors that are designed to meet marketable cost targets. The developed load cell would also facilitate a field-test program for surveying the primary in-service loads that are passed through the fifth wheel, thereby aiding advancement in the structural design of tractors, semitrailers, dollies and components.

6. In tractor-semitrailers for which both the fifth-wheel and the trailer axle(s) are instrumented, the rollover threshold of the vehicle combination can be estimated within approximately ± 10 percent by computing a weighted average of the respective axle-liftoff limits—that is, by averaging between tractor and semitrailer values for axle-liftoff threshold, as weighted by the loads deduced to be carried on the respective axle sets.

7. The RSA concept of roll-stability estimation is inherently constrained in its accuracy limits by the substantial nonlinearities in stiffness of leaf-spring suspension in the vicinity of axle liftoff. Where sensors are installed on units whose suspension properties are known at the time of manufacture, the uncertainty in nonlinear behavior on the equipped vehicle unit can be eliminated by treatment within the RSA algorithm. For fleets that purchase their own semitrailers with consistent suspension properties (and perhaps wheelbases, as well) the performance of a tractor-based RSA system, alone, could be made high, indeed. Nevertheless, RSA performance concerns would probably arise when such tractors are later sold to other users hauling a diversity of semitrailers whose parameter values vary widely.

8. The presentation of estimated rollover limits and instantaneous lateral-acceleration demand using a graphical driver display was practicably demonstrated here. Nevertheless, human factors issues related to the display presentation and even the broader cognitive and behavioral aspects of driver response to such information have not been explored.

9. The prospect that RSA-based information would have utility for fleet-safety management seems great. Because the information can be readily processed in light of known rollover probability data, there is a very real likelihood that a fleet could directly appraise its rollover risks on an ongoing basis, thereby giving objective

guidance for implementing countermeasures and for measuring their effectiveness in normal operations, soon after they are applied.

10. In summary, this project provides a real-world validation of the practicality of the RSA concept of identifying vehicle properties while the vehicle is in operation. That is, the rollover threshold and wheel-liftoff limits have been effectively determined for an actual tractor-semitrailer vehicle during normal driving.

4.2 Conclusions Relating to the RAMS System

1. The RAMS system developed for this project demonstrates proof of the viability of the concept of using electronic braking to improve the roll stability and tracking response of a doubles combination in obstacle-avoidance situations.

2. A particular design involving articulation-rate damping and dolly steering, as achieved through side-to-side braking at each axle of the trailers and the dolly, has been shown to be effective in reducing rearward amplification.

3. The RAMS concept is that it constitutes a standby control device that is rarely called into action. Reflecting this philosophy, the implemented RAMS prototype was designed to detect that a significant rearward-amplification response was pending by sampling the steering activity at the tractor, above a selected threshold for vehicle speed. Other implementations that would not depend upon tractor-based triggering of RAMS control are certainly of interest since they would appeal to a broader set of market scenarios. In any case, RAMS activation should be so rare that the system function plays no part in tire or brake wear nor in any concern for fuel efficiency.

4. Relative to the prospect for a RAMS controller that does not employ any measurement from the tractor, it has been observed that right-left brake actuations are remarkably phased with right-left peaks in tire load. This serendipitous outcome may point the way toward a relatively simple, trailer-only, RAMs implementation wherever trailer air suspensions afford a simple means of measuring air pressures as a simple surrogate for wheel load.

5. The level of RAMS performance (expressed by the approximate 40 percent reduction in rearward amplification on a western doubles combination) is comparable to that which has been shown by the use of dual-drawbar dollies. Accordingly, the RAMS approach should be ranked with dual-drawbar dollies by those considering possible future strategies for controlling the configuration of combination vehicles on behalf of traffic safety.

5.0 RECOMMENDATIONS

The following future steps are recommended for facilitating real-world implementation of the examined concepts:

5.1 RELATING TO THE RSA SYSTEM

1) Further study of the autocorrelation technique for estimating semitrailer wheelbase from force data measured at the fifth-wheel load cell. Major improvement in autocorrelation processing would eliminate the need to assume any semitrailer parameter values, thereby opening the way for a broadly-applicable, tractor-based, RSA system.

2) Study the sensitivity of RSA roll stability estimations to the performance of the enabling force and/or moment sensors. This general subject addresses the effort to find the necessary and sufficient specifications of truly marketable RSA packages. Assuming that sensor accuracy and the range of measurement tend to drive sensor cost, thus determining the ultimate marketability of RSA products, study of the trade-offs between prediction accuracy and sensor quality is central to the arrival at product-ready approaches. Such trade-off studies should be conducted for both tractor-based and semitrailer-based systems.

3) Study of the market potential for the alternative system types. While market-assessments may be best done by private companies, the results are also pertinent to further government involvement in this subject area since additional public investment should go only where safety-enhancing implementations are likely to happen. Market study should, for example, explore the relative attractiveness of:

   A) the in-cab (display) type of RSA application, employed as either
      1) a training aid, for acquainting new drivers with the relationships between driving style, vehicle roll stability levels, and rollover risks or
      2) an aid in the continuous usage of a vehicle in service

   B) the off-line usage of RSA measurements that were only recorded (i.e., not displayed) on-board

   If the type-A application were thought to be a popular avenue, it would clearly call for an intensive human-factors investigation that the latter application does not. On the other hand, successful development of the latter application requires that work be done to assimilate rollover-accident data within an overall software package that uses RSA raw data to predict fleet rollover risk. The package should also provide a means for gradually folding in fleet-specific data to the risk prediction so that a

more and more credible basis is established to underpin fleet-safety policy. This outlook would suggest that RSA results be "calibrated," so to speak, against the rollover accidents that are still occurring at some rate within the RSA-equipped fleet.

5.2 Relating to the RAMS System

1. Although the particular design created in this study performs well, there could be other designs that have features that would make them more attractive for deployment. For example, research into the possibility of a trailer-only RAMS implementation package is recommended. This would mean that the system could work with any tractor and that only trailer manufacturers or suppliers would be involved in providing a system for deployment. Such a feature could then be marketed as self-contained within the trailer EBS package.

2. It is further recommended that other design algorithms (i.e., control-objective functions, as discussed herein) be developed for achieving the RAMS function. As in the previous recommendation, the goal would be to discover systems with practical and pragmatic advantages over the system shown here. In particular, RAMS arrangements that operated on yaw acceleration, yaw-rate damping as the dominant criteria for energizing brakes on the rearmost axle in the train, and roll-related braking activations should be considered and tested if analysis shows them to be effective.

Given the success of the RAMS concept on a doubles combination, the effectiveness of RAMS for controlling the rearward amplification of a triples combination should be tested and demonstrated. Clearly, there is every reason to expect that RAMS would so effectively tame rearward amplification in triples combinations as to offer a compelling new type of "quid pro quo" option for the safety-effective allowance of triples, nationwide.

6.0 REFERENCES

1. Ervin, R. D.; Winkler, C. B. 1987. *The influence of braking efficiency on the probability of wheel lockup.* University of Michigan Transportation Research Institute. 13 p. Also published in *SAE Transactions 1987.* Volume 96. Warrendale, SAE, 1988. Report No. SAE 870334.

2. Winkler, C. B.; Bogard, S. E.; Bowen, M. A.; Ganduri, S. M.; Lindquist, D. J. 1995. *An operational field test of long combination vehicles using ABS and C-dollies. Volume I: Final technical report.* University of Michigan Transportation Research Institute. 168 p. Sponsor: National Highway Traffic Safety Administration, Washington, D.C. Report No. UMTRI-95-45-1.

3. Ervin, R. D.; Mathew, A. 1988. *Reducing the risk of spillage in the transportation of chemical wastes by truck. Final report.* University of Michigan Transportation Research Institute. 25 p. Sponsor: Rohm and Haas, Bristol, Pa. Report No. UMTRI-88-28

4. Mallikarjunarao, C.; Fancher, P. S. 1978. *Analysis of the directional response characteristics of double tankers.* University of Michigan Highway Safety Research Institute. 20 p. Report No. SAE 781064.

5. Fancher, P., Winkler, C., Ervin, R., Zhang, H. 1997. "Using braking to control the lateral motion of full trailers." University of Michigan Transportation Research Institute. *The Dynamics of Vehicles on Roads and on Tracks: Proceedings of the 15th IAVSD Symposium.* Lisse, Swets & Zeitlinger.

6. Fancher, P.; Zhang, H.; Winkler, C. 1996. "The use of braking for controlling the lateral motion of full trailers." University of Michigan Transportation Research Institute. 19 p. *International Symposium on Advanced Vehicle Control. Proceedings. Volume 1.* Aachen, Peter List, Kartographie und Druck. Pp. 527-545.

7. Hazemoto, T. 1973. *Analysis of lateral stability for doubles.* Mitsubishi Motors Corporation, Japan. 18 p. Report No. SAE 730688

8. Strandberg, L.; Nordstroem, O.; Nordmark, S. 1975. "Safety problems in commercial vehicle handling." Statens Vaeg-och Trafikinstitut, Fack, Sweden. 66 p. *Commercial Vehicle Braking and Handling Symposium. Proceedings.* Ann Arbor, Highway Safety Research Institute, 1975. Pp. 463-528.

9. Ervin, R. D.; Fancher, P. S.; Gillespie, T. D.; Winkler, C. B.; Wolfe, A. 1978. *Ad hoc study of certain safety-related aspects of double-bottom tankers. Final report.* University of Michigan Highway Safety Research Institute. 78 p. Sponsor: Michigan State Office of Highway Safety Planning, Lansing. Report No. UM-HSRI-78-18-1.

10. Winkler, C. B.; Fancher, P. S.; Carsten, O.; Mathew, A.; Dill, P. 1986. *Improving the dynamic performance of multitrailer vehicles: a study of innovative dollies. Volume I - technical report. Final report.* University of Michigan University Transportation Research Institute. 246 p. Sponsor: Federal Highway Administration, Washington, D.C. Report No. UMTRI-86-26-1/ FHWA/RD-86/161.

11. Winkler, C. B.; Fancher, P. S.; Bareket, Z.; Bogard, S. E.; Johnson, G.; Karamihas, S. M.; Mink, C. E. 1992. *Heavy vehicle size and weight: test procedures for minimum safety performance standards. Final technical report.* University of Michigan Transportation Research Institute. 118 p. Sponsor: National Highway Traffic Safety Administration, Washington, D.C. Report No. UMTRI-92-13/ DOT/HS 807 855.

Appendix A: "Smart Truck" Suspension Tests

This document reports on suspension testing performed for the Smart Truck project. The steer axle, trailing drive axle, and one of the trailer axles of a 6-axle doulbes combination were tested. The tests were performed primarily to characterize suspension properties relevant to roll stability of the vehicle. Table A-1 summarizes the axles that were tested.

Table A-1. Smart Truck Suspensions.

Axle Class	Steer	Drive, Tandem†	Trailer, Single
Suspension Type	Single	Trailing Arm	Trailing Arm
Spring Type	Taper Leaf (2)	Air	Air
Rating (per axle)	12,000 lbs	20,000 lbs	20,000 lbs
Vehicle Manufacurer	Freightliner		Fruehauf
Vehicle ID	VIN 1FUYSXZB5UP556581		Model FBB9-F1-28

† Only the trailing axle of the tandem set was tested.

TESTING PROGRAM

Testing of the functional performance of the suspensions listed in table A-1 was done to measure: the vertical spring rate, suspension roll stiffness (including auxiliary stiffness), the roll center height, the roll steer performance, the lateral compliance, and the aligning moment steer. Table A-2 describes the measurement program for the steer axle. For the steer axle the roll motion and lateral force tests were performed at suspension loads of 14000, 12000, 10000, 7500, and 5000 lbs. The aligning moment test was performed at a suspension load of 12000 lbs. Table A-3 describes the measurement program for the drive and trailer axles. Only the trailing drive axle was tested. The vertical motion, roll motion, lateral force, and aligning moment, tests were performed at nominal suspension loads of 20000, 18000, 16000, 14000, 8000, and 4000 lbs for the drive axle. The vertical motion, roll motion, and tests were performed at nominal suspension loads of 25800, 20800, 15300, 10400, and 5900 lbs for the trailer axle. The aligning moment test for the trailer axle was performed at a suspension load of 20800 lbs.

The test results corresponding to each entry in the tables are reported in reduced and graphical form. The graphical data, provided at the end of this appendix, provide the functional relationships between the independent and dependent variables of interest. The reduced parameters, provided in the "Results" section, represent idealized (usually linear) stiffness or kinematic properties derived from the graphical data.

TEST DEFINITIONS

All suspension measurements were conducted using the UMTRI heavy vehicle suspension measurement facility. The facility is described in detail in SAE Technical Paper 800906. In all tests, the frame of the vehicle is held fixed and the suspension is exercised by moving the facility "table" vertically, in roll, or by applying tire shear forces using the "wheel pads."

Table A-2. Steer Axle Suspension Measurement Program.

Test	Measurement	Reduced Numerics	Data Plots
Vertical motion	Vertical rate	Boundary tables, beta, linear coefficients	F_Z vs Z
Roll motion	Roll rate	Total roll stiffness, Auxiliary roll stiffness	M_X vs Roll
	Roll center	Roll center height	Y_{REF} vs Roll
	Roll steer	Roll steer coefficient	Steer vs Roll
Aligning moment	Aligning moment steer	Linear coefficient, freeplay, model parameters	Steer vs M_Z
Lateral force	Lateral compliance	Linear coefficient	Y vs F_Y

Table A-3. Drive and Trailer Axle Suspension Measurement Program.

Test	Measurement	Reduced Numerics	Data Plots
Vertical motion	Vertical rate	Boundary tables, beta	F_Z vs Z
Roll motion	Roll rate	Total roll stiffness, Auxiliary roll stiffness	M_X vs Roll
	Roll center	Roll center height	Y_{REF} vs Roll
	Roll steer	Roll steer coefficient	Steer vs Roll
Lateral force	Lateral compliance	Linear coefficient	Y vs F_Y
	Lateral force steer	Linear coefficient	Steer vs F_Y
Aligning moment	Aligning moment steer	Linear coefficient	Steer vs M_Z

Force measurements are made with load cell systems located in each of the wheel pads. Thus, in general and except where noted, the reported forces in the data are absolute values measured at the tire/road interface. Resulting motions of the suspension and wheels are measured with several potentiometric devices. Generally, these motion measurements are relative (not absolute) and are referenced to the fixed frame of the vehicle.

The following paragraphs outline the test procedure for the four physical test types listed in tables A-2 and A-3.

Vertical motion: The suspension is exercised by vertical motion of the table. Table motion is controlled by a force and moment feedback servo-system so that roll moment applied to the suspension is held constant at zero while vertical load on the suspension is varied over the range of interest. Force and moment control servo-systems are also used to maintain zero levels of tire shear force and moment.

Roll motion: The suspension is exercised by roll motion of the table. Table motion is controlled by a force and moment feedback servo-system so that the total vertical load applied to the suspension is held constant at the desired value while total roll moment on the suspension is varied over the range of interest. Force and moment control servo-systems are also used to maintain zero levels of tire shear force and moment. This force and moment control mode allows the motion of the suspension to be determined by the suspension geometry, rather than by facility geometry.

Lateral force: The suspension is exercised by the application of lateral tire shear force. Prior to the test, the suspension is loaded vertically to the desired level (with zero roll moment). During the test, the table is controlled by feedback of the vertical position of the right and left axle spindles so that the *vertical and roll position of the axle is held fixed.* (As a result, vertical and roll motions, and especially their influence on steer, are not allowed to influence the test, but vertical load on individual tires will change some during the test. Total vertical load may also change slightly.) The force and moment control servo-systems of the wheel pads are used to vary the lateral force at each tire while longitudinal force and aligning moment are held fixed at zero. Lateral force loading is equal at each wheel throughout the test.

Aligning moment: The suspension is exercised by the application of aligning moments at each tire pair. Prior to the test, the suspension is loaded vertically to the desired level (with zero roll moment). During the test, the table is controlled by feedback of the vertical position of the right and left axle spindles so that the *vertical and roll position of the axle is held fixed.* (As a result, vertical and roll motions, and especially their influence on steer, are not allowed to influence the test, but vertical load on individual tires will change some during the test. Total vertical load may also change slightly.) The force and moment control servo-systems of the wheel pads are used to vary the aligning moment at each tire while longitudinal and lateral force are held fixed at zero. Aligning moment is equal at each wheel throughout the test.

RESULTS

The graphical data collected for the suspensions are provided at the end of this appendix. At least one graph is produced from each test. Each graph identifies the data file, test type, vertical load (if applicable), and other pertinent information. The graphs also provide definitions of the dependent and independent variables, including the units and sign convention. Any explanation needed for interpretation of the graphs is provided in this section.

Reduced data appear in tables A-5 through A-19, and are discussed in this section. Many of the reduced numerics are simply linear coefficients indicating the nominal slope of the related graphical data. The slopes presented are taken from the data at the nominal suspension operating point for the test, often at the origin of the data graph. Note that, due to nonlinearity of the graphical data, other values may be appropriate for "off-center" conditions.

Vertical Motion

The vertical force-deflection behavior is characterized during the vertical motion test. The functional relationship that results from the test is a plot of vertical load versus suspension deflection. The plots provide the suspension spring rate *as measured at the wheel spindle,* that is, they do not include compliance of the tire. In all plots, the vertical

load is measured at the ground, not at the spring, so it includes the unsprung weight of the suspension.

Vertical spring rate

The stiffness properties relevant to roll stability derived from the vertical motion test are linear spring rate and coulomb friction level at a specified operating point (see tables A-5 through A-7), and tables describing the compression and extension boundaries of the force-deflection data (see tables A-8 through A-19). The stiffness of the suspension springs, in combination with their lateral separation, determine the contribution of vertical rate to roll stiffness. The linear spring rate is simply the slope of the vertical force-deflection plot at the operating point. For the drive and trailer axles, a set of extension and compression boundaries is given of each nominal load condition, because each condition implies a different air bag pressure at ride height.

Roll Motion

The suspension total roll stiffness, auxiliary roll stiffness, roll center height, and roll steer coefficient are all reduced from the results of the roll motion test. (See tables A-5 through A-7.)

Total roll stiffness

The plots entitled "Axle Roll Rate" present roll moment about the suspension roll center versus the roll angle of the axle. The slope of this plot is the total roll stiffness of an axle.

The total roll stiffness of the steer axle decreased with nominal suspension load. This is because the auxiliary roll stiffness decreased with load. The total roll stiffness of the drive and trailer axles was fairly consistent over a broad range of suspension loads.

Auxiliary roll stiffness

The roll stiffness of most suspensions is higher than the stiffness dictated by the vertical spring rate of the suspension and the spring spacing. Some portion of the overall roll stiffness of a suspension can usually be attributed to auxiliary mechanisms, such as lateral links or stabilizer bars. Roll motion test data and vertical motion test data are applied to a simple suspension model (based on the UMTRI exponential spring model) to determine what portion of the total roll stiffness is accounted for by the vertical spring rate and what portion derives from auxiliary stiffness.

Most of the stiffness in the drive and trailer axles stems from resistance of the trailing arms to twisting. Thus, the auxiliary stiffness accounts for most of the total roll stiffness.

Roll center height

The roll center is defined as the *instant center of axle roll motion with respect to the fixed frame of the vehicle*. The roll center is assumed to be *on the centerline* of the vehicle and its height is relative to the simulated ground plane. Roll center height is determined from the slope of the Roll Center Height plot (lateral vs. roll motion of the axle). The slope

of the plot a zero roll angle is determined and used in the following formula to calculate h_{rc}, the height of the suspension roll center above the simulated ground plane.

$$h_{rc} = h_a + 57.3 \bullet \left.\frac{\partial y_a}{\partial \phi_a}\right|_{\phi_a = 0} \qquad \text{(A-1)}$$

where: ϕ_a is the roll motion of the axle, y_a is the lateral motion of the axle at an arbitrary height, h_a, above the simulated ground plane. As expected, the roll center height of the suspensions lowered with increasing load. The change is due largely to the compression of the suspension springs and tires (making the fixed frame closer to "ground").

Roll steer coefficient

The roll steer coefficient is the slope of the Roll Steer plots at zero roll angle. This coefficient indicates the steer response of the suspension that results from roll motion. For the steer axle roll steer was moderate and positive and decreased with suspension load. For the drive axle roll steer was moderate and negative and increased with suspension load. For the trailer axle roll steer was moderate and positive and increased with suspension load.

Lateral Force

Lateral force compliance coefficient

The lateral compliance coefficient given is the slope of the linear portion of the Lateral Force Compliance plot. (See tables A-5 through A-7.) That is, the coefficient indicates the lateral motion response of the axle as results from the sum of the two tire lateral forces. Note that the values reported in tables A-5 through A-7 are lateral motion of the axle per *total* lateral force applied to the suspension, not lateral force per side.

Although the lateral force compliance coefficient is given as a linear coefficient, the lateral force compliance behavior is often nonlinear. In such cases, a portion of the lateral motion of the suspension in response to lateral force is due to lash (restricted by coulomb friction). For the trailer axle, the lateral compliance characteristic showed a distict decrease in slope for lateral loads above 800 lbs per wheel. For this reason, a separate linear coefficient is given in table A-7 for lateral loads above and below 800 lbs per wheel.

Lateral force steer coefficient

The lateral force steer coefficient is the slope of the Lateral Force Compliance Steer plot at the zero lateral force condition. The coefficient indicates the steer response of the suspension that results from the from the sum of the two tire lateral forces. Note that the values reported in tables A-6 and A-7 are steer of the axle per *total* lateral force applied to the suspension, not lateral force per side. This test was not performed on the steer axle, because it was too difficult to obtain results that did not include the influence of aligning moment steer.

Aligning Moment

The aligning moment steer coefficient for the drive and trailer axles is the slope of the Aligning Moment Compliance Steer plots. (See tables A-6 and A-7.) Note that the aligning moment used is the average of that applied to the two wheel sets. The coefficient indicates the steer response of the suspension that results from the sum of tire aligning moments. Although the aligning moment compliance steer is given as a linear coefficient, the aligning moment behavior is sometimes nonlinear. In such cases, a portion of the steer of the suspension in response to aligning moment is due to lash.

The aligning moment compliance steer of the front axle was measured at a suspension load of 12000 lbs. The steering gear and tie rod stiffness values are derived from the slopes of the linear portions of the Aligning Moment Compliance Steer plots. The calculated spring values were deduced from the model shown in figure A-1 and the following:

$$K_S = 2 \cdot \left(\partial SAL / \partial MZAV\right)^{-1}$$

$$K_T = \left[\left(\partial SAR / \partial MZAV\right) - \left(\partial SAL / \partial MZAV\right)\right]^{-1} \qquad \text{(A-2)}$$

Table A-4 provides the results.

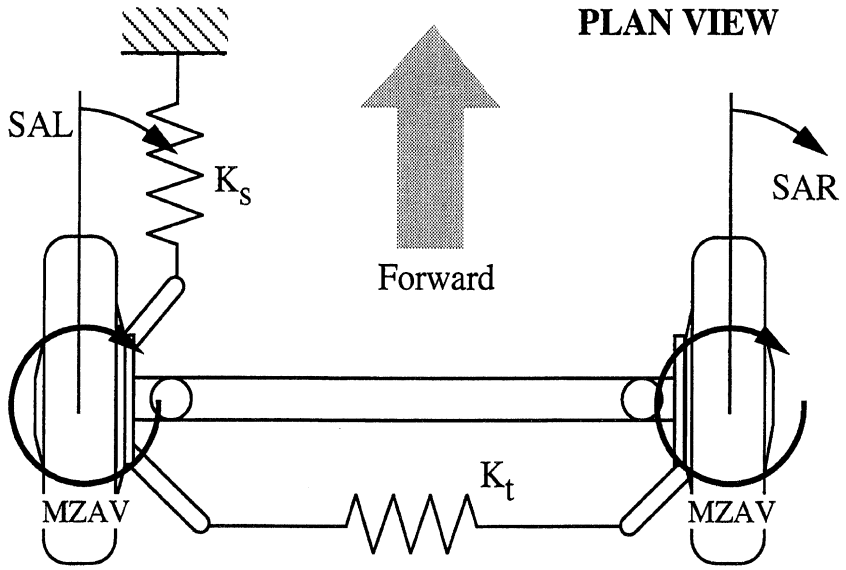

Figure A-1. Aligning moment compliance steer model.

Table A-4. Steering System Model Parameters.

Freeplay (deg)	*Measured Compliance (deg/in-lb)*		*Calculated Spring Values (in-lb/deg)*	
	$\frac{\partial SAR}{\partial MZAV}$	$\frac{\partial SAL}{\partial MZAV}$	K_S	K_T
.25	$.235 \times 10^{-3}$	$.194 \times 10^{-3}$	10,310	24,390

Table A-5. Reduced Data, Steer Axle.

At a Nominal Suspension Load of:	*5000 lbs*	*7500 lbs*	*10000 lbs*	*12000 lbs*	*14000 lbs*
Vertical Stiffness (lb/in)	1560	1510	1460	1445	1465
Coulomb Friction (lbs)	205	218	201	200	208
Total Roll Stiffness (in-lb/deg)	28,800	26,000	24,200	23,000	22,600
Auxiliary Roll Stiffness (in-lb/deg)	14,500	12,000	10,500	9,500	8,500
Roll Center Height, above ground (in)	21.2	20.0	19.2	18.5	18.0
Roll Steer Coefficient (deg/deg)	.145	.133	.104	.075	.059
Lateral Compliance Coeff (in/lb)	$.595x10^{-4}$	$.600x10^{-4}$	$.550x10^{-4}$	$.580x10^{-4}$	$.540x10^{-4}$

Table A-6. Reduced Data, Trailing Drive Axle.

At a Nominal Suspension Load of:	*4000 lbs*	*8000 lbs*	*14000 lbs*
Nominal Air Bag Pressure (psi)	8	26	51
Vertical Stiffness (lb/in)	562	968	1460
Coulomb Friction (lbs)	416	560	780
Total Roll Stiffness (in-lb/deg)	110,500	109,500	106,500
Auxiliary Roll Stiffness (in-lb/deg)	107,500	105,000	100,000
Roll Center Height, above ground (in)	31.3	31.0	30.7
Roll Steer Coefficient (deg/deg)	-.125	-.125	-.108
Lateral Compliance Coeff (in/lb)	$.156x10^{-4}$	$.163x10^{-4}$	$.143x10^{-4}$
Lateral Compliance Steer (deg/lb)	$.680x10^{-5}$	$.106x10^{-4}$	$.655x10^{-5}$
Aligning Moment Steer Coeff (deg/in-lb)	$.485x10^{-5}$	$.411x10^{-4}$	$.494x10^{-5}$

Table 6. (cont) Reduced Data, Trailing Drive Axle.

At a Nominal Suspension Load of:	*16000 lbs*	*18000 lbs*	*20000 lbs*
Nominal Air Bag Pressure (psi)	58	65	70.5
Vertical Stiffness (lb/in)	1605	1785	1980
Coulomb Friction (lbs)	735	640	755
Total Roll Stiffness (in-lb/deg)	105,000	106,000	107,000
Auxiliary Roll Stiffness (in-lb/deg)	95,000	95,000	95,000
Roll Center Height, above ground (in)	31.3	30.4	30.3
Roll Steer Coefficient (deg/deg)	-1.06	-.104	-.098
Lateral Compliance Coeff (in/lb)	$.139x10^{-4}$	$.142x10^{-4}$	$.143x10^{-4}$
Lateral Compliance Steer (deg/lb)	$.710x10^{-5}$	$.580x10^{-5}$	$.616x10^{-5}$
Aligning Moment Steer Coeff (deg/in-lb)	$.458x10^{-5}$	$.434x10^{-4}$	$.455x10^{-5}$

Table A-7. Reduced Data, Trailer Axle.

At a Nominal Suspension Load of:	*5900 lbs*	*10400 lbs*	*15300 lbs*	*20800 lbs*	*25800 lbs*
Nominal Bag Pressure (psi)	20	40	60	80	100
Vertical Stiffness (lb/in)	760	1110	1540	1950	2580
Coulomb Friction (lbs)	345	535	780	610	560
Total Roll Stiffness (in-lb/deg)	124,000	119,000	119,500	124,000	125,000
Auxiliary Roll Stiffness (in-lb/deg)	117,000	111,000	106,000	104,000	105,000
Roll Center Height, above ground (in)	25.9	25.2	25.1	24.5	24.4
Roll Steer Coefficient (deg/deg)	.104	.125	.133	.143	.162
Lateral Compliance Coeff (in/lb)	$.735 \times 10^{-4}$	$.770 \times 10^{-4}$	$.850 \times 10^{-4}$	$.830 \times 10^{-4}$	$.790 \times 10^{-4}$
Lateral Compliance Steer (deg/lb)	$-.372 \times 10^{-4}$	$-.346 \times 10^{-4}$	$-.377 \times 10^{-4}$	$-.375 \times 10^{-4}$	$-.389 \times 10^{-4}$
Aligning Moment Steer Coeff (deg/in-lb)	–	–	–	$.656 \times 10^{-5}$	–

Table A-8. Steer Axle Spring Boundary Tables.

Compression Envelope		*Extension Envelope*	
Deflection (in)	Force (lbs)	Deflection (in)	Force (lbs)
.77	441	.84	441
1.23	1492	1.56	1695
1.88	2610	2.56	3220
3.28	4712	4.12	5492
4.65	6678	5.33	7288
5.54	8000	5.71	7966
5.74	8576	5.93	9085
5.90	9424		

Table A-9. Drive Axle Spring Boundary Tables, Nominal Load of 4000 lbs, Air Bags at 8 PSI.

Compression Envelope		*Extension Envelope*	
Deflection (in)	Force (lbs)	Deflection (in)	Force (lbs)
1.24	1180	1.37	712
2.82	1770	2.73	1058
3.96	2339	4.03	1525
4.98	2990	5.13	2237
5.85	3824	5.94	2929
6.74	4759	6.55	3783
6.95	5186	6.95	4658
6.99	6183	7.02	4983
		7.04	5898

Table A-10. Drive Axle Spring Boundary Tables, Nominal Load of 8000 lbs, Air Bags at 26 PSI.

Compression Envelope		*Extension Envelope*	
Deflection (in)	Force (lbs)	Deflection (in)	Force (lbs)
.82	1915	.96	1407
2.06	2932	2.06	2119
3.48	3847	3.48	2831
4.61	4932	4.36	3542
5.69	6424	5.29	4525
6.46	7746	6.01	5678
7.02	8932	6.69	7136
7.08	10458	7.08	8390
		7.15	10390

Table A-11. Drive Axle Spring Boundary Tables, Nominal Load of 14000 lbs, Air Bags at 50.5 PSI.

Compression Envelope		*Extension Envelope*	
Deflection (in)	Force (lbs)	Deflection (in)	Force (lbs)
.67	3420	.78	2946
1.93	4939	2.84	4892
3.74	7122	3.80	5793
4.72	8688	4.84	7217
5.75	10776	5.78	9115
6.71	13339	6.55	11251
7.20	15237	7.11	13434
		7.20	14573

Table A-12. Drive Axle Spring Boundary Tables, Nominal Load of 16000 lbs, Air Bags at 58 PSI.

Compression Envelope		*Extension Envelope*	
Deflection (in)	Force (lbs)	Deflection (in)	Force (lbs)
.92	3851	.85	3234
1.38	4610	2.43	5085
2.78	6556	3.67	6414
3.65	7742	4.61	7932
4.45	8976	5.25	9166
5.32	10780	6.12	11444
6.21	13105	6.63	13200
7.02	15668	7.02	15003

Table A-13. Drive Axle Spring Boundary Tables, Nominal Load of 18000 lbs, Air Bags at 65 PSI.

Compression Envelope		*Extension Envelope*	
Deflection (in)	Force (lbs)	Deflection (in)	Force (lbs)
.89	4224	.80	3573
1.79	5742	2.15	5308
4.04	9159	3.87	7532
5.07	11329	5.09	9810
6.03	13715	5.85	11871
6.88	16644	6.51	13986
		6.99	15885

Table A-14. Drive Axle Spring Boundary Tables, Nominal Load of 20000 lbs, Air Bags at 71.5 PSI.

Compression Envelope		*Extension Envelope*	
Deflection (in)	Force (lbs)	Deflection (in)	Force (lbs)
.83	4790	.89	4302
1.92	6634	2.71	6905
3.62	9400	4.12	8858
4.90	11949	5.09	10864
5.87	14444	5.76	12654
6.40	16125	6.53	15312
6.88	17807	6.92	17102

Table A-15. Trailer Axle Spring Boundary Tables, Nominal Load of 5900 lbs, Air Bags at 20 PSI.

Compression Envelope		*Extension Envelope*	
Deflection (in)	Force (lbs)	Deflection (in)	Force (lbs)
1.55	1232	1.71	1178
2.51	1720	3.47	1856
3.71	2398	4.69	2453
4.74	3076	5.75	3212
5.70	3917	6.48	3944
6.57	4893	7.30	5110
7.47	6276	7.83	6303
8.36	8093	8.36	7849

Table A-16. Trailer Axle Spring Boundary Tables, Nominal Load of 10400 lbs, Air Bags at 40 PSI.

Compression Envelope		*Extension Envelope*	
Deflection (in)	Force (lbs)	Deflection (in)	Force (lbs)
1.72	2386	1.70	2169
4.07	4664	3.53	3525
5.69	6617	4.73	4393
6.73	8461	6.05	5749
7.86	11281	6.91	7214
8.64	13776	7.47	8461
8.82	16434	8.28	11064
		8.76	13505
		8.84	16163

Table A-17. Trailer Axle Spring Boundary Tables, Nominal Load of 15300 lbs, Air Bags at 60 PSI.

Compression Envelope		*Extension Envelope*	
Deflection (in)	Force (lbs)	Deflection (in)	Force (lbs)
1.74	3464	1.86	3281
3.65	6088	3.41	4929
5.23	8529	4.91	6576
6.35	10786	5.95	8041
6.99	12434	6.79	9627
7.86	15180	7.63	11885
8.74	18658	8.16	13898
8.96	20000	8.94	17986
		9.12	20000

Table A-18. Trailer Axle Spring Boundary Tables, Nominal Load of 20800 lbs, Air Bags at 80 PSI.

Compression Envelope		*Extension Envelope*	
Deflection (in)	Force (lbs)	Deflection (in)	Force (lbs)
1.68	4441	1.78	4383
3.39	7495	3.28	6573
4.87	10549	4.94	9512
5.82	12739	5.86	11356
6.85	15966	6.64	13431
7.98	20173	7.19	15505
		8.23	20231

Table A-19. Trailer Axle Spring Boundary Tables, Nominal Load of 25800 lbs, Air Bags at 100 PSI.

Compression Envelope		*Extension Envelope*	
Deflection (in)	Force (lbs)	Deflection (in)	Force (lbs)
1.44	4671	1.48	4305
1.72	6014	1.74	5708
2.80	8332	2.62	7234
4.01	11444	3.79	9736
5.67	15837	5.01	12786
6.39	17973	5.91	15105
7.13	20597	6.61	17729
		7.21	20414

Measured by UMTRI for Smart Truck
Freightliner Tractor

Data file: FRTLNS00.ERD

Single Steer Axle Suspension

Aligning Moment Compliance Steer

6 April 96
Suspension: Taper-Leaf (2)

Suspension Load: 12000 lb.

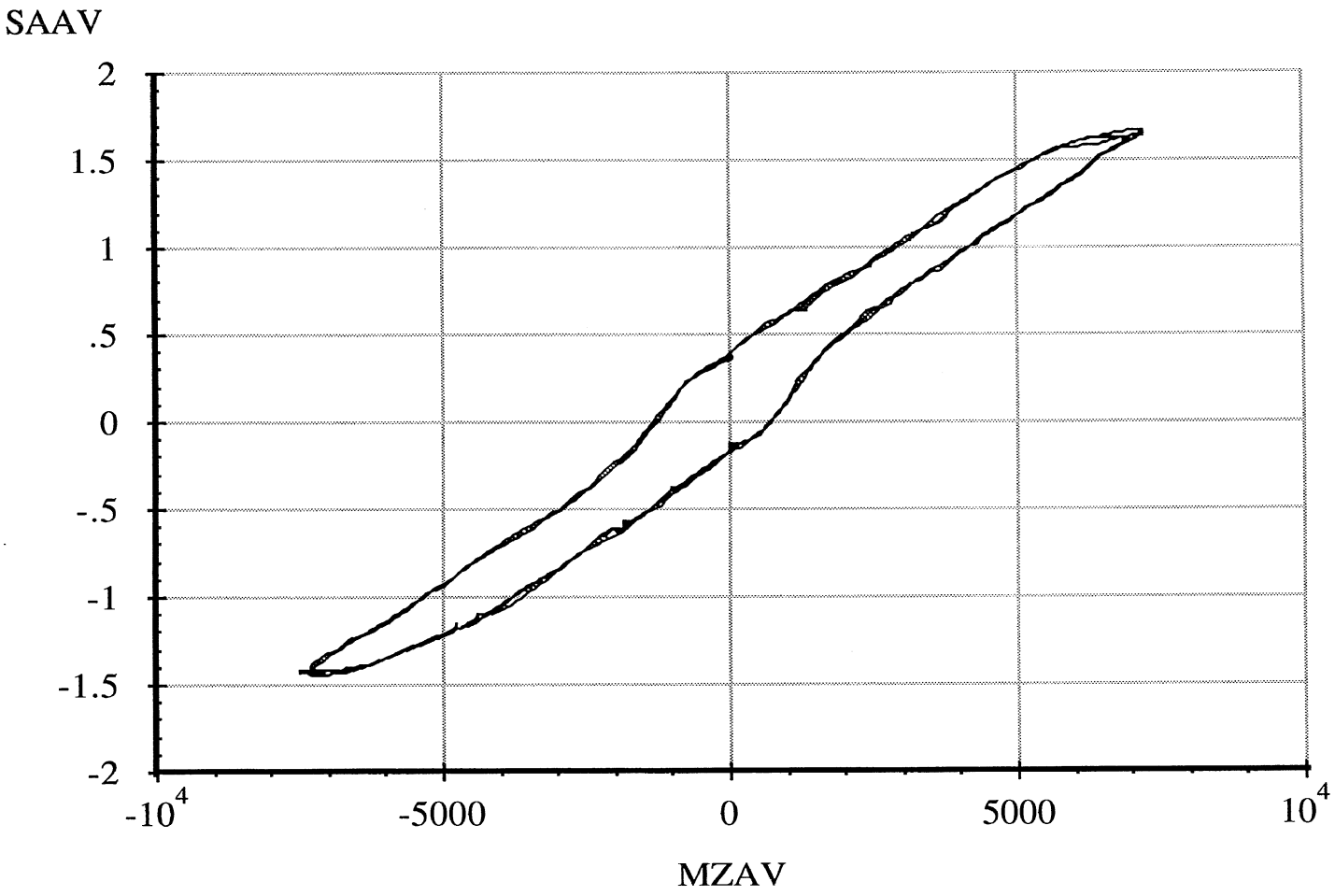

Abscissa (X): Average axle aligning moment (MZAV); in-lb per wheel; applied to both wheels simultaneously; downward (right hand rule) moment vector, positive.

Ordinate (Y): Average steer angle (SAAV); degrees; steer toward right, positive.

*Note: Brakes on. Engine on. Position Control. Steering Wheel Locked.

Measured by UMTRI for Smart Truck
Freightliner Tractor

Single Steer Axle Suspension

6 April 96
Suspension: Taper-Leaf (2)

Data file: FRTLNS00.ERD

Left Wheel Aligning Moment Compliance Steer

Suspension Load: 12000 lb.

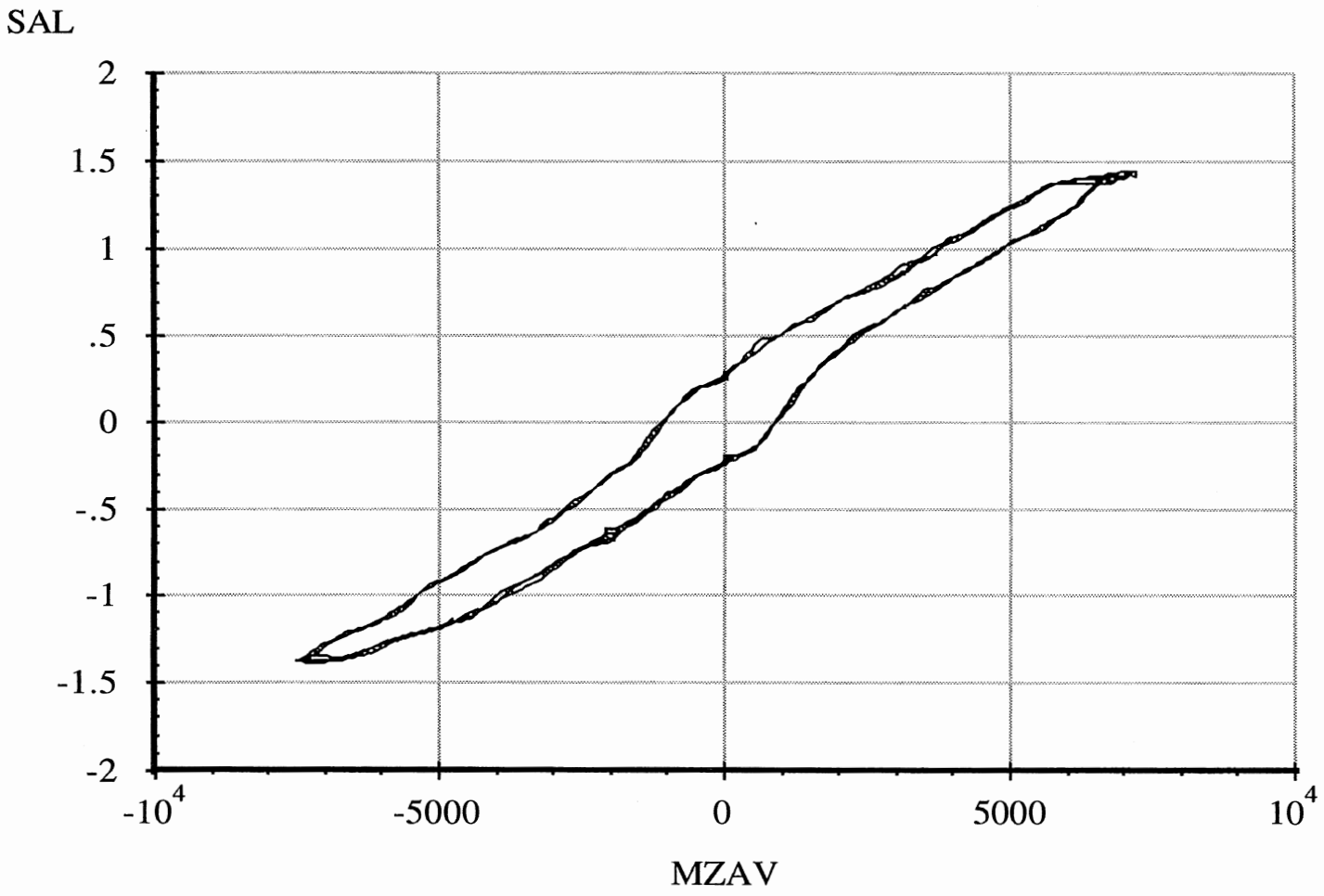

Abscissa (X): Average axle aligning moment (MZAV); in-lb per wheel; applied to both wheels simultaneously; downward (right hand rule) moment vector, positive.

Ordinate (Y): Left wheel steer angle (SAL); degrees; steer toward right, positive.

*Note: Brakes on. Engine on. Position Control. Steering Wheel Locked.

Measured by UMTRI for Smart Truck
Freightliner Tractor

6 April 96
Suspension: Taper-Leaf (2)

Single Steer Axle Suspension

Data file: FRTLNS00.ERD

Right Wheel Aligning Moment Compliance Steer

Suspension Load: 12000 lb.

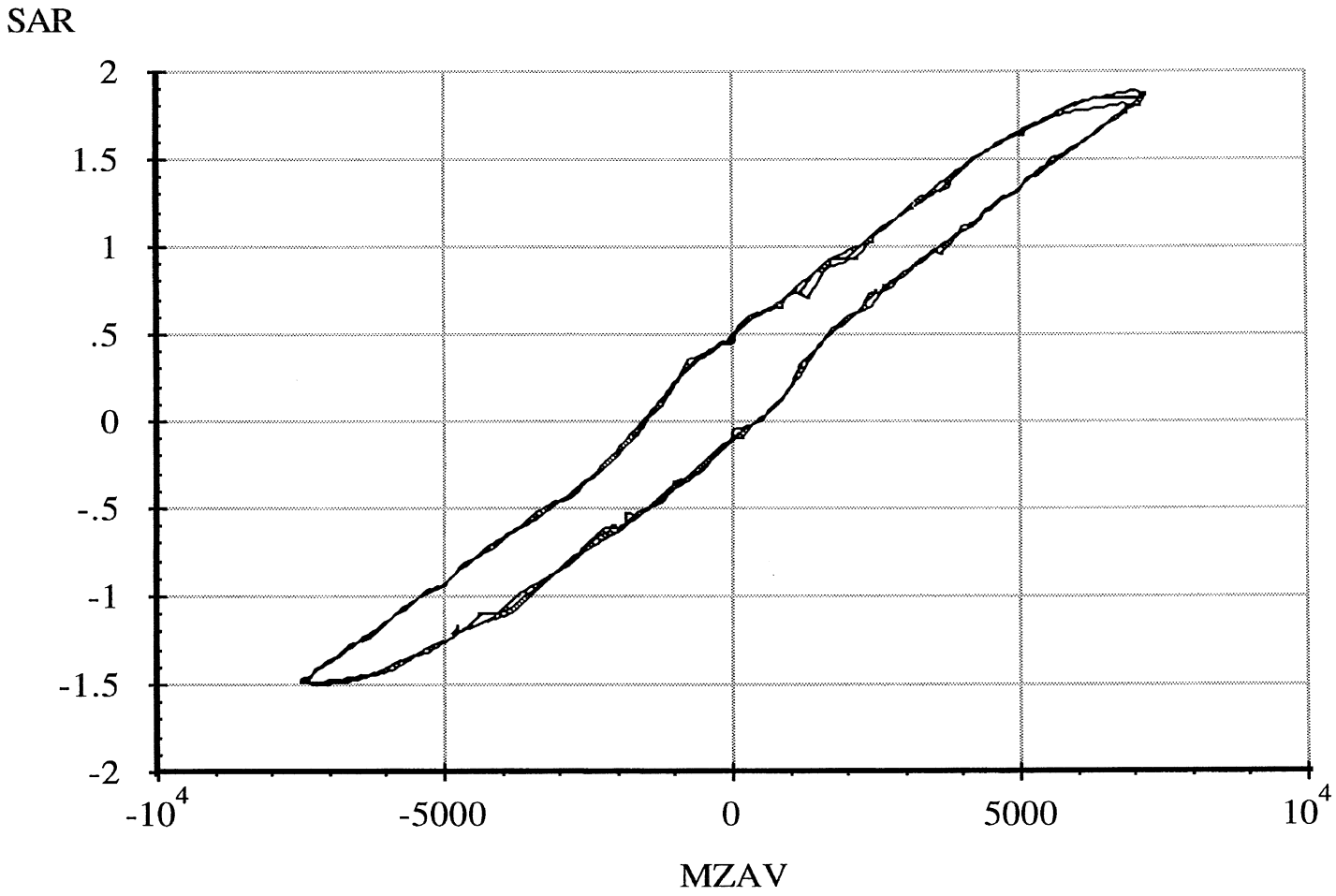

Abscissa (X): Average axle aligning moment (MZAV); in-lb per wheel; applied to both wheels simultaneously; downward (right hand rule) moment vector, positive.

Ordinate (Y): Right wheel steer angle (SAR); degrees; steer toward right, positive.

*Note: Brakes on. Engine on. Position Control. Steering Wheel Locked.

Measured by UMTRI for Smart Truck
Freightliner Tractor

Data file: FRTLNS01.ERD

Single Steer Axle Suspension

6 April 96
Suspension: Taper-Leaf (2)

Average Vertical Spring Rate

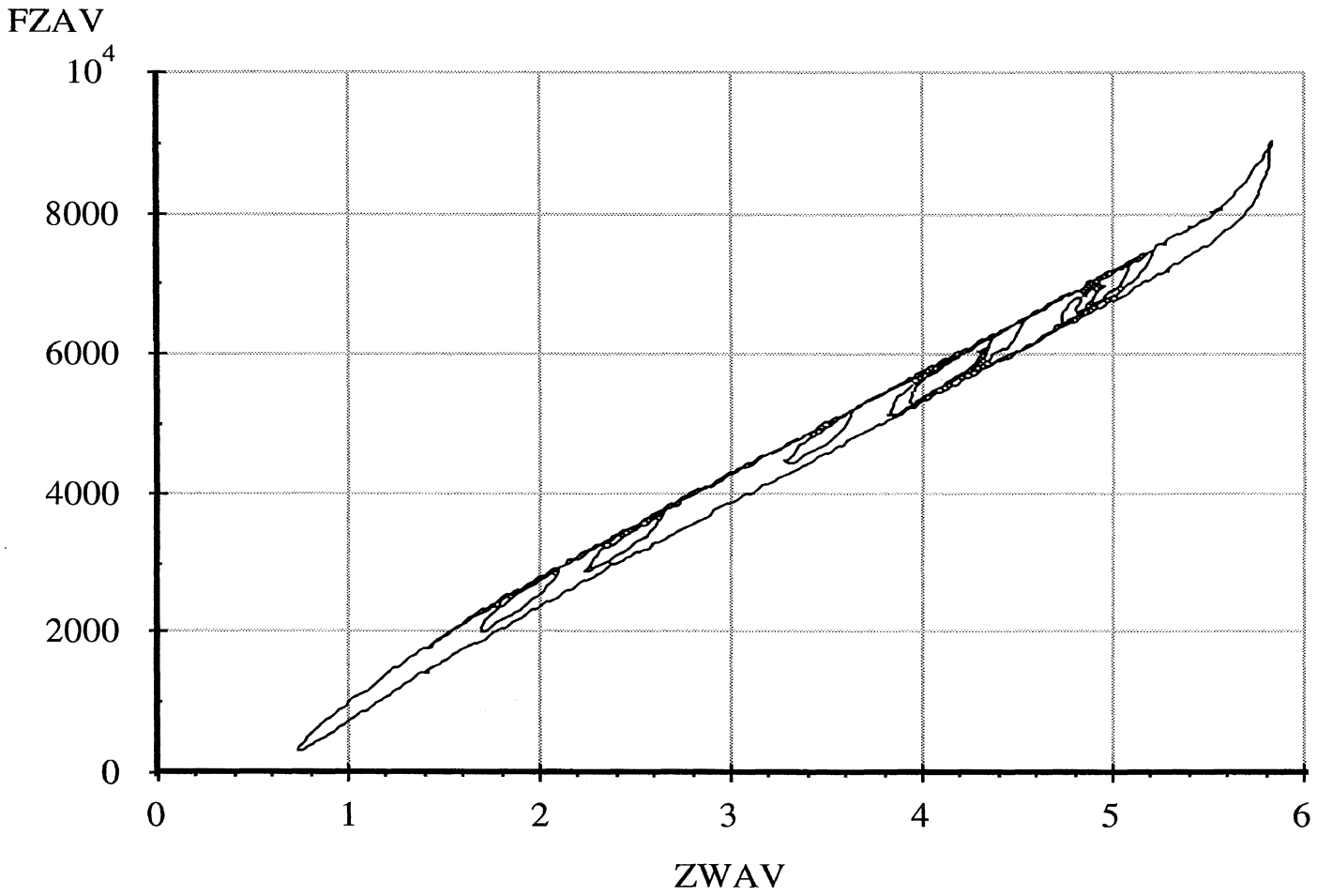

Abscissa (X): Average vertical wheel displacement (ZWAV); inches; spring compression, positive.

Ordinate (Y): Average vertical wheel load (FZAV); pounds; spring compression, positive.

*Note: Brakes on. Position control. Pitman arm blocked.

Measured by UMTRI for Smart Truck
Freightliner Tractor

Data file: FRTLNS06.ERD

Single Steer Axle Suspension

Axle Roll Rate

6 April 96
Suspension: Taper-Leaf (2)

Suspension Load: 14000 lb.

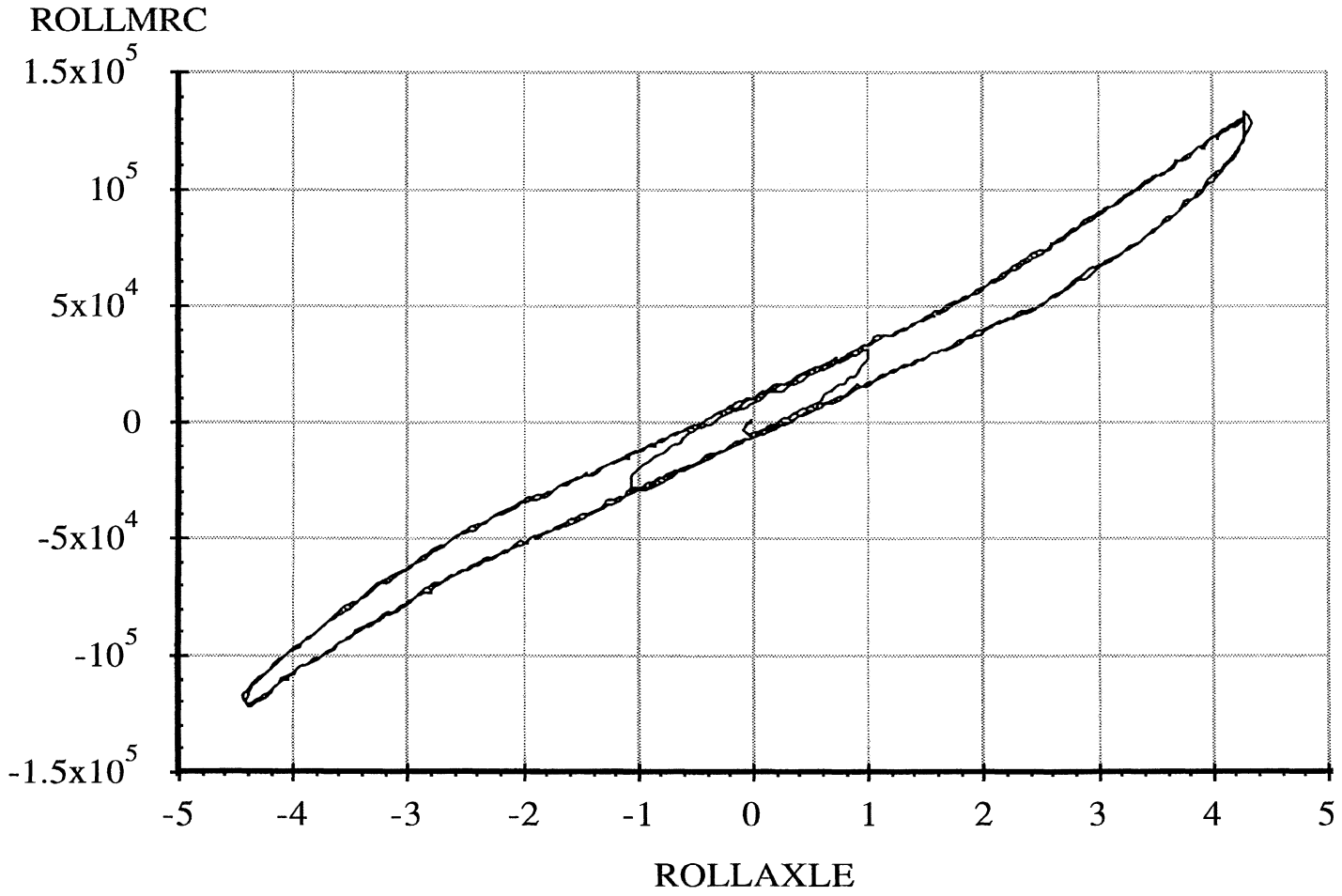

Abscissa (X): Axle roll angle (ROLLAXLE); degrees; right side compressed, positive.

Ordinate (Y): Axle roll moment about the roll center (ROLLMRC); in-lb; right side compressed, positive.

*Note: Brakes on. Force control. Pitman arm blocked.

Measured by UMTRI for Smart Truck
Freightliner Tractor

Data file: FRTLNS06.ERD

Single Steer Axle Suspension

Roll Center Height

6 April 96
Suspension: Taper-Leaf (2)

Suspension Load: 14000 lb.

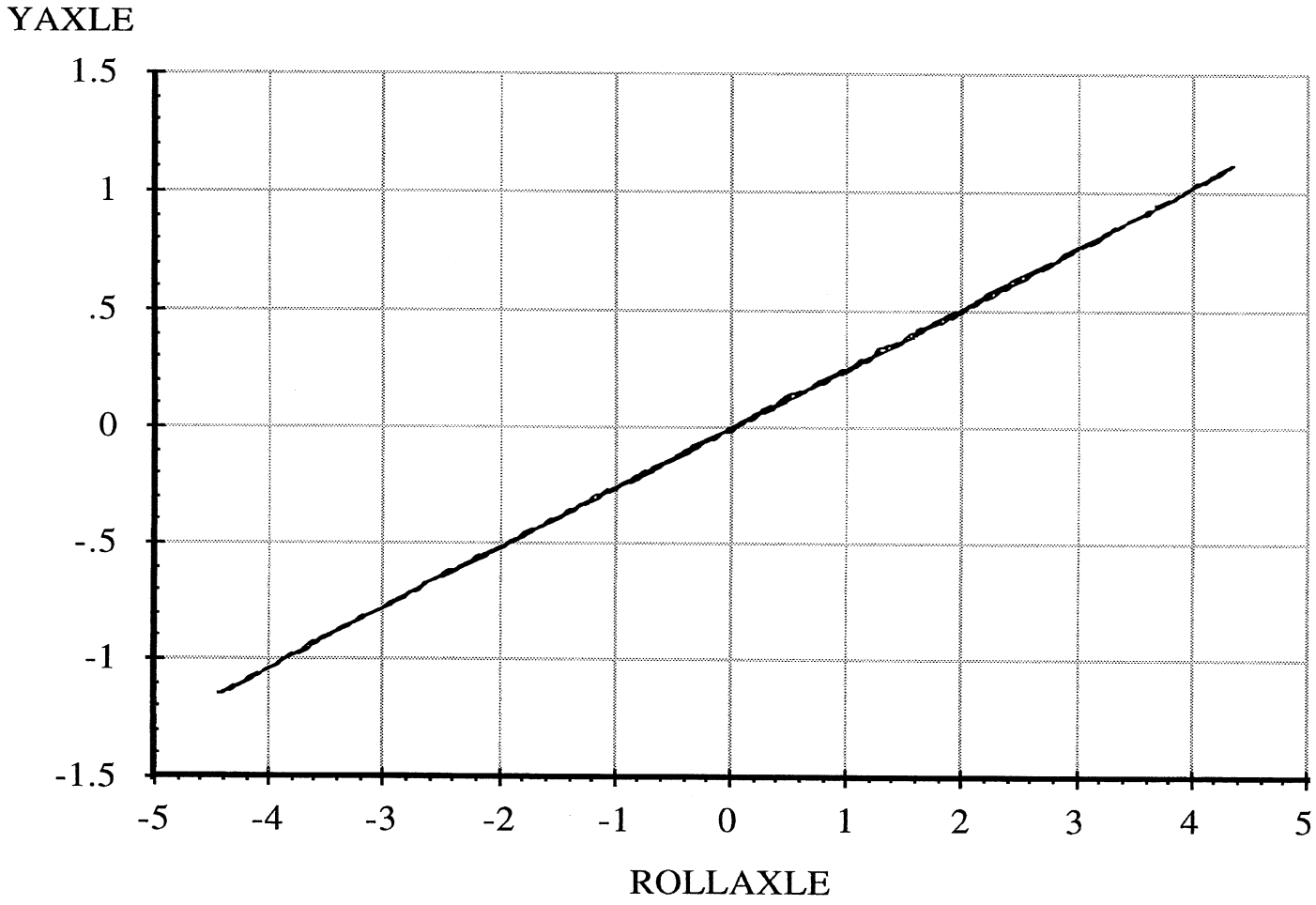

Abscissa (X): Axle roll angle (ROLLAXLE); degrees; right side compressed, positive.

Ordinate (Y): Axle reference point lateral translation (YAXLE); inches; motion toward right, positive.

*Note: Brakes on. Force control. Pitman arm blocked. Reference height of 3.25 inches.

Measured by UMTRI for Smart Truck
Freightliner Tractor

Data file: FRTLNS06.ERD

Single Steer Axle Suspension

Roll Steer

6 April 96
Suspension: Taper-Leaf (2)

Suspension Load: 14000 lb.

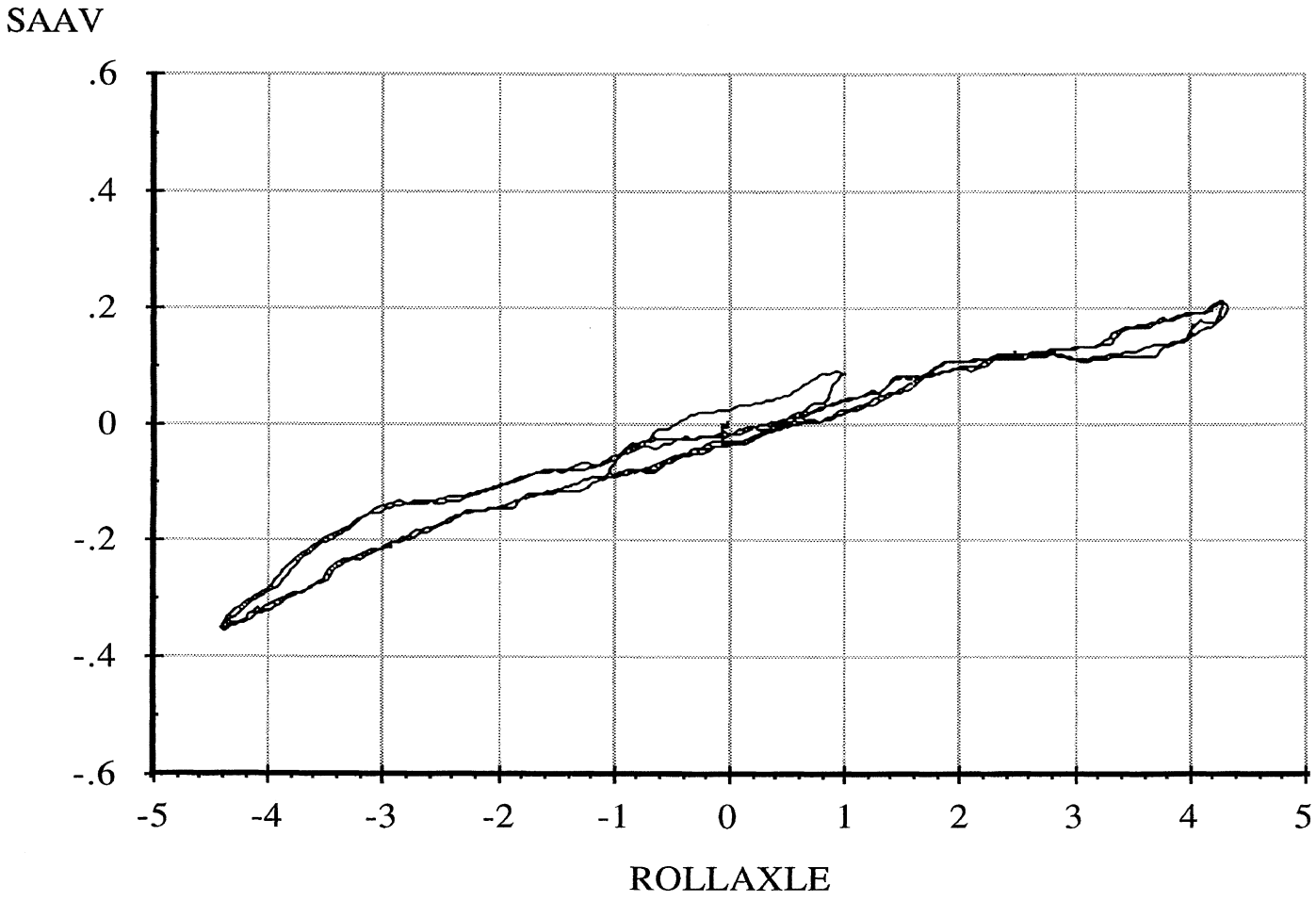

Abscissa (X): Axle roll angle (ROLLAXLE); degrees; right side compressed, positive.

Ordinate (Y): Average steer angle (SAAV); degrees; steer toward right, positive.

*Note: Brakes on. Force control. Pitman arm blocked.

Measured by UMTRI for Smart Truck
Freightliner Tractor

Data file: FRTLNS05.ERD

Single Steer Axle Suspension

Axle Roll Rate

6 April 96
Suspension: Taper-Leaf (2)

Suspension Load: 12000 lb.

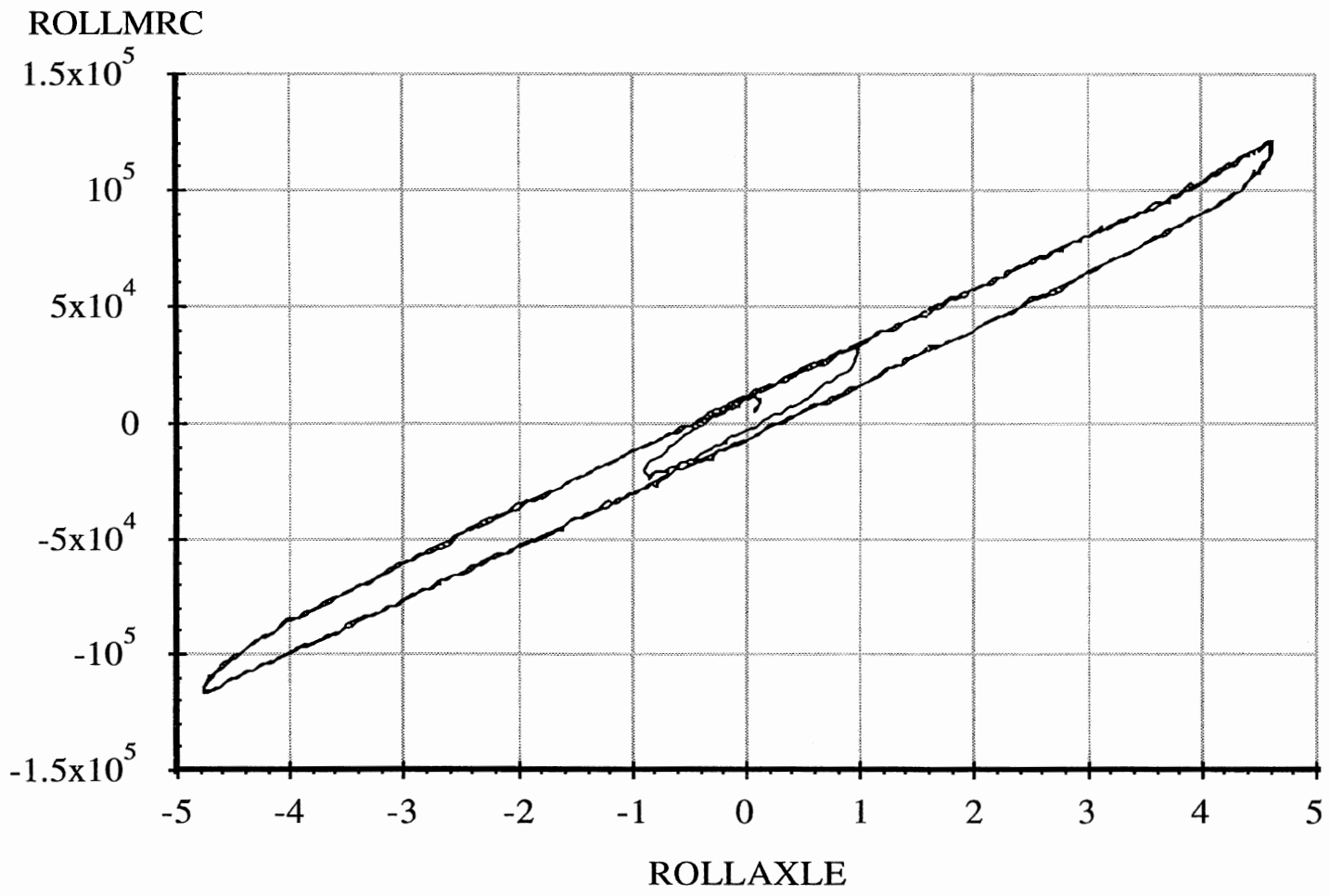

Abscissa (X): Axle roll angle (ROLLAXLE); degrees; right side compressed, positive.

Ordinate (Y): Axle roll moment about the roll center (ROLLMRC); in-lb; right side compressed, positive.

*Note: Brakes on. Force control. Pitman arm blocked.

Measured by UMTRI for Smart Truck
Freightliner Tractor

Data file: FRTLNS05.ERD

Single Steer Axle Suspension

Roll Center Height

6 April 96
Suspension: Taper-Leaf (2)

Suspension Load: 12000 lb.

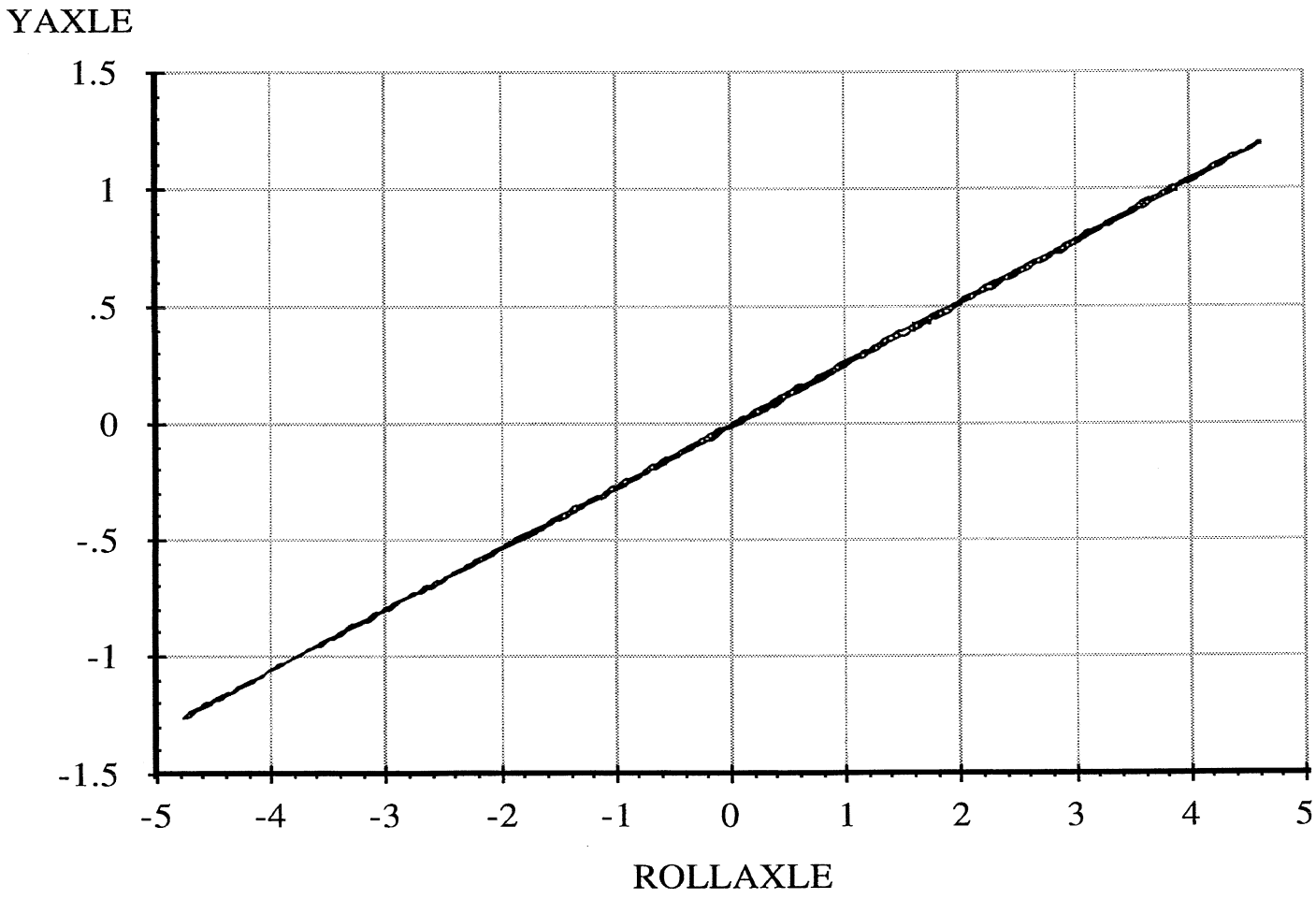

Abscissa (X): Axle roll angle (ROLLAXLE); degrees; right side compressed, positive.

Ordinate (Y): Axle reference point lateral translation (YAXLE); inches; motion toward right, positive.

*Note: Brakes on. Force control. Pitman arm blocked. Reference height of 3.44 inches.

Measured by UMTRI for Smart Truck
Freightliner Tractor

Data file: FRTLNS05.ERD

Single Steer Axle Suspension

Roll Steer

6 April 96
Suspension: Taper-Leaf (2)

Suspension Load: 12000 lb.

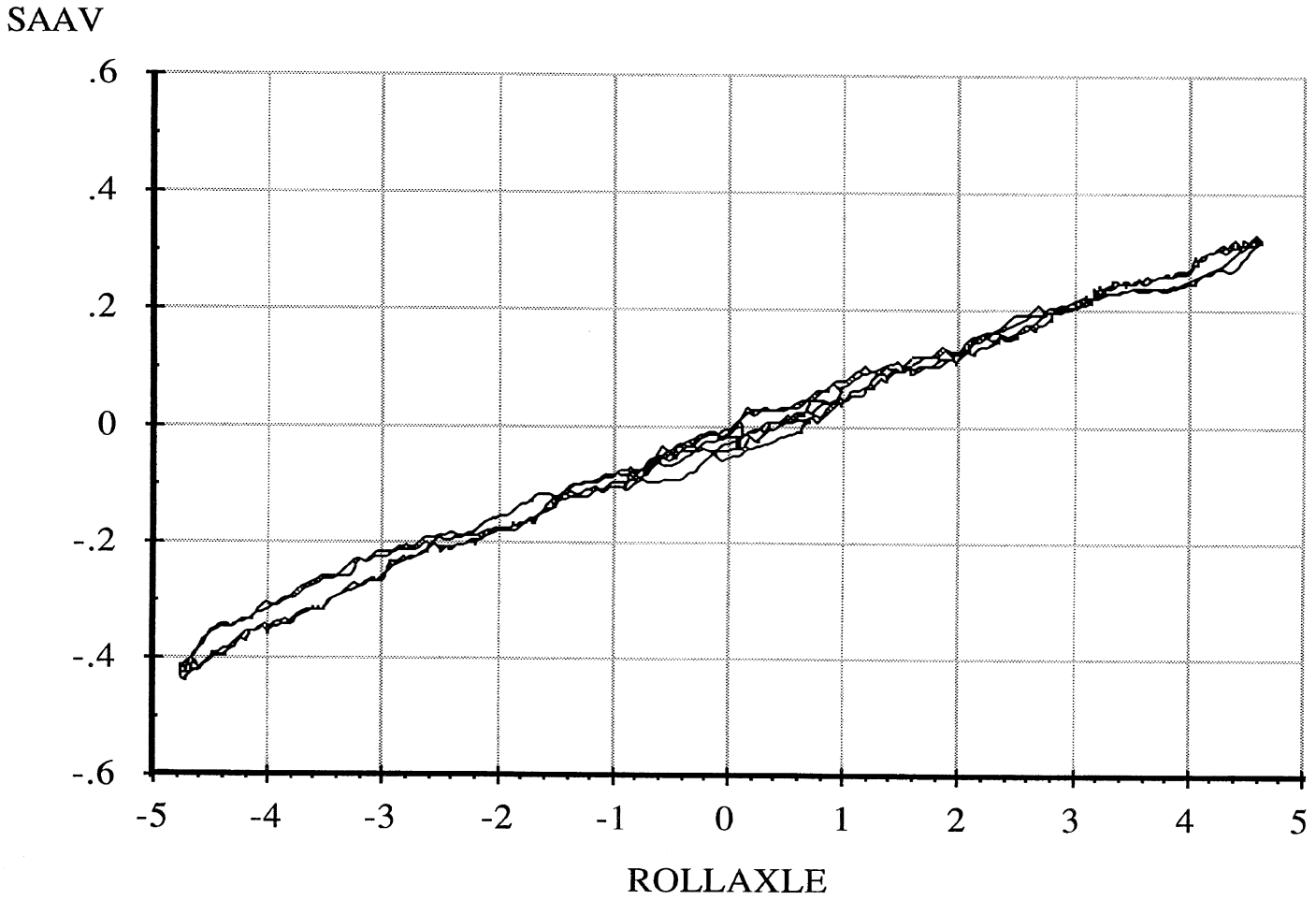

Abscissa (X): Axle roll angle (ROLLAXLE); degrees; right side compressed, positive.

Ordinate (Y): Average steer angle (SAAV); degrees; steer toward right, positive.

*Note: Brakes on. Force control. Pitman arm blocked.

Measured by UMTRI for Smart Truck
Freightliner Tractor

Data file: FRTLNS04.ERD

Single Steer Axle Suspension

Axle Roll Rate

6 April 96
Suspension: Taper-Leaf (2)

Suspension Load: 10000 lb.

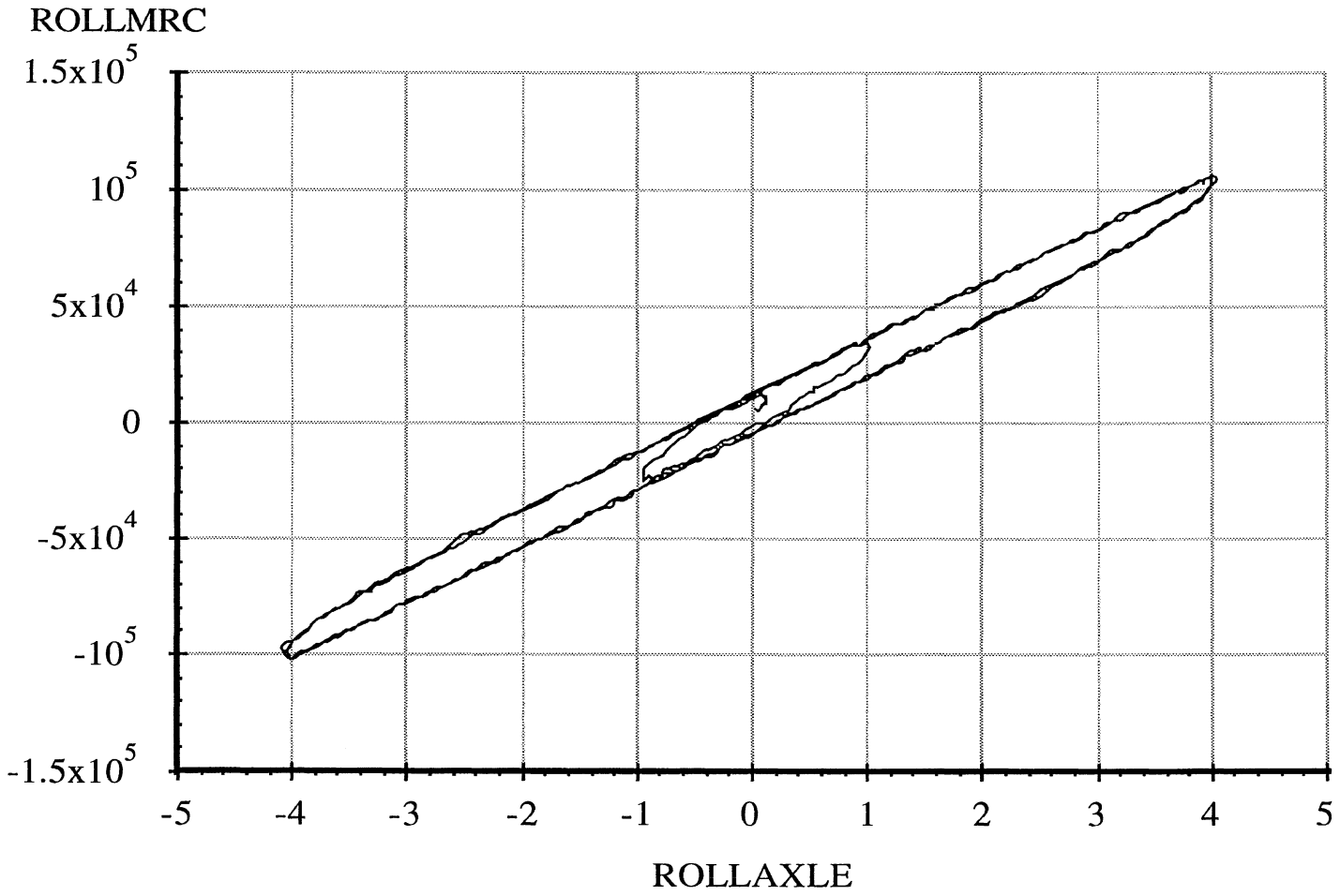

Abscissa (X): Axle roll angle (ROLLAXLE); degrees; right side compressed, positive.

Ordinate (Y): Axle roll moment about the roll center (ROLLMRC); in-lb; right side compressed, positive.

*Note: Brakes on. Force control. Pitman arm blocked.

Measured by UMTRI for Smart Truck
Freightliner Tractor

Data file: FRTLNS04.ERD

Single Steer Axle Suspension

Roll Center Height

6 April 96
Suspension: Taper-Leaf (2)

Suspension Load: 10000 lb.

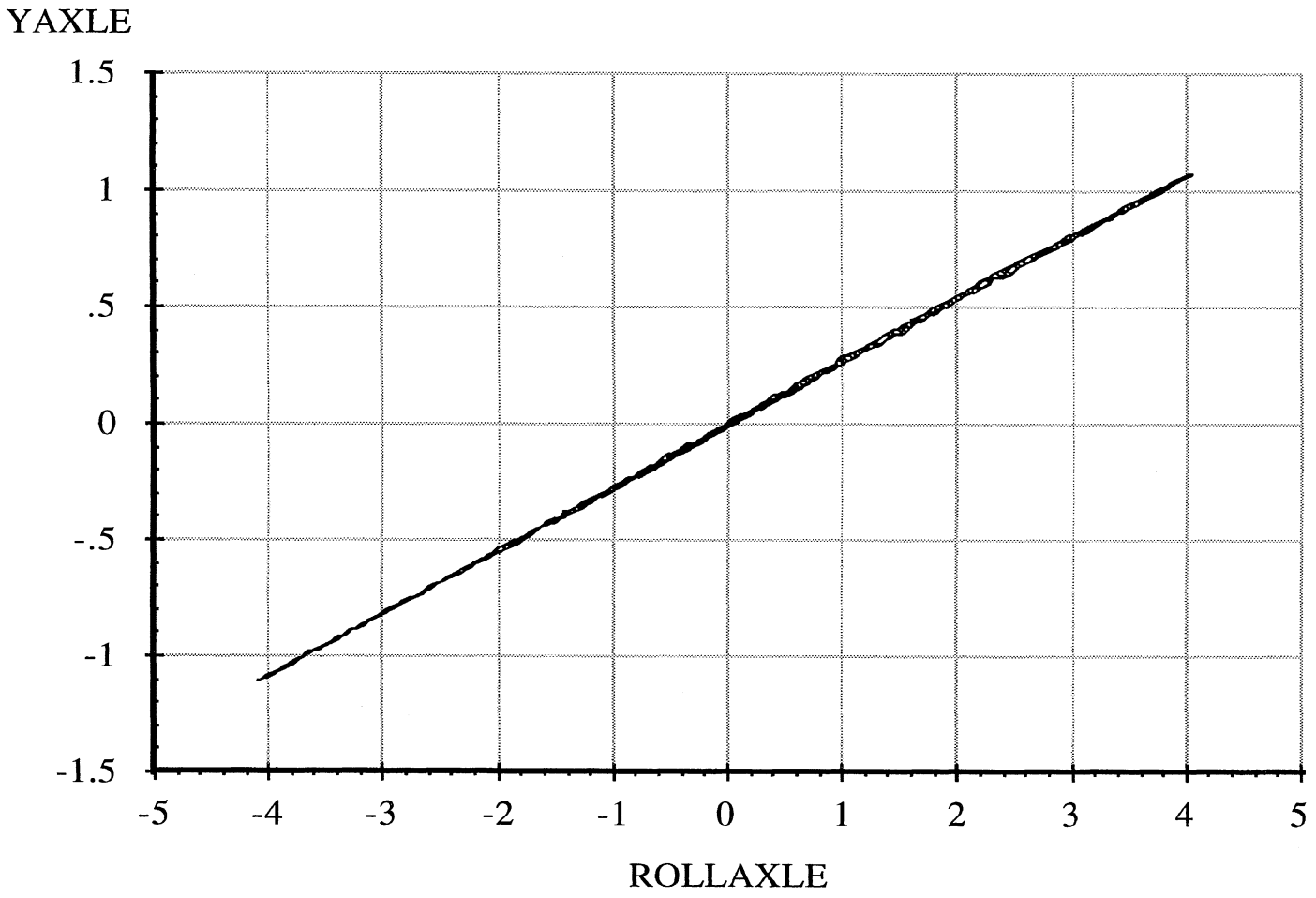

Abscissa (X): Axle roll angle (ROLLAXLE); degrees; right side compressed, positive.

Ordinate (Y): Axle reference point lateral translation (YAXLE); inches; motion toward right, positive.

*Note: Brakes on. Force control. Pitman arm blocked. Reference height of 3.75 inches.

Measured by UMTRI for Smart Truck
Freightliner Tractor

Data file: FRTLNS04.ERD

Single Steer Axle Suspension

Roll Steer

6 April 96
Suspension: Taper-Leaf (2)

Suspension Load: 10000 lb.

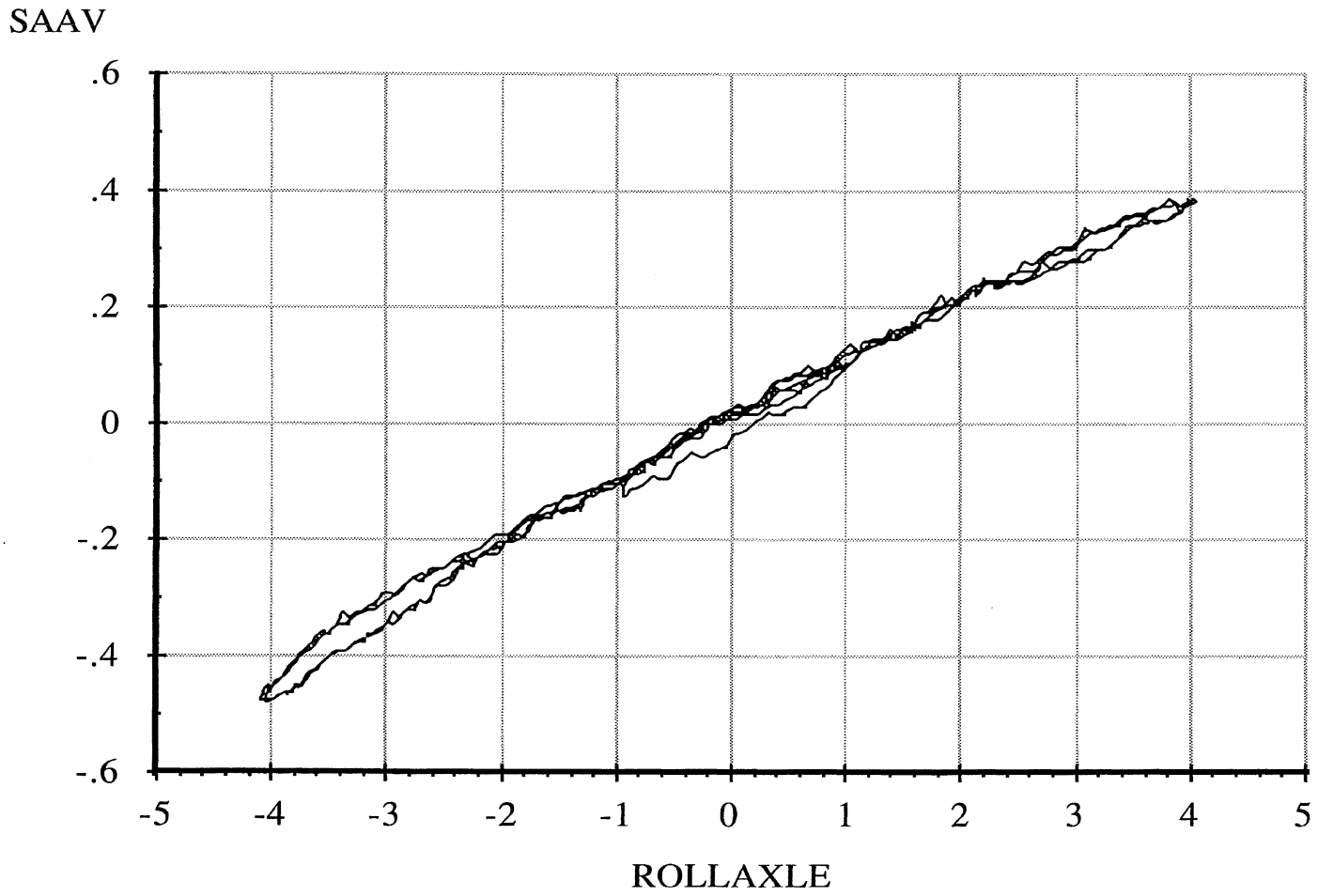

Abscissa (X): Axle roll angle (ROLLAXLE); degrees; right side compressed, positive.

Ordinate (Y): Average steer angle (SAAV); degrees; steer toward right, positive.

*Note: Brakes on. Force control. Pitman arm blocked.

Measured by UMTRI for Smart Truck
Freightliner Tractor

Data file: FRTLNS03.ERD

Single Steer Axle Suspension

Axle Roll Rate

6 April 96
Suspension: Taper-Leaf (2)

Suspension Load: 7500 lb.

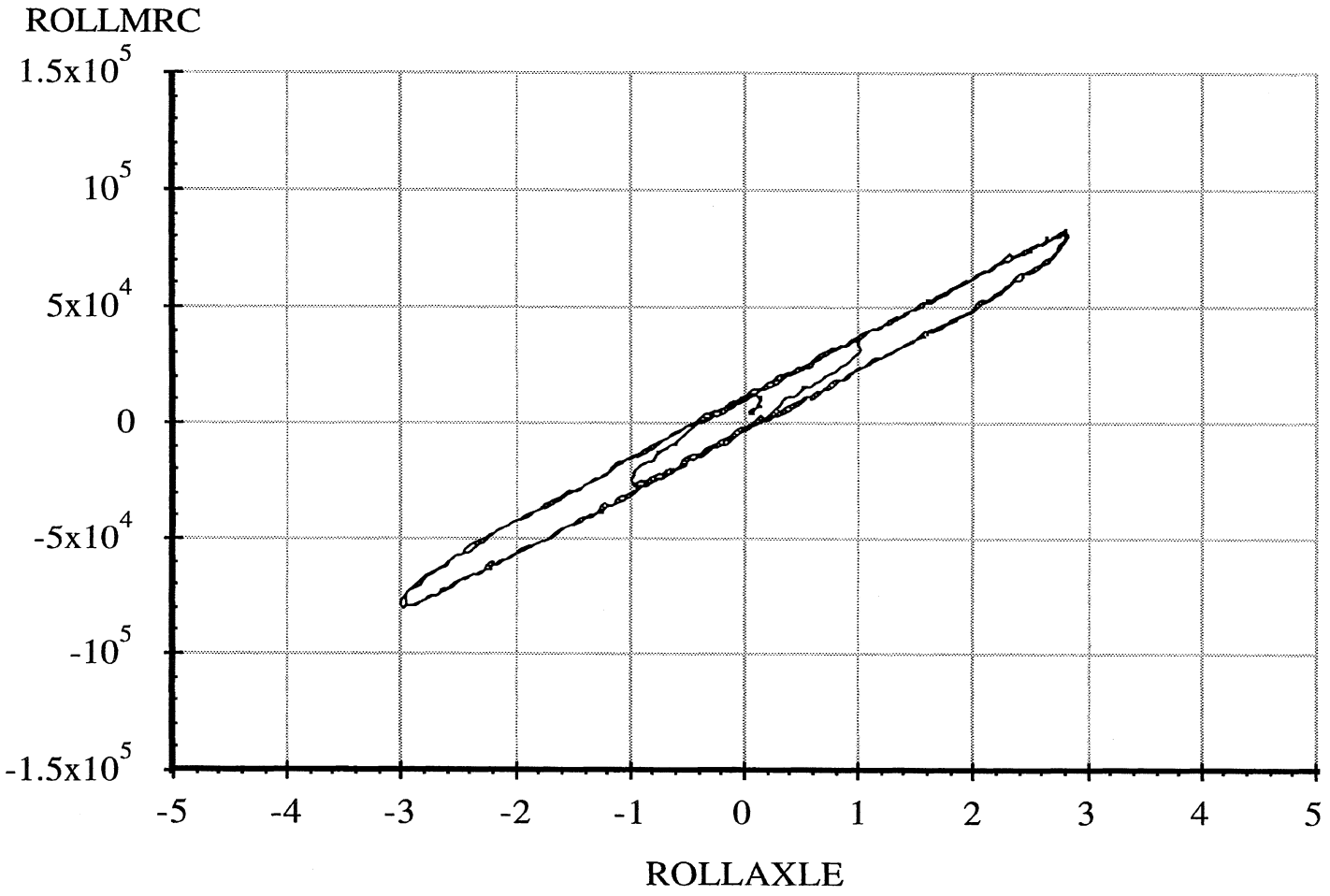

Abscissa (X): Axle roll angle (ROLLAXLE); degrees; right side compressed, positive.

Ordinate (Y): Axle roll moment about the roll center (ROLLMRC); in-lb; right side compressed, positive.

*Note: Brakes on. Force control. Pitman arm blocked.

Measured by UMTRI for Smart Truck
Freightliner Tractor

Data file: FRTLNS03.ERD

Single Steer Axle Suspension

Roll Center Height

6 April 96
Suspension: Taper-Leaf (2)

Suspension Load: 7500 lb.

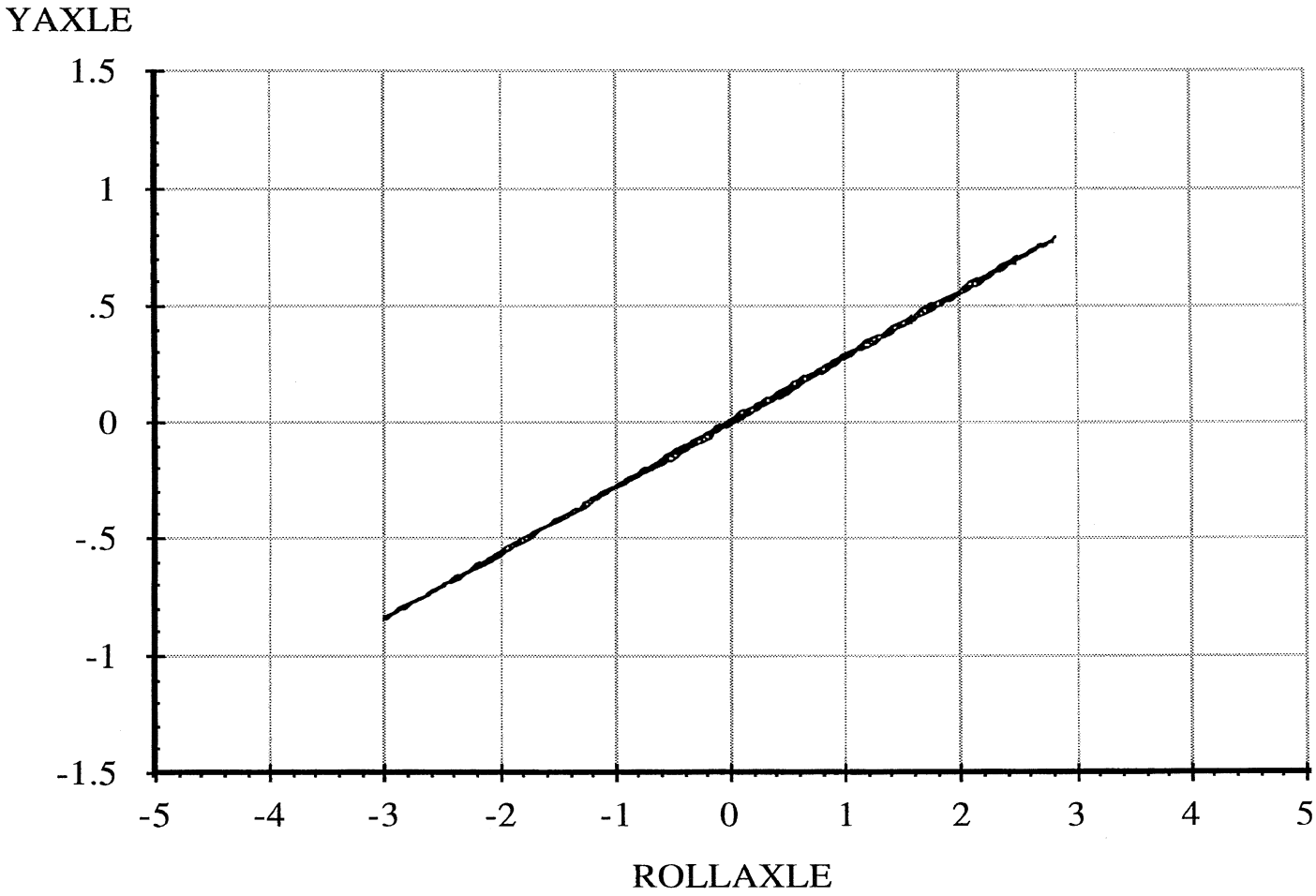

Abscissa (X): Axle roll angle (ROLLAXLE); degrees; right side compressed, positive.

Ordinate (Y): Axle reference point lateral translation (YAXLE); inches; motion toward right, positive.

*Note: Brakes on. Force control. Pitman arm blocked. Reference height of 4.00 inches.

Measured by UMTRI for Smart Truck
Freightliner Tractor

Data file: FRTLNS03.ERD

Single Steer Axle Suspension

Roll Steer

6 April 96
Suspension: Taper-Leaf (2)

Suspension Load: 7500 lb.

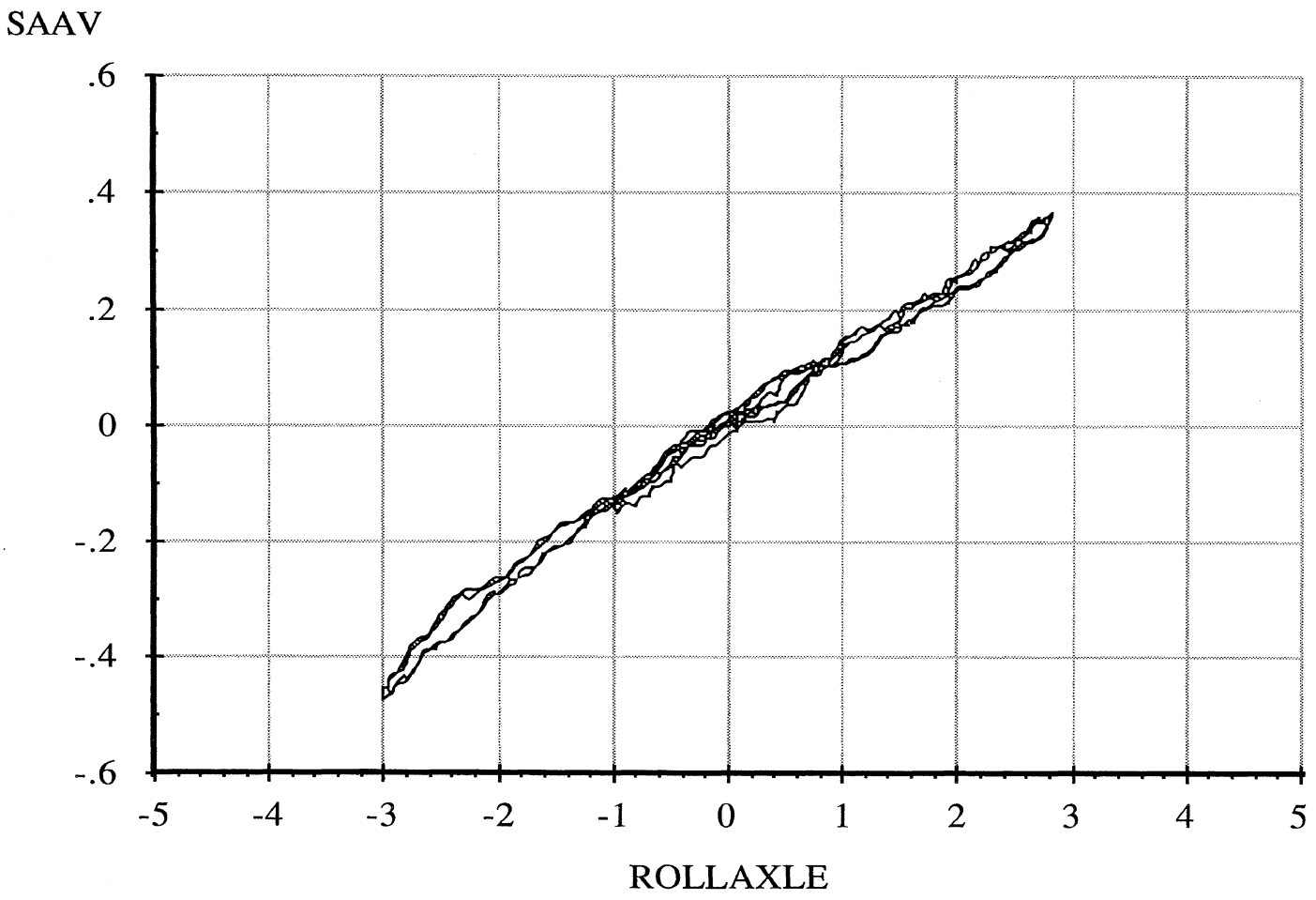

Abscissa (X): Axle roll angle (ROLLAXLE); degrees; right side compressed, positive.

Ordinate (Y): Average steer angle (SAAV); degrees; steer toward right, positive.

*Note: Brakes on. Force control. Pitman arm blocked.

Measured by UMTRI for Smart Truck
Freightliner Tractor

Data file: FRTLNS02.ERD

Single Steer Axle Suspension

Axle Roll Rate

6 April 96
Suspension: Taper-Leaf (2)

Suspension Load: 5000 lb.

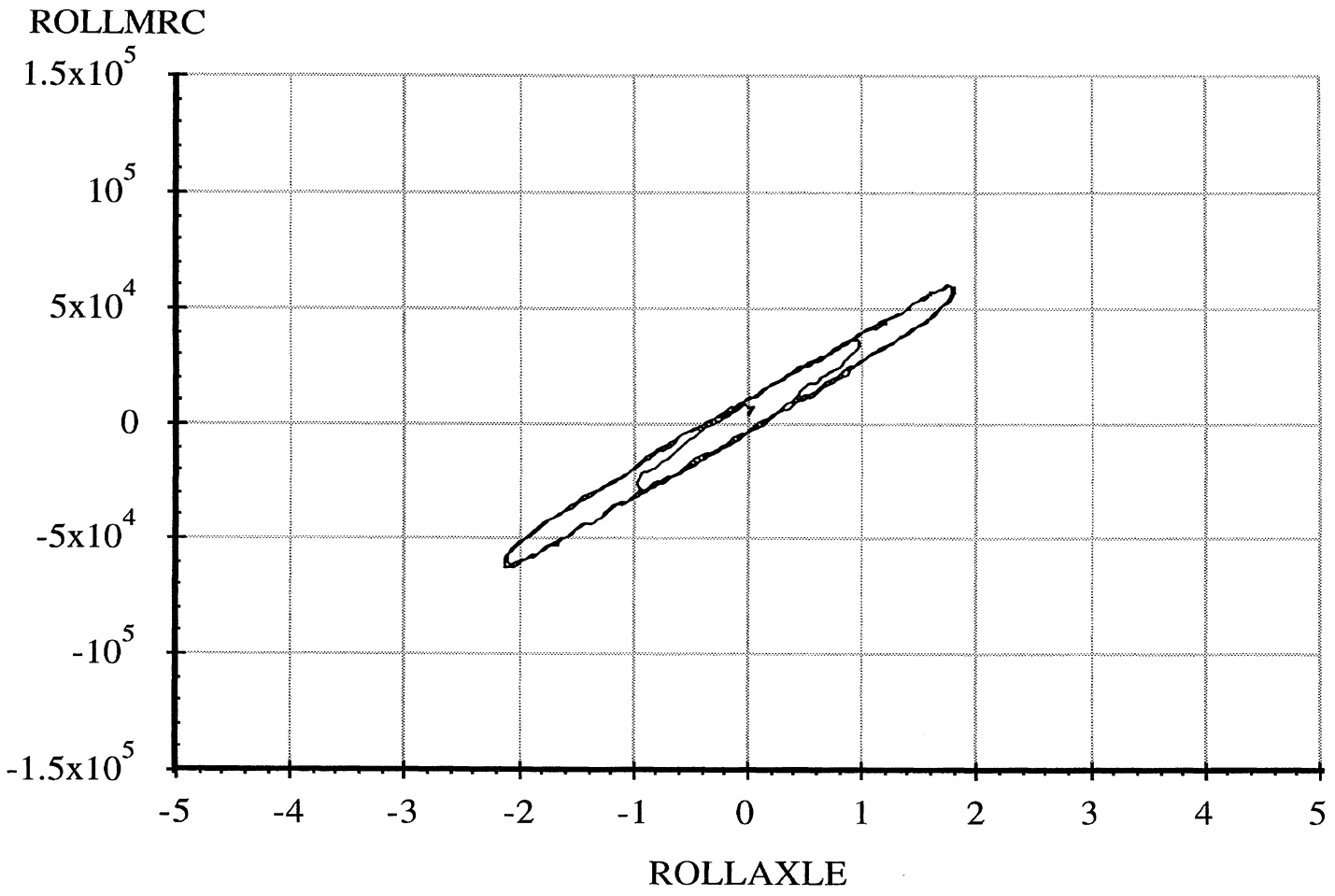

Abscissa (X): Axle roll angle (ROLLAXLE); degrees; right side compressed, positive.

Ordinate (Y): Axle roll moment about the roll center (ROLLMRC); in-lb; right side compressed, positive.

*Note: Brakes on. Force control. Pitman arm blocked.

Measured by UMTRI for Smart Truck
Freightliner Tractor

Data file: FRTLNS02.ERD

Single Steer Axle Suspension

Roll Center Height

6 April 96
Suspension: Taper-Leaf (2)

Suspension Load: 5000 lb.

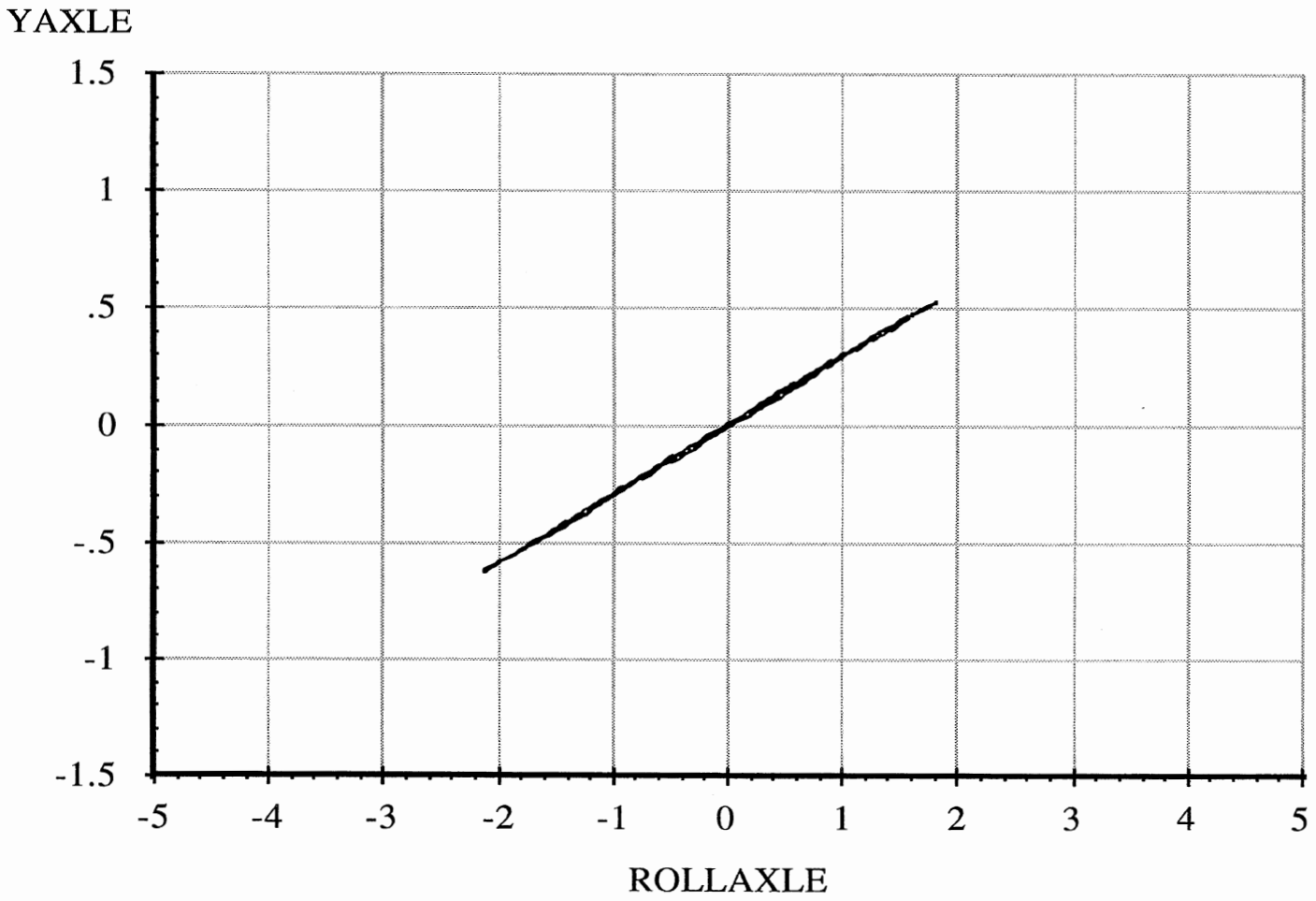

Abscissa (X): Axle roll angle (ROLLAXLE); degrees; right side compressed, positive.

Ordinate (Y): Axle reference point lateral translation (YAXLE); inches; motion toward right, positive.

*Note: Brakes on. Force control. Pitman arm blocked. Reference height of 4.25inches.

Measured by UMTRI for Smart Truck
Freightliner Tractor

Data file: FRTLNS02.ERD

Single Steer Axle Suspension

Roll Steer

6 April 96
Suspension: Taper-Leaf (2)

Suspension Load: 5000 lb.

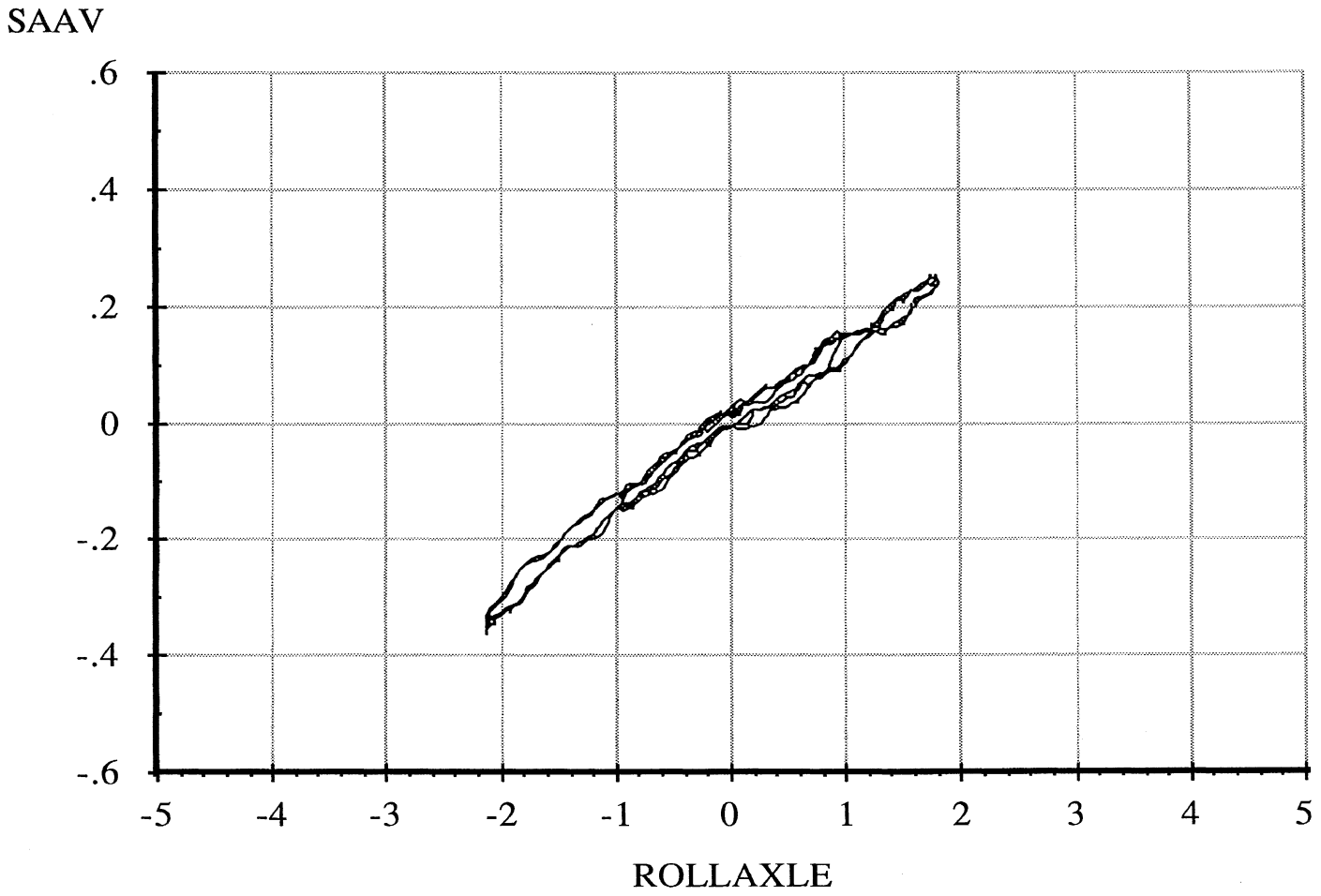

Abscissa (X): Axle roll angle (ROLLAXLE); degrees; right side compressed, positive.

Ordinate (Y): Average steer angle (SAAV); degrees; steer toward right, positive.

*Note: Brakes on. Force control. Pitman arm blocked.

Measured by UMTRI for Smart Truck
Freightliner Tractor

Data file: FRTLNS16.ERD

Single Steer Axle Suspension

Lateral Force Compliance

6 April 96
Suspension: Taper-Leaf (2)

Suspension Load: 14000 lb.

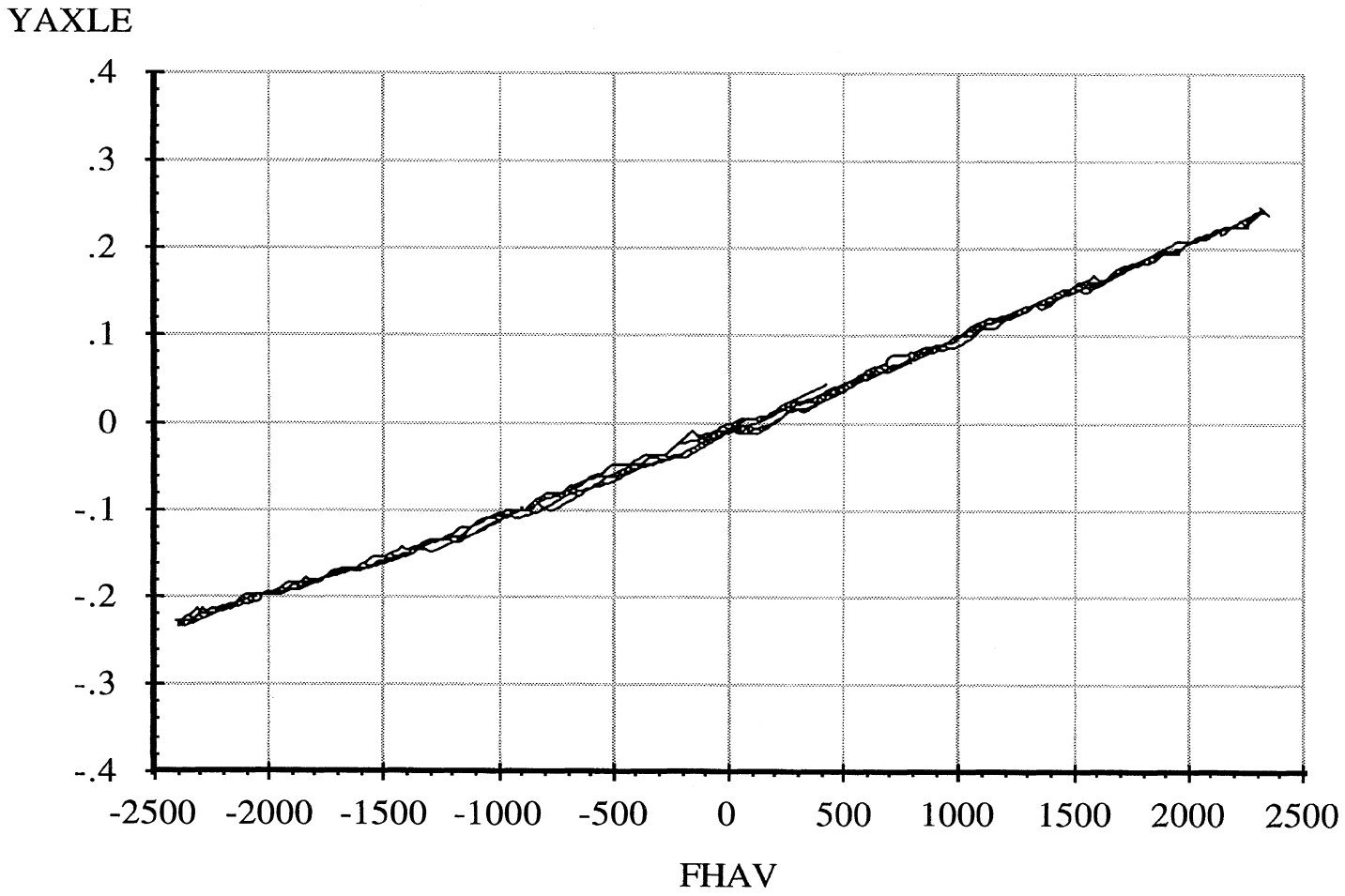

Abscissa (X): Average axle lateral force (FHAV); pounds; applied to both wheels simultaneously; force applied toward right, positive.

Ordinate (Y): Axle lateral translation (YAXLE); inches; motion toward right, positive.

*Note: Brakes on. Position control. Pitman arm blocked.

Measured by UMTRI for Smart Truck
Freightliner Tractor

Data file: FRTLNS15.ERD

Single Steer Axle Suspension

Lateral Force Compliance

6 April 96
Suspension: Taper-Leaf (2)

Suspension Load: 12000 lb.

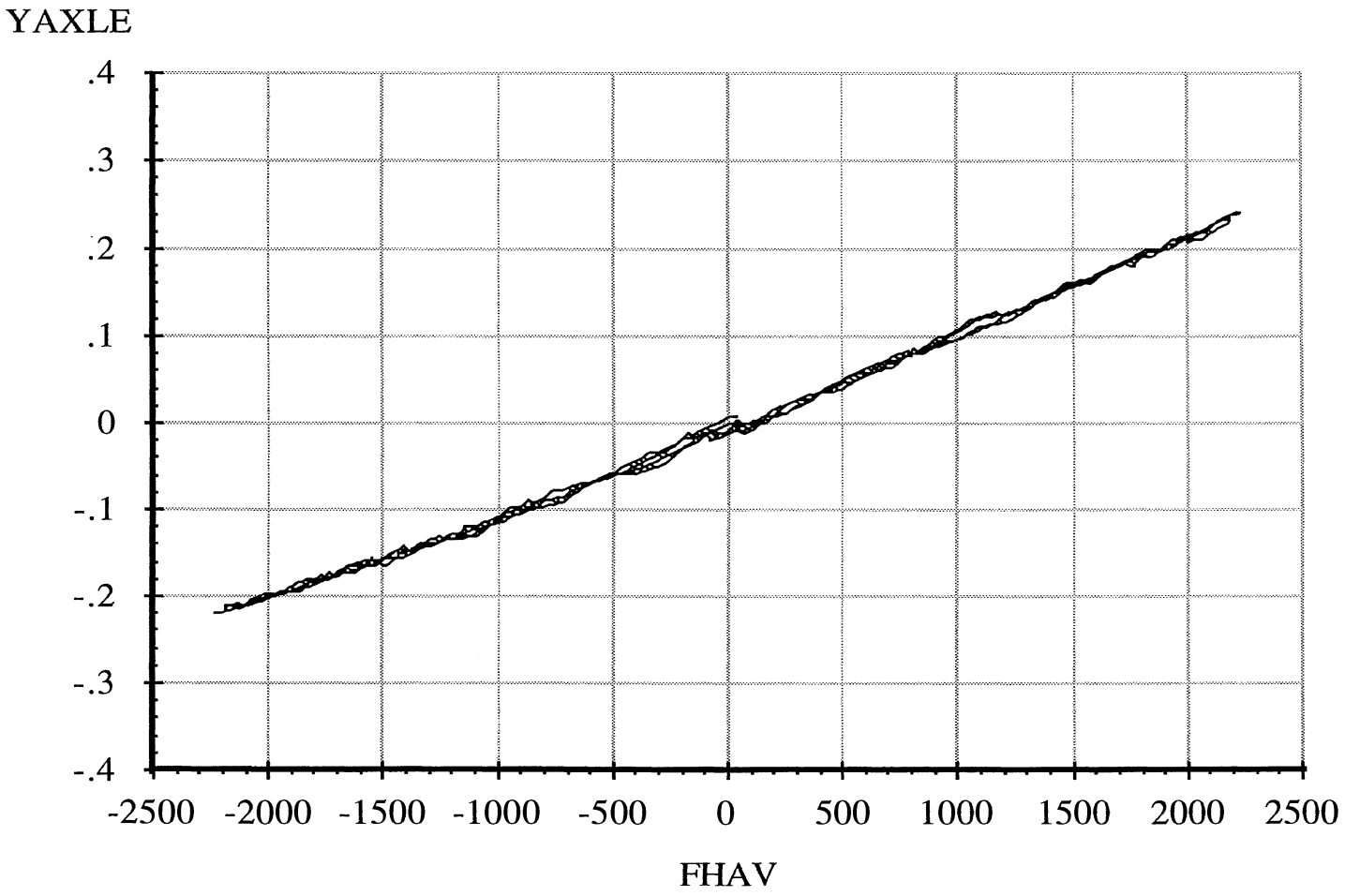

Abscissa (X): Average axle lateral force (FHAV); pounds; applied to both wheels simultaneously; force applied toward right, positive.

Ordinate (Y): Axle lateral translation (YAXLE); inches; motion toward right, positive.

*Note: Brakes on. Position control. Pitman arm blocked.

Measured by UMTRI for Smart Truck
Freightliner Tractor

Data file: FRTLNS14.ERD

Single Steer Axle Suspension

Lateral Force Compliance

6 April 96
Suspension: Taper-Leaf (2)

Suspension Load: 10000 lb.

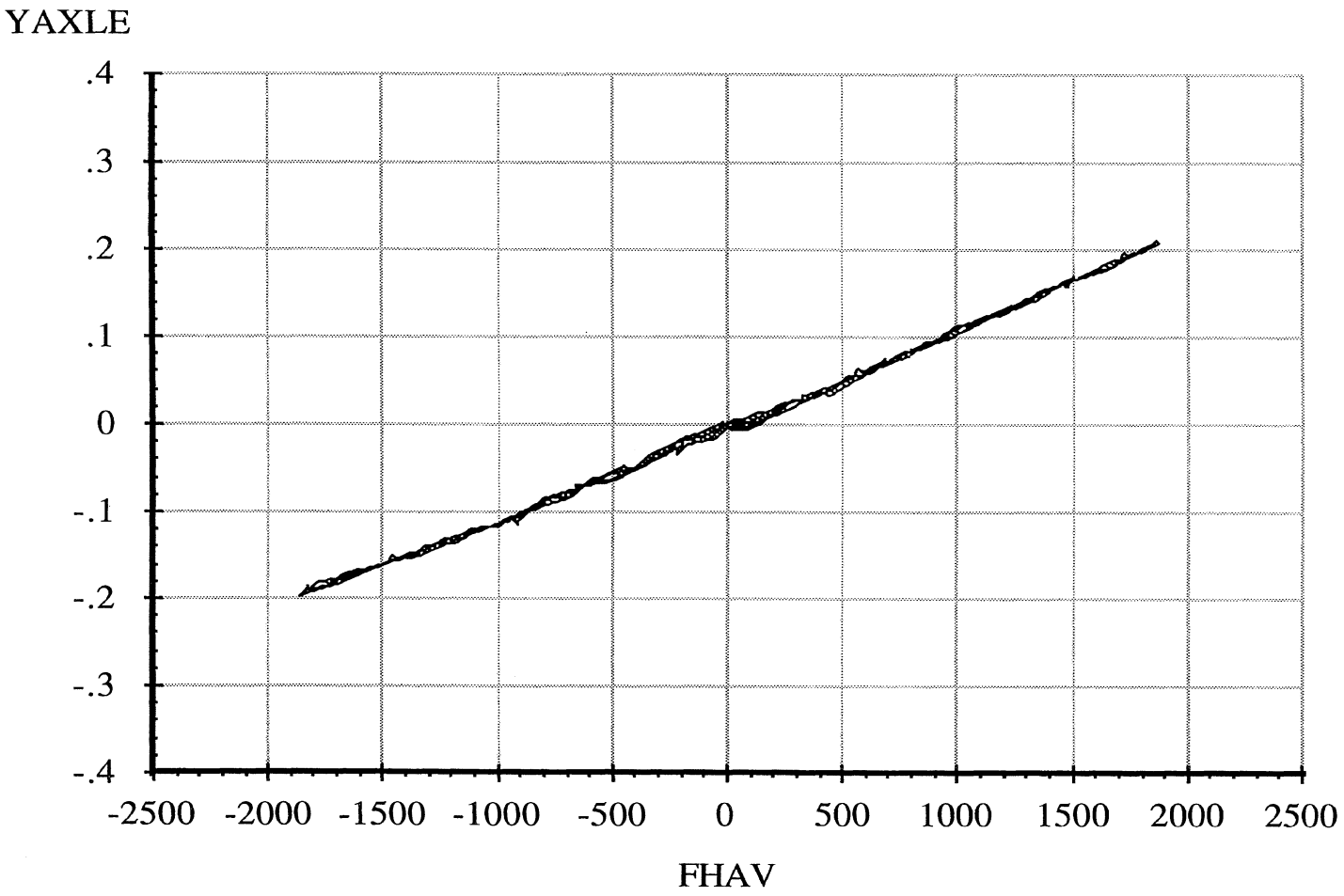

Abscissa (X): Average axle lateral force (FHAV); pounds; applied to both wheels simultaneously; force applied toward right, positive.

Ordinate (Y): Axle lateral translation (YAXLE); inches; motion toward right, positive.

*Note: Brakes on. Position control. Pitman arm blocked.

Measured by UMTRI for Smart Truck
Freightliner Tractor

Data file: FRTLNS13.ERD

Single Steer Axle Suspension

Lateral Force Compliance

6 April 96
Suspension: Taper-Leaf (2)

Suspension Load: 7500 lb.

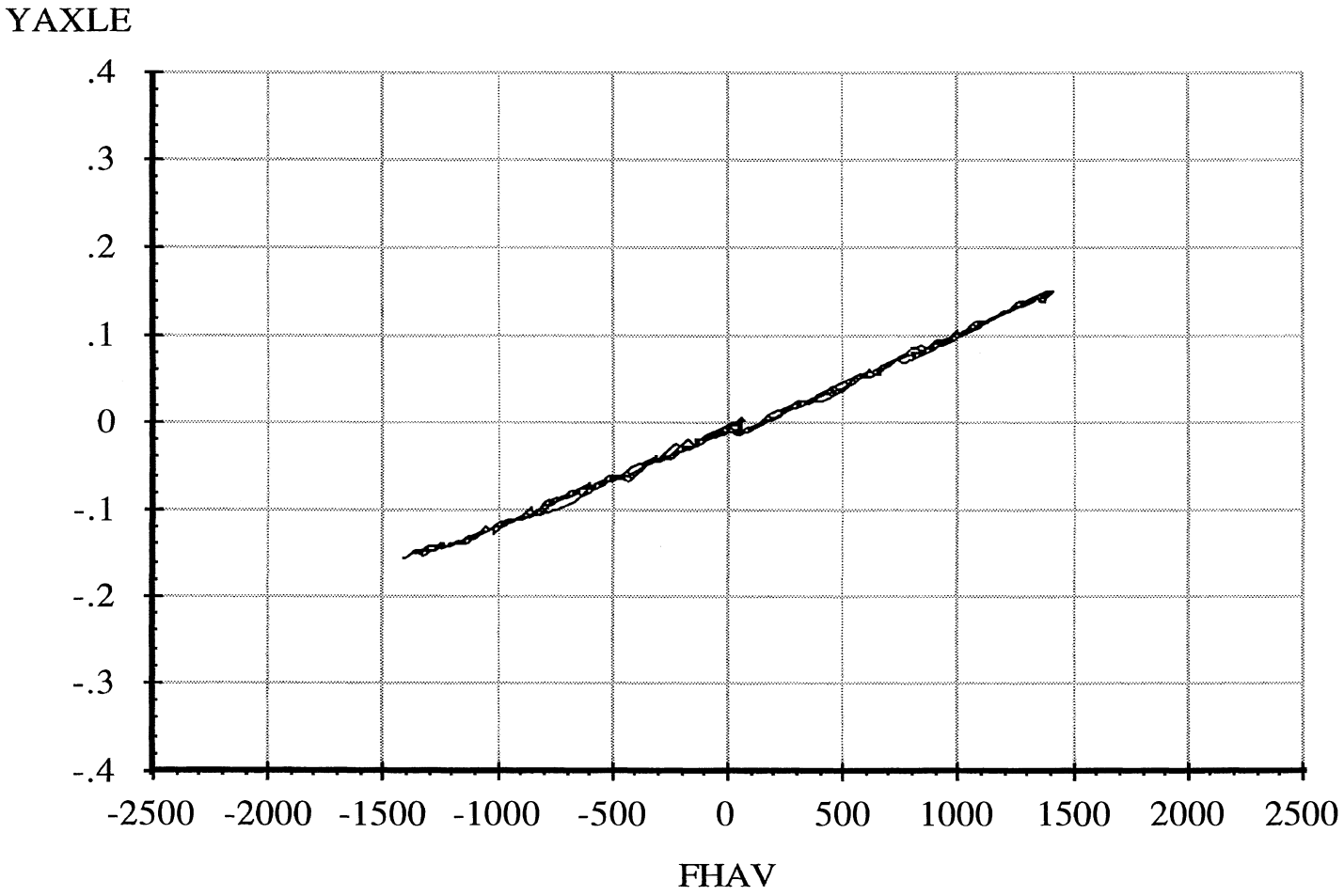

Abscissa (X): Average axle lateral force (FHAV); pounds; applied to both wheels simultaneously; force applied toward right, positive.

Ordinate (Y): Axle lateral translation (YAXLE); inches; motion toward right, positive.

*Note: Brakes on. Position control. Pitman arm blocked.

Measured by UMTRI for Smart Truck
Freightliner Tractor

Data file: FRTLNS12.ERD

Single Steer Axle Suspension

Lateral Force Compliance

6 April 96
Suspension: Taper-Leaf (2)

Suspension Load: 5000 lb.

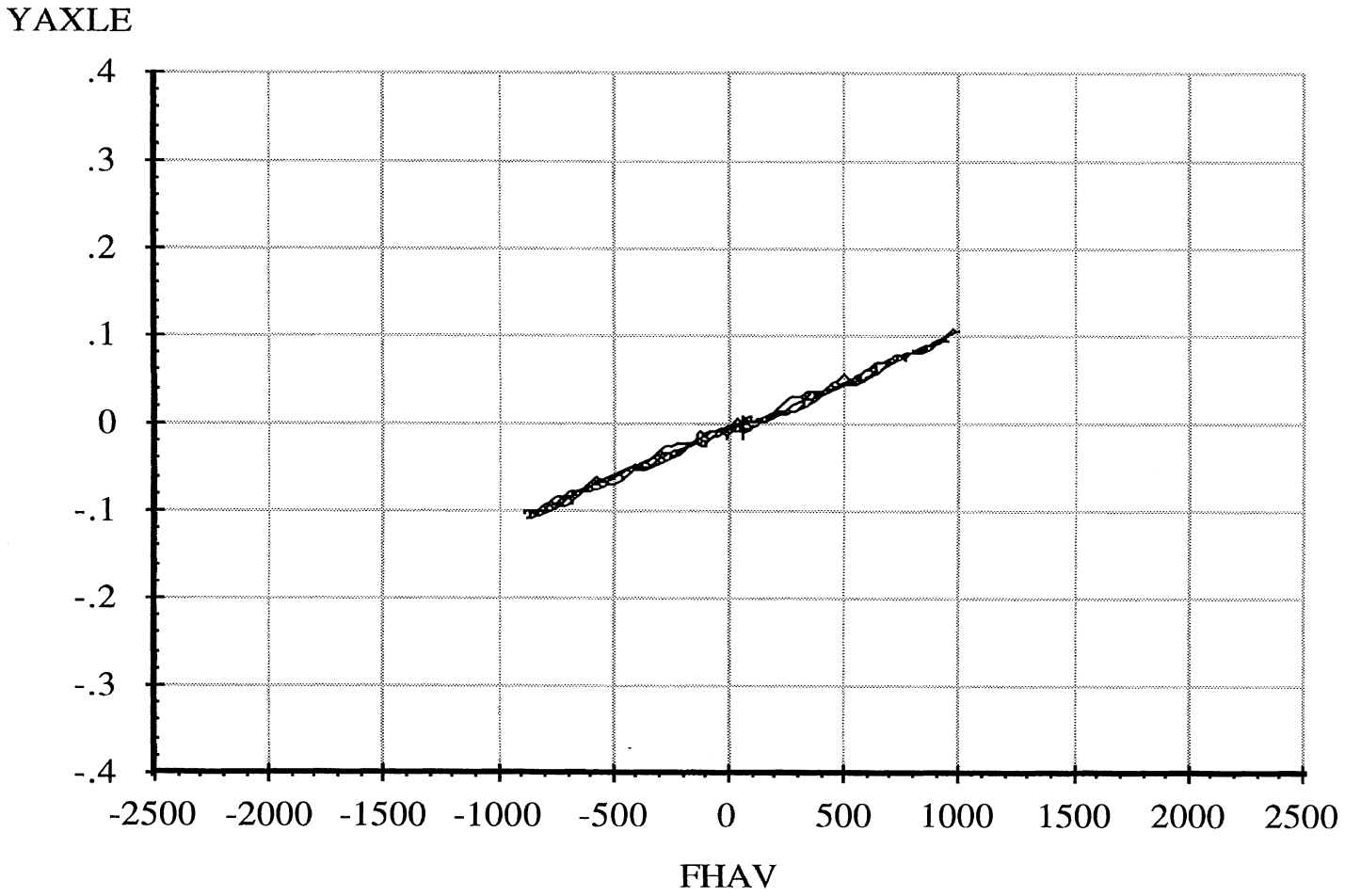

Abscissa (X): Average axle lateral force (FHAV); pounds; applied to both wheels simultaneously; force applied toward right, positive.

Ordinate (Y): Axle lateral translation (YAXLE); inches; motion toward right, positive.

*Note: Brakes on. Position control. Pitman arm blocked.

Measured by UMTRI for Smart Truck
Freightliner Tractor

Data file: FRTLNG50.ERD

Drive Axle Suspension, Trailing Only

Average Vertical Spring Rate

6 April 96
Suspension: Trailing Arm (2LU)

Nominal Suspension Load: 20000 lb.

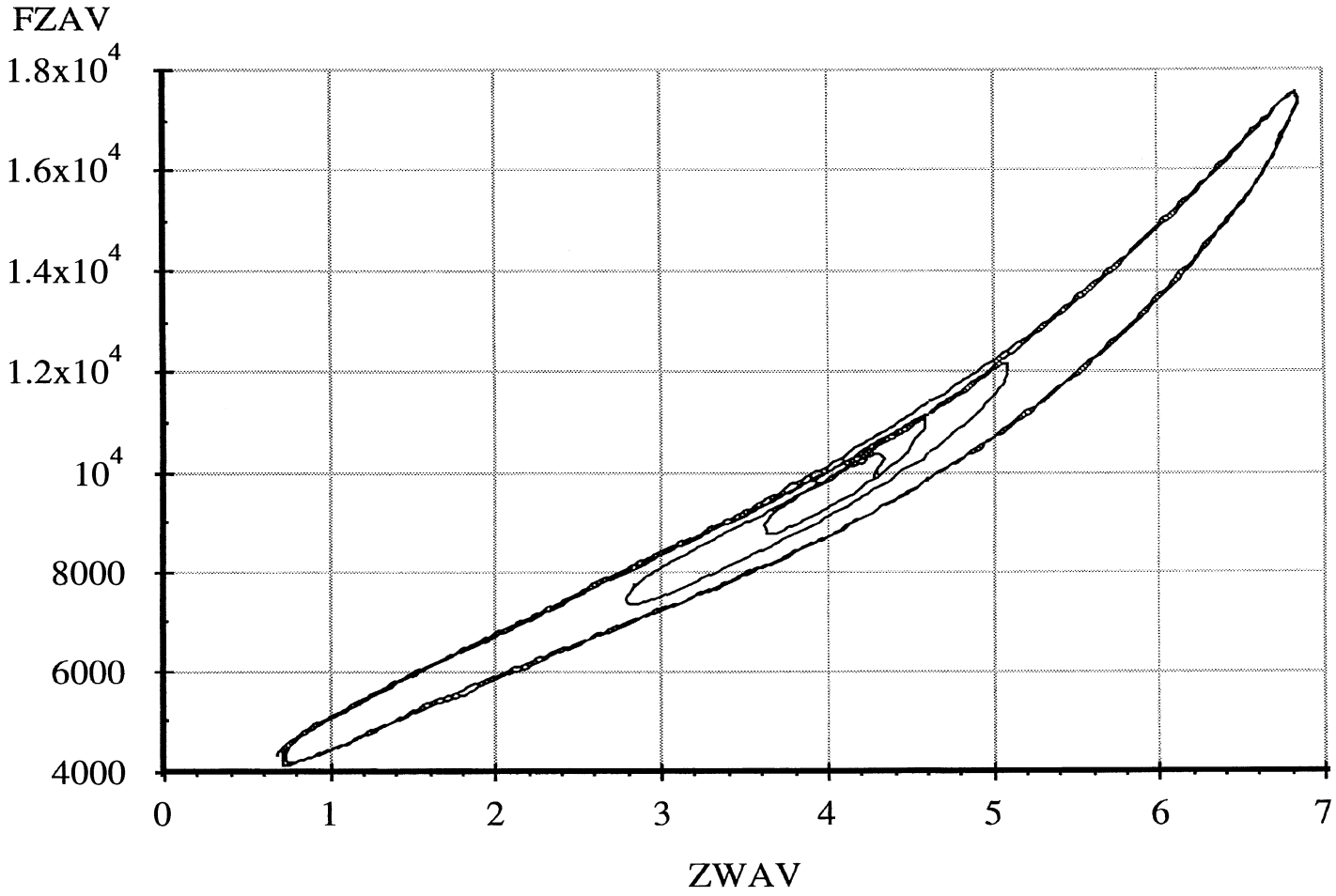

Abscissa (X): Average vertical wheel displacement (ZWAV); inches; spring compression, positive.

Ordinate (Y): Average vertical wheel load (FZAV); pounds; spring compression, positive.

*Note: Brakes on. Position control. Air bags inflated to 70.5 psi. Low side of vertical.

Measured by UMTRI for Smart Truck
Freightliner Tractor

Data file: FRTLNG54.ERD

Drive Axle Suspension, Trailing Only

Average Vertical Spring Rate

6 April 96
Suspension: Trailing Arm (2LU)

Nominal Suspension Load: 20000 lb.

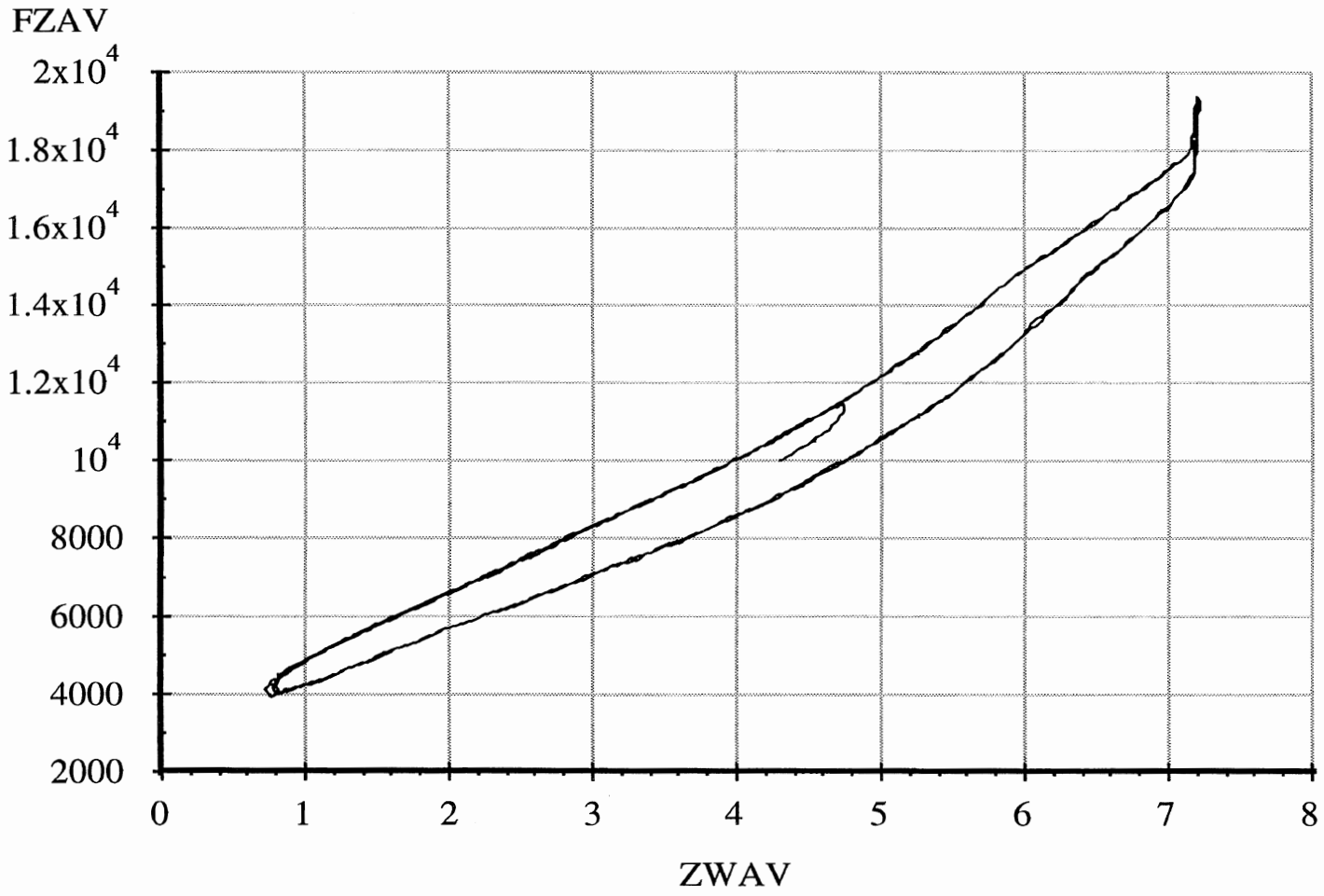

Abscissa (X): Average vertical wheel displacement (ZWAV); inches; spring compression, positive.

Ordinate (Y): Average vertical wheel load (FZAV); pounds; spring compression, positive.

*Note: Brakes on. Position control. Air bags inflated to 70.5 psi. High side of vertical.

Measured by UMTRI for Smart Truck
Freightliner Tractor

Data file: FRTLNG51.ERD

Drive Axle Suspension, Trailing Only

Axle Roll Rate

6 April 96
Suspension: Trailing Arm (2LU)

Suspension Load: 20000 lb.

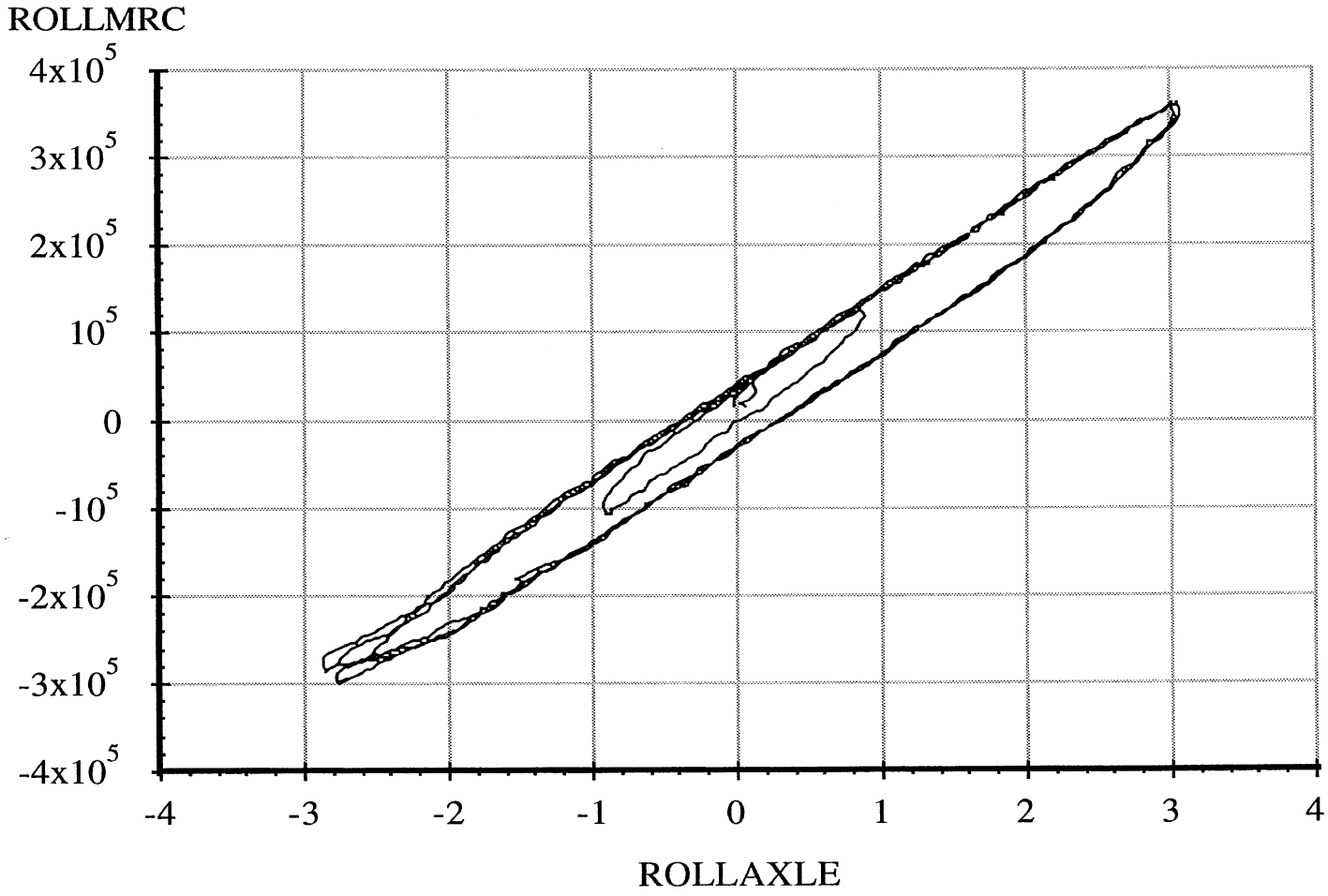

Abscissa (X): Axle roll angle (ROLLAXLE); degrees; right side compressed, positive.

Ordinate (Y): Axle roll moment about the roll center (ROLLMRC); in-lb; right side compressed, positive.

*Note: Brakes on. Force control. Air bags inflated to 70.5 psi.

Measured by UMTRI for Smart Truck
Freightliner Tractor

Data file: FRTLNG51.ERD

Drive Axle Suspension, Trailing Only

Roll Center Height

6 April 96
Suspension: Trailing Arm (2LU)

Suspension Load: 20000 lb.

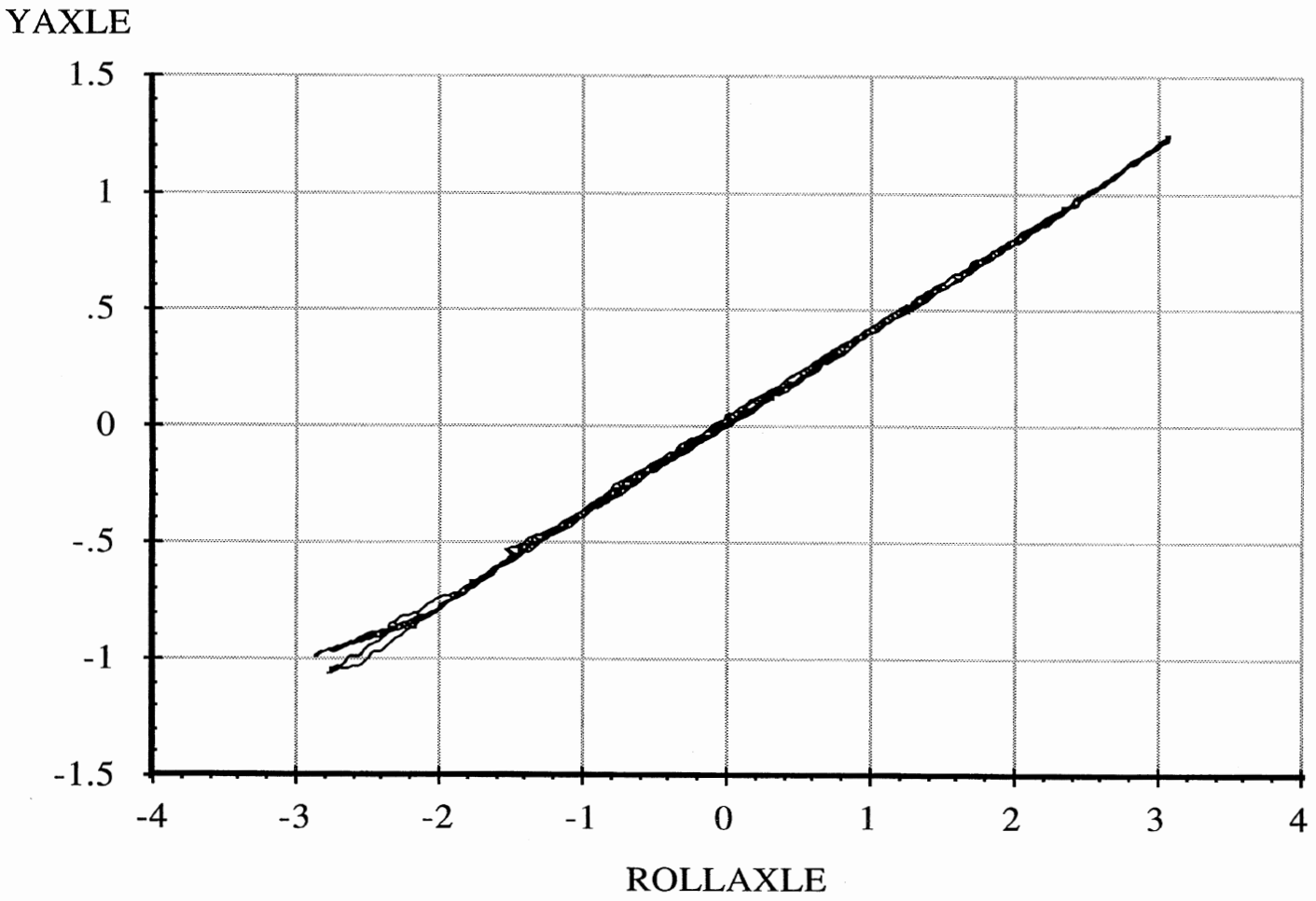

Abscissa (X): Axle roll angle (ROLLAXLE); degrees; right side compressed, positive.

Ordinate (Y): Axle reference point lateral translation (YAXLE); inches; motion toward right, positive.

*Note: Brakes on. Force control. Air bags inflated to 70.5 psi. Reference height of 7.69 inches.

Measured by UMTRI for Smart Truck
Freightliner Tractor

Data file: FRTLNG51.ERD

Drive Axle Suspension, Trailing Only

Roll Steer

6 April 96
Suspension: Trailing Arm (2LU)

Suspension Load: 20000 lb.

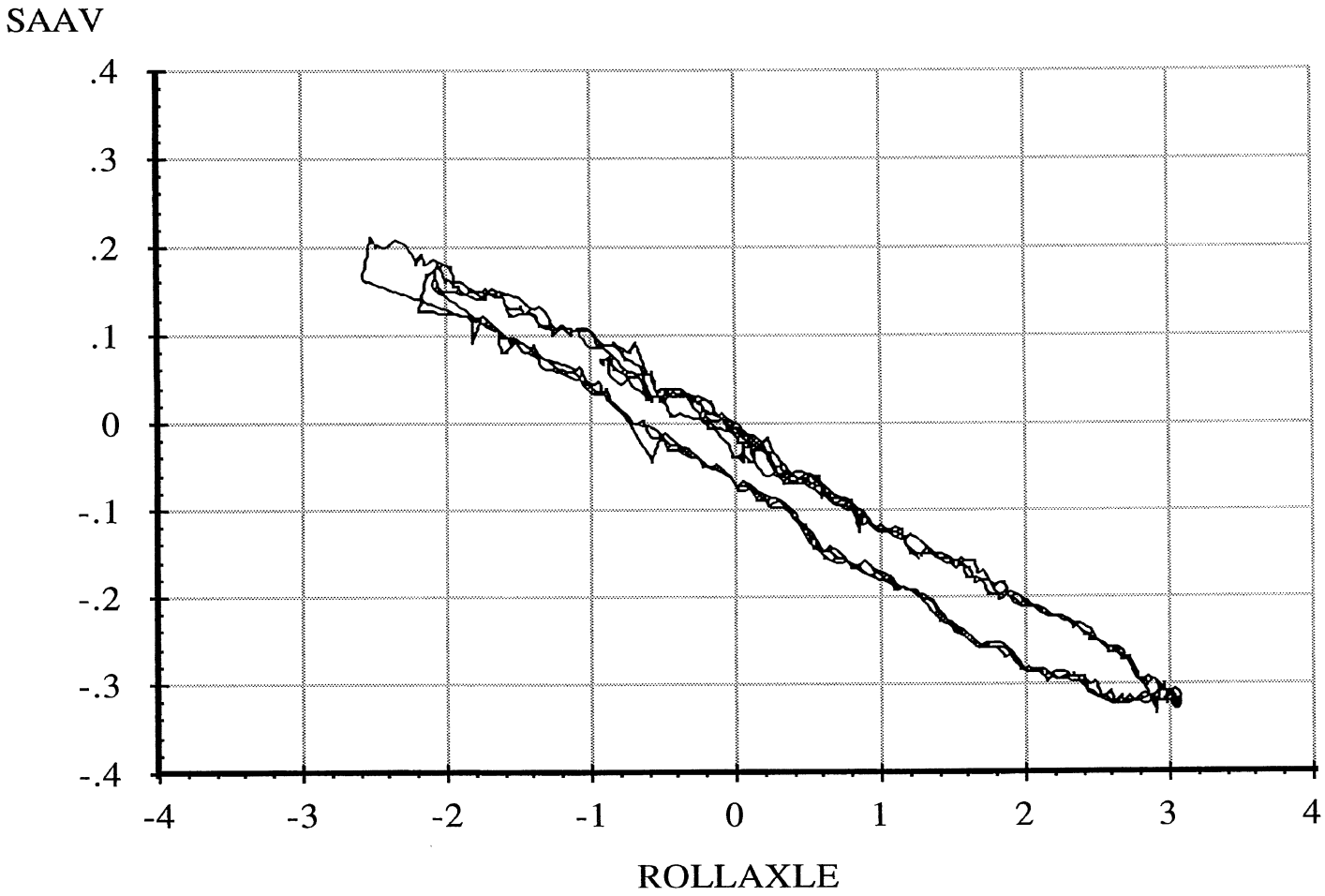

Abscissa (X): Axle roll angle (ROLLAXLE); degrees; right side compressed, positive.

Ordinate (Y): Average steer angle (SAAV); degrees; steer toward right, positive.

*Note: Brakes on. Force control. Air bags inflated to 70.5 psi.

Measured by UMTRI for Smart Truck
Freightliner Tractor

Data file: FRTLNG52.ERD

Drive Axle Suspension, Trailing Only

Lateral Force Compliance

6 April 96
Suspension: Trailing Arm (2LU)

Suspension Load: 20000 lb.

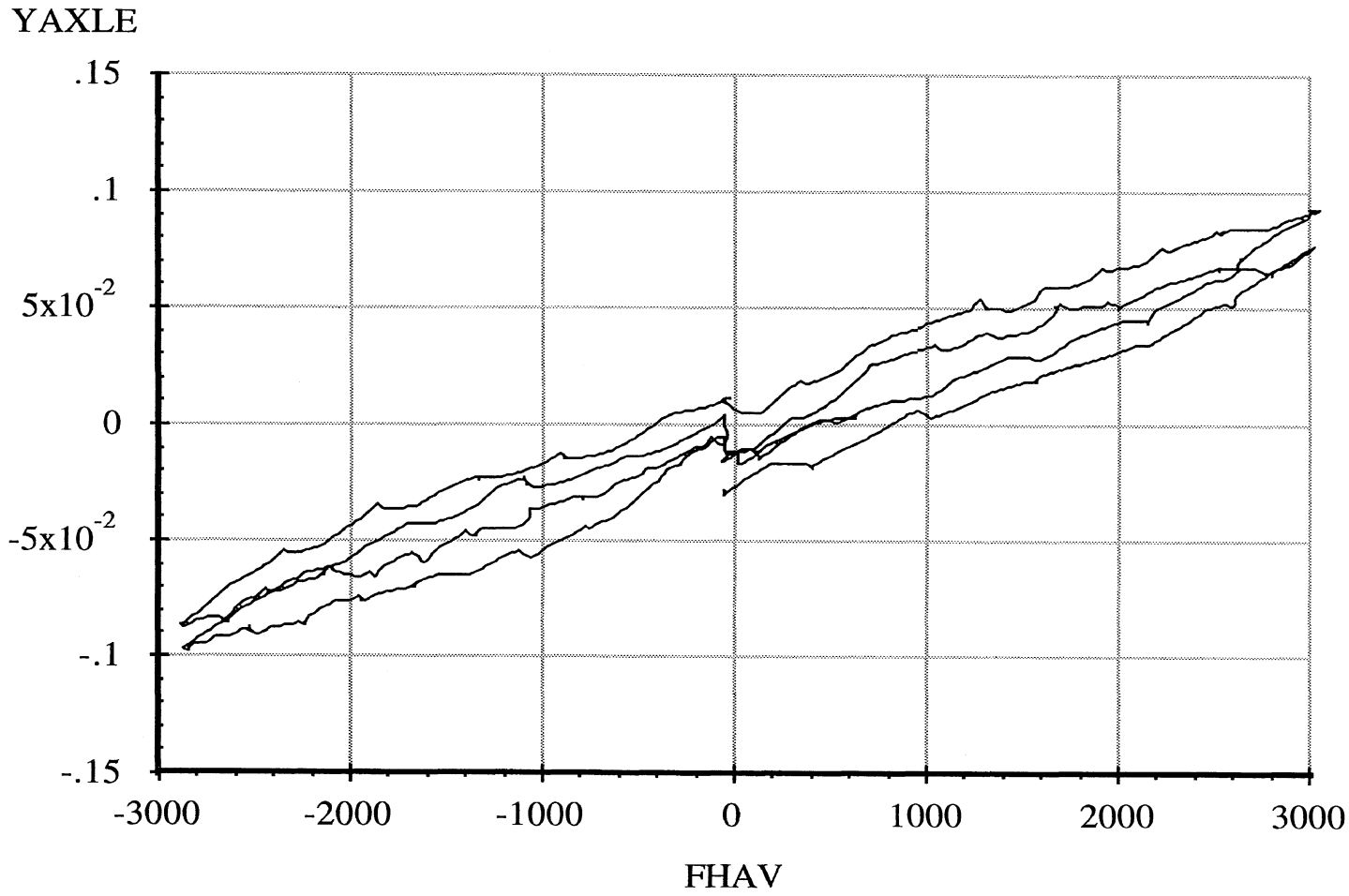

Abscissa (X): Average axle lateral force (FHAV); pounds; applied to both wheels simultaneously; force applied toward right, positive.

Ordinate (Y): Axle lateral translation (YAXLE); inches; motion toward right, positive.

*Note: Brakes on. Position control. Air bags inflated to 70.5 psi. Reference height of 7.69 inches.

Measured by UMTRI for Smart Truck
Freightliner Tractor

Data file: FRTLNG52.ERD

Drive Axle Suspension, Trailing Only

Lateral Force Steer

6 April 96
Suspension: Trailing Arm (2LU)

Suspension Load: 20000 lb.

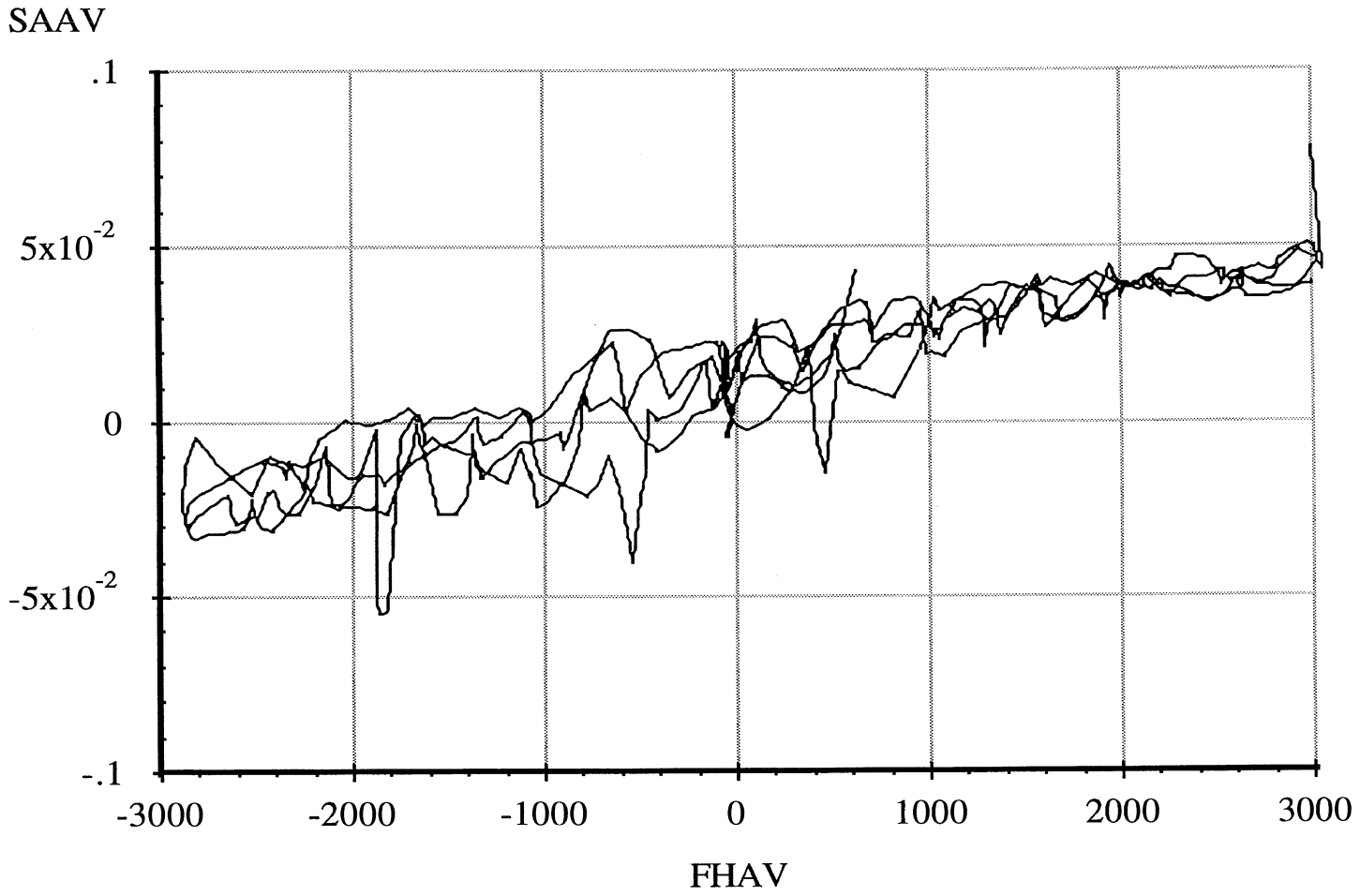

Abscissa (X): Average axle lateral force (FHAV); pounds; applied to both wheels simultaneously; force applied toward right, positive.

Ordinate (Y): Average steer angle (SAAV); degrees; steer toward right, positive.

*Note: Brakes on. Position control. Air bags inflated to 70.5 psi.

Measured by UMTRI for Smart Truck
Freightliner Tractor

Data file: FRTLNG53.ERD

Drive Axle Suspension, Trailing Only

Aligning Moment Compliance Steer

6 April 96
Suspension: Trailing Arm (2LU)

Suspension Load: 20000 lb.

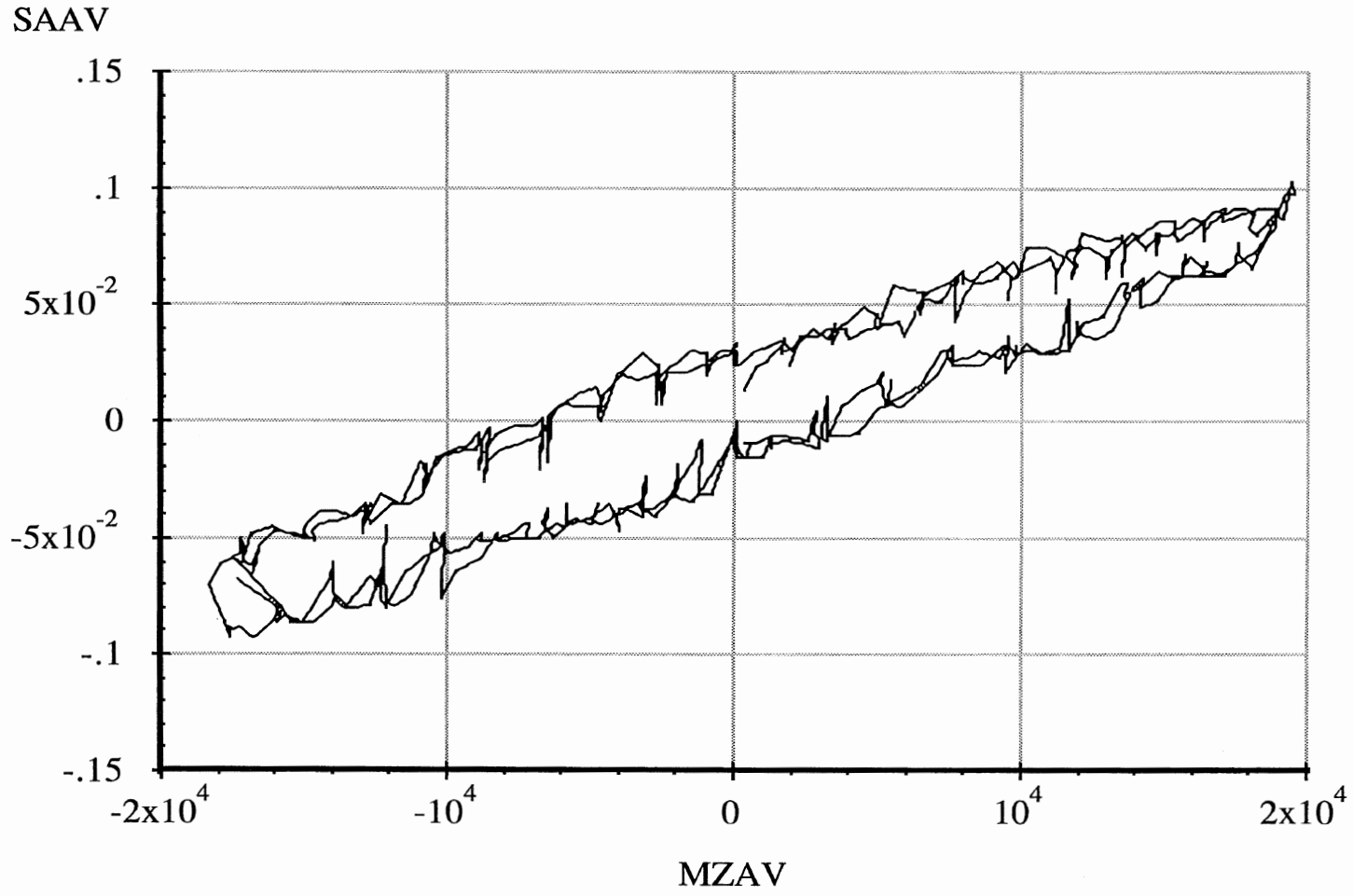

Abscissa (X): Average axle aligning moment (MZAV); in-lb per wheel; applied to both wheels simultaneously; downward (right hand rule) moment vector, positive.

Ordinate (Y): Average steer angle (SAAV); degrees; steer toward right, positive.

*Note: Brakes on. Position control. Air bags inflated to 70.5 psi.

Measured by UMTRI for Smart Truck
Freightliner Tractor

Data file: FRTLNG40.ERD

Drive Axle Suspension, Trailing Only

Average Vertical Spring Rate

6 April 96
Suspension: Trailing Arm (2LU)

Nominal Suspension Load: 18000 lb.

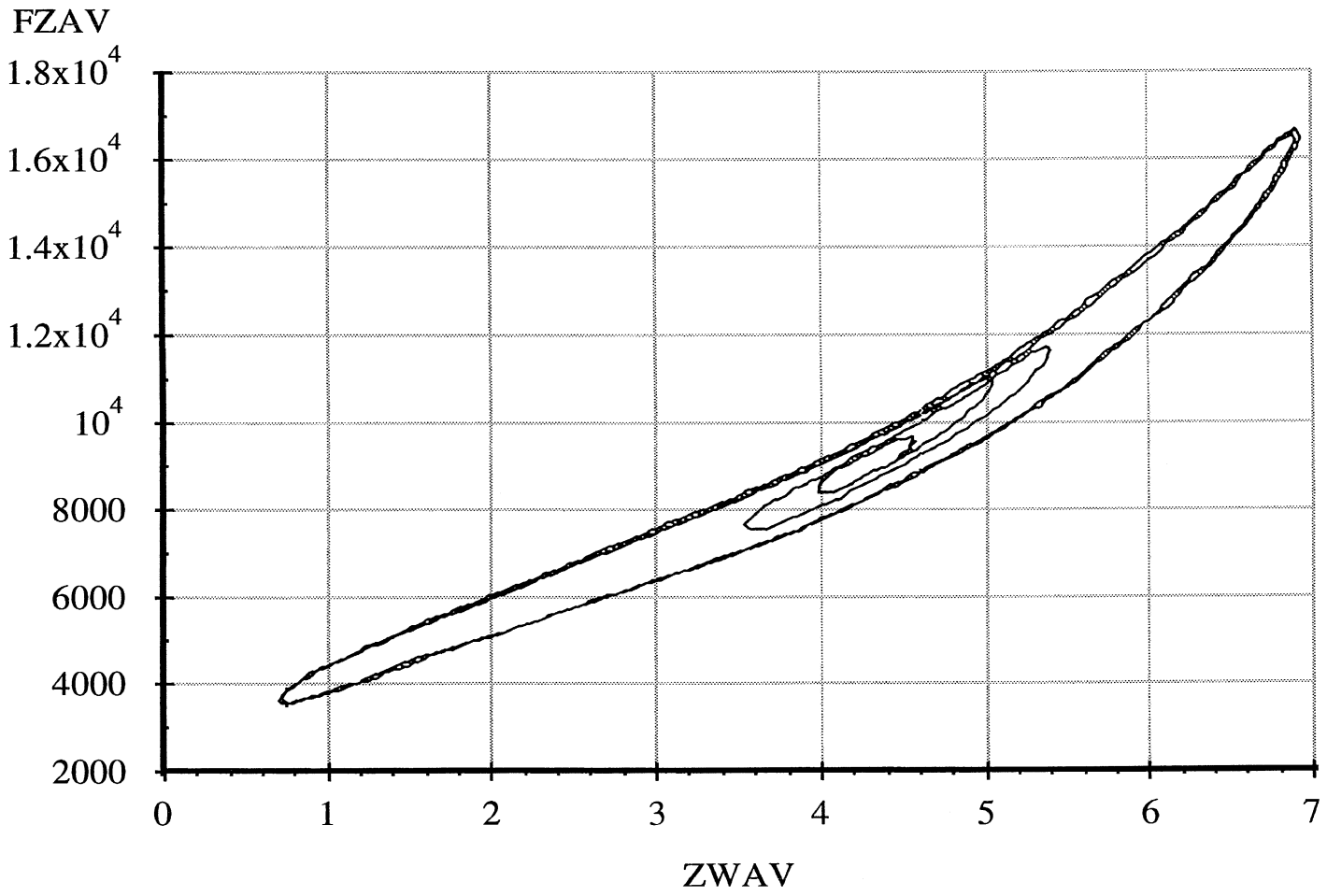

Abscissa (X): Average vertical wheel displacement (ZWAV); inches; spring compression, positive.

Ordinate (Y): Average vertical wheel load (FZAV); pounds; spring compression, positive.

*Note: Brakes on. Position control. Air bags inflated to 65 psi. Low side of vertical.

Measured by UMTRI for Smart Truck
Freightliner Tractor

Data file: FRTLNG44.ERD

Drive Axle Suspension, Trailing Only

Average Vertical Spring Rate

6 April 96
Suspension: Trailing Arm (2LU)

Nominal Suspension Load: 18000 lb.

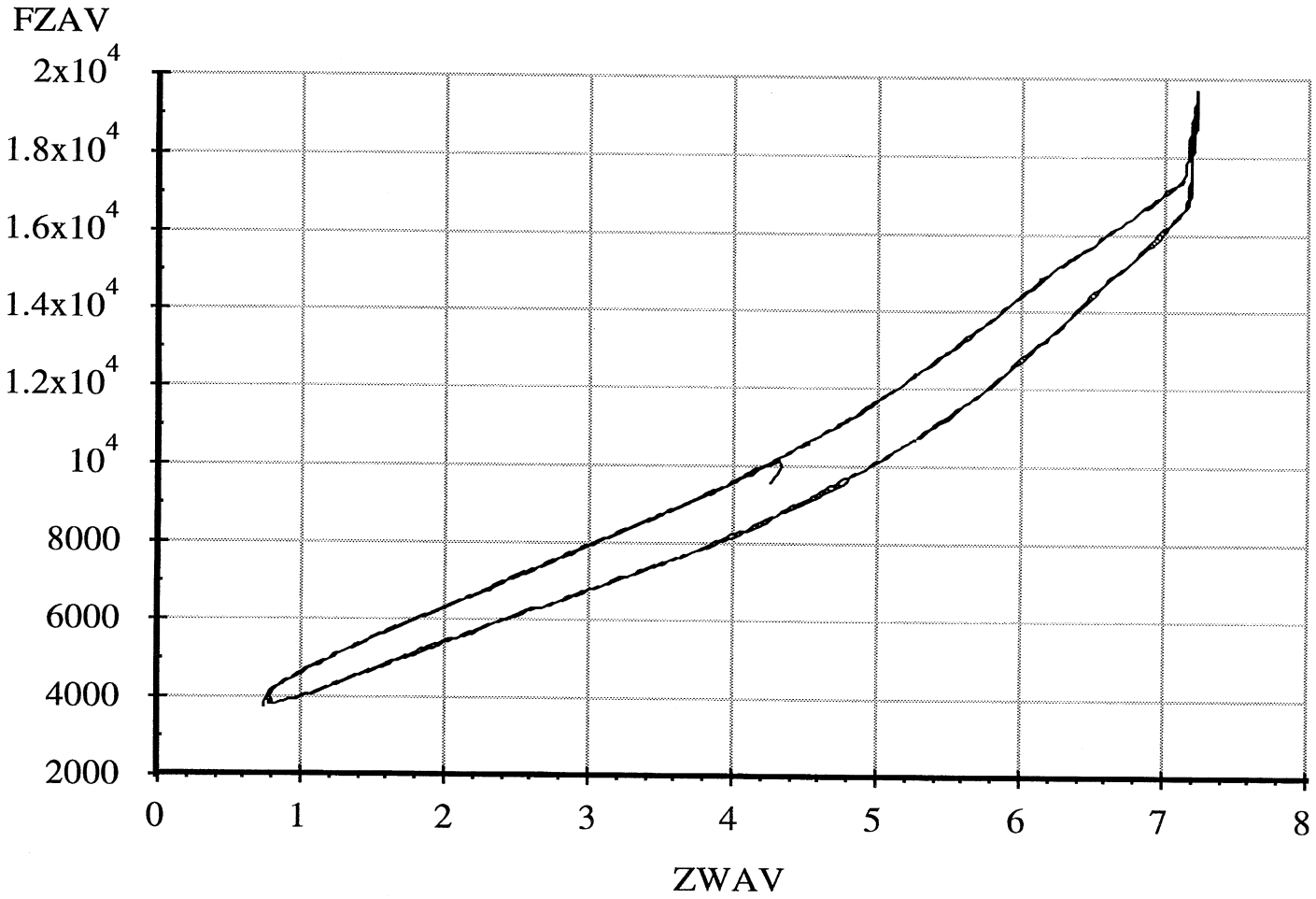

Abscissa (X): Average vertical wheel displacement (ZWAV); inches; spring compression, positive.

Ordinate (Y): Average vertical wheel load (FZAV); pounds; spring compression, positive.

*Note: Brakes on. Position control. Air bags inflated to 65 psi. High side of vertical.

Measured by UMTRI for Smart Truck
Freightliner Tractor

Data file: FRTLNG41.ERD

Drive Axle Suspension, Trailing Only

Axle Roll Rate

6 April 96
Suspension: Trailing Arm (2LU)

Suspension Load: 18000 lb.

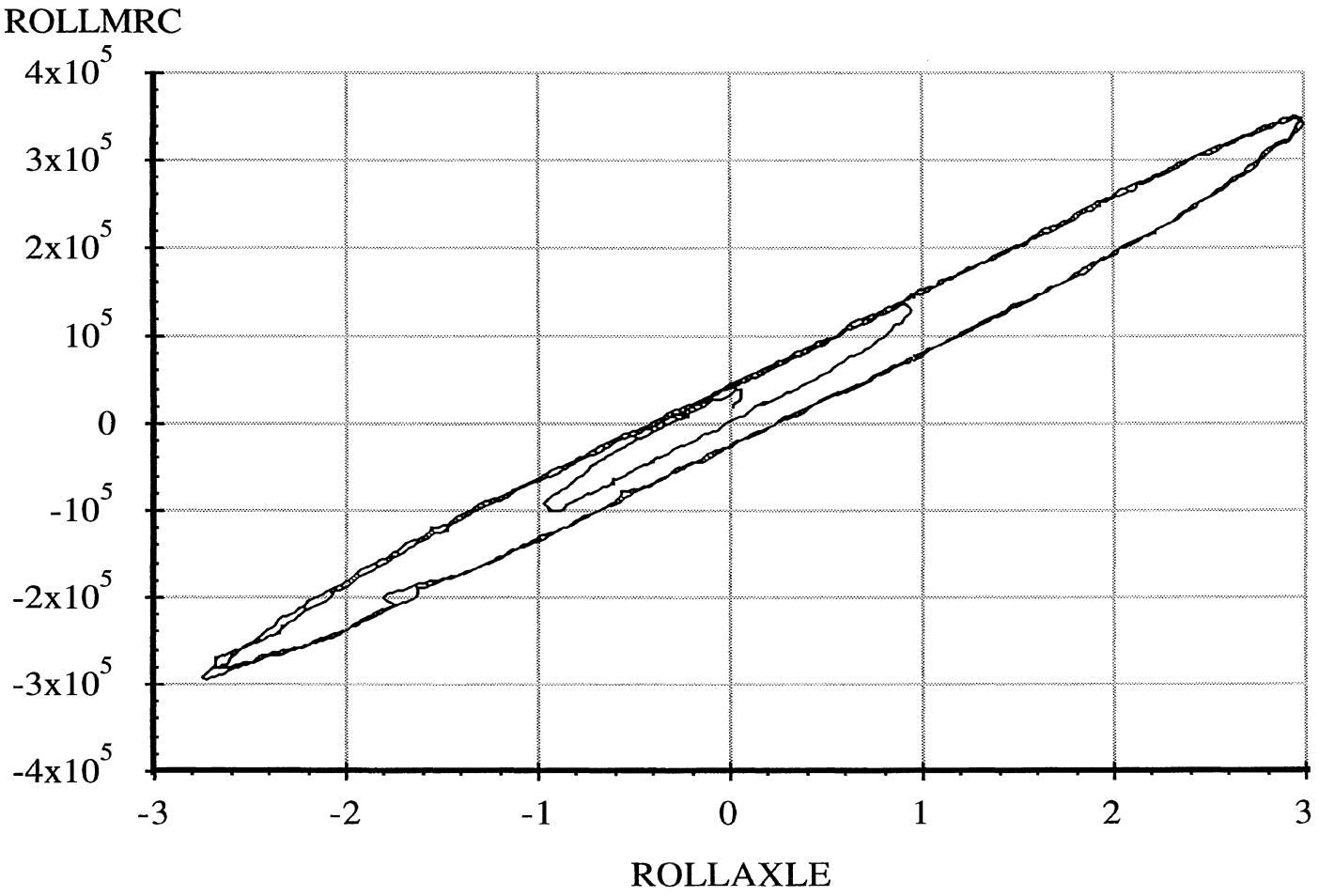

Abscissa (X): Axle roll angle (ROLLAXLE); degrees; right side compressed, positive.

Ordinate (Y): Axle roll moment about the roll center (ROLLMRC); in-lb; right side compressed, positive.

*Note: Brakes on. Force control. Air bags inflated to 65 psi.

Measured by UMTRI for Smart Truck
Freightliner Tractor

Data file: FRTLNG41.ERD

Drive Axle Suspension, Trailing Only

Roll Center Height

6 April 96
Suspension: Trailing Arm (2LU)

Suspension Load: 18000 lb.

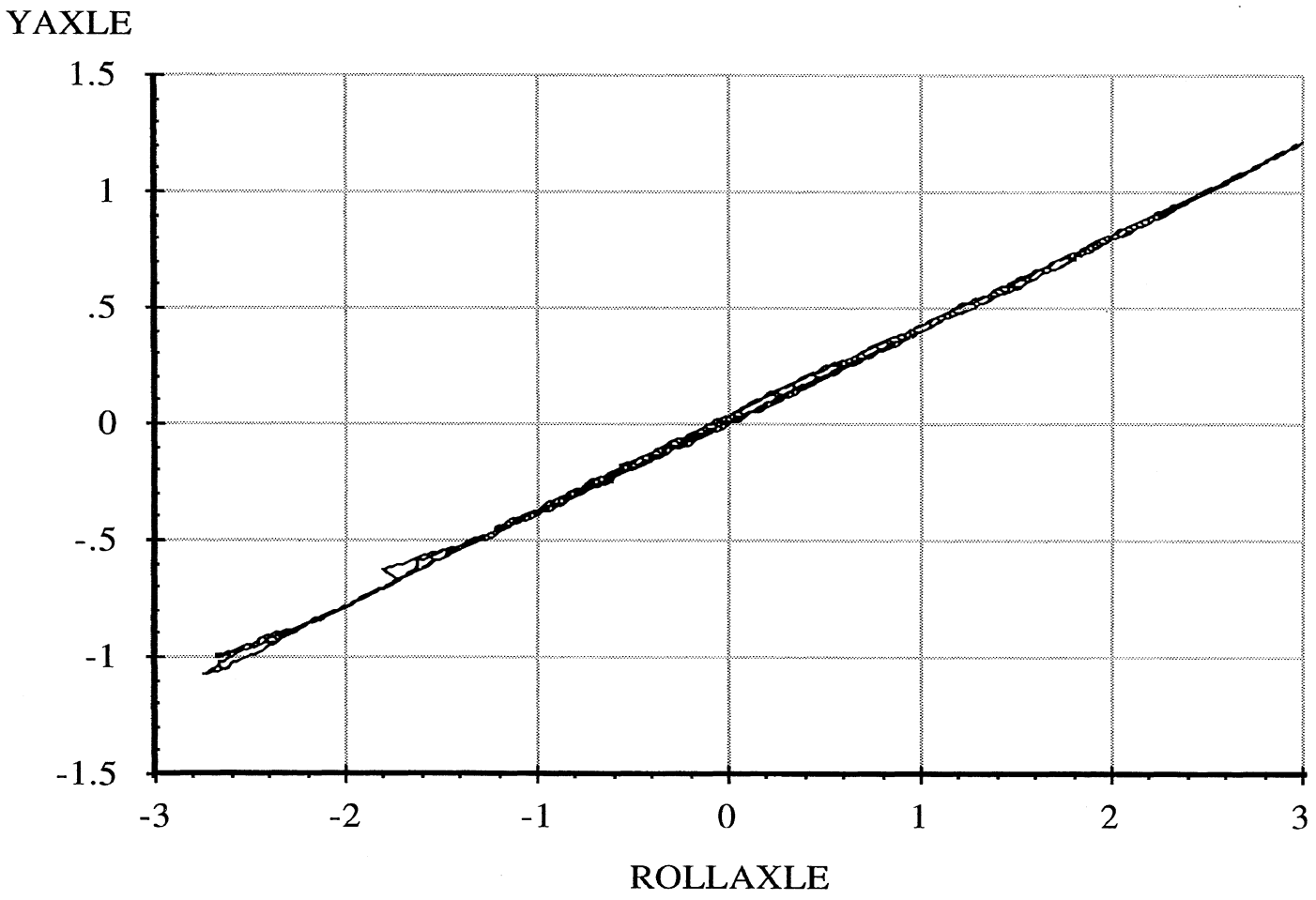

Abscissa (X): Axle roll angle (ROLLAXLE); degrees; right side compressed, positive.

Ordinate (Y): Axle reference point lateral translation (YAXLE); inches; motion toward right, positive.

*Note: Brakes on. Force control. Air bags inflated to 65 psi. Reference height of 7.81 inches.

Measured by UMTRI for Smart Truck
Freightliner Tractor

Data file: FRTLNG41.ERD

Drive Axle Suspension, Trailing Only

Roll Steer

6 April 96
Suspension: Trailing Arm (2LU)

Suspension Load: 18000 lb.

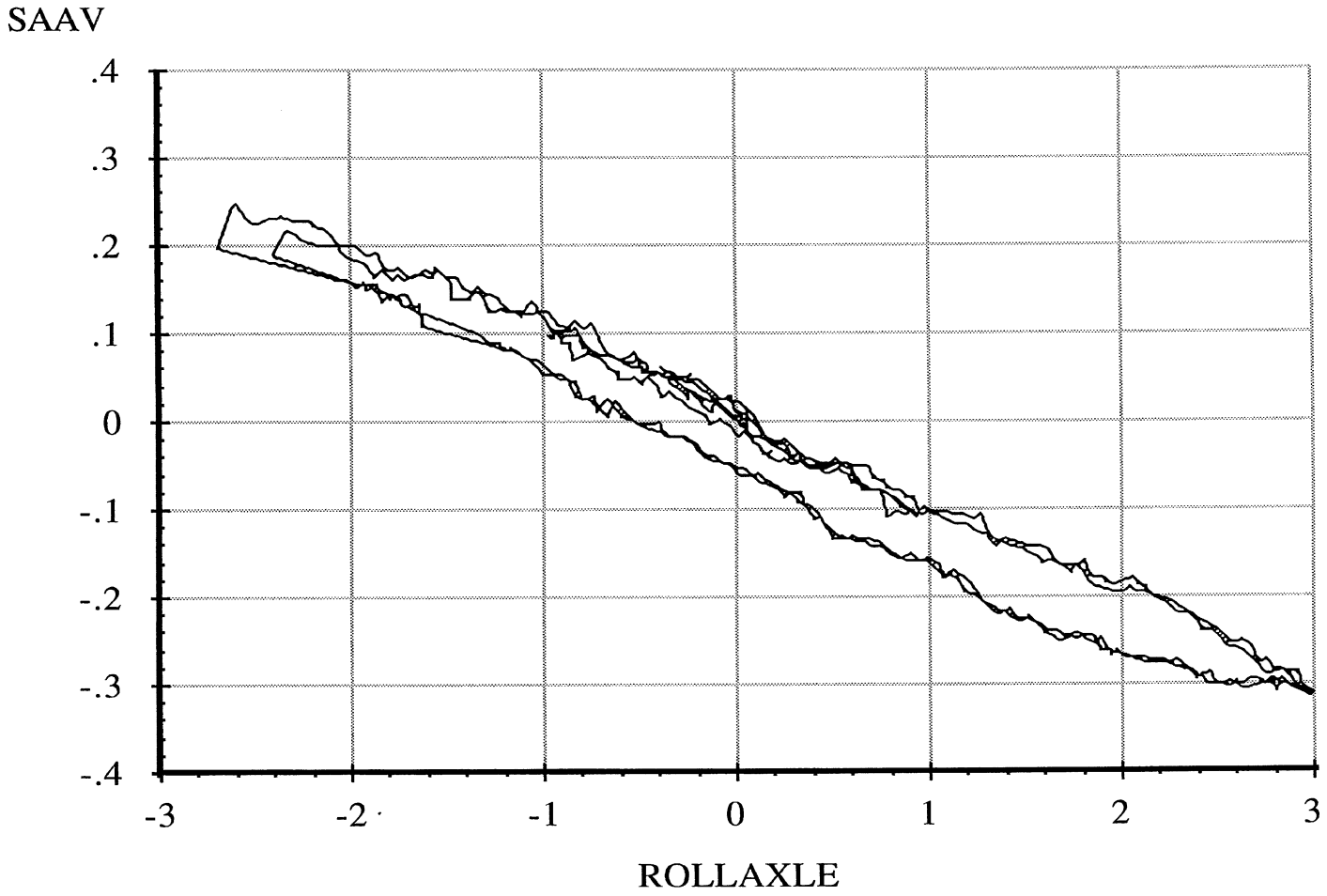

Abscissa (X): Axle roll angle (ROLLAXLE); degrees; right side compressed, positive.

Ordinate (Y): Average steer angle (SAAV); degrees; steer toward right, positive.

*Note: Brakes on. Force control. Air bags inflated to 65 psi.

Measured by UMTRI for Smart Truck
Freightliner Tractor

Data file: FRTLNG42.ERD

Drive Axle Suspension, Trailing Only

Lateral Force Compliance

6 April 96
Suspension: Trailing Arm (2LU)

Suspension Load: 18000 lb.

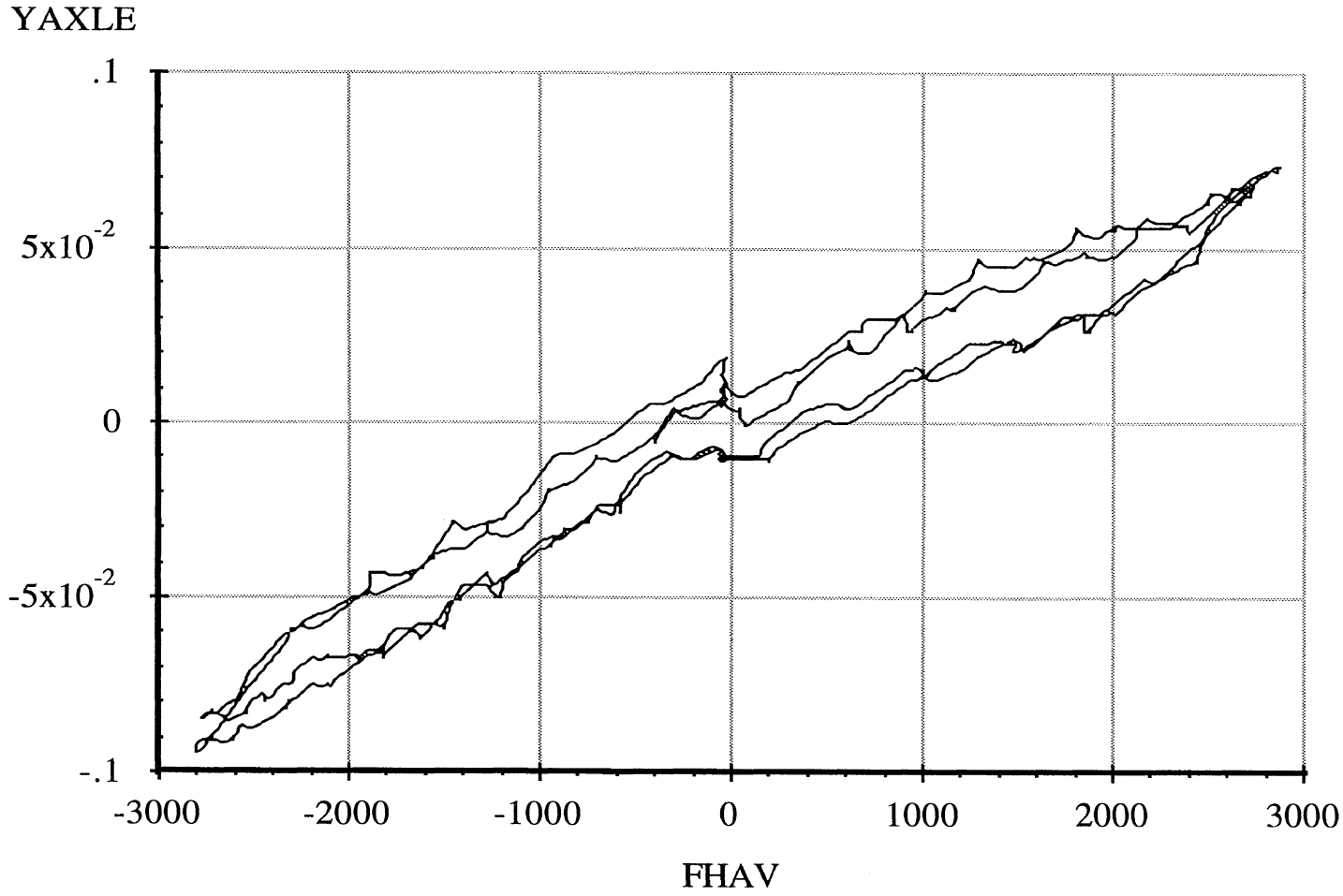

Abscissa (X): Average axle lateral force (FHAV); pounds; applied to both wheels simultaneously; force applied toward right, positive.

Ordinate (Y): Axle lateral translation (YAXLE); inches; motion toward right, positive.

*Note: Brakes on. Position control. Air bags inflated to 65 psi. Reference height of 7.81 inches.

Measured by UMTRI for Smart Truck
Freightliner Tractor

Data file: FRTLNG42.ERD

Drive Axle Suspension, Trailing Only

Lateral Force Steer

6 April 96
Suspension: Trailing Arm (2LU)

Suspension Load: 18000 lb.

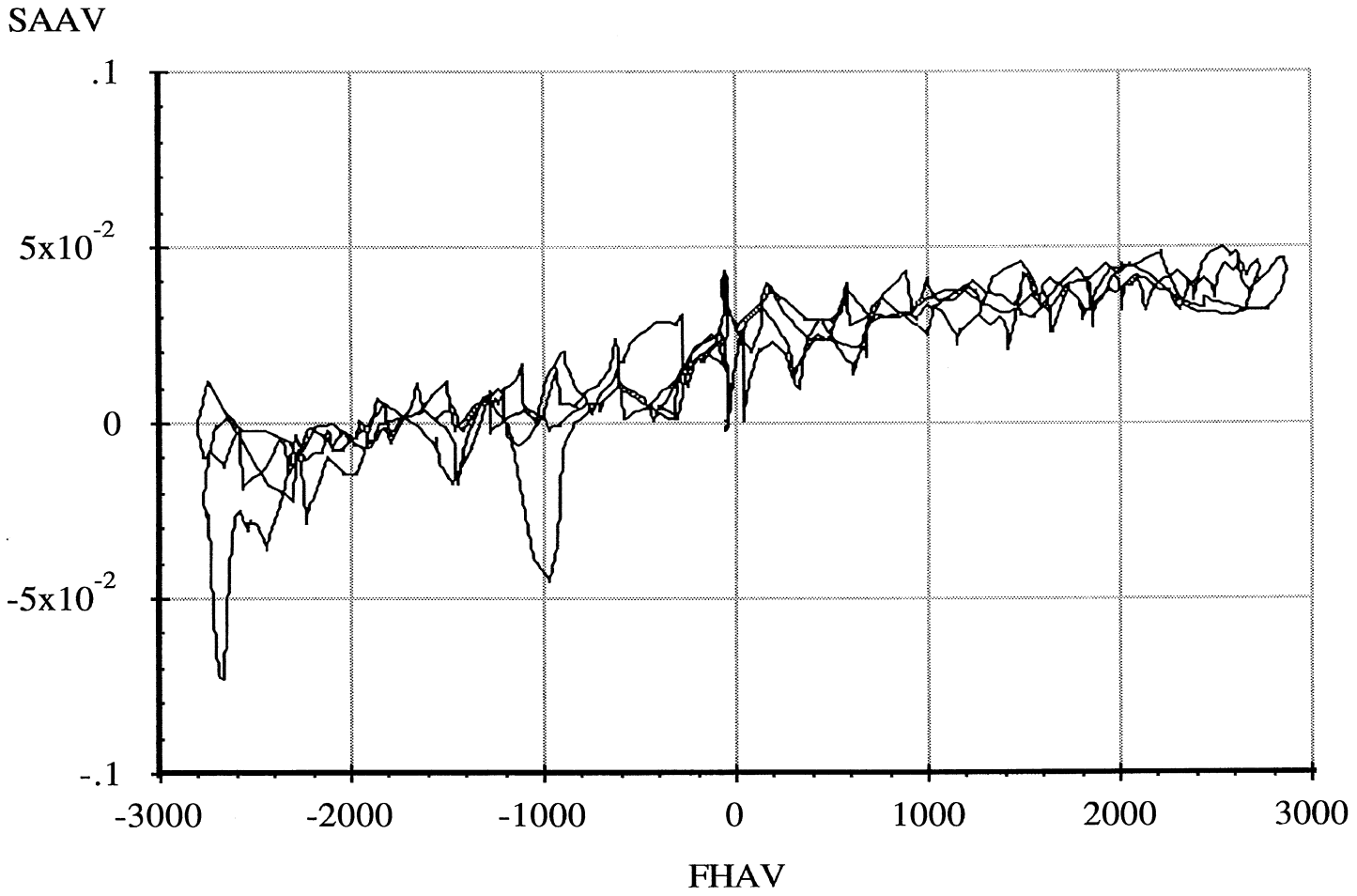

Abscissa (X): Average axle lateral force (FHAV); pounds; applied to both wheels simultaneously; force applied toward right, positive.

Ordinate (Y): Average steer angle (SAAV); degrees; steer toward right, positive.

*Note: Brakes on. Position control. Air bags inflated to 65 psi.

Measured by UMTRI for Smart Truck
Freightliner Tractor

Drive Axle Suspension, Trailing Only

6 April 96
Suspension: Trailing Arm (2LU)

Data file: FRTLNG43.ERD

Aligning Moment Compliance Steer

Suspension Load: 18000 lb.

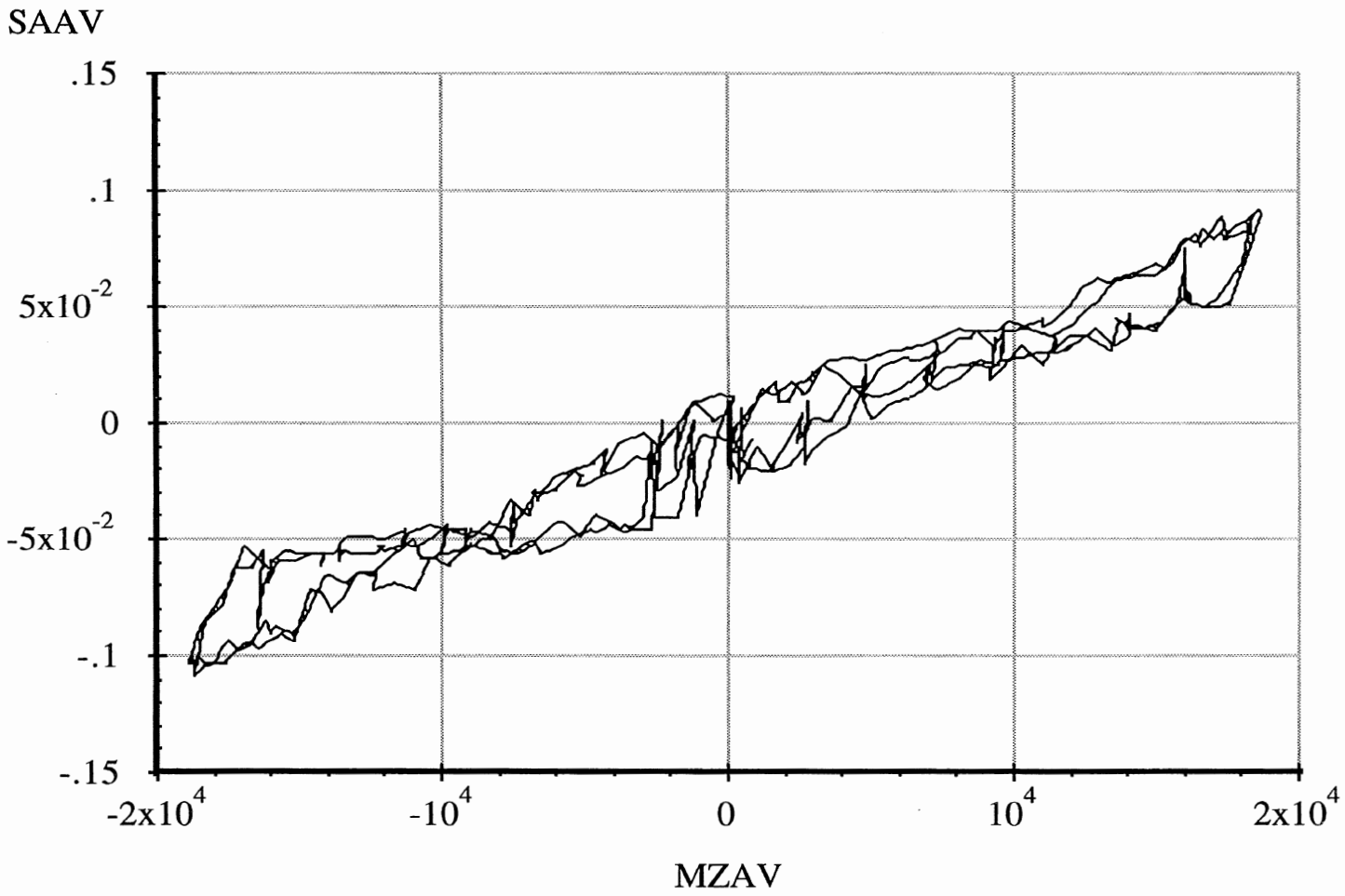

Abscissa (X): Average axle aligning moment (MZAV); in-lb per wheel; applied to both wheels simultaneously; downward (right hand rule) moment vector, positive.

Ordinate (Y): Average steer angle (SAAV); degrees; steer toward right, positive.

*Note: Brakes on. Position control. Air bags inflated to 65 psi.

Measured by UMTRI for Smart Truck
Freightliner Tractor

Data file: FRTLNG30.ERD

Drive Axle Suspension, Trailing Only

Average Vertical Spring Rate

6 April 96
Suspension: Trailing Arm (2LU)

Nominal Suspension Load: 16000 lb.

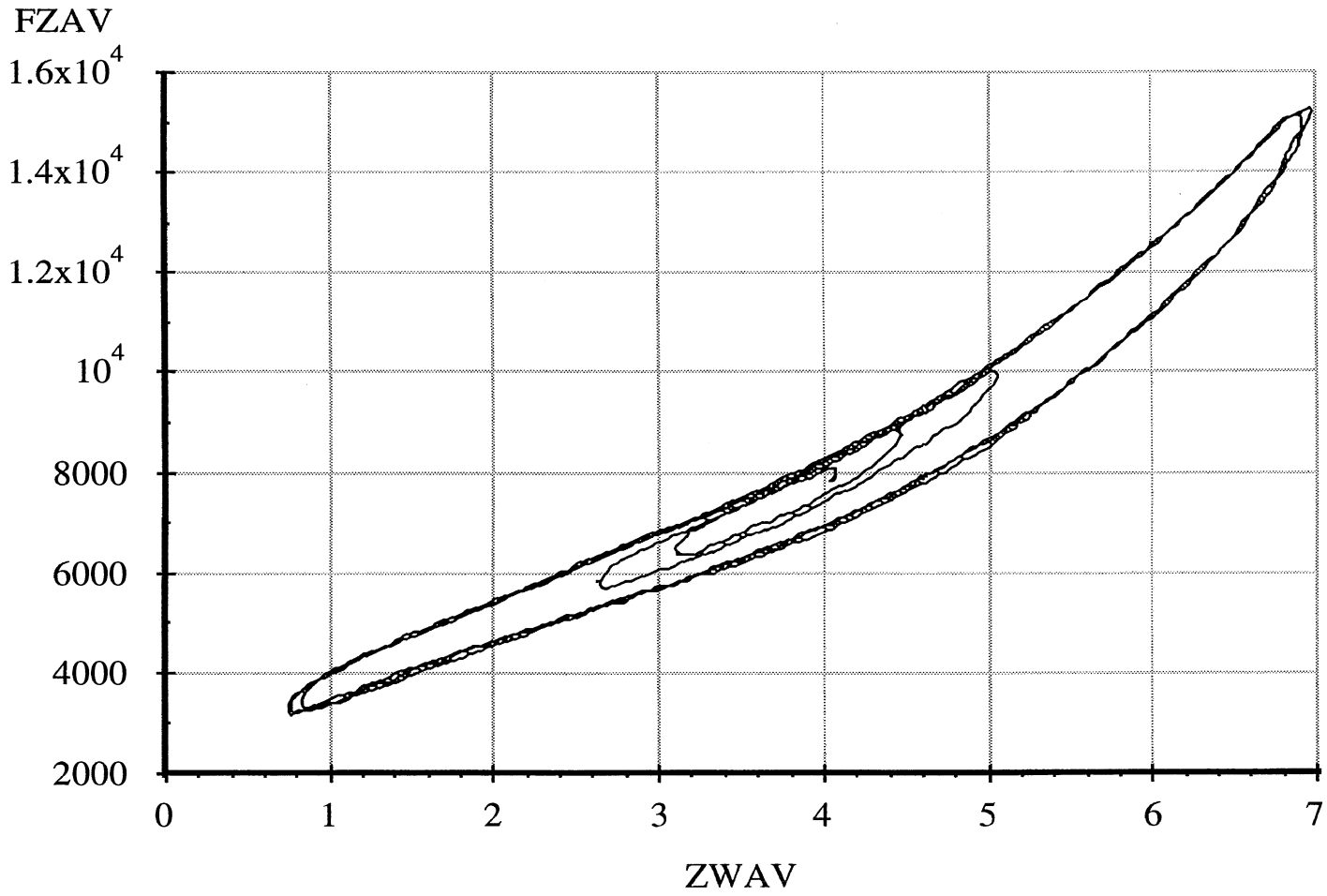

Abscissa (X): Average vertical wheel displacement (ZWAV); inches; spring compression, positive.

Ordinate (Y): Average vertical wheel load (FZAV); pounds; spring compression, positive.

*Note: Brakes on. Position control. Air bags inflated to 58 psi. Low side of vertical.

Measured by UMTRI for Smart Truck
Freightliner Tractor

Data file: FRTLNG34.ERD

Drive Axle Suspension, Trailing Only

Average Vertical Spring Rate

6 April 96
Suspension: Trailing Arm (2LU)

Nominal Suspension Load: 16000 lb.

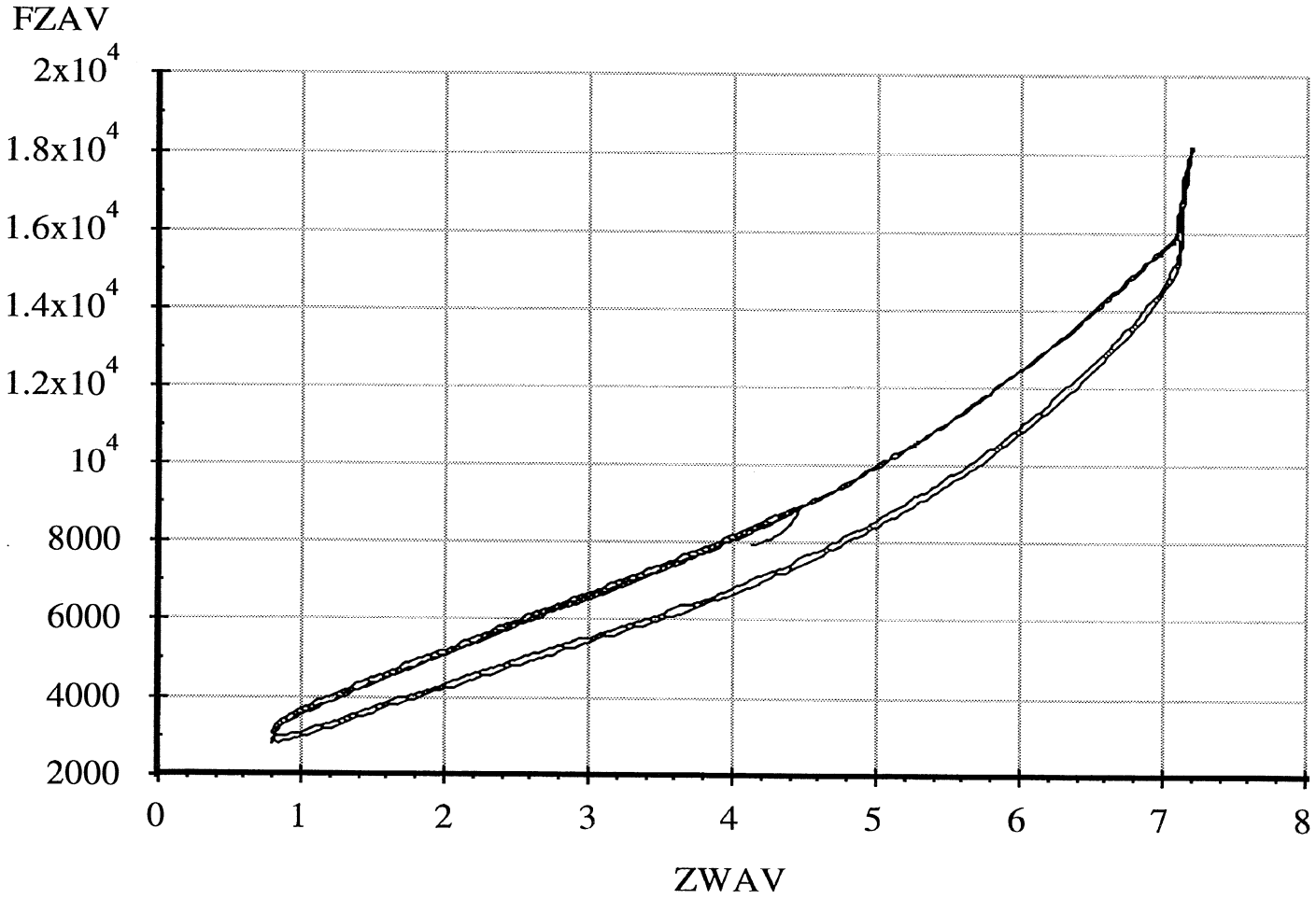

Abscissa (X): Average vertical wheel displacement (ZWAV); inches; spring compression, positive.

Ordinate (Y): Average vertical wheel load (FZAV); pounds; spring compression, positive.

*Note: Brakes on. Position control. Air bags inflated to 58 psi. High side of vertical.

Measured by UMTRI for Smart Truck
Freightliner Tractor

Data file: FRTLNG31.ERD

Drive Axle Suspension, Trailing Only

Axle Roll Rate

6 April 96
Suspension: Trailing Arm (2LU)

Suspension Load: 16000 lb.

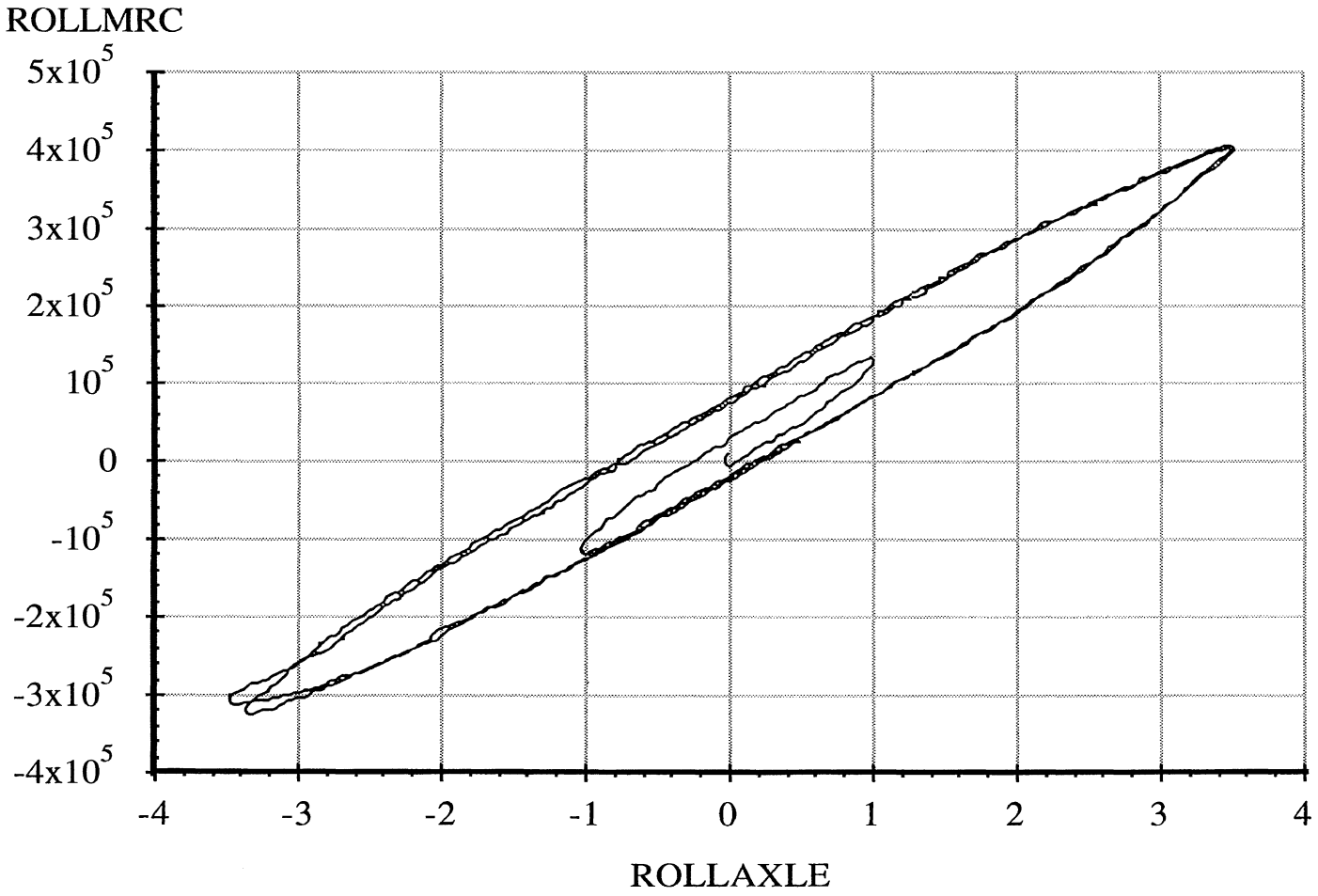

Abscissa (X): Axle roll angle (ROLLAXLE); degrees; right side compressed, positive.

Ordinate (Y): Axle roll moment about the roll center (ROLLMRC); in-lb; right side compressed, positive.

*Note: Brakes on. Force control. Air bags inflated to 58 psi.

Measured by UMTRI for Smart Truck
Freightliner Tractor

Data file: FRTLNG31.ERD

Drive Axle Suspension, Trailing Only

Roll Center Height

6 April 96
Suspension: Trailing Arm (2LU)

Suspension Load: 16000 lb.

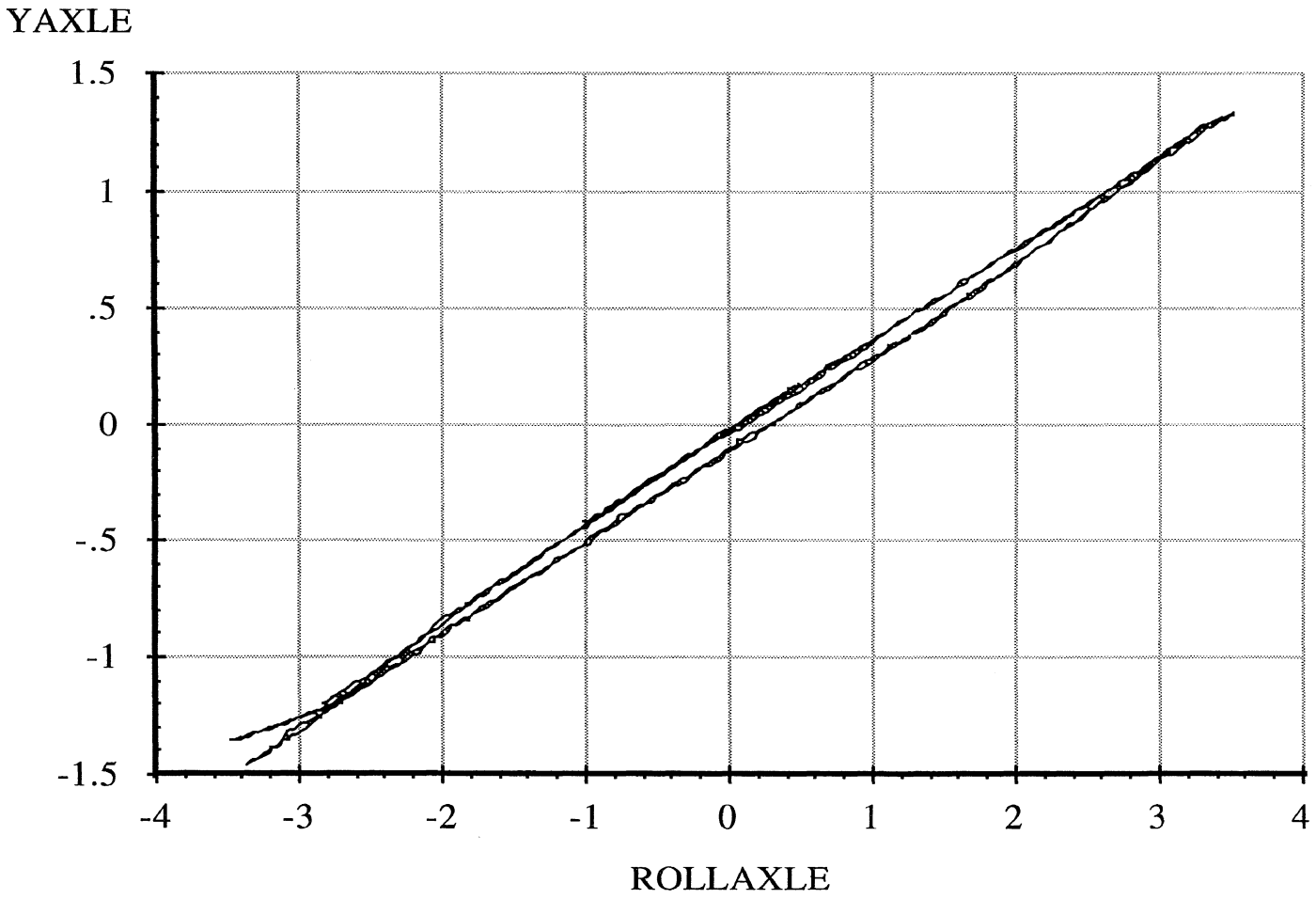

Abscissa (X): Axle roll angle (ROLLAXLE); degrees; right side compressed, positive.

Ordinate (Y): Axle reference point lateral translation (YAXLE); inches; motion toward right, positive.

*Note: Brakes on. Force control. Air bags inflated to 58 psi. Reference height of 7.88 inches.

Measured by UMTRI for Smart Truck
Freightliner Tractor

Data file: FRTLNG31.ERD

Drive Axle Suspension, Trailing Only

Roll Steer

6 April 96
Suspension: Trailing Arm (2LU)

Suspension Load: 16000 lb.

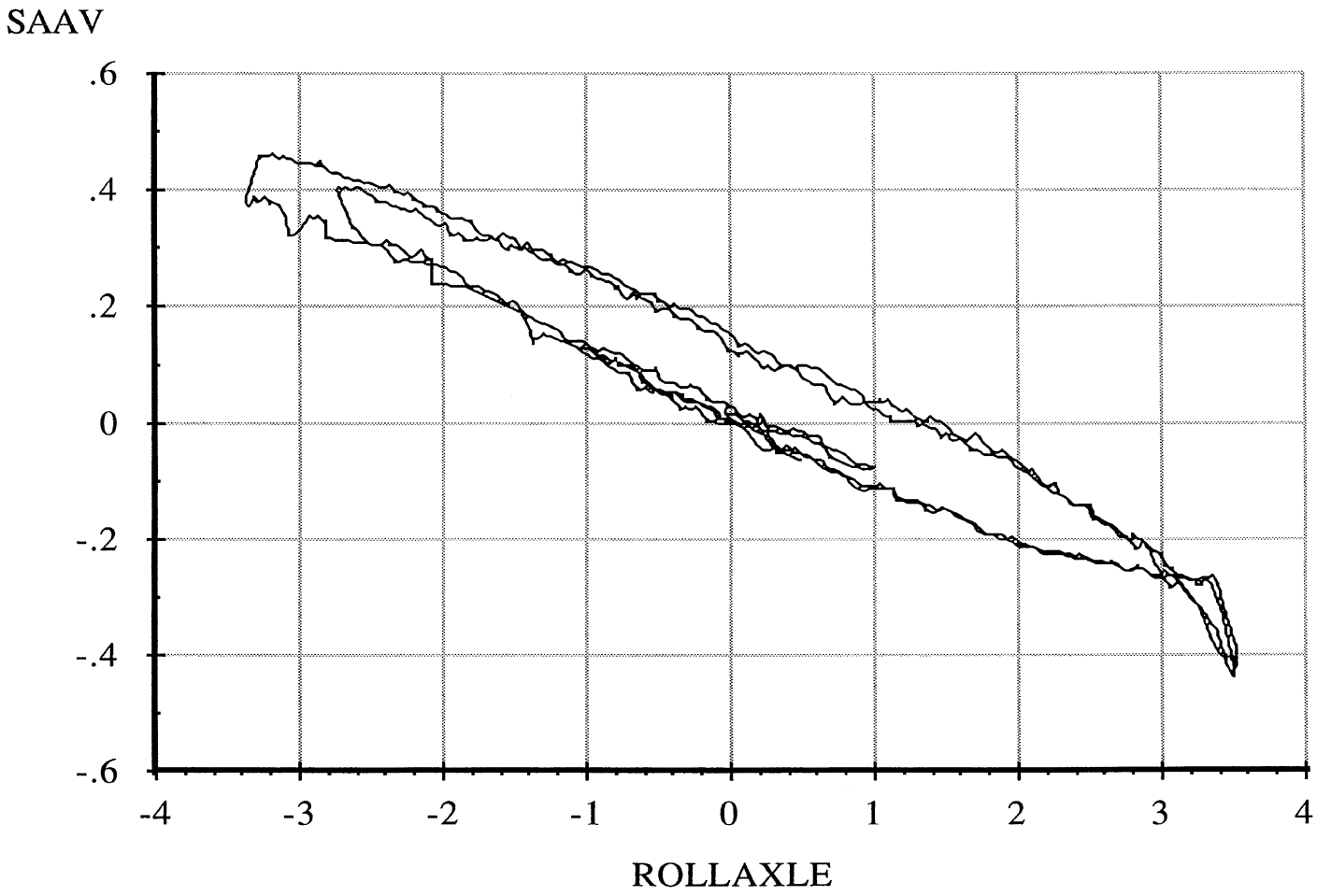

Abscissa (X): Axle roll angle (ROLLAXLE); degrees; right side compressed, positive.

Ordinate (Y): Average steer angle (SAAV); degrees; steer toward right, positive.

*Note: Brakes on. Force control. Air bags inflated to 58 psi.

Measured by UMTRI for Smart Truck
Freightliner Tractor

Data file: FRTLNG32.ERD

Drive Axle Suspension, Trailing Only

Lateral Force Compliance

6 April 96
Suspension: Trailing Arm (2LU)

Suspension Load: 16000 lb.

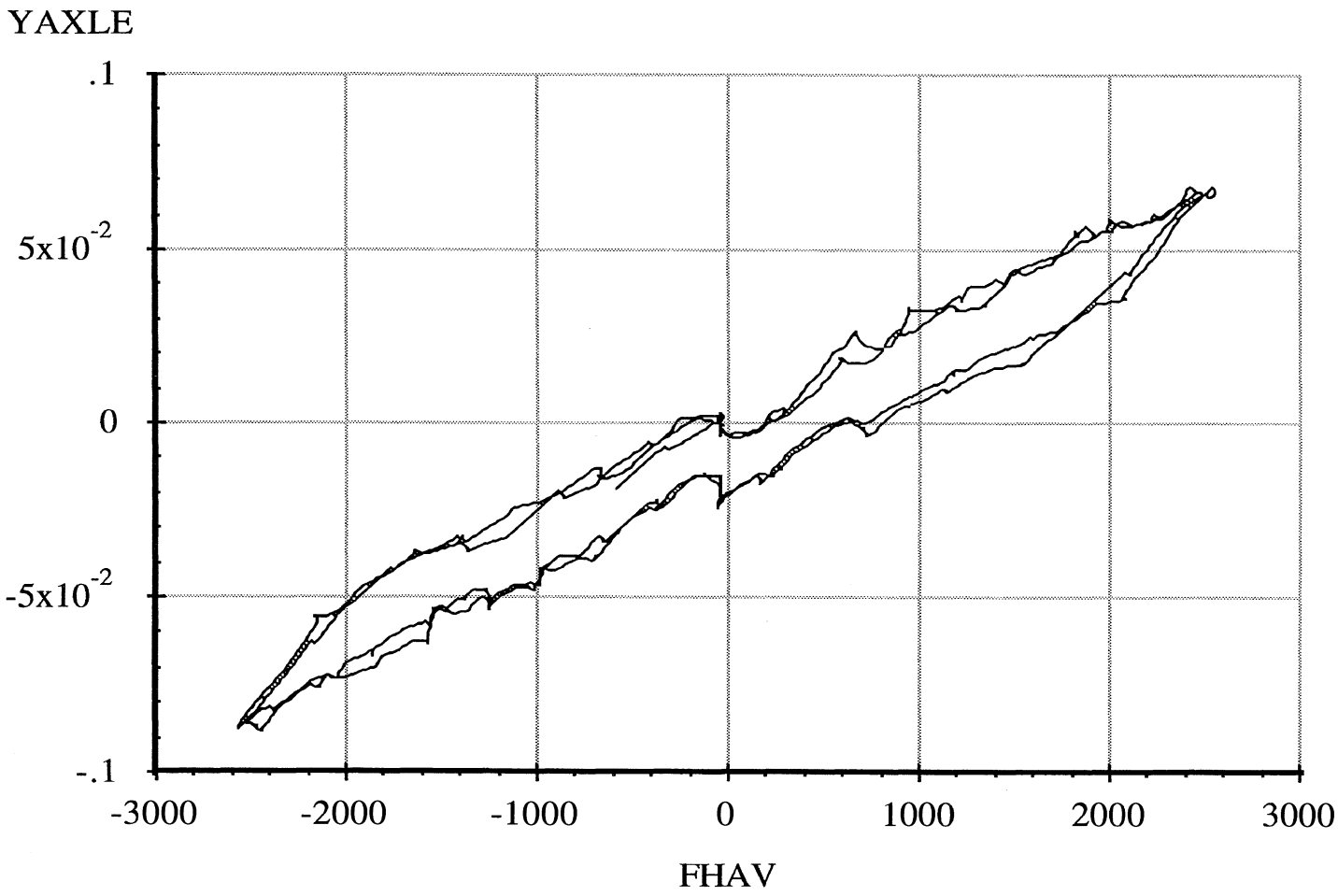

Abscissa (X): Average axle lateral force (FHAV); pounds; applied to both wheels simultaneously; force applied toward right, positive.

Ordinate (Y): Axle lateral translation (YAXLE); inches; motion toward right, positive.

*Note: Brakes on. Position control. Air bags inflated to 58 psi. Reference height of 7.88 inches.

Measured by UMTRI for Smart Truck
Freightliner Tractor

Data file: FRTLNG32.ERD

Drive Axle Suspension, Trailing Only

Lateral Force Steer

6 April 96
Suspension: Trailing Arm (2LU)

Suspension Load: 16000 lb.

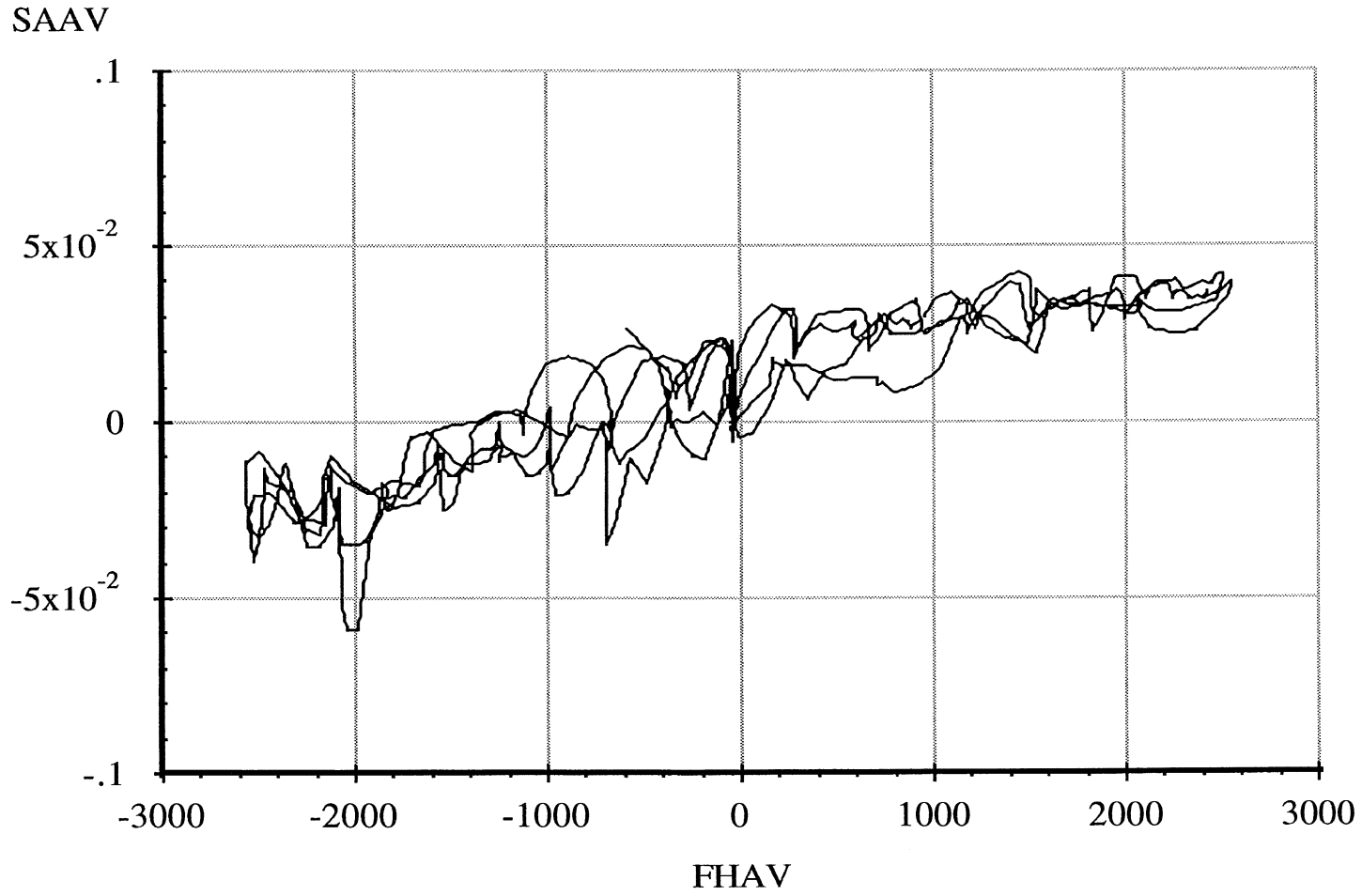

Abscissa (X): Average axle lateral force (FHAV); pounds; applied to both wheels simultaneously; force applied toward right, positive.

Ordinate (Y): Average steer angle (SAAV); degrees; steer toward right, positive.

*Note: Brakes on. Position control. Air bags inflated to 58 psi.

Measured by UMTRI for Smart Truck
Freightliner Tractor

Data file: FRTLNG33.ERD

Drive Axle Suspension, Trailing Only

Aligning Moment Compliance Steer

6 April 96
Suspension: Trailing Arm (2LU)

Suspension Load: 16000 lb.

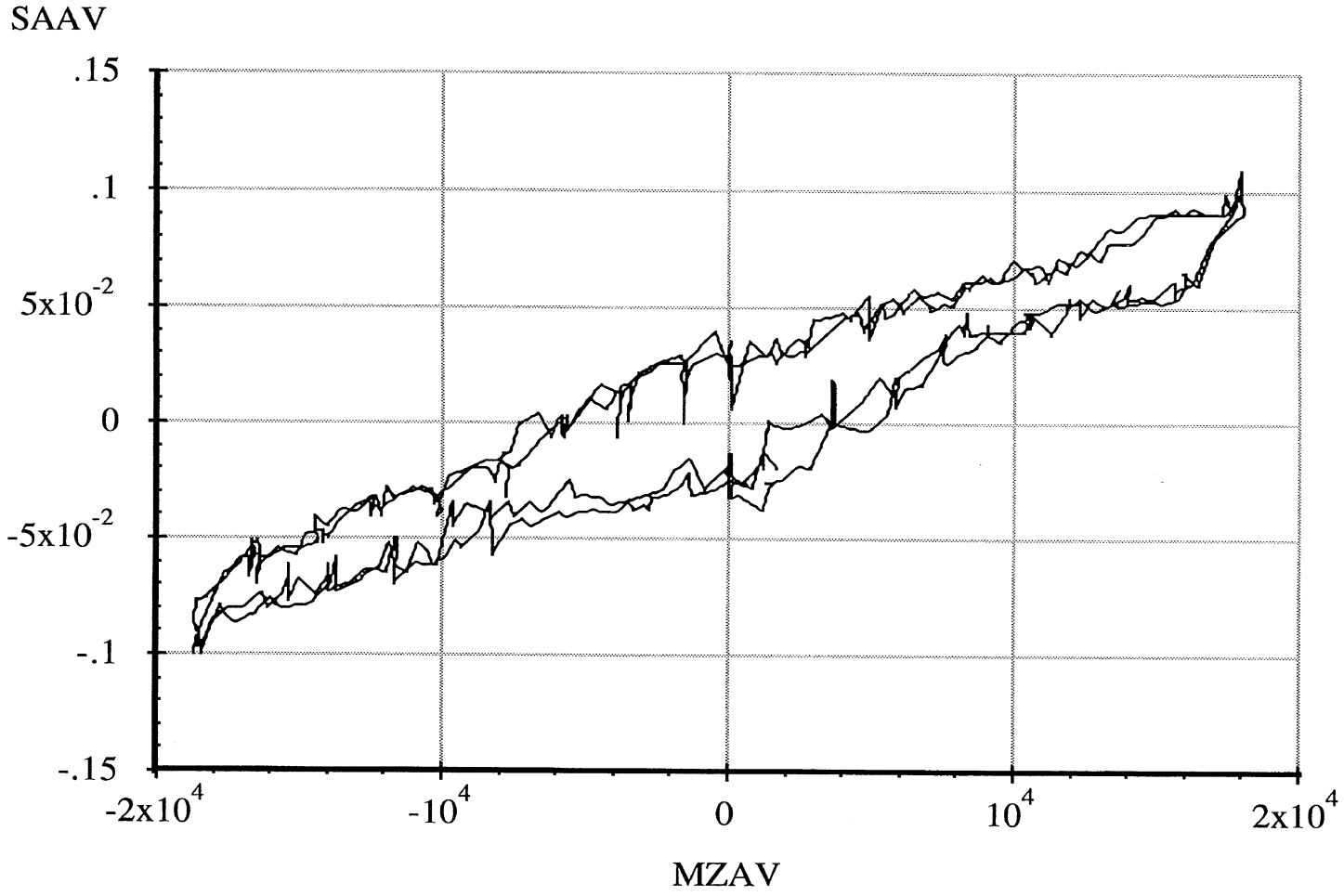

Abscissa (X): Average axle aligning moment (MZAV); in-lb per wheel; applied to both wheels simultaneously; downward (right hand rule) moment vector, positive.

Ordinate (Y): Average steer angle (SAAV); degrees; steer toward right, positive.

*Note: Brakes on. Position control. Air bags inflated to 58 psi.

Measured by UMTRI for Smart Truck
Freightliner Tractor

Data file: FRTLNG20.ERD

Drive Axle Suspension, Trailing Only

Average Vertical Spring Rate

6 April 96
Suspension: Trailing Arm (2LU)

Nominal Suspension Load: 14000 lb.

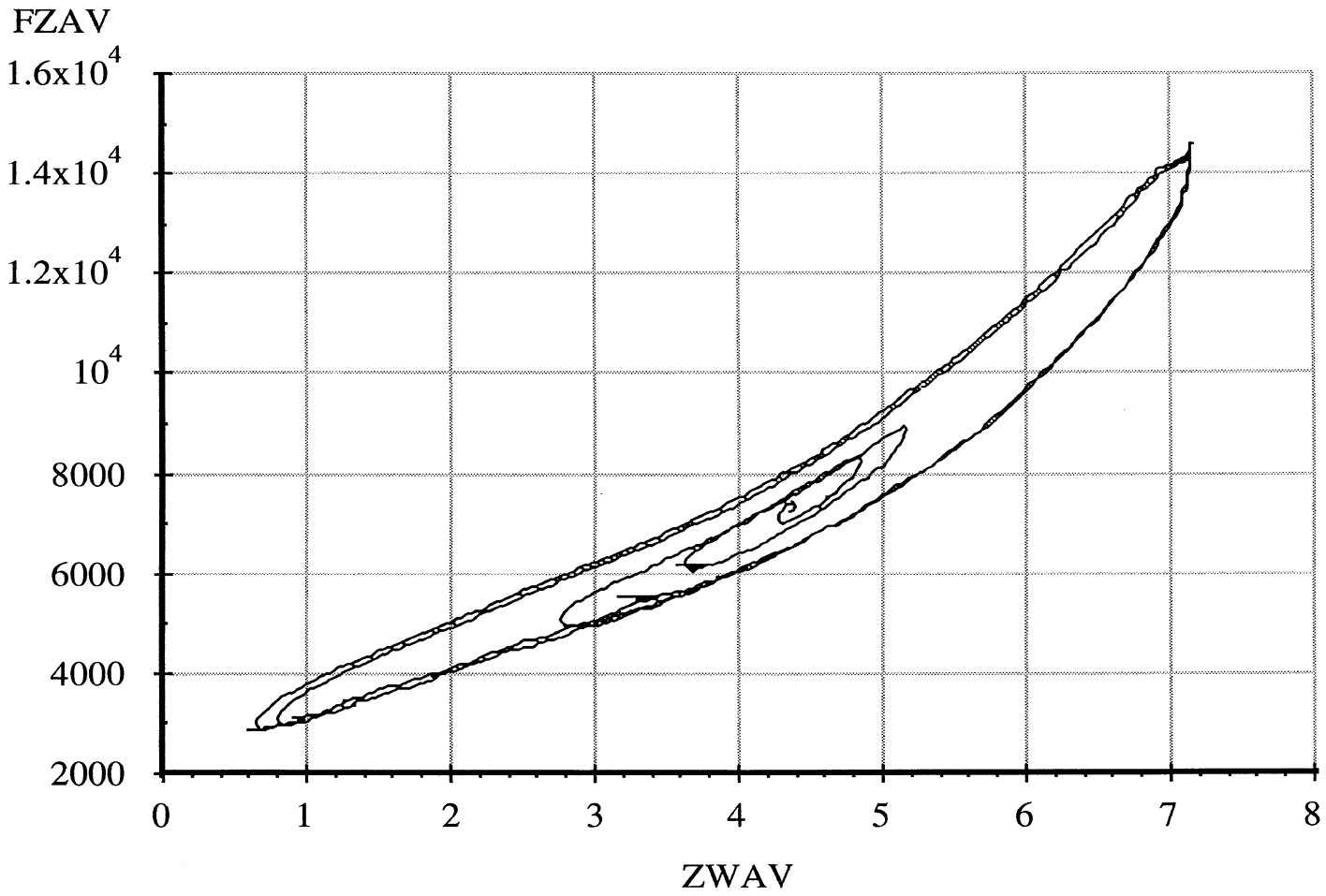

Abscissa (X): Average vertical wheel displacement (ZWAV); inches; spring compression, positive.

Ordinate (Y): Average vertical wheel load (FZAV); pounds; spring compression, positive.

*Note: Brakes on. Position control. Air bags inflated to 51 psi.

Measured by UMTRI for Smart Truck
Freightliner Tractor

Data file: FRTLNG21.ERD

Drive Axle Suspension, Trailing Only

Axle Roll Rate

6 April 96
Suspension: Trailing Arm (2LU)

Suspension Load: 14000 lb.

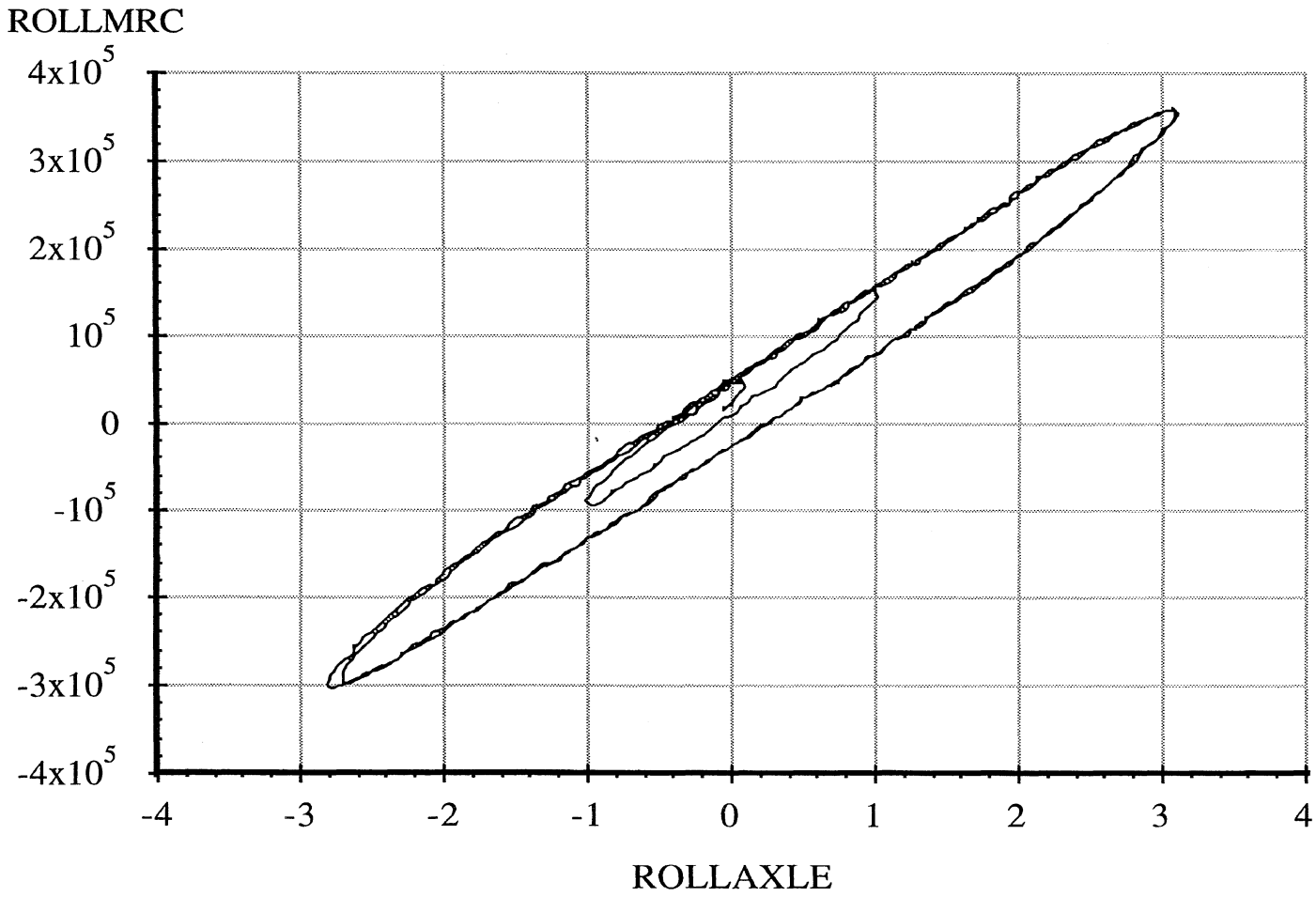

Abscissa (X): Axle roll angle (ROLLAXLE); degrees; right side compressed, positive.

Ordinate (Y): Axle roll moment about the roll center (ROLLMRC); in-lb; right side compressed, positive.

*Note: Brakes on. Force control. Air bags inflated to 51 psi.

Measured by UMTRI for Smart Truck
Freightliner Tractor

Data file: FRTLNG21.ERD

Drive Axle Suspension, Trailing Only

Roll Center Height

6 April 96
Suspension: Trailing Arm (2LU)

Suspension Load: 14000 lb.

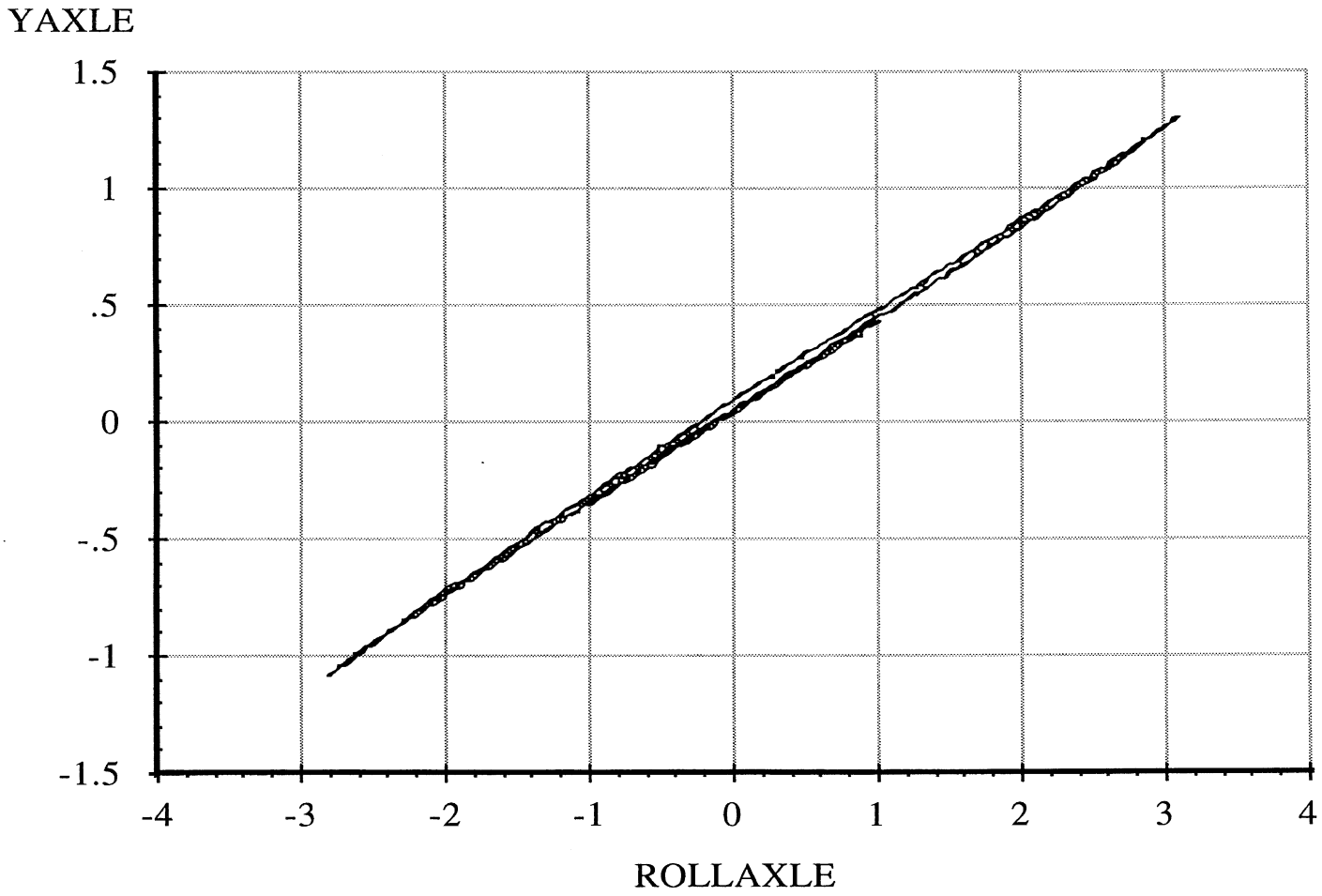

Abscissa (X): Axle roll angle (ROLLAXLE); degrees; right side compressed, positive.

Ordinate (Y): Axle reference point lateral translation (YAXLE); inches; motion toward right, positive.

*Note: Brakes on. Force control. Air bags inflated to 58 psi. Reference height of 8.00 inches.

Measured by UMTRI for Smart Truck
Freightliner Tractor

Data file: FRTLNG21.ERD

Drive Axle Suspension, Trailing Only

Roll Steer

6 April 96
Suspension: Trailing Arm (2LU)

Suspension Load: 14000 lb.

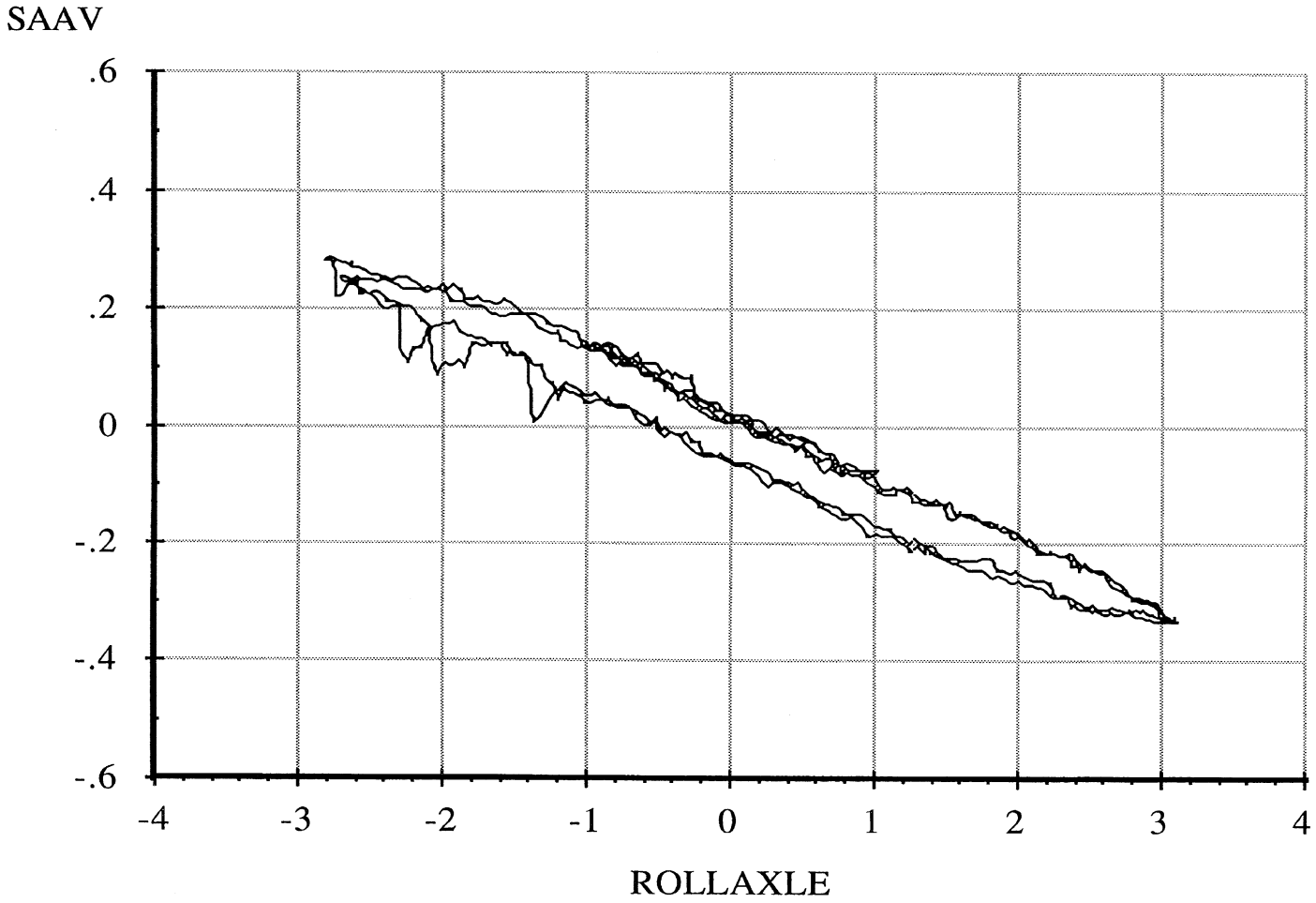

Abscissa (X): Axle roll angle (ROLLAXLE); degrees; right side compressed, positive.

Ordinate (Y): Average steer angle (SAAV); degrees; steer toward right, positive.

*Note: Brakes on. Force control. Air bags inflated to 51 psi.

Measured by UMTRI for Smart Truck
Freightliner Tractor

Data file: FRTLNG22.ERD

Drive Axle Suspension, Trailing Only

Lateral Force Compliance

6 April 96
Suspension: Trailing Arm (2LU)

Suspension Load: 14000 lb.

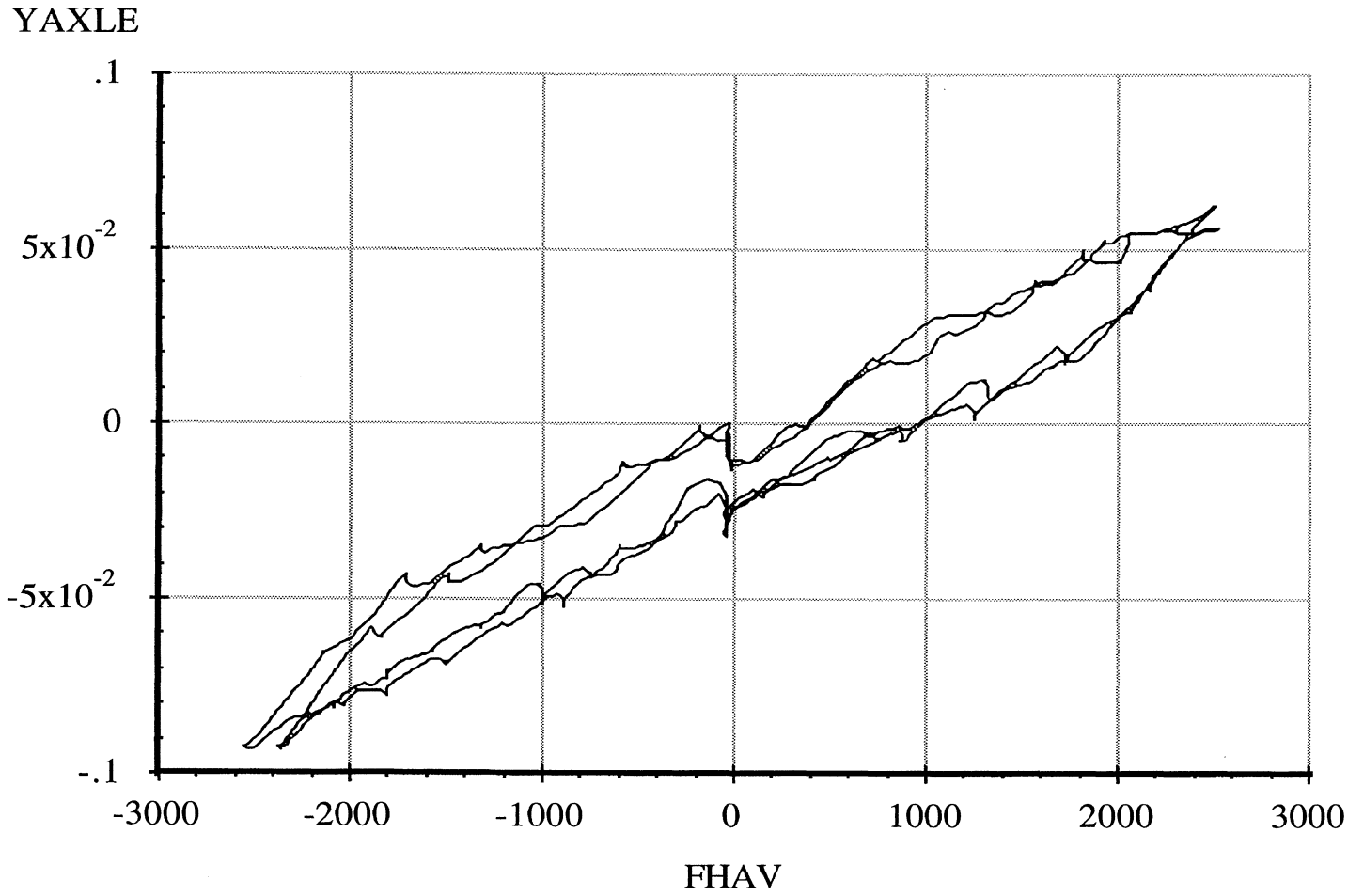

Abscissa (X): Average axle lateral force (FHAV); pounds; applied to both wheels simultaneously; force applied toward right, positive.

Ordinate (Y): Axle lateral translation (YAXLE); inches; motion toward right, positive.

*Note: Brakes on. Position control. Air bags inflated to 51 psi. Reference height of 8.00 inches.

Measured by UMTRI for Smart Truck
Freightliner Tractor

Data file: FRTLNG23.ERD

Drive Axle Suspension, Trailing Only

Aligning Moment Compliance Steer

6 April 96
Suspension: Trailing Arm (2LU)

Suspension Load: 14000 lb.

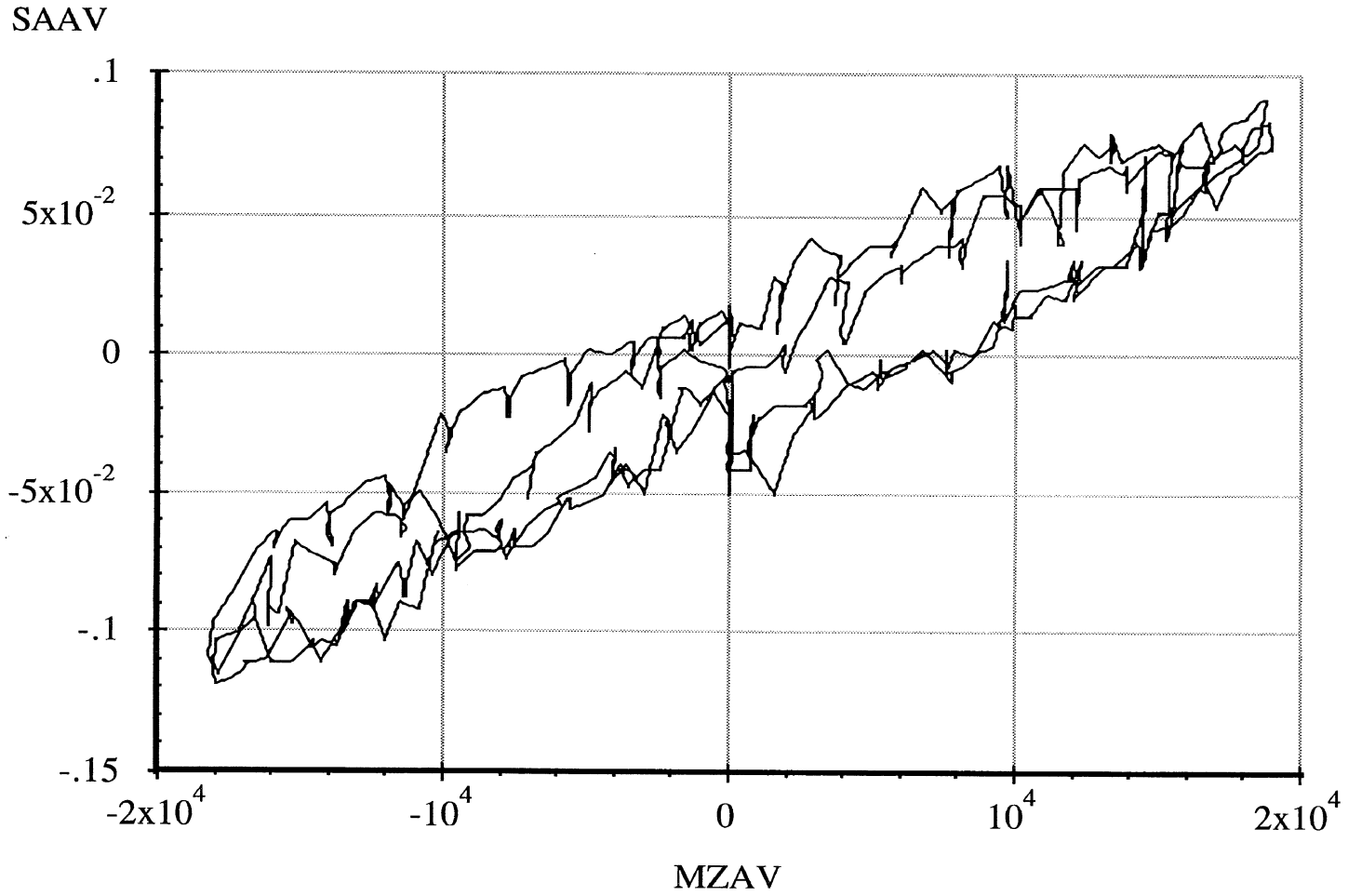

Abscissa (X): Average axle aligning moment (MZAV); in-lb per wheel; applied to both wheels simultaneously; downward (right hand rule) moment vector, positive.

Ordinate (Y): Average steer angle (SAAV); degrees; steer toward right, positive.

*Note: Brakes on. Position control. Air bags inflated to 51 psi.

Measured by UMTRI for Smart Truck
Freightliner Tractor

Data file: FRTLNG00.ERD

Drive Axle Suspension, Trailing Only

Average Vertical Spring Rate

6 April 96
Suspension: Trailing Arm (2LU)

Nominal Suspension Load: 8000 lb.

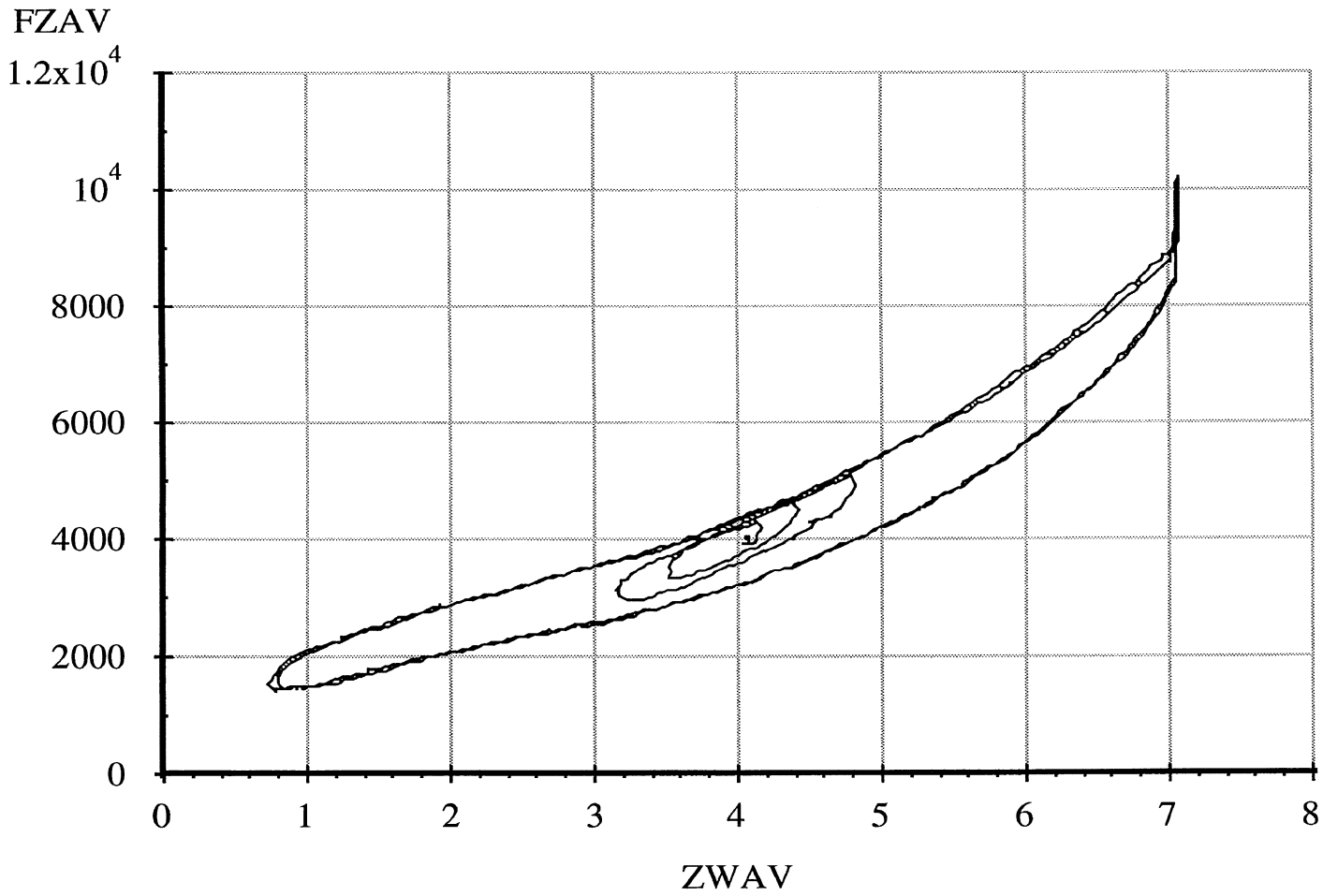

Abscissa (X): Average vertical wheel displacement (ZWAV); inches; spring compression, positive.

Ordinate (Y): Average vertical wheel load (FZAV); pounds; spring compression, positive.

*Note: Brakes on. Position control. Air bags inflated to 26 psi. Low side of vertical.

Measured by UMTRI for Smart Truck
Freightliner Tractor

Data file: FRTLNG01.ERD

Drive Axle Suspension, Trailing Only

Axle Roll Rate

6 April 96
Suspension: Trailing Arm (2LU)

Suspension Load: 8000 lb.

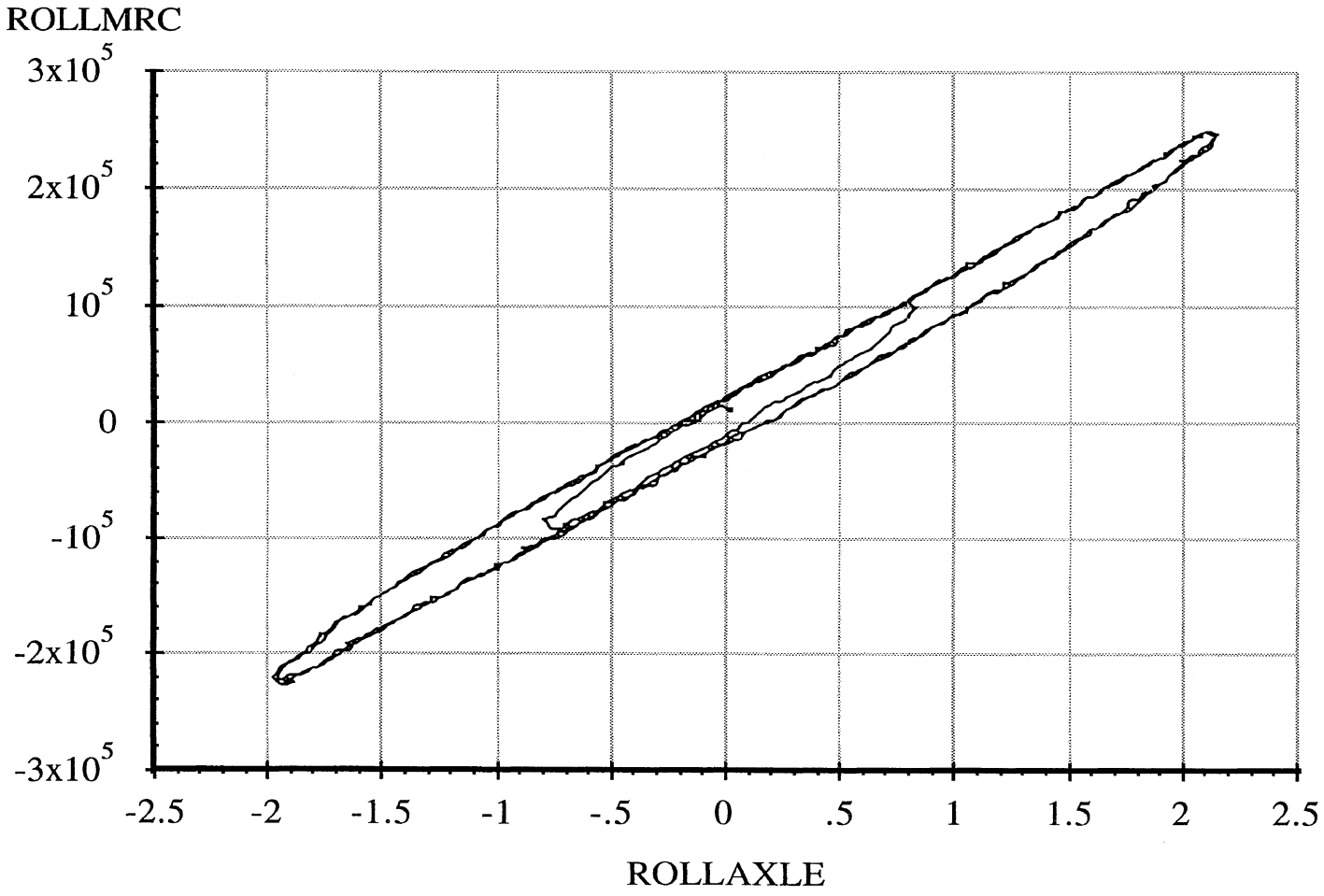

Abscissa (X): Axle roll angle (ROLLAXLE); degrees; right side compressed, positive.

Ordinate (Y): Axle roll moment about the roll center (ROLLMRC); in-lb; right side compressed, positive.

*Note: Brakes on. Force control. Air bags inflated to 26 psi.

Measured by UMTRI for Smart Truck
Freightliner Tractor

Data file: FRTLNG01.ERD

Drive Axle Suspension, Trailing Only

Roll Center Height

6 April 96
Suspension: Trailing Arm (2LU)

Suspension Load: 8000 lb.

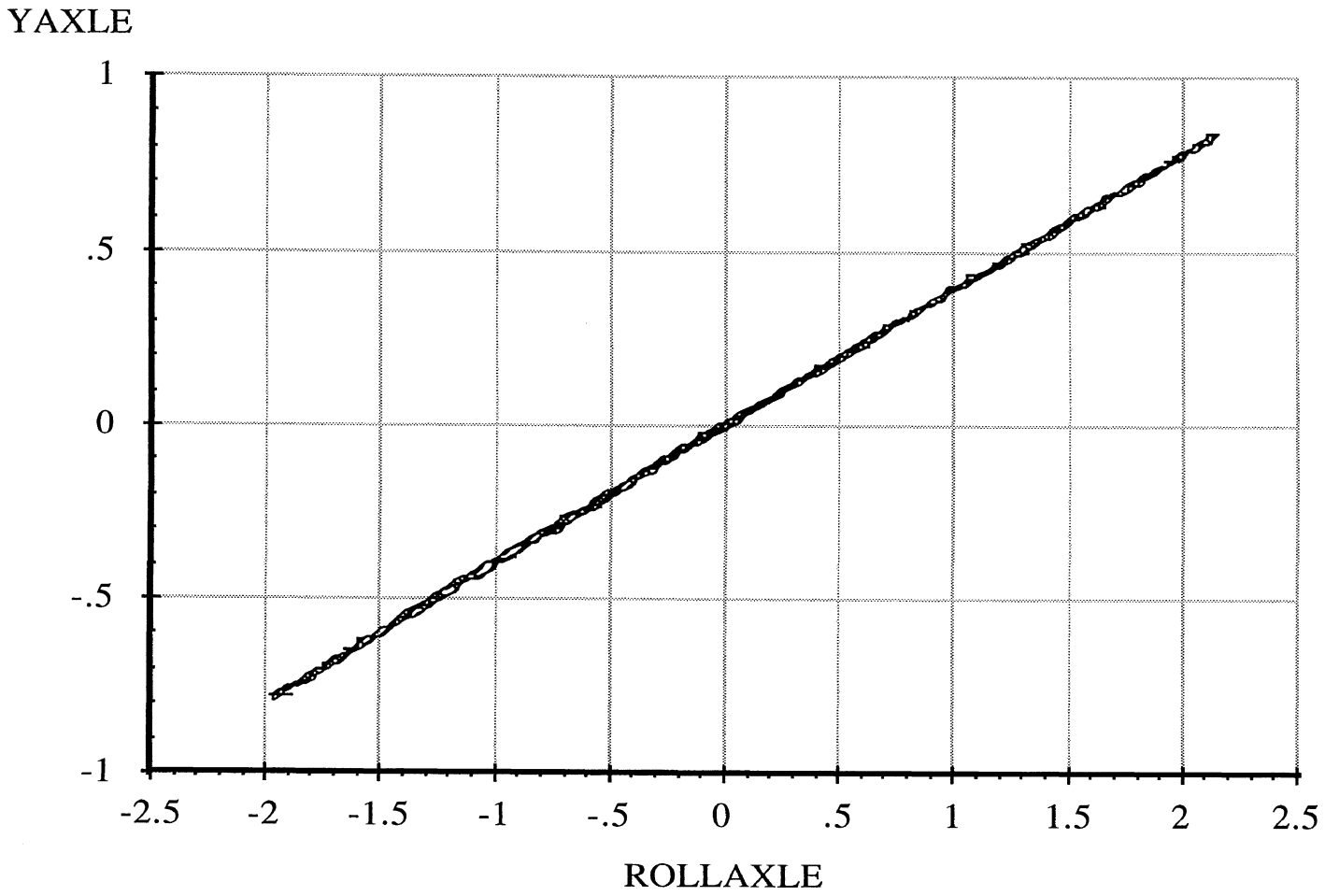

Abscissa (X): Axle roll angle (ROLLAXLE); degrees; right side compressed, positive.

Ordinate (Y): Axle reference point lateral translation (YAXLE); inches; motion toward right, positive.

*Note: Brakes on. Force control. Air bags inflated to 26 psi. Reference height of 8.31 inches.

Measured by UMTRI for Smart Truck
Freightliner Tractor

Data file: FRTLNG01.ERD

Drive Axle Suspension, Trailing Only

Roll Steer

6 April 96
Suspension: Trailing Arm (2LU)

Suspension Load: 8000 lb.

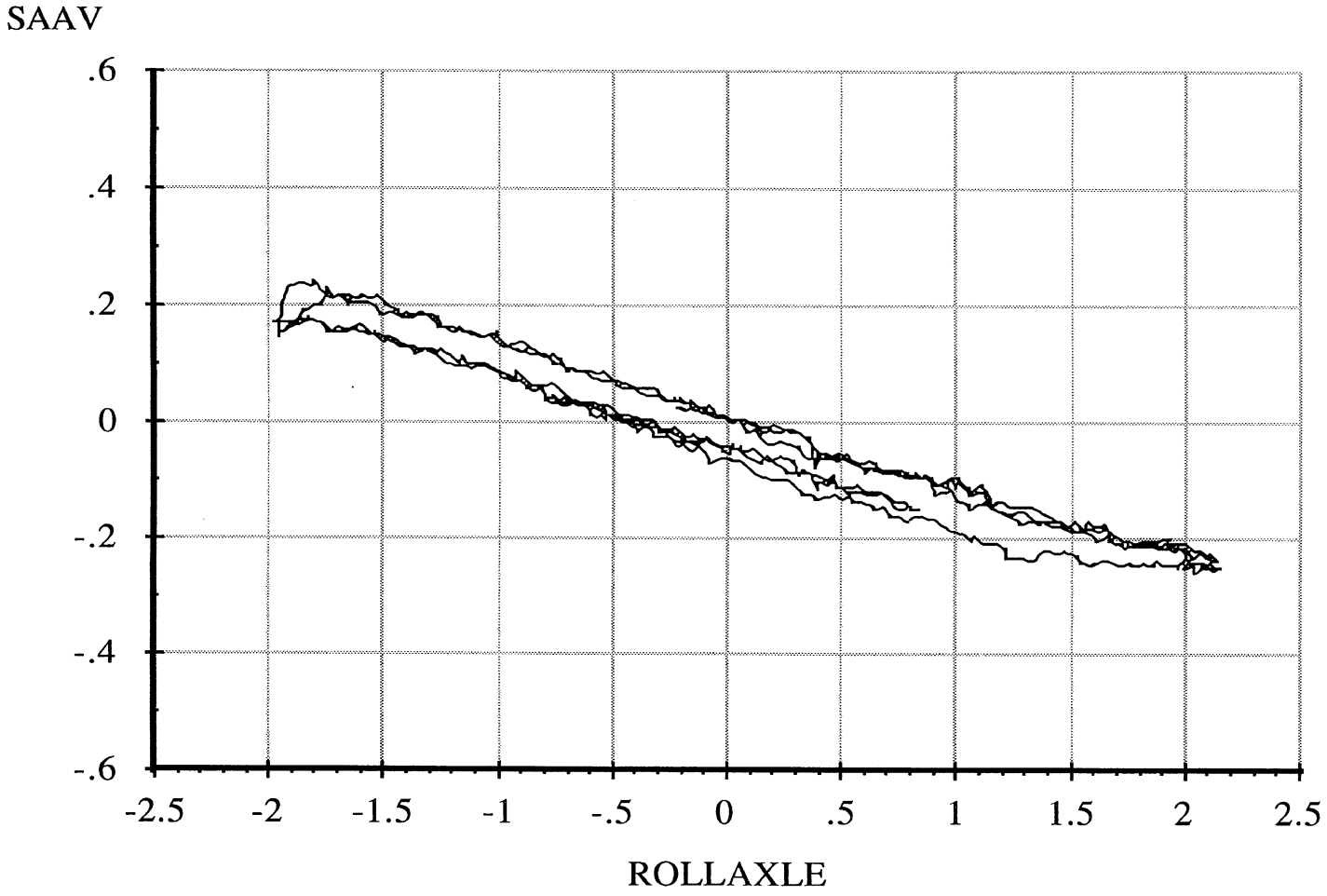

Abscissa (X): Axle roll angle (ROLLAXLE); degrees; right side compressed, positive.

Ordinate (Y): Average steer angle (SAAV); degrees; steer toward right, positive.

*Note: Brakes on. Force control. Air bags inflated to 26 psi.

Measured by UMTRI for Smart Truck
Freightliner Tractor

Data file: FRTLNG02.ERD

Drive Axle Suspension, Trailing Only

Lateral Force Compliance

6 April 96
Suspension: Trailing Arm (2LU)

Suspension Load: 8000 lb.

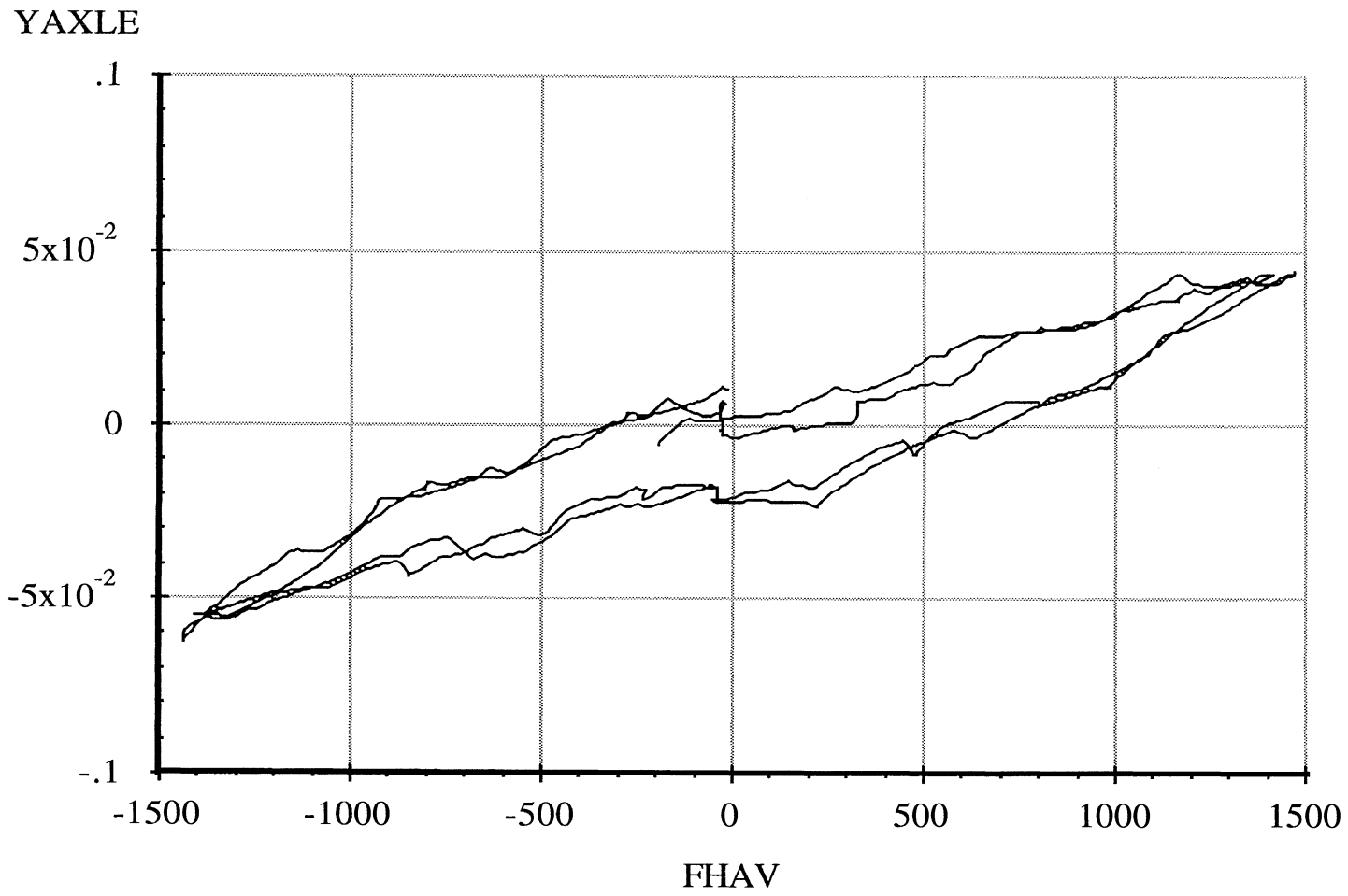

Abscissa (X): Average axle lateral force (FHAV); pounds; applied to both wheels simultaneously; force applied toward right, positive.

Ordinate (Y): Axle lateral translation (YAXLE); inches; motion toward right, positive.

*Note: Brakes on. Position control. Air bags inflated to 26 psi. Reference height of 8.31 inches.

Measured by UMTRI for Smart Truck
Freightliner Tractor

Data file: FRTLNG02.ERD

Drive Axle Suspension, Trailing Only

Lateral Force Steer

6 April 96
Suspension: Trailing Arm (2LU)

Suspension Load: 8000 lb.

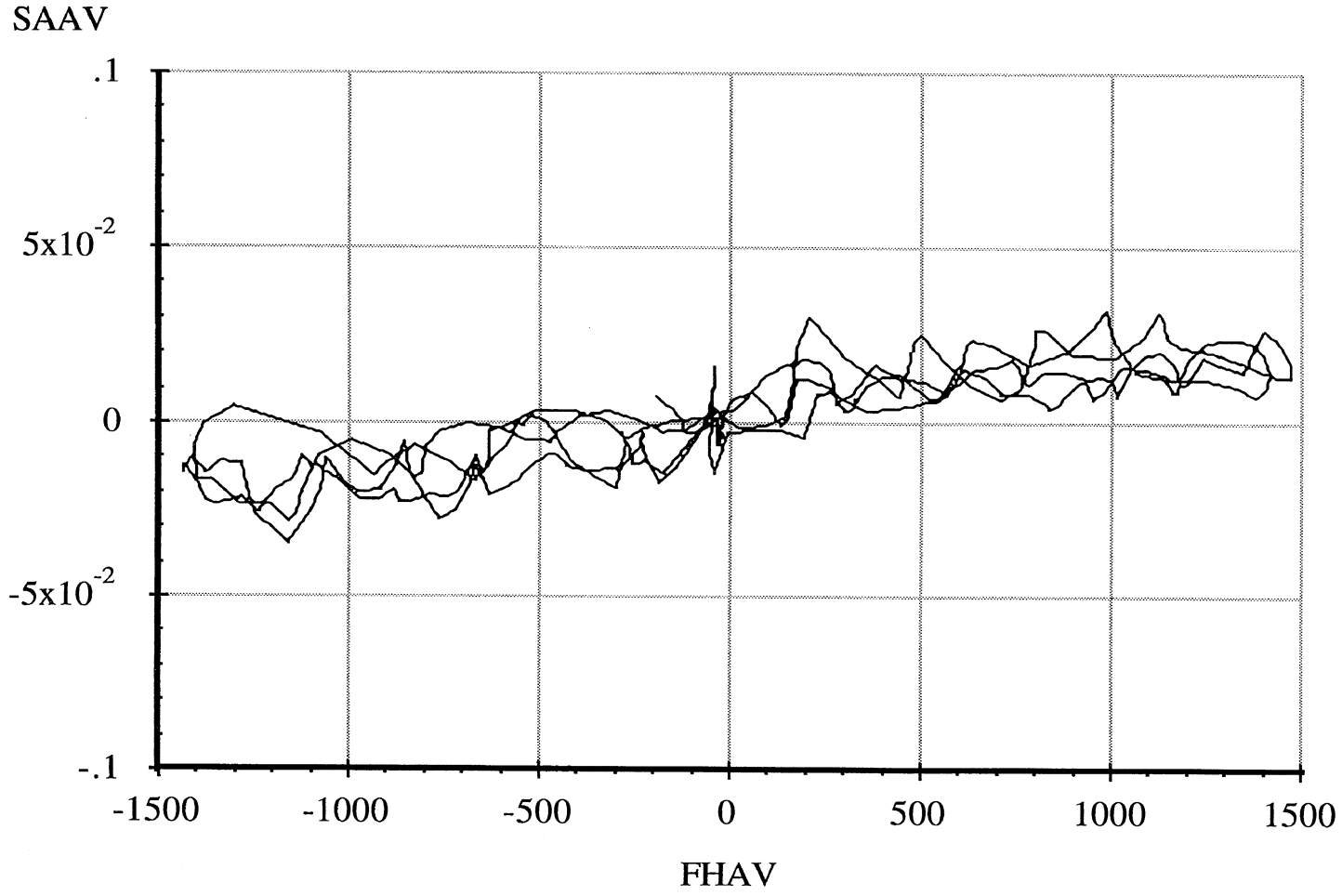

Abscissa (X): Average axle lateral force (FHAV); pounds; applied to both wheels simultaneously; force applied toward right, positive.

Ordinate (Y): Average steer angle (SAAV); degrees; steer toward right, positive.

*Note: Brakes on. Position control. Air bags inflated to 26 psi.

Measured by UMTRI for Smart Truck
Freightliner Tractor

Drive Axle Suspension, Trailing Only

6 April 96
Suspension: Trailing Arm (2LU)

Data file: FRTLNG03.ERD

Aligning Moment Compliance Steer

Suspension Load: 8000 lb.

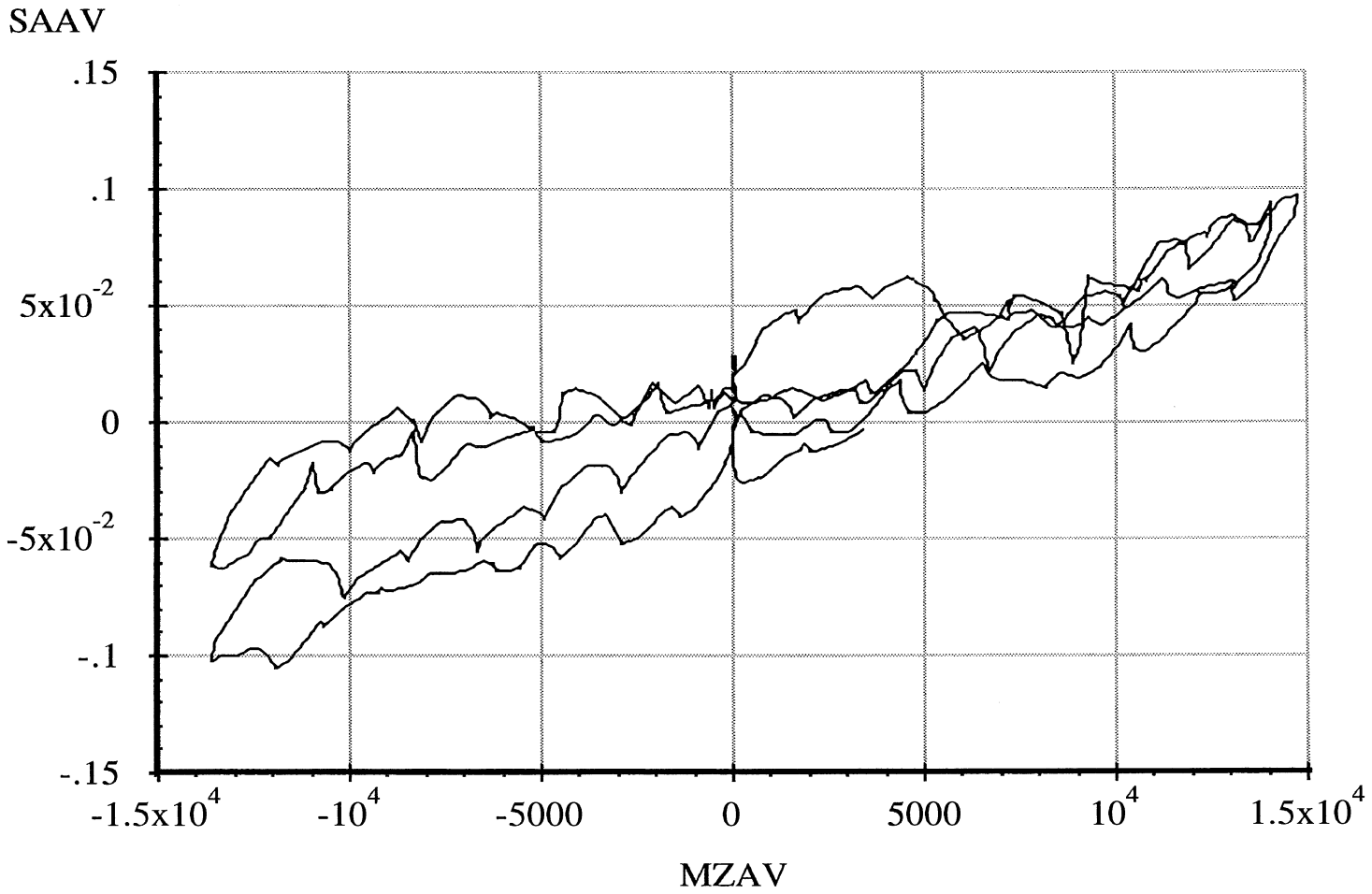

Abscissa (X): Average axle aligning moment (MZAV); in-lb per wheel; applied to both wheels simultaneously; downward (right hand rule) moment vector, positive.

Ordinate (Y): Average steer angle (SAAV); degrees; steer toward right, positive.

*Note: Brakes on. Position control. Air bags inflated to 26 psi.

Measured by UMTRI for Smart Truck
Freightliner Tractor

Data file: FRTLNG00.ERD

Drive Axle Suspension, Trailing Only

Average Vertical Spring Rate

6 April 96
Suspension: Trailing Arm (2LU)

Nominal Suspension Load: 4000 lb.

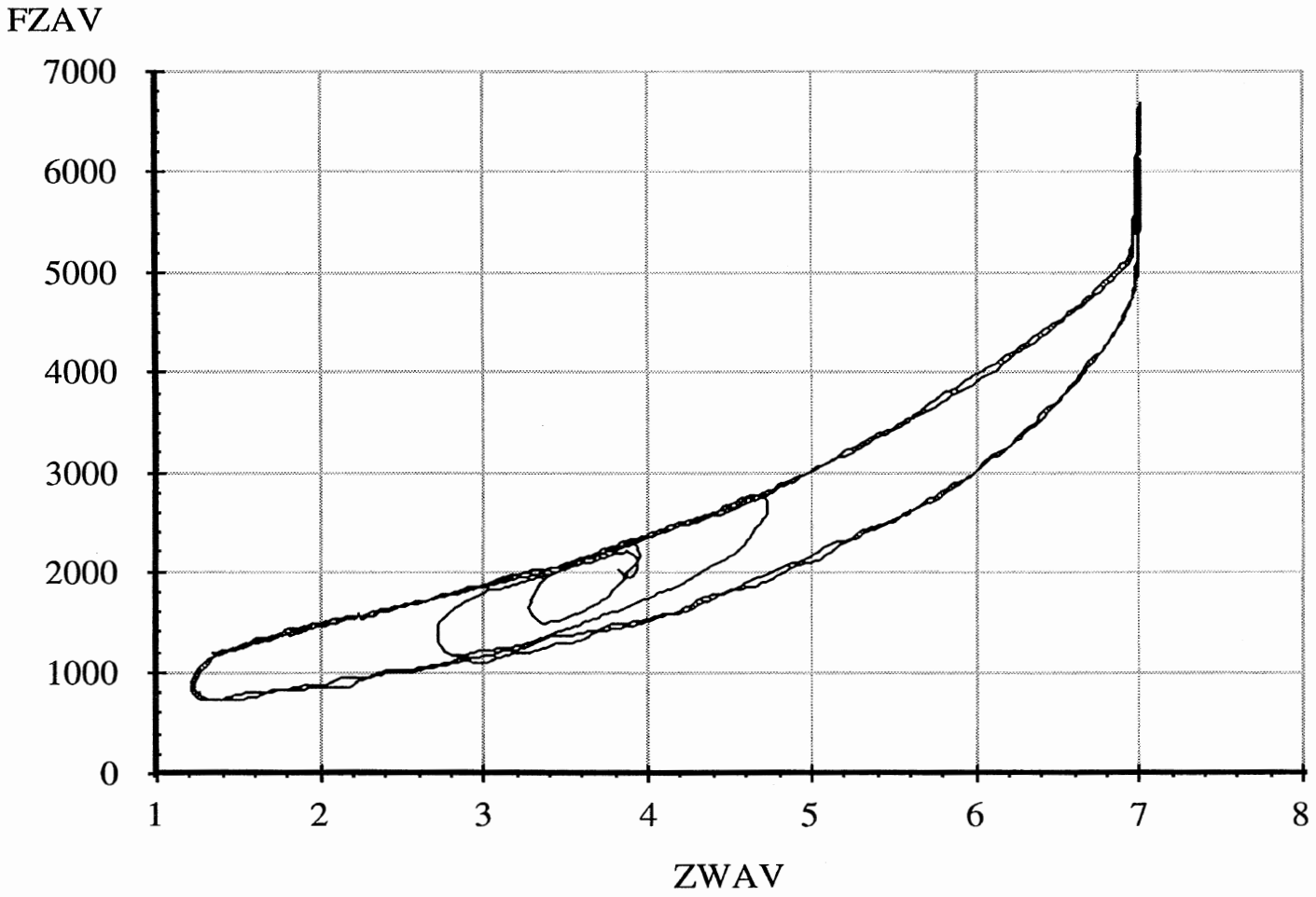

Abscissa (X): Average vertical wheel displacement (ZWAV); inches; spring compression, positive.

Ordinate (Y): Average vertical wheel load (FZAV); pounds; spring compression, positive.

*Note: Brakes on. Position control. Air bags inflated to 8 psi.

Measured by UMTRI for Smart Truck
Freightliner Tractor

Data file: FRTLNG11.ERD

Drive Axle Suspension, Trailing Only

Axle Roll Rate

6 April 96
Suspension: Trailing Arm (2LU)

Suspension Load: 4000 lb.

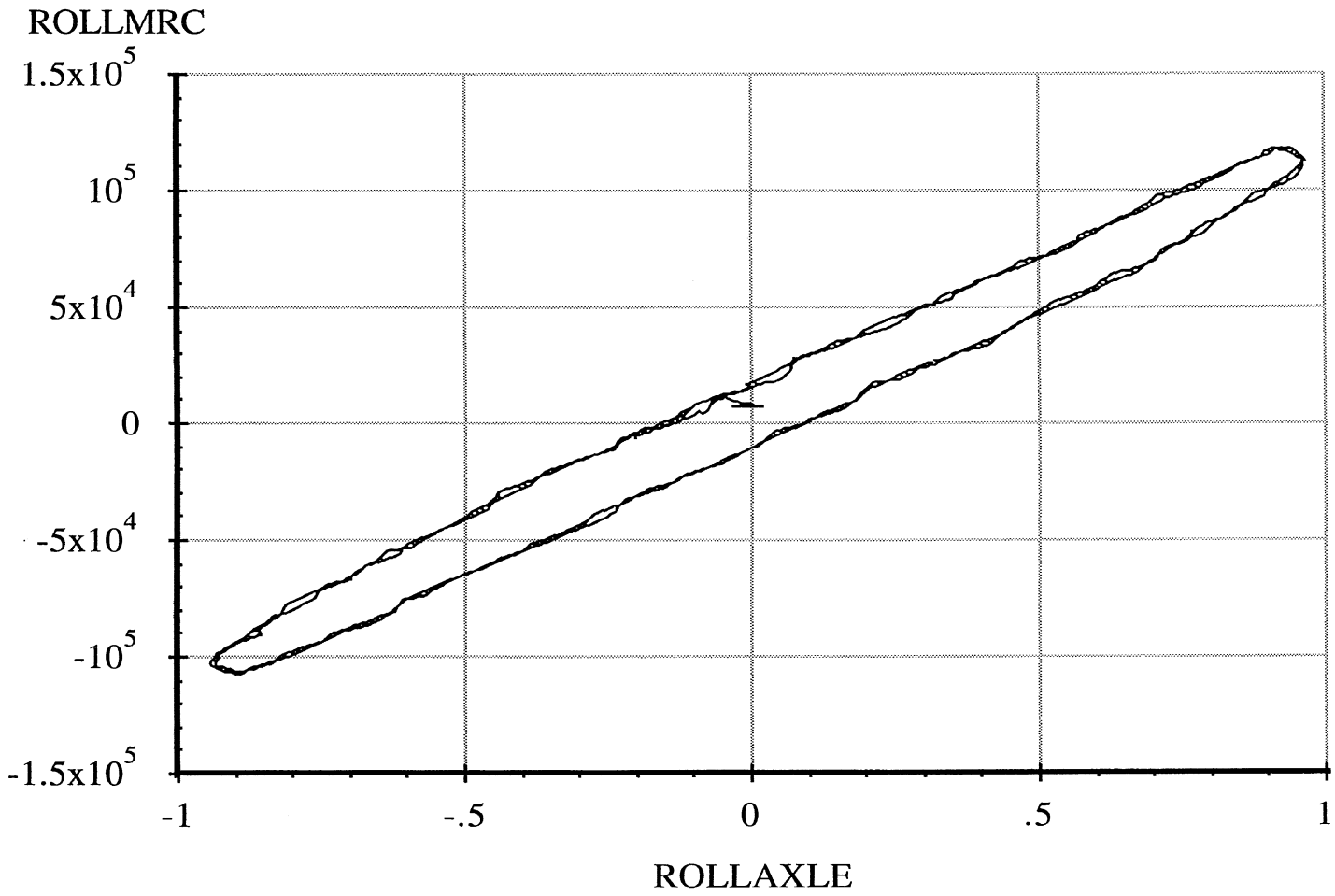

Abscissa (X): Axle roll angle (ROLLAXLE); degrees; right side compressed, positive.

Ordinate (Y): Axle roll moment about the roll center (ROLLMRC); in-lb; right side compressed, positive.

*Note: Brakes on. Force control. Air bags inflated to 8 psi.

Measured by UMTRI for Smart Truck
Freightliner Tractor

Data file: FRTLNG11.ERD

Drive Axle Suspension, Trailing Only

Roll Center Height

6 April 96
Suspension: Trailing Arm (2LU)

Suspension Load: 4000 lb.

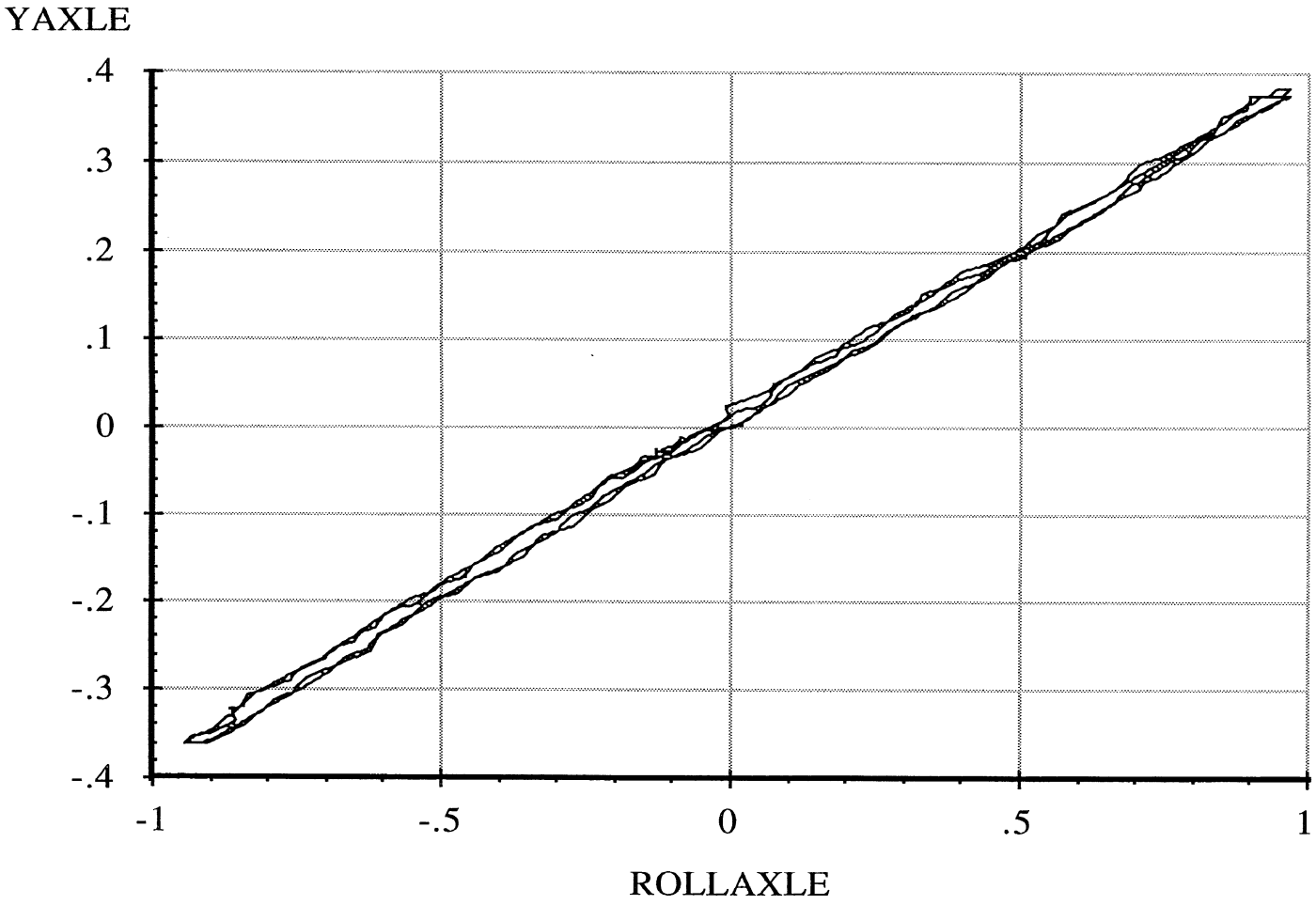

Abscissa (X): Axle roll angle (ROLLAXLE); degrees; right side compressed, positive.

Ordinate (Y): Axle reference point lateral translation (YAXLE); inches; motion toward right, positive.

*Note: Brakes on. Force control. Air bags inflated to 8 psi. Reference height of 8.56 inches.

Measured by UMTRI for Smart Truck
Freightliner Tractor

Data file: FRTLNG11.ERD

Drive Axle Suspension, Trailing Only

Roll Steer

6 April 96
Suspension: Trailing Arm (2LU)

Suspension Load: 4000 lb.

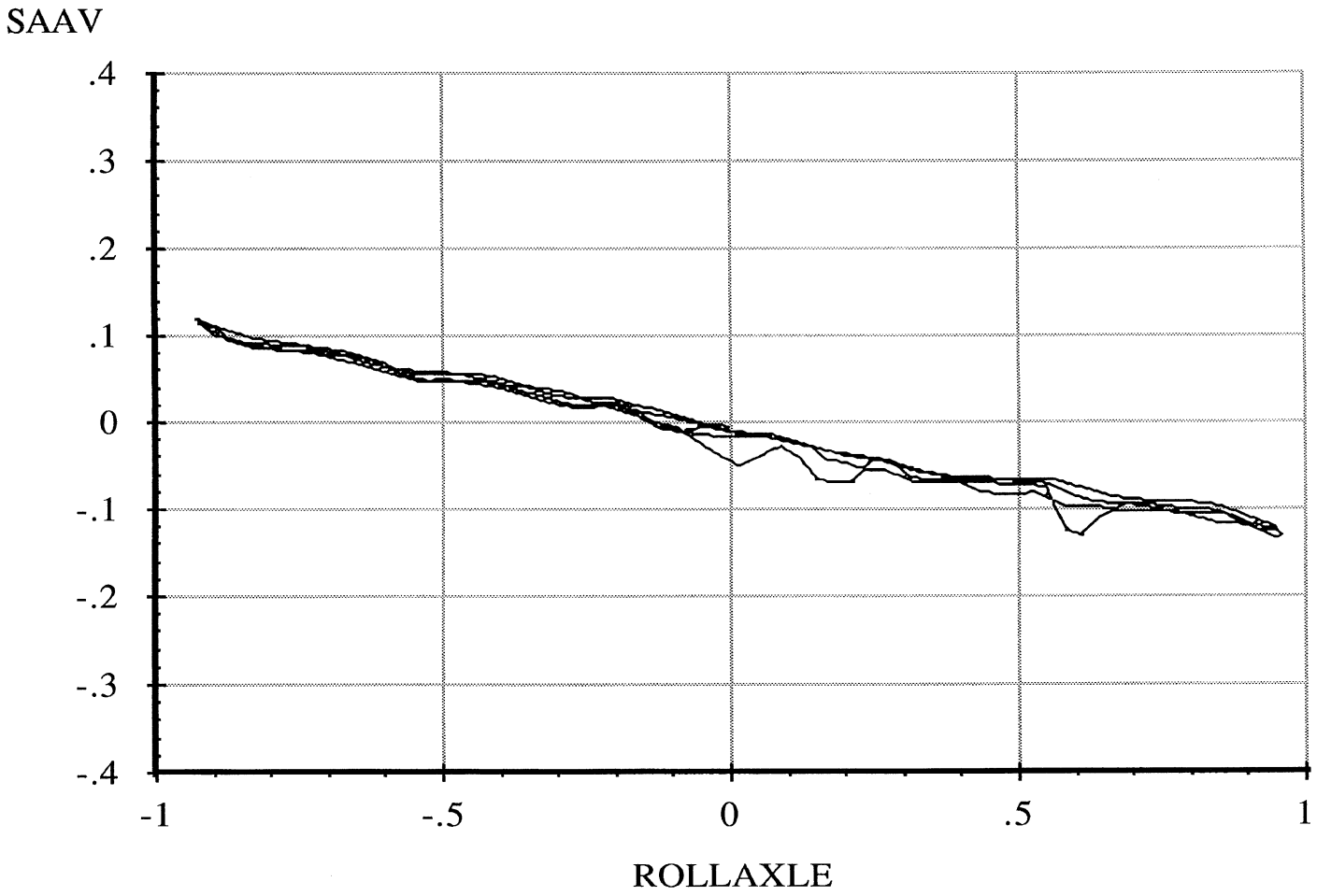

Abscissa (X): Axle roll angle (ROLLAXLE); degrees; right side compressed, positive.

Ordinate (Y): Average steer angle (SAAV); degrees; steer toward right, positive.

*Note: Brakes on. Force control. Air bags inflated to 8 psi.

Measured by UMTRI for Smart Truck
Freightliner Tractor

Data file: FRTLNG12.ERD

Drive Axle Suspension, Trailing Only

Lateral Force Compliance

6 April 96
Suspension: Trailing Arm (2LU)

Suspension Load: 4000 lb.

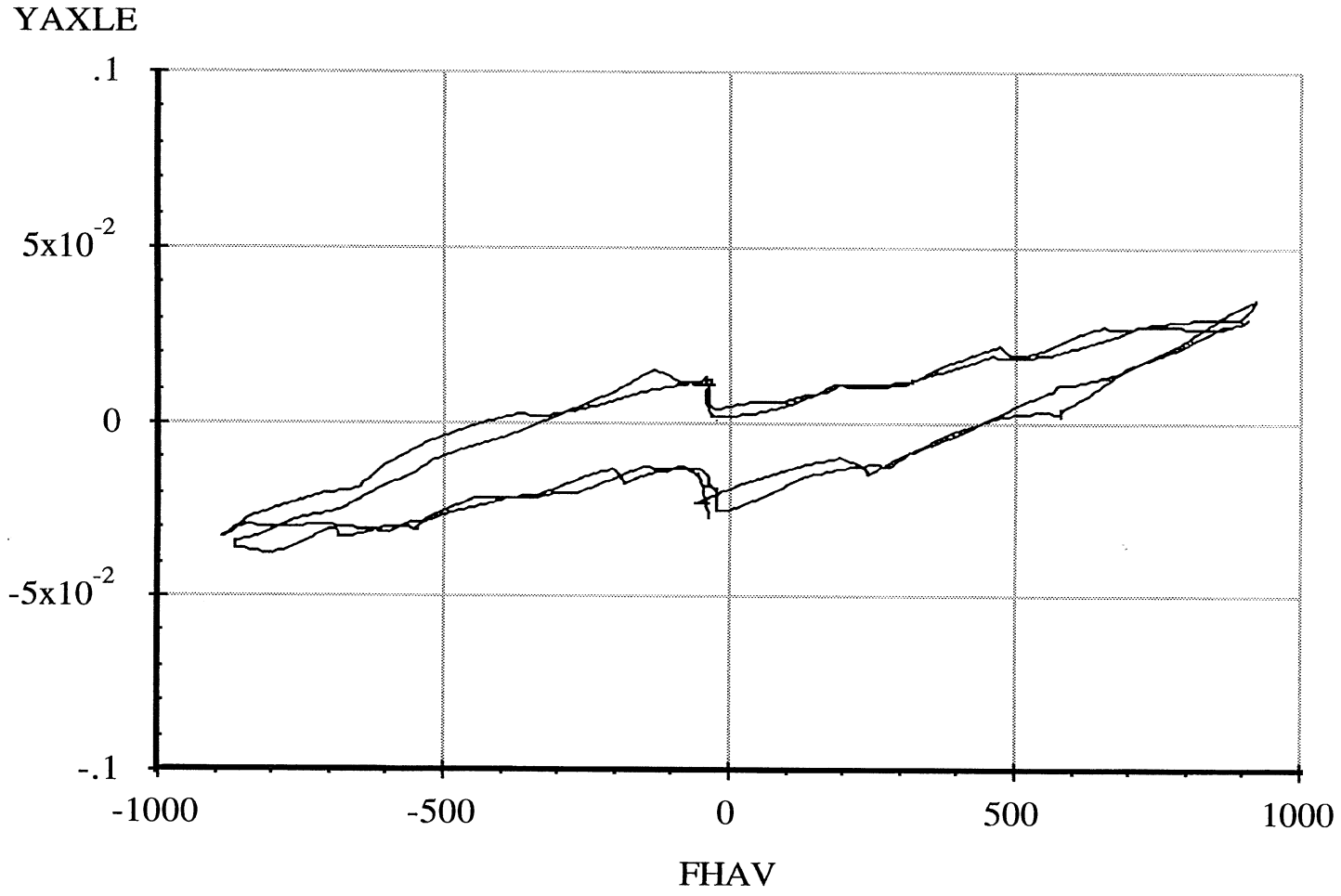

Abscissa (X): Average axle lateral force (FHAV); pounds; applied to both wheels simultaneously; force applied toward right, positive.

Ordinate (Y): Axle lateral translation (YAXLE); inches; motion toward right, positive.

*Note: Brakes on. Position control. Air bags inflated to 8 psi. Reference height of 8.56 inches.

Measured by UMTRI for Smart Truck
Freightliner Tractor

Data file: FRTLNG12.ERD

Drive Axle Suspension, Trailing Only

Lateral Force Steer

6 April 96
Suspension: Trailing Arm (2LU)

Suspension Load: 4000 lb.

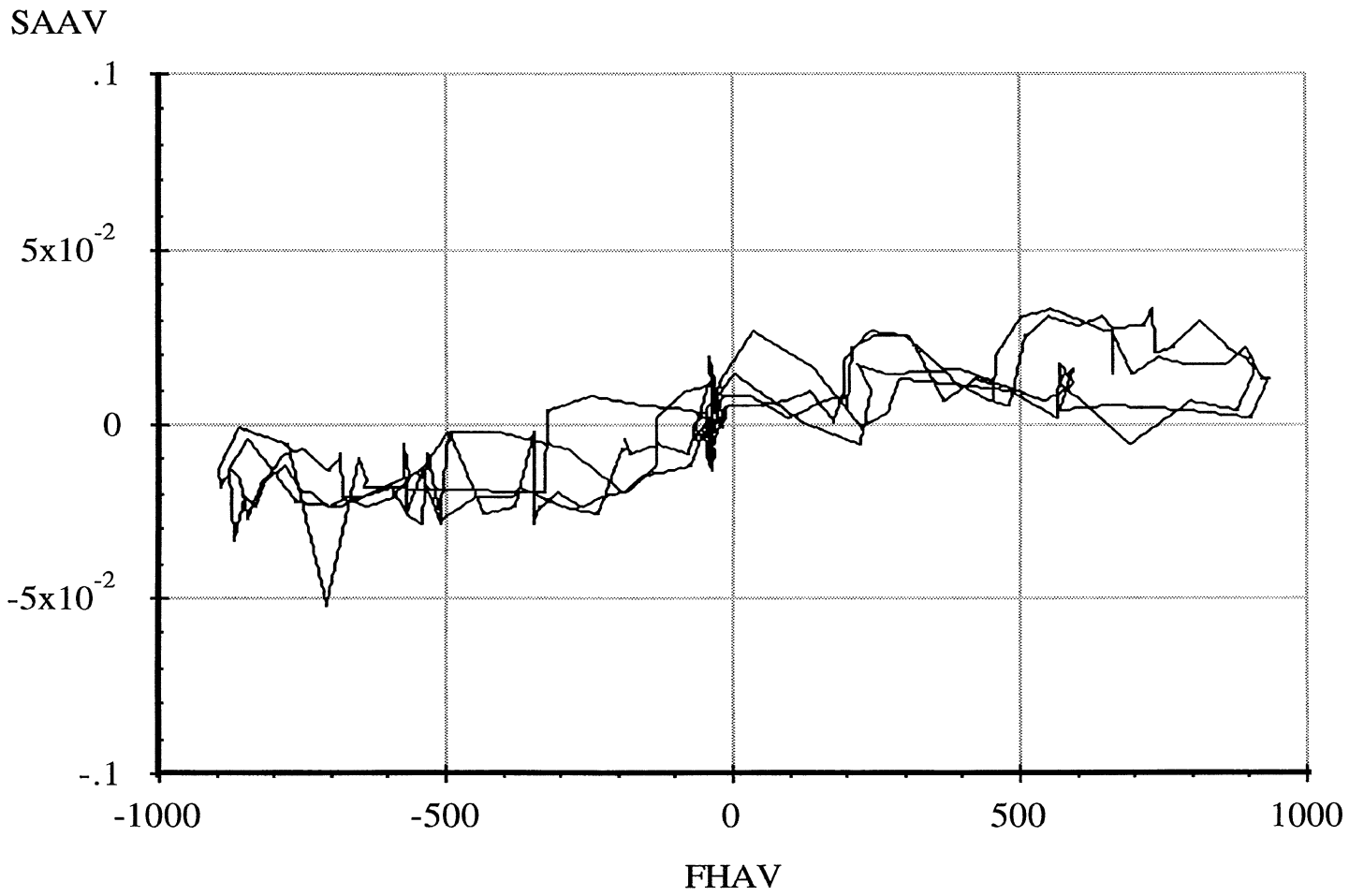

Abscissa (X): Average axle lateral force (FHAV); pounds; applied to both wheels simultaneously; force applied toward right, positive.

Ordinate (Y): Average steer angle (SAAV); degrees; steer toward right, positive.

*Note: Brakes on. Position control. Air bags inflated to 8 psi.

Measured by UMTRI for Smart Truck
Freightliner Tractor

Data file: FRTLNG13.ERD

Drive Axle Suspension, Trailing Only

Aligning Moment Compliance Steer

6 April 96
Suspension: Trailing Arm (2LU)

Suspension Load: 4000 lb.

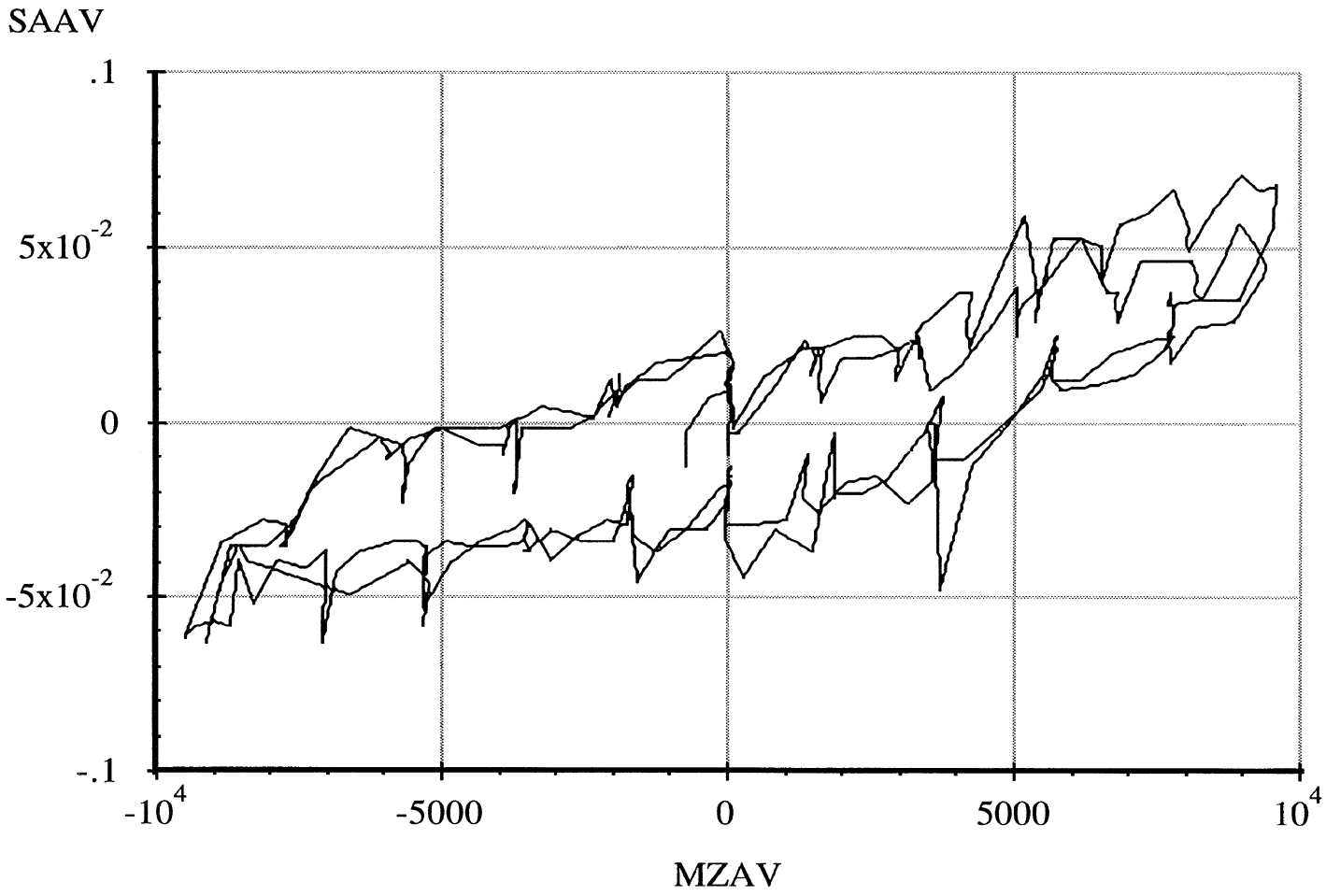

Abscissa (X): Average axle aligning moment (MZAV); in-lb per wheel; applied to both wheels simultaneously; downward (right hand rule) moment vector, positive.

Ordinate (Y): Average steer angle (SAAV); degrees; steer toward right, positive.

*Note: Brakes on. Position control. Air bags inflated to 8 psi.

Measured by UMTRI for Smart Truck
Fruehauf Model FBB9-F1-28

Data file: SMTTRL05.ERD

Single Trailer Axle Suspension

Average Vertical Spring Rate

4 Jan 98
Suspension: Trailing Arm (WT)

Nominal Suspension Load: 25800 lb.

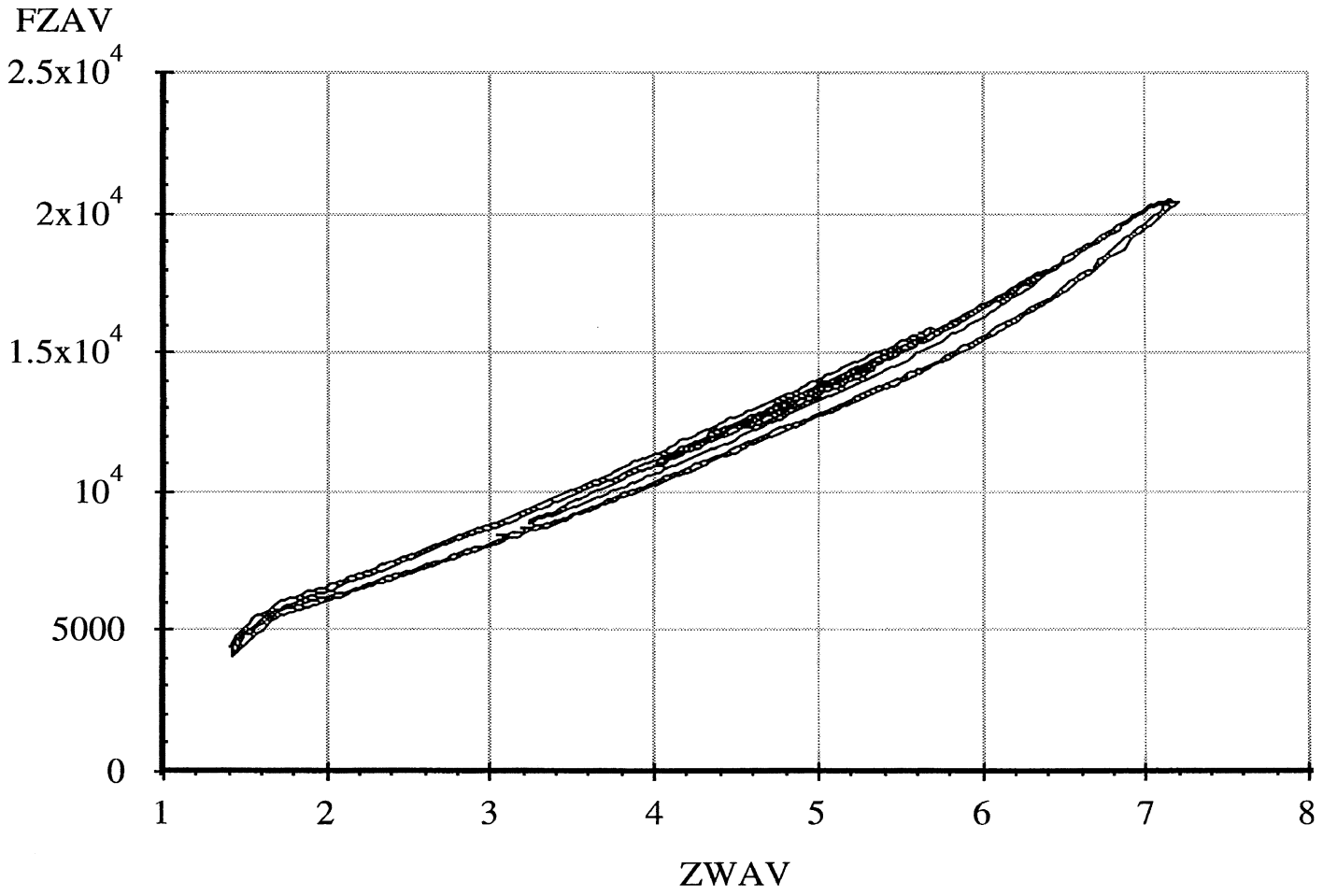

Abscissa (X): Average vertical wheel displacement (ZWAV); inches; spring compression, positive.

Ordinate (Y): Average vertical wheel load (FZAV); pounds; spring compression, positive.

*Note: Brakes on. Position control. Air bags inflated to 100 psi.

Measured by UMTRI for Smart Truck
Fruehauf Model FBB9-F1-28

Data file: SMTTRL15.ERD

Single Trailer Axle Suspension

Axle Roll Rate

4 Jan 98
Suspension: Trailing Arm (WT)

Suspension Load: 25800 lb.

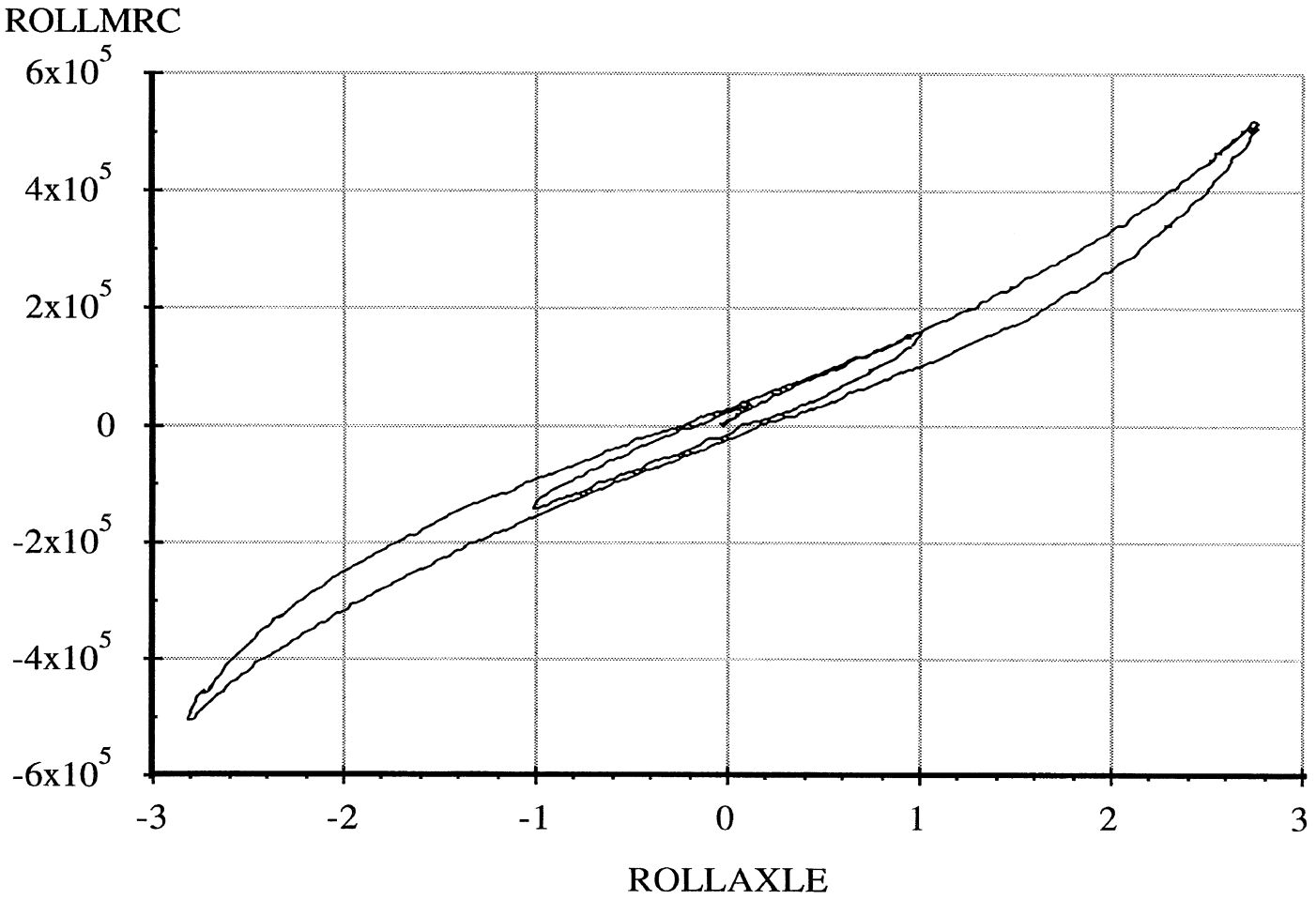

Abscissa (X): Axle roll angle (ROLLAXLE); degrees; right side compressed, positive.

Ordinate (Y): Axle roll moment about the roll center (ROLLMRC); in-lb; right side compressed, positive.

*Note: Brakes on. Force control. Air bags inflated to 100 psi.

Measured by UMTRI for Smart Truck
Fruehauf Model FBB9-F1-28

Data file: SMTTRL15.ERD

Single Trailer Axle Suspension

Roll Center Height

4 Jan 98
Suspension: Trailing Arm (WT)

Suspension Load: 25800 lb.

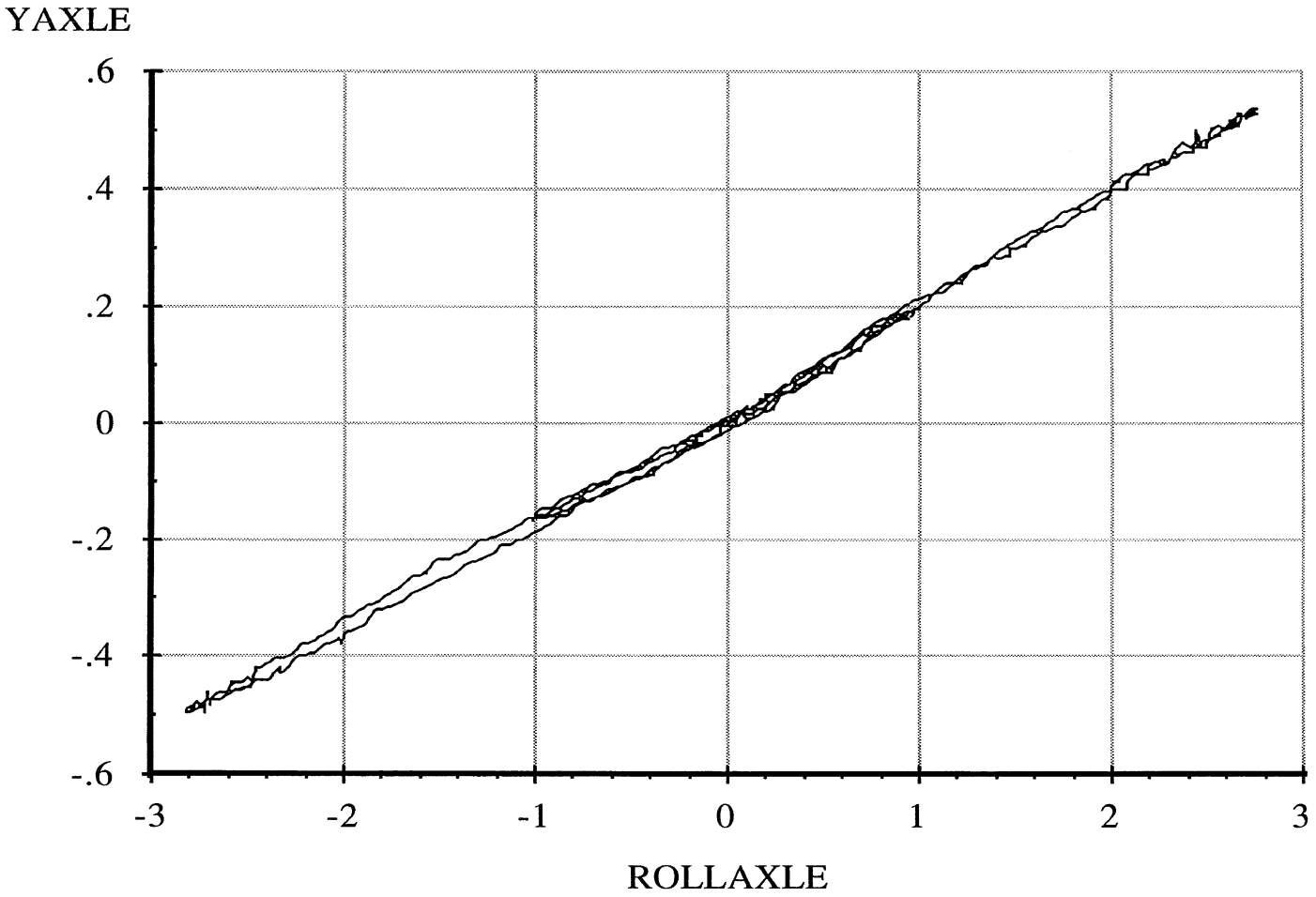

Abscissa (X): Axle roll angle (ROLLAXLE); degrees; right side compressed, positive.

Ordinate (Y): Axle reference point lateral translation (YAXLE); inches; motion toward right, positive.

*Note: Brakes on. Force control. Air bags inflated to 100 psi. Reference height of 13.69 inches.

Measured by UMTRI for Smart Truck
Fruehauf Model FBB9-F1-28

Data file: SMTTRL15.ERD

Single Trailer Axle Suspension

Roll Steer

4 Jan 98
Suspension: Trailing Arm (WT)

Suspension Load: 25800 lb.

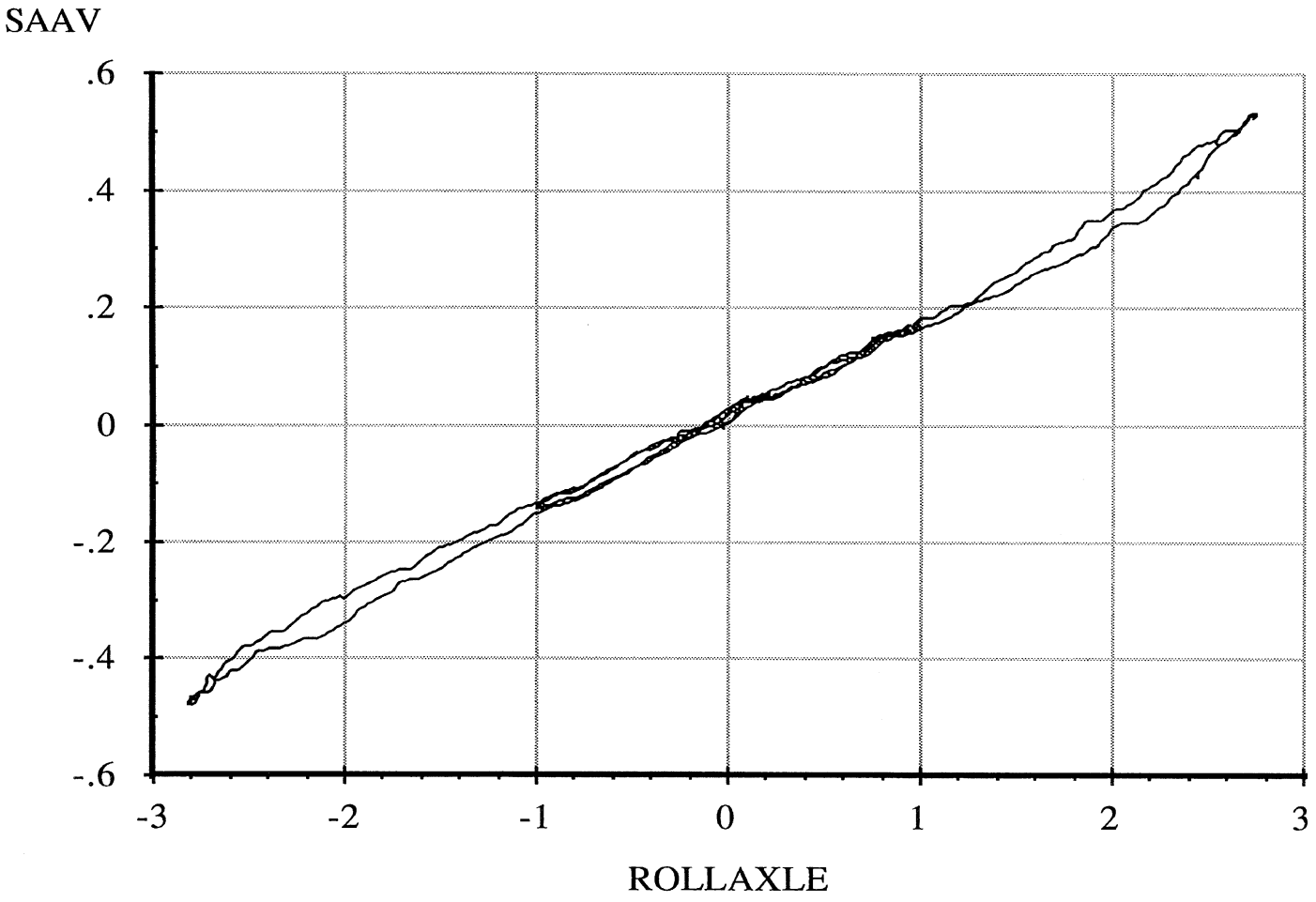

Abscissa (X): Axle roll angle (ROLLAXLE); degrees; right side compressed, positive.

Ordinate (Y): Average steer angle (SAAV); degrees; steer toward right, positive.

*Note: Brakes on. Force control. Air bags inflated to 100 psi.

Measured by UMTRI for Smart Truck
Fruehauf Model FBB9-F1-28

Data file: SMTTRL25.ERD

Single Trailer Axle Suspension

Lateral Force Compliance

4 Jan 98
Suspension: Trailing Arm (WT)
Suspension Load: 25800 lb.

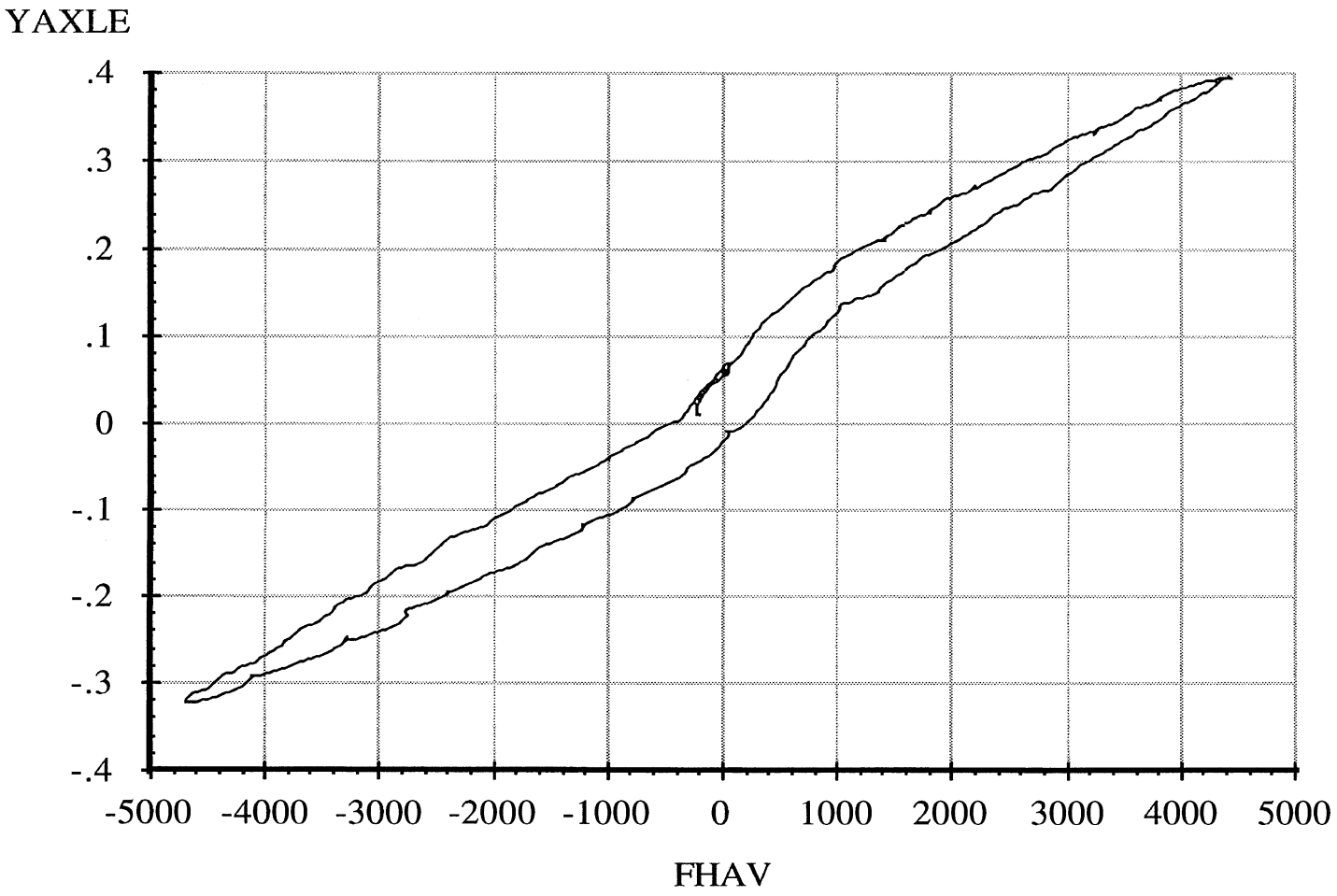

Abscissa (X): Average axle lateral force (FHAV); pounds; applied to both wheels simultaneously; force applied toward right, positive.

Ordinate (Y): Axle lateral translation (YAXLE); inches; motion toward right, positive.

*Note: Brakes on. Position control. Air bags inflated to 100 psi. Reference height of 13.69 inches.

Measured by UMTRI for Smart Truck
Fruehauf Model FBB9-F1-28

Data file: SMTTRL25.ERD

Single Trailer Axle Suspension

Lateral Force Steer

4 Jan 98
Suspension: Trailing Arm (WT)

Suspension Load: 25800 lb.

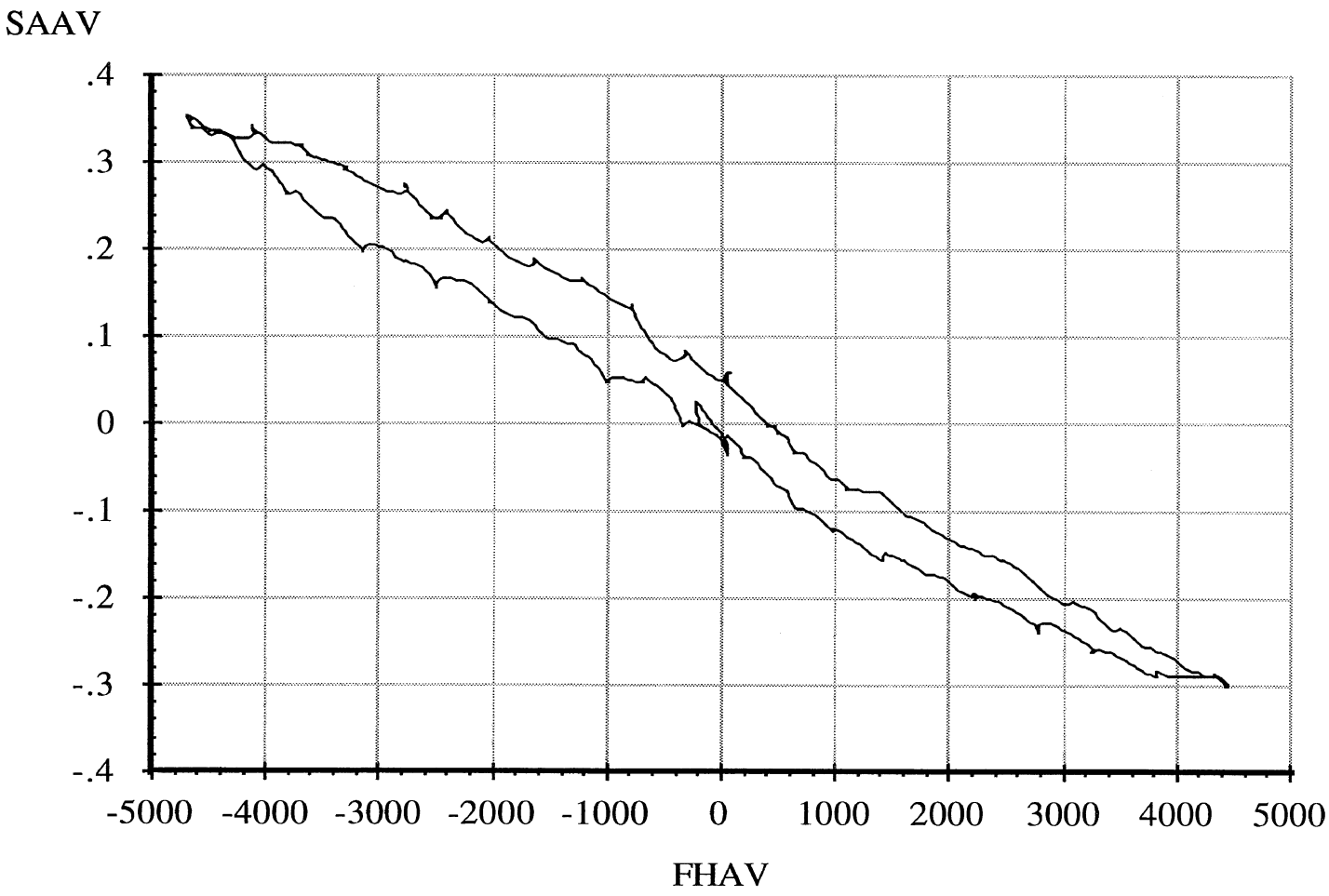

Abscissa (X): Average axle lateral force (FHAV); pounds; applied to both wheels simultaneously; force applied toward right, positive.

Ordinate (Y): Average steer angle (SAAV); degrees; steer toward right, positive.

*Note: Brakes on. Position control. Air bags inflated to 100 psi.

Measured by UMTRI for Smart Truck
Fruehauf Model FBB9-F1-28

Data file: SMTTRL04.ERD

Single Trailer Axle Suspension

Average Vertical Spring Rate

4 Jan 98
Suspension: Trailing Arm (WT)

Nominal Suspension Load: 20800 lb.

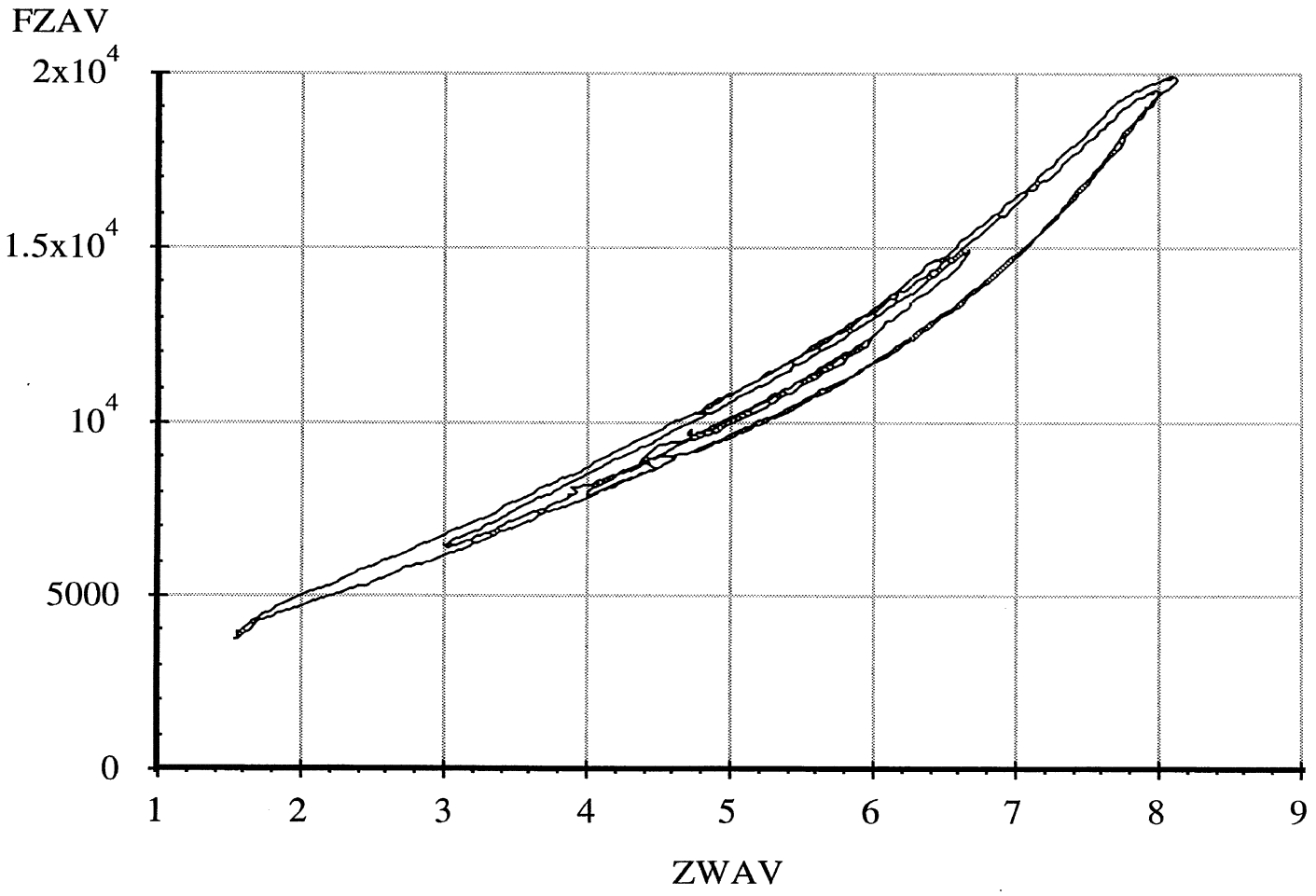

Abscissa (X): Average vertical wheel displacement (ZWAV); inches; spring compression, positive.

Ordinate (Y): Average vertical wheel load (FZAV); pounds; spring compression, positive.

*Note: Brakes on. Position control. Air bags inflated to 80 psi.

Measured by UMTRI for Smart Truck
Fruehauf Model FBB9-F1-28

Data file: SMTTRL14.ERD

Single Trailer Axle Suspension

Axle Roll Rate

4 Jan 98
Suspension: Trailing Arm (WT)

Suspension Load: 20800 lb.

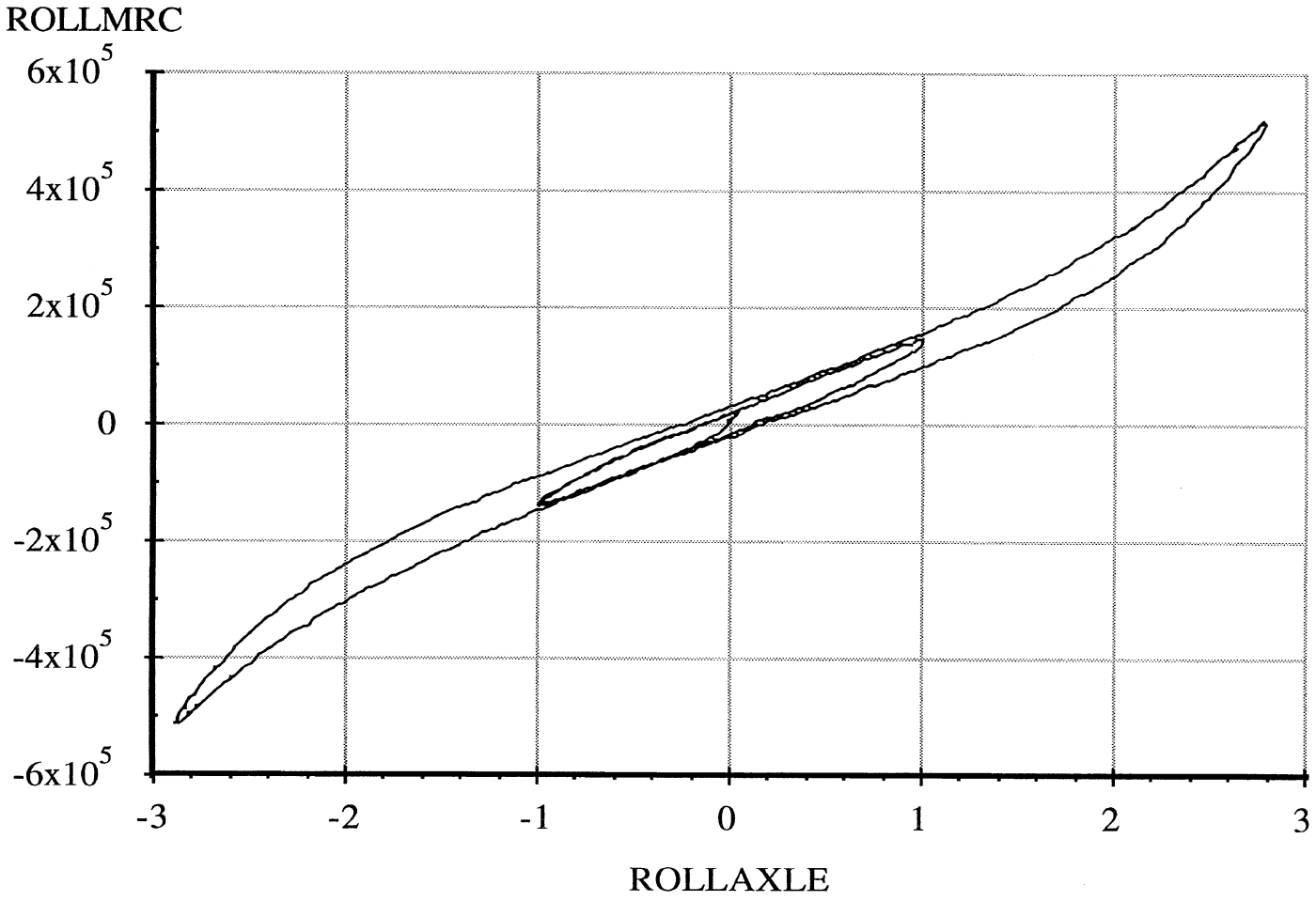

Abscissa (X): Axle roll angle (ROLLAXLE); degrees; right side compressed, positive.

Ordinate (Y): Axle roll moment about the roll center (ROLLMRC); in-lb; right side compressed, positive.

*Note: Brakes on. Force control. Air bags inflated to 80 psi.

APPENDIX B. MAPS OF THE RSA ROAD COURSES

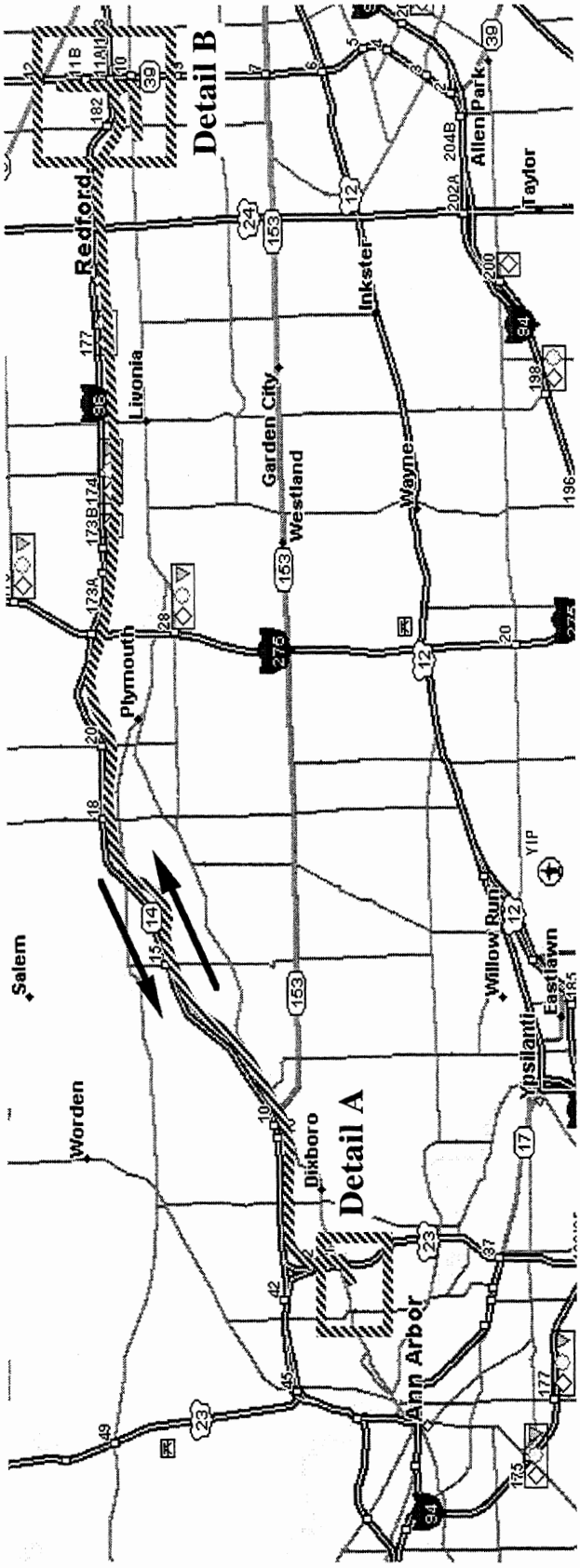

Figure B-1. RSA test route #1

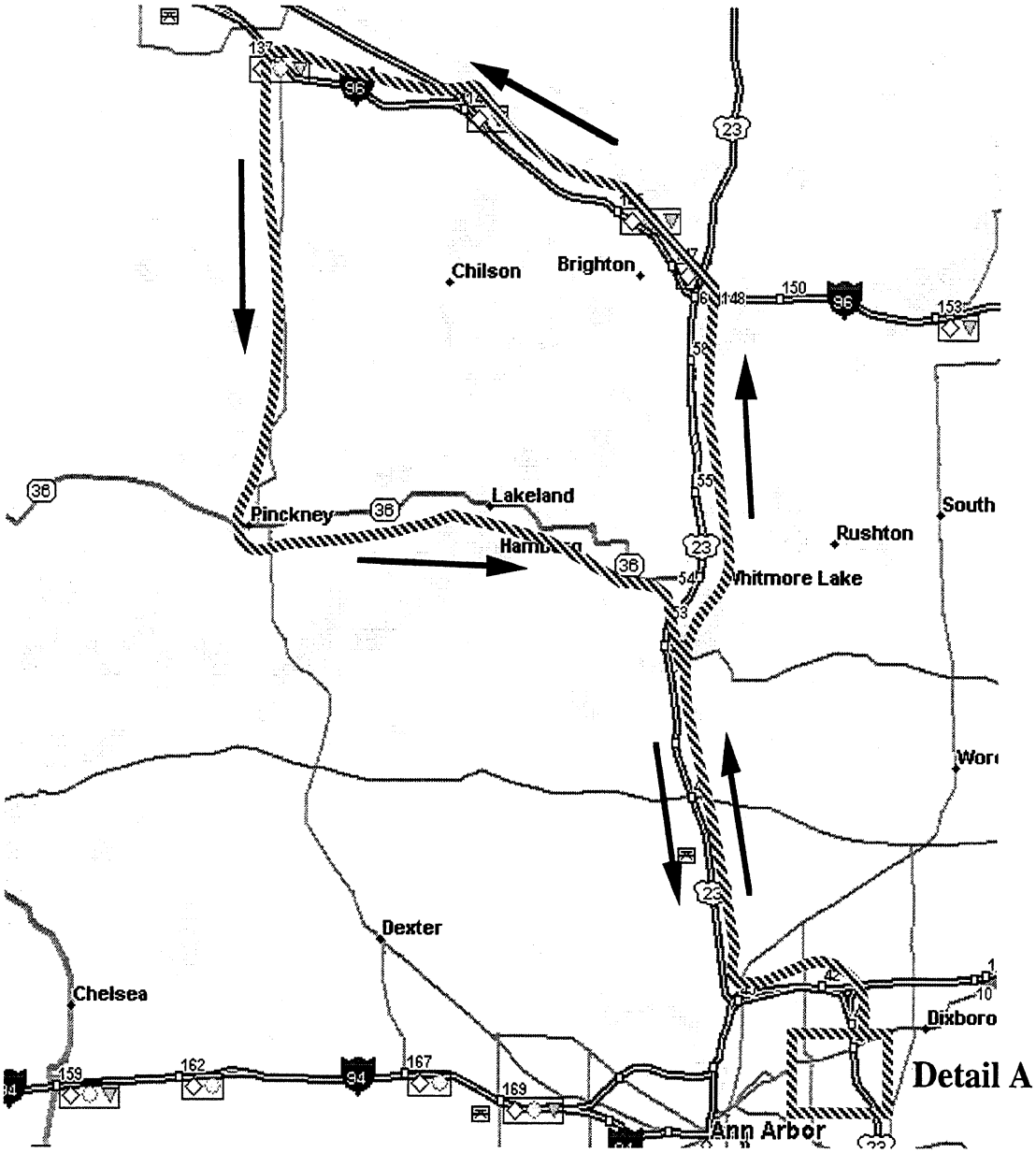

Figure B-2. RSA test route #2

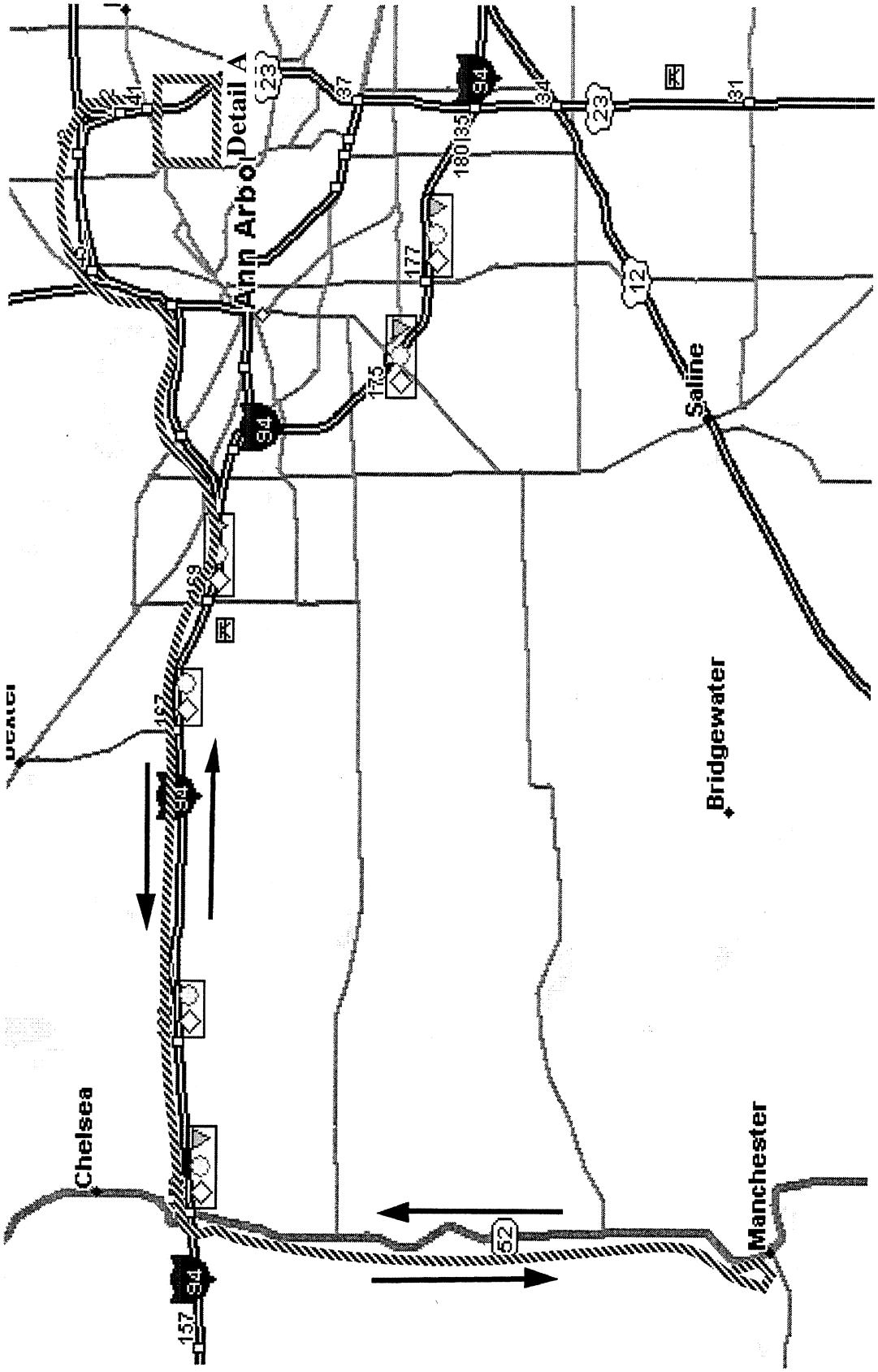

Figure B-3. RSA test route #3

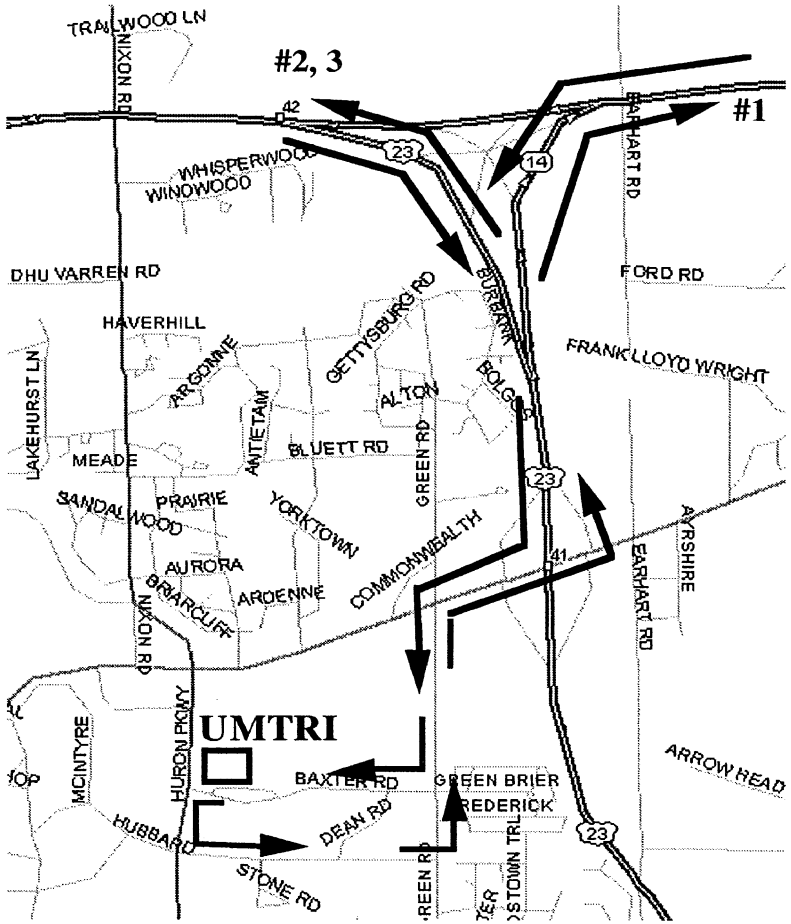

Figure B-4. Detail of RSA test routes in Ann Arbor

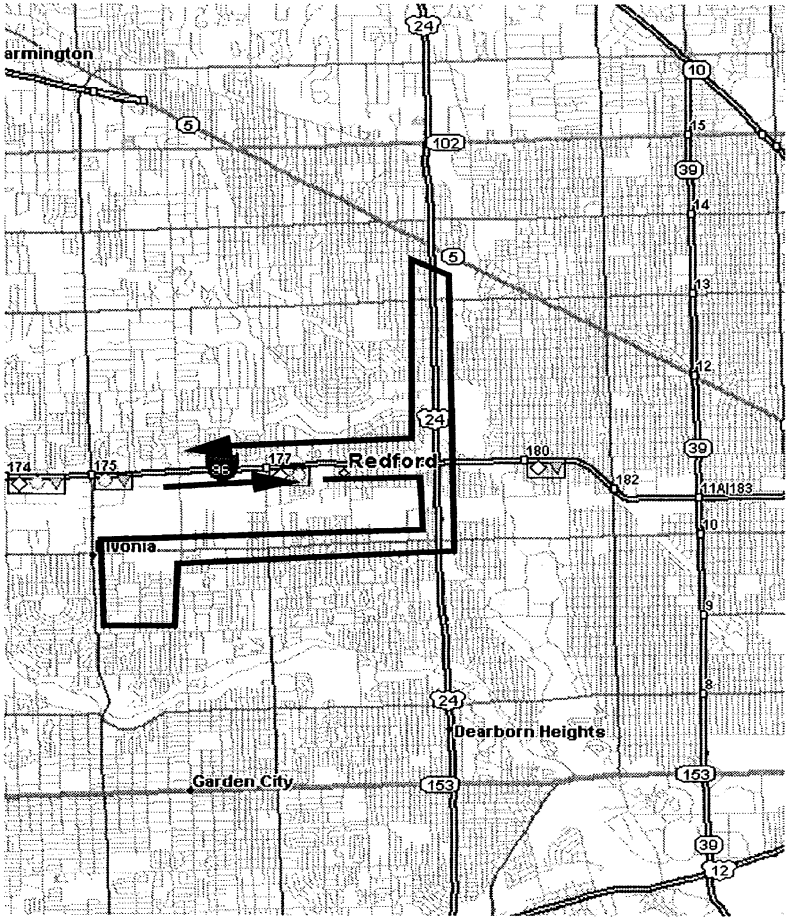

Figure B-5. Detail of RSA test route in Dearborn

APPENDIX C

1. INTRODUCTION

The Roll Stability Advisor (RSA) as envisaged in its most comprehensive form would have the capability to assess the stability of any attached semitrailer by means of only the use of instrumentation mounted on the tractor, with no assumptions being made about knowledge of semitrailer properties, and using only such information as can be gathered during maneuvers that occur during normal highway/city driving. This task is quite a challenging one given the number of and accuracy with which semitrailer parameters have to be estimated in real world conditions where all measurements are contaminated with varying levels of noise and the signal levels for the most part are fairly low due to the routine and non-exciting (in the dynamic sense) maneuvers that large tractor-semitrailer combinations execute. This appendix details the approaches taken to achieve the above goal, the degree of success attained in doing so and the areas in which improvement may be necessary.

The fundamental task in developing the RSA system is to predict the critical lateral acceleration at which the tractor-semitrailer combination rolls over. This may be subdivided into predicting the level of lateral accelerations for semitrailer axle liftoff, and tractor axle respectively, and then determining which of the two limits represents the critical value for overall vehicle rollover. The approach taken in this study considers only steady state maneuvers. While dynamic effects certainly affect truck stability, the steady state limits provide valuable information, especially from the point of view of this particular effort which is to develop a system that attempts to inform or the driver about the stability of the semitrailer and helps him/her suitably modify driving aggressiveness.

The task of developing the RSA system consisted of the following steps: (i) development of a model that describes the physics of the tractor-semitrailer system (ii) development of algorithms that draw upon the previously derived model and the available measurements to estimate semitrailer parameters and (iii) prediction of critical accelerations for tractor and semitrailer rollover.

II. MODELING OF TRACTOR-SEMITRAILER SYSTEM

1.1 Pitch plane model

Figure C.1 is a free body diagram of a semitrailer in pitch plane. The dynamic equilibrium can be written as

$$\sum F_x = 0 \qquad F_{x5} - F_r - F_a - m_2 g \sin\theta - m_2 a_{x2} = 0 \tag{1.1}$$

$$\sum F_z = 0 \qquad F_{z5} + W_r - m_2 g \cos\theta - m_2 a_{z2} = 0 \tag{1.2}$$

$$\sum M_{Ay} = 0 \qquad -F_{z5}L + F_{x5}h_5 + m_2 gb\cos\theta - m_2 g h_{CG}\sin\theta - m_2 a_{x2} h_{CG} \;)$$

$$- F_a h_a + m_2 a_{z2} b - [\Phi_P + m_2 (b^2 + {h_{CG}}^2)]\dot{P} = 0 \tag{1.3}$$

where Φ_P is the pitch inertia moment, and $\dot{P}$ pitch acceleration. The definitions of other parameters can be seen from Figure C.1.

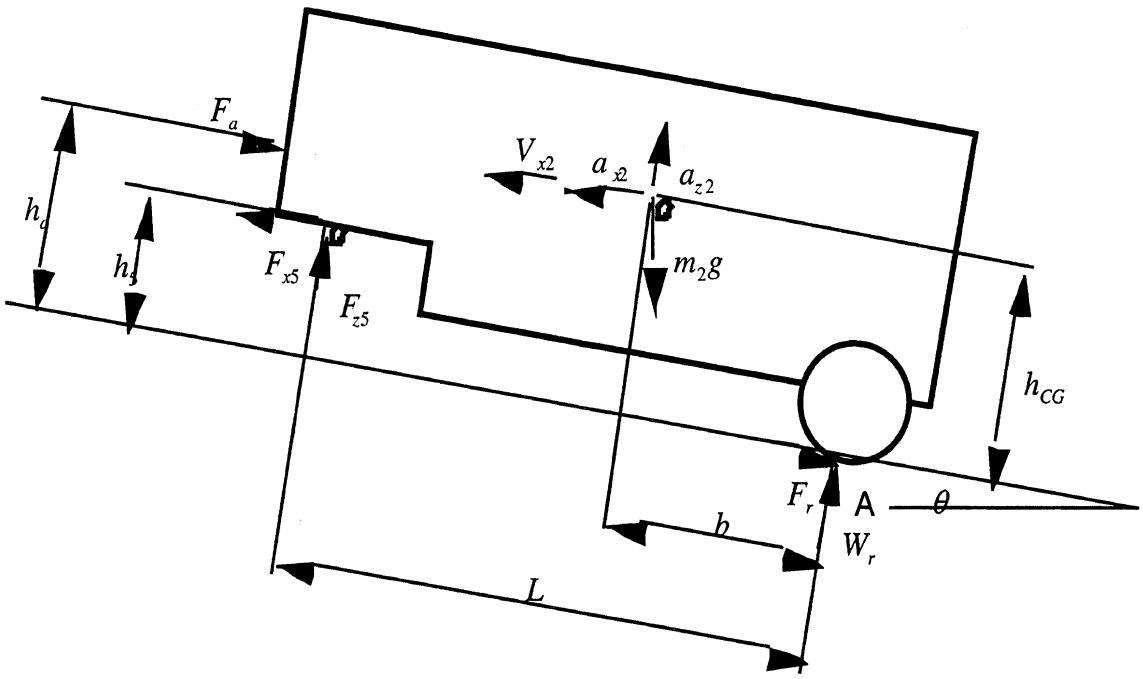

Figure C.1. Free body diagram of a semitrailer in pitch plane

If the change of rolling resistance characteristics between roadway and tires is ignored, the rolling resistance coefficient can be expressed as

$$f = f_0 + f_v V_x \tag{1.4}$$

where V_x is the vehicle speed, f_0 and f_v are two constants. According to [1], the aerodynamic drag is

$$F_a = f_{v2} V_x^2 \tag{1.5}$$

where f_{v2} is a constant. Substituting equation (1.4) and (1.5) into (1.1) yields

$$F_{x5} - W_r(f_0 + f_v V_{x2}) - f_{v2} V_{x2}^2 - m_2 g \sin\theta - m_2 a_{x2} = 0 \tag{1.6}$$

From equation (1.2), we have

$$W_r = -F_{z5} + m_2 g \cos\theta + m_2 a_{z2} \tag{1.7}$$

Substituting equation (1.7) into (1.6) yields

$$F_{x5} - (-F_{z5} + m_2 g \cos\theta + m_2 a_{z2}) \cdot (f_0 + f_v V_{x2}) - f_{v2} V_{x2}^2 - m_2 g \sin\theta - m_2 a_{x2} = 0 \tag{1.8}$$

When the road slope and cross slope are very small, $\sin\theta$ and $\cos\theta$ can be approximated by 0 and 1. Equation (1.3) and (1.8) are rewritten into:

$$-F_{z5} L + F_{x5} h_5 + m_2 g b - m_2 a_{x2} h_{CG} - F_a h_a + m_2 a_{z2} b - [\Phi_P + m_2 (b^2 + h_{CG}{}^2)]\dot{P} = 0 \tag{1.9}$$

and

$$F_{x5} - (-F_{z5} + m_2 g + m_2 a_{z2}) \cdot (f_0 + f_v V_{x2}) - f_{v2} V_{x2}^2 - m_2 a_{x2} = 0 \tag{1.10}$$

Rearranging it produces

$$F_{z5} = \frac{m_2 g b}{L} + \frac{h_5}{L} F_{x5} - \frac{m_2 h_{CG}}{L} a_{x2} + m_2 \frac{b}{L} a_{z2} - \frac{h_a}{L} f_{v2} V_{x2}^2 - \frac{\Phi_P + m_2 (b^2 + h_{CG}{}^2)}{L} \dot{P} \tag{1.11}$$

and

$$F_{x5} = f_0 m_2 g + m_2 a_{x2} - f_0 F_{z5} + f_0 m_2 a_{z2} + f_v m_2 g V_{x2} + f_v m_2 a_{z2} V_{x2} - f_v V_{x2} F_{z5} + f_{v2} V_{x2}^2 \tag{1.12}$$

Equation (1.11) and (1.12) are the pitch plane models for semitrailer. Since the pitch acceleration and vertical acceleration of semitrailer are included in the models, we call them full models.

When the pitch acceleration and vertical acceleration of the semitrailer are ignored, equation (1.11) and (1.12) can be simplified into

$$F_{z5} = \frac{m_2 g b}{L} + \frac{h_5}{L} F_{x5} - \frac{m_2 h_{CG}}{L} a_{x2} - \frac{h_a}{L} f_{v2} V_{x2}^2 \tag{1.13}$$

and

$$F_{x5} = f_0 m_2 g + m_2 a_{x2} - f_0 F_{z5} + f_v m_2 g V_{x2} - f_v V_{x2} F_{z5} + f_{v2} V_{x2}^2 \tag{1.14}$$

Equations (1.13) and (1.14) are the simplified pitch plane models for the semitrailer.

2.2. Roll Plane Model

Figure.2.1 and 2.2 are the free body diagrams of a semitrailer respectively in roll plane at the semitrailer CG and in space. Since the roll moments about the roll axis should be in equilibrium, we have

$$M_{x2}\cos\psi + M_{x3}\cos\psi - m_2 a_y[(h_{cg} - h_{rcg})\cos\phi - e\sin\phi]\cos\psi$$
$$-m_2 g[(h_{cg} - h_{rcg})\sin\phi + e\cos\phi]\cos\psi = 0 \qquad (2.1)$$

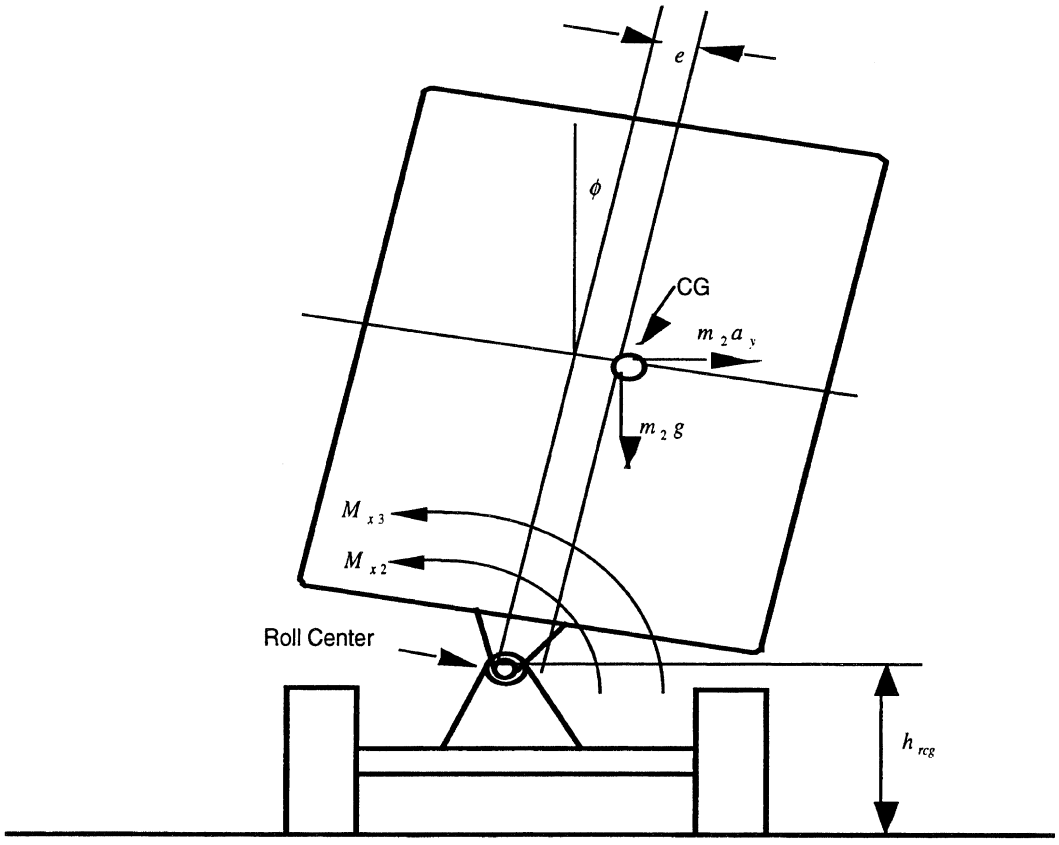

Figure C.2 A free body diagram of a semitrailer in roll plane at the semitrailer CG

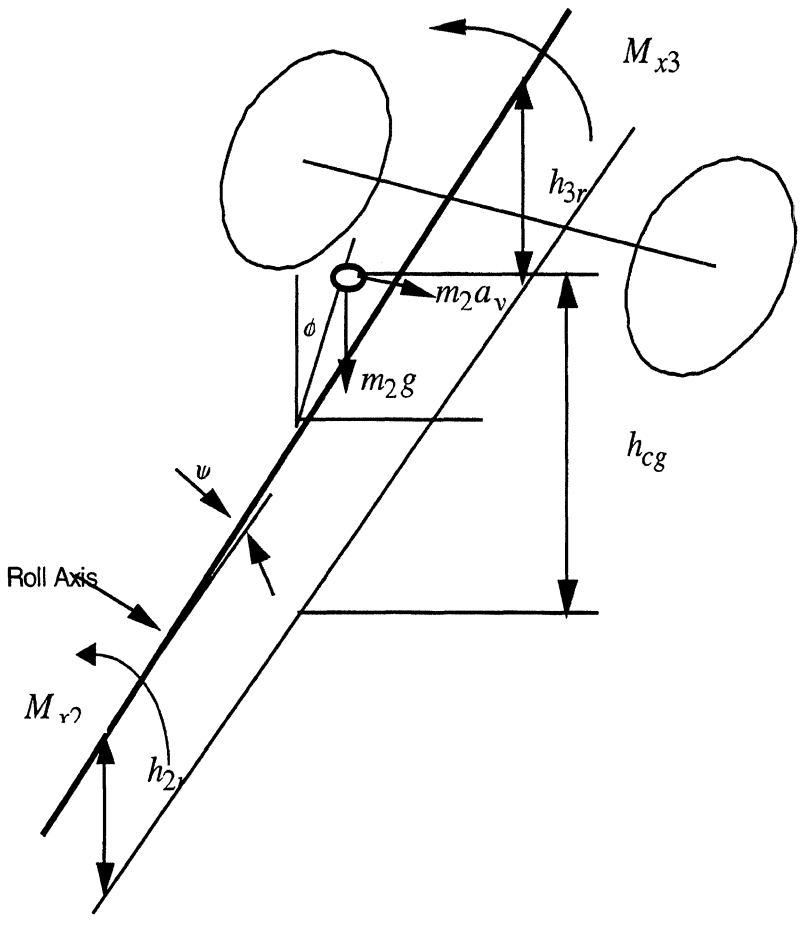

Figure C.3. Free body diagram of a semitrailer in space

where ψ is the angle between the roll center line of semitrailer (assumed to be small), and M_{x3} is the roll moment sustained by semitrailer rear suspension. If a linear roll model

$$M_{x3} = K_{r3}\phi \tag{2.2}$$

is used to represent the roll characteristics of axle 3 (the combination of suspension and tires at the semitrailer rear axle), equation (2.1) can be rewritten into

$$M_{x2} + K_{r3}\phi - m_2 a_y[(h_{cg} - h_{rcg})\cos\phi - e\sin\phi] - m_2 g[(h_{cg} - h_{rcg})\sin\phi + e\cos\phi] = 0. \tag{2.3}$$

where K_{r3} is the roll stiffness of axle 3. Since roll angle ϕ is a small quantity, its cosine and sin can be approximated by 1 and itself. In this case, equation (2.3) can be simplified into

$$M_{x2} + K_{3r}\phi - m_2 a_y[(h_{cg} - h_{rcg}) - e\phi] - m_2 g[(h_{cg} - h_{rcg})\phi + e] = 0 \tag{2.4}$$

or

$$M_{x5} = m_2 ge + \left[m_2 g(h_{cg} - h_{rcg}) - K_{3r}\right]\phi + \left[m_2(h_{cg} - h_{rcg})\right]a_y - m_2 e a_y \phi - (h_5 - h_{2r})F_{y5} \quad (2.7)$$

Equation (2.7) defines the roll plane behavior of the semitrailer.

III. ESTIMATION OF SEMITRAILER PARAMETERS

Identifying the roll stability limits of the vehicle combination essentially involves estimating the semitrailer properties, since the overall roll behavior of the combination is determined by the semitrailer and the tractor, but the tractor's parameters can be assumed to be known to the tractor manufacturer and thus to the OEM supplied computing system that monitors roll stability. This section describes the procedure and details the algorithm used to determine semitrailer parameters and presents the results of the scheme as applied off-line (in a batch processing and not recursive mode) to data obtained from a number of different highway runs, under various loading conditions.

At the outset of the project it was envisaged that semitrailer wheelbase could be estimated either through computing the autocorrelation of the road vibrations as measured at the fifth wheel and observing the time delay between the resulting peaks or through a linear regression scheme applied to the measurements involved in the semitrailer pitch plane model. However, examination of the autocorrelation and the semitrailer pitch plane data showed that the sensitivity of the signals to the semitrailer wheelbase was too low and the noise levels in the data too high to provide sufficiently accurate estimates. Without knowledge of the semitrailer wheelbase, estimation of the semitrailer rear suspension stiffness $K_{3\phi}$ becomes impossible. Hence, it was assumed that for the rest of this study it would be assumed that $K_{3\phi}$ would be assumed to be known. Such an assumption would be valid and would provide a useful system when the operator of a fleet, uses a number of identical semitrailers which is quite often the case with most commercial truck operations. The procedure used to estimate semitrailer properties is then presented in the flowchart in Figure C.4.

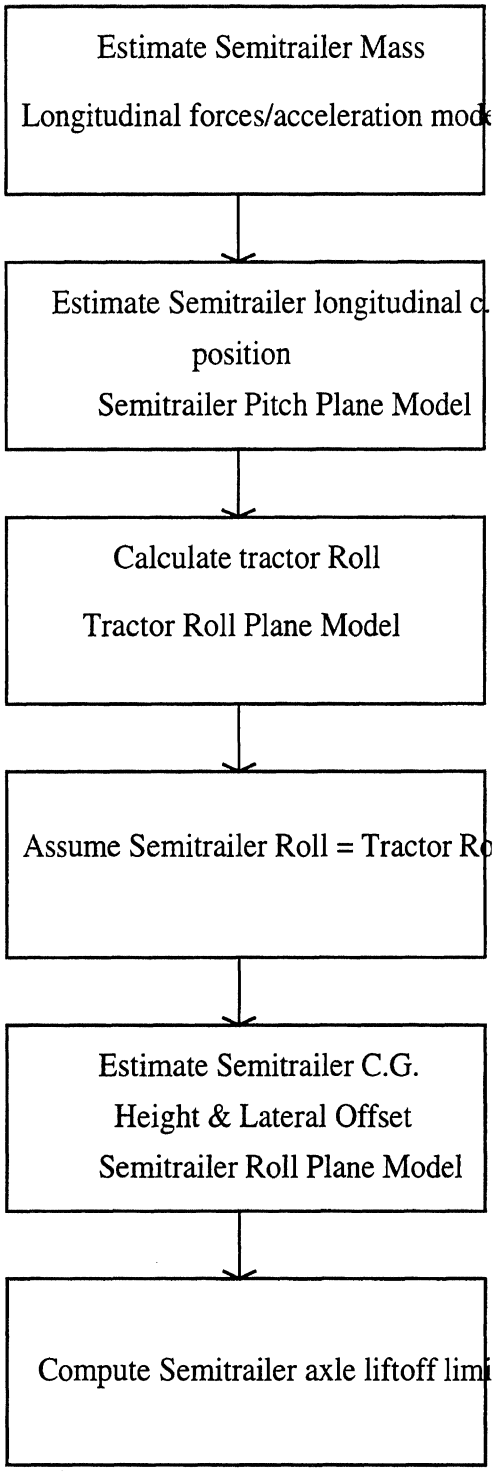

Figure C.4. Semitrailer roll limits estimation procedure

Detailed below is the algorithm for computing semitrailer parameters.

3.1. Semitrailer Mass

Semitrailer mass is computed from the longitudinal force/acceleration balance equation of the semitrailer pitch plane model. Recall equation (2.1.14).

$$F_{x5} = f_0 m_2 g + m_2 a_{x2} - f_0 F_{z5} + f_v m_2 g V_{x2} - f_v V_{x2} F_{z5} + f_{v2} V_{x2}^2 \tag{3.1.1}$$

Semitrailer mass m_2 can then be calculated through linear regression. Note that m_2 obtained from this equation represents total semitrailer mass while in later computations it is necessary to use semitrailer sprung mass. Therefore the approximation of m_2 to the semitrailer sprung mass is improved by assuming that the unsprung mass is about 5% of the total mass and then subtracting that portion from the total.

3.2 Semitrailer Center of Gravity longitudinal position

This is computed from the moment balance equation of the pitch plane model. Again, recall equation (2.1.13).

$$F_{z5} = \frac{m_2 g b}{L} + \frac{h_5}{L} F_{x5} - \frac{m_2 h_{CG}}{L} a_{x2} - \frac{h_a}{L} f_{v2} V_{x2}^2 \tag{3.1.2}$$

The longitudinal position of the c.g., b, can then be calculated through linear regression. As noted earlier it was found that the signal-noise ratio of the data was too low for the calculation of either semitrailer wheelbase, L, or c.g. height, h_{cg}, using this equation.

3.3. Tractor and Semitrailer roll angle

Tractor roll angle is computed using the following equation (derived from a model of the tractor roll plane behavior).

$$\phi_1 = \frac{-\{M_{x5} + f_{y5}(h_5 - h_{1r}) + m_1 a_y (h_{cgtractor} - h_{1r})\}}{\{m_1 g (h_{cgtractor} - h_{1r}) - K_{\phi 1}\}} \tag{3.1.3}$$

where, h_{1r} is the height of the tractor roll center, m_1 is that portion of the tractor sprung mass that is borne by the axle that supports the fifth wheel and $K_{\phi 1}$ is the effective roll stiffness of the tractor rear axle. Semitrailer roll angle ϕ_2 is then assumed to be equal to the tractor roll angle, since the tractor rear frame segment and the semitrailer fifth wheel coupling are assumed to have a high torsional stiffness about the roll axis.

3.4. Semitrailer center of gravity height and lateral offset

The position of the semitrailer c.g. can then be calculated from the semitrailer roll plane model equation (2.2.7).

$$M_{x5} = m_2 ge + \left[m_2 g(h_{cg} - h_{rcg}) - K_{3r}\right]\phi_2 + \left[m_2(h_{cg} - h_{rcg})\right]a_y - m_2 e a_y \phi_2 - (h_5 - h_{2r})F_{y5} \quad (3.1.4)$$

3.5. Semitrailer axle liftoff limits

One useful estimate of the rollover threshold is the level of maneuver severity at which the semitrailer axle just lifts off from the ground. In order to compute this limit it is first necessary to write the roll plane equations for the semitrailer axle.

From measurements of the lateral acceleration and the previously calculated roll angle the relationship between these quantities is established by the following model.

$$\phi_2 = a_0 + a_1 * a_y \quad (3.1.5)$$

where a_0 and a_1 are coefficients that are computed through linear regression.

Then,

$$a_y m_2 h_{2r} - K_{\phi 2}\phi_2 - m_2 \frac{b}{L}\frac{T}{2} - m_2 e = 0 \quad (3.1.6)$$

where T is the semitrailer track width.

The limits for left and right turns are different due to the lateral offset of the semitrailer c.g. and can be calculated by combining equations (3.1.5 and 3.1.6). The critical acceleration for a left turn is given by,

$$a_{ylcritical} = \frac{\left\{m_2 \frac{b}{L}\frac{T}{2} - m_2 e + a_0\right\}}{(m_2 h_{2r} - K_{\phi 2} a_1)} \quad (3.1.7)$$

and that for a right turn is given by,

$$a_{yrcritical} = \frac{\left\{m_2 \frac{b}{L}\frac{T}{2} + m_2 e + a_0\right\}}{(m_2 h_{2r} - K_{\phi 2} a_1)} \quad (3.1.8)$$

4. COMPARISON BETWEEN MEASURED AND COMPUTED RESULTS

The above algorithm was validated through off-line computation of the trailer axle liftoff limits using test data gathered during several normal driving runs performed under different loading conditions as described earlier in the report. The following table presents the actual height and c.g. offset of the the semitrailer mass and the semitrailer

axle liftoff limits as measured from tilt table experiments, and the corresponding estimates produced by the prediction algorithm for each of the test runs.

Run	Actual h_{cg} (in)	Actual c.g. offset (in)	$a_{yliftoff}$ (tilt table) (g's)		Estimated h_{cg} (in)	Estimated c.g. offset (in)	Estimated $a_{yliftoff}$ (g's)	
			Left turn	Right turn			Left turn	Right turn
1.	96.5	0.0	0.29	0.29	92.3	0.2	0.29	0.30
2.	80.4	0.0	0.38	0.38	82.2	-0.2	0.36	0.35
3.	80.4	0.0	0.38	0.38	81.8	0.1	0.37	0.37
4.	90.8	6.3	0.25	0.33	93.2	4.7	0.22	0.36
5.	84.1	6.3	0.28	0.38	88.1	4.3	0.24	0.37
6.	93.5	0.0	0.35	0.35	96.5	0.6	0.3	0.31
7.	90.8	6.3	0.25	0.35	89.4	4.0	0.23	0.36
8.	90.8	6.3	0.25	0.35	88.1	4.2	0.22	0.36
9.	84.1	6.3	0.28	0.38	81.4	4.2	0.25	0.39
10.	90.8	6.3	0.25	0.33	92.0	4.3	0.23	0.36

Table C.1. Results of roll stability algorithm implementation

Figure C.5 shows the actual versus the predicted semitrailer c.g. heights for each of the runs. It can be seen that the predictions are within about ±3in of the actual heights. Examining the table for the predictions of the lateral offset of the c.g., shows that the predictions are consistently lower than the actual values. However the variation in the roll stability between those for the left and right turns, is greater than the actual variation. This is probably due to the existence of some factors in the algorithm that are compensating (acting against one another) in their effects on the predictions of the lateral offset and the overal stability limits respectively.

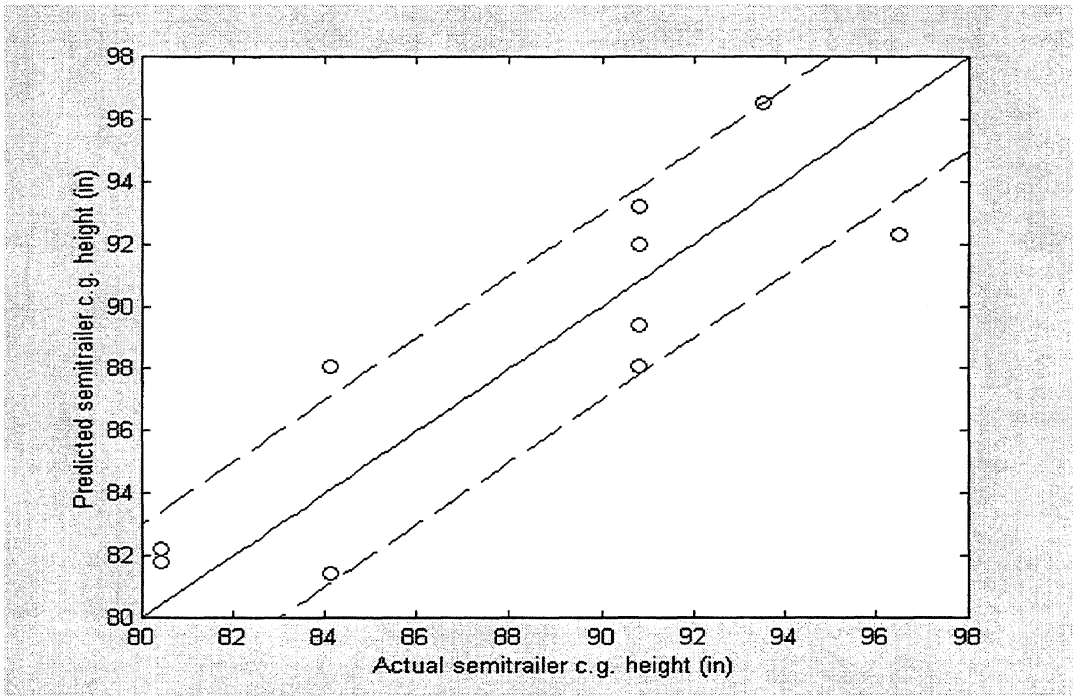

Figure C.5. Plot of actual versus predicted semitrailer c.g. heights (with ±3 in error bounds)

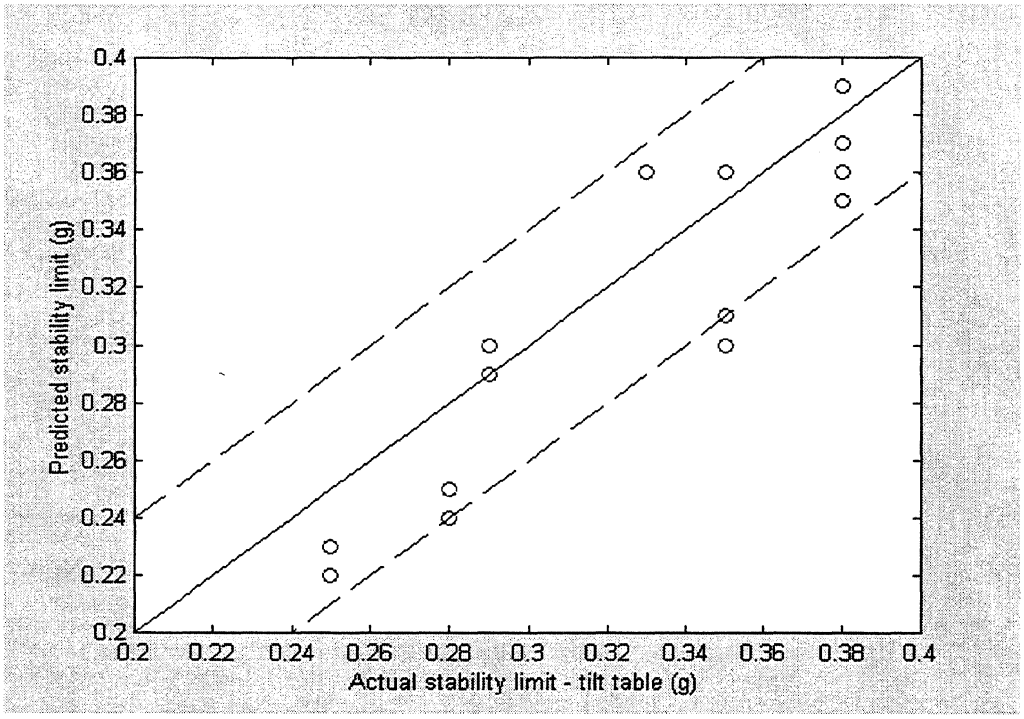

Figure C.6. Plot of actual versus predicted stability with 0.04 error bounds (dashed lines)

Figure C.6 shows a plot of the actual versus predicted stability limits for each of the runs. In the case of the offset loads the left and right stability limits were calculated from knowledge of the left and right wheel loads. Note that there are 20 points on the plot but not all of them can be distinguished since some of the points coincide due to

being rounded down to 2 decimal places. It can be seen that 95% (19/20) predictions lie within 0.04 g's of the actual value. It also appears that the prediction algorithm tends to produce conservative estimates, i.e., stability limits that are lower than the actual values. Some tweaking of the algorithm could achieve scatter that is more centered and could lie within a smaller error band.

The original intention of the project was to develop the capability of predicting tractor-semitrailer combination roll limits using only tractor based (fifth wheel) measurements and knowledge of tractor properties. However, the approach of estimating the semitrailer wheelbase from the autocorrelation of road roughness excited vibrations proved infeasible. Some of the possible reasons for this may be, (i) the tractor and traile wheelbases were very similar making it impossible to distinguish their respective peaks in the autocorrelation and (ii) the presence of other resonances in the vehicle structure which caused vibrations that drowned out the road excited vibrations. Further study is necessary to test if the autocorrelation method could be sufficiently improved, or if some other means could be developed to produce accurate wheelbase estimates. Further it is not entirely certain that, even with a good estimate of the semitrailer wheelbase the pitch plane data, was of sufficiently high quality (in terms of the signal to noise ratio) to produce accurate estimates of the semitrailer c.g. height. Therefore this study was performed with an assumed knowledge of the semitrailer rear suspension roll stiffness. While this does restrict the usefulness of the scheme to those situations in which such knowledge is available, such a scenario could exist in a number of cases especially when the operator of a fleet of trucks uses a number of identical semitrailers.

5. CONCLUSION

This appendix presented, in detail, the derivation and implementation of an algorithm designed to predict semitrailer parameters and roll stability behavior using measurements made by a tractor based (fifth wheel) sensor. The algorithm was implemented and tested off line, but is simple enough to be implemented on-board the vehicle without being unduly demanding in terms of computing capabilities. The prediction algorithm produced relatively accurate (within ±0.04g) estimates of the roll stability limits of the semitrailer. How useful this level of prediction accuracy is, will depend on the application and the behavioral adaptations that it produces in drivers. These and other questions regarding the extent of quantitative improvement in safety that such a system can provide can only be answered by a long term study examining its implementation on a fleet of trucks.

APPENDIX D
UMTRI FIFTH-WHEEL LOAD TRANSDUCER
—USERS' GUIDE—

The UMTRI fifth-wheel load transducer was created for the NHTSA under Cooperative Agreement number DTNH22-95-H-07002 and is the property of NHTSA. It is intended to measure all four primary loads which a semitrailer applies to a tractor (or dolly) through the fifth wheel. These loads, diagrammed in figure 1, are:

F_x longitudinal (fore/aft) force,
F_y lateral (sideways) force,
F_z vertical force,
M_x overturning (roll) moment.

The UMTRI fifth-wheel load transducer system measures these loads by replacing the standard fifth-wheel chairs with specially-made chairs, each of which are a four-component load transducer. The four signals from an individual chair are combined appropriately by a data reduction matrix calculation to yield the three forces (longitudinal, lateral, and vertical) and one moment (overturning) acting on that chair. In turn these values for both the left and right chairs are combined by a matrix calculation to determine the total loads on the fifth wheel.

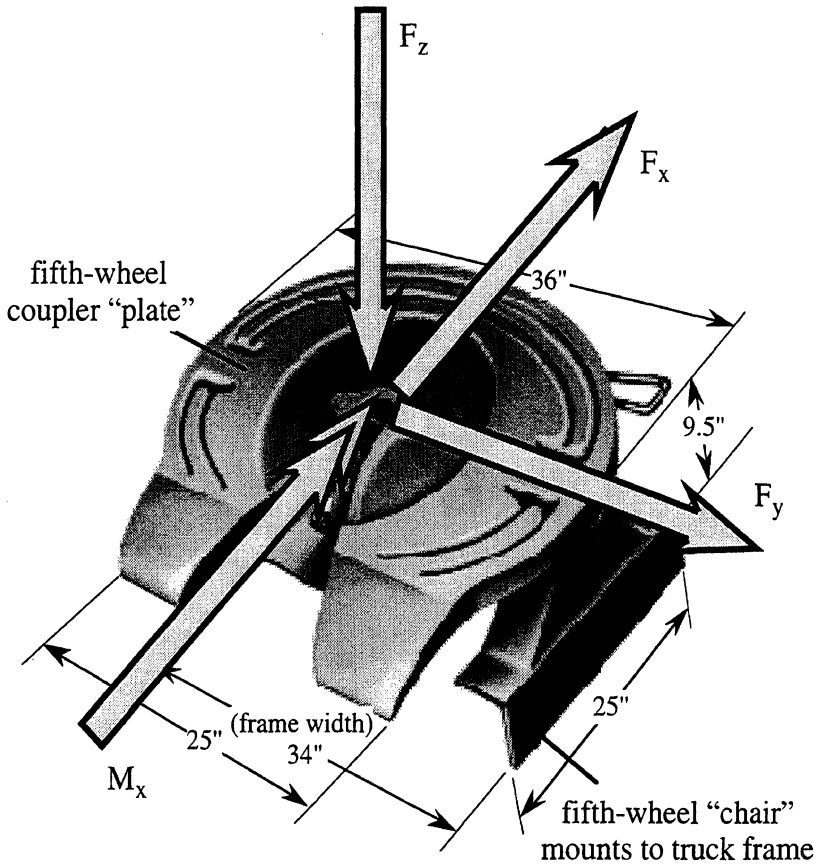

Figure 1. A standard fifth-wheel with loads and nomenclature

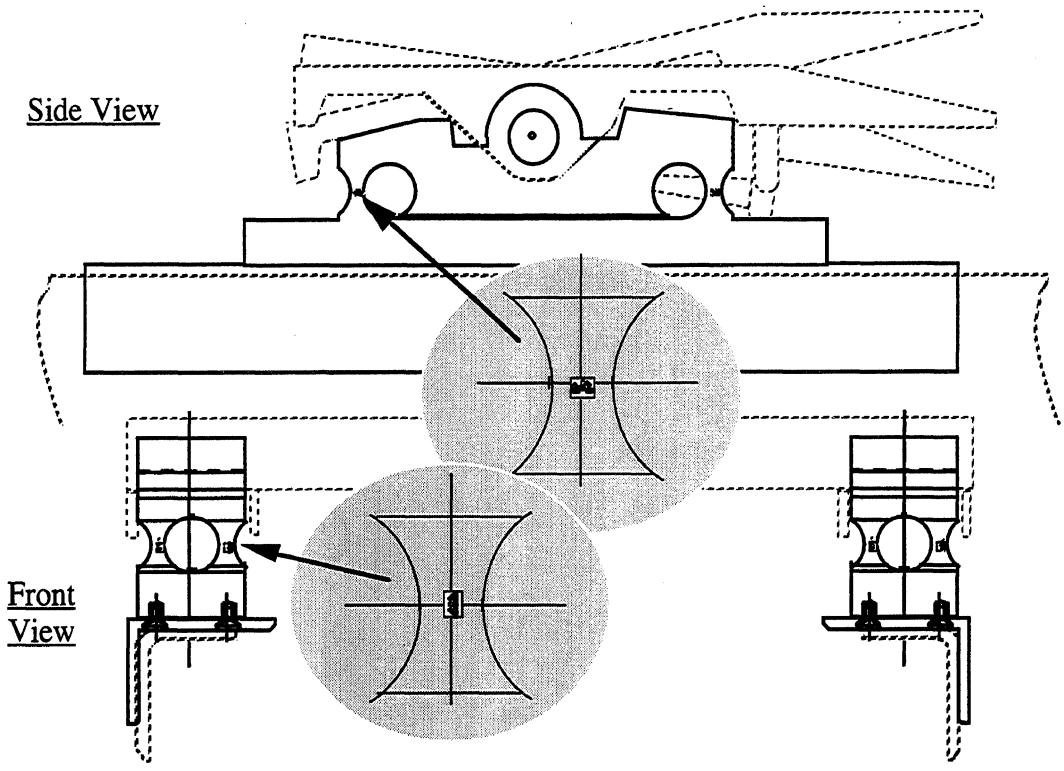

Figure 2. General design of the UMTRI fifth-wheel load transducer

Figure 2 is a sketch which shows the general design of the transducer system. The transducer has approximately the same overall dimensions as the standard chair shown in figure 1. However, this chair is cut from a solid block of high-strength steel in a manner such that all loads applied to it by the fifth-wheel plate flow down into the truck frame through four precisely-machined posts, each of which have twelve strain gauges applied.

The calibration process (of May, 1998) showed the nominal accuracy of these cells to be in the range of one to two percent. Additional test have shown the cells to be rather insensitive to twisting and bending loads applied through their base. (This is an especially important issue for a fifth-wheel load cell since it is normal for the typical commercial truck frame to flex substantially during use). Calibration loading is depicted in figure 3 and results are reviewed in tables 1 and 2. The loads for the base-distortion sensitivity tests are depicted in figure 4 with results presented in table 3.

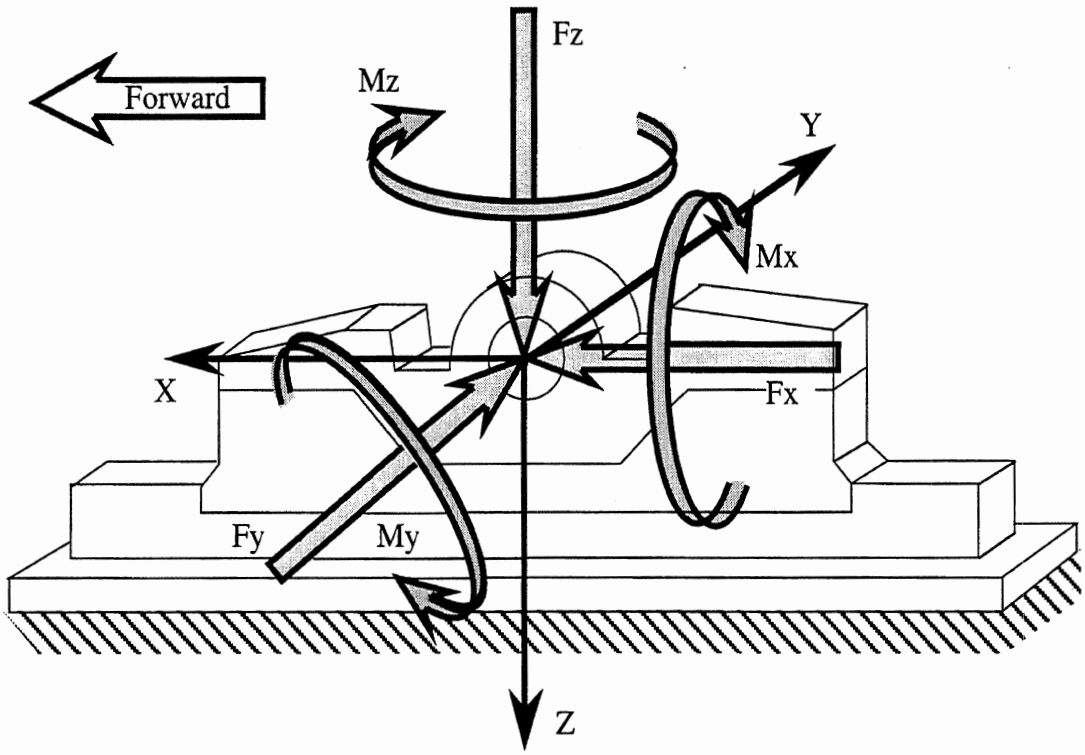

Fx, Fy, Fz, Mx, My, and Mz loads are applied through the load cell to ground.
Load cell transduces only Fx, Fy, Fz, and Mx.

Figure 3. Load-cell calibration tests

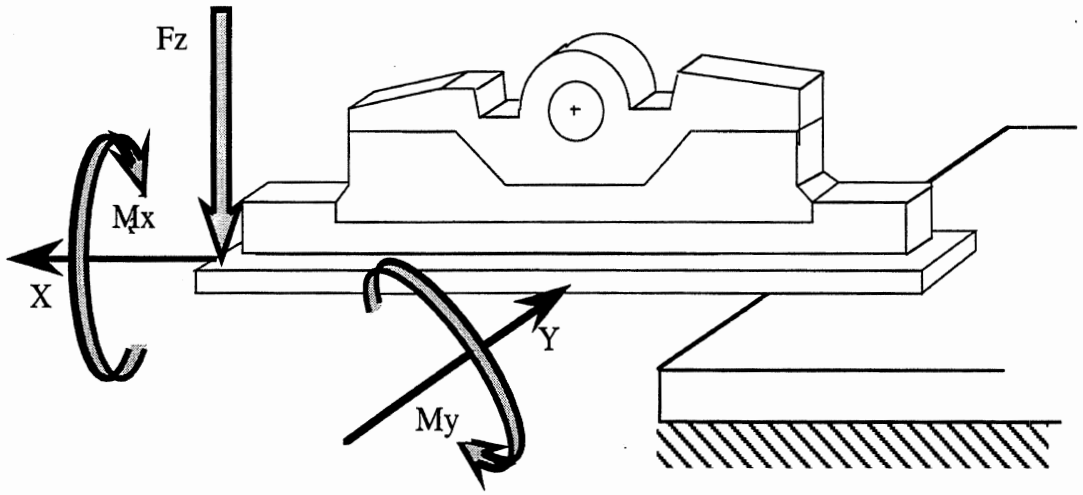

Loads are applied through base to ground.
NO loads are applied through the load cell.

Figure 4. Base distortion tests

Table 1. Calibration results—UMTRI 5th-Wheel Load Cell #1

Calibration of May, 1998

Test Conditions*

Peak values of applied loads

Test	Fx [kilo lb]	Fy [kilo lb]	Fz [kilo lb]	Mx [kilo in-lb]	My [kilo in-lb]	Mz [kilo in-lb]
1	20.3					
2	21.1					
3	20.2					40.3
4	21.2					42.5
5	20.5					-41.1
6	-20.4					40.9
7	-20.9					41.8
8	-20.8					-41.5
9	-20.4					-40.8
10	-22.6					
11	-22.6					
12	-22.6					
13	22.9					
14	23.4					
15		22.3				
16		22.5				
17		20.0				-40.0
18		19.9				-39.8
19		20.0				-40.0
20		19.0				38.0
21		19.0				38.0
22		20.0		-40.0		
23		20.0		-40.0		
24		21.2		42.4		
25		20.7		41.4		
26		-21.2				
27		-20.6				
28		-21.0				42.0
29		-20.5				41.1
30		-20.8				-41.7
31		-20.9				-41.8
32		-21.0		-42.0		
33		-21.0		-41.9		
34		-21.0		42.1		
35		-21.1		42.2		
36			20.8			
37			22.4			
38			22.9	45.7		
39			22.8	45.7		
40			17.1	-34.1		
41			16.7	-33.3		
42			23.7			
43			24.0			
44			10.3		-20.5	
45			10.5		-21.0	
46			10.5		21.0	
47			-20.8			
48			-20.8			

Load Cell Evaluation

Correlation coefficients (r^2)				
Test	Fx	Fy	Fz	Mx
All**	0.999998	0.999996	0.999786	0.999880

Errors in measured loads								
Test	Fx [lb]		Fy [lb]		Fz [lb]		Mx [in-lb]	
	Peak to peak	RMS	Peak to peak	RMS	Peak to peak	RMS	Peak to peak	RMS
All**	69	12	132	15	545	80	599	118
***	0.5%	0.1%	0.6%	0.1%	2.3%	0.3%	2.1%	1.3%
1	68	14	22	12	120	43	37	7
2	91	43	25	15	122	54	49	18
3	75	29	28	10	126	45	82	19
4	96	13	29	10	141	45	95	26
5	59	14	31	12	131	51	53	10
6	55	30	28	10	111	42	213	103
7	50	14	31	15	103	35	194	85
8	45	12	8	1	155	63	166	69
9	51	13	7	2	155	69	172	72
10	67	13	18	7	149	72	57	24
11	59	14	20	7	142	54	55	13
12	78	13	16	5	142	57	56	21
13	95	36	25	12	152	71	43	11
14	58	16	22	12	147	68	45	10
15	12	5	68	16	316	130	163	89
16	9	3	59	16	320	139	218	61
17	12	2	66	19	261	88	541	212
18	15	4	64	16	269	109	469	251
19	15	5	59	19	266	120	571	250
20	12	5	104	13	273	113	614	288
21	14	5	105	12	277	100	672	313
22	10	4	67	12	171	67	235	76
23	9	3	74	16	171	72	286	91
24	11	5	54	12	562	235	620	252
25	10	2	61	12	513	228	632	217
26	7	1	161	48	298	126	313	144
27	6	1	54	9	280	133	237	130
28	16	5	94	11	295	128	370	142
29	17	8	43	13	287	139	281	141
30	9	2	46	12	282	141	391	184
31	11	5	66	12	280	141	386	178
32	6	1	49	14	188	82	236	65
33	8	1	57	11	175	77	226	59
34	9	3	50	17	525	259	891	303
35	11	5	49	18	529	258	833	255
36	16	7	46	13	217	114	380	167
37	8	4	57	22	257	146	323	118
38	14	6	17	6	286	133	401	146
39	14	5	18	4	266	121	376	120
40	10	2	55	18	211	100	408	97
41	9	3	51	17	198	100	387	102
42	20	10	69	25	262	138	407	137
43	21	7	71	26	260	133	450	144
44	14	6	11	3	47	22	113	28
45	13	5	10	2	42	17	111	32
46	9	3	19	5	63	33	148	41
47	20	9	94	41	86	42	245	95
48	16	7	95	47	90	43	281	136

*Loads smoothly applied from zero to maximum to zero over approximately 30 seconds.

**Results for all tests combined are after digital filtering at 5 hz. (Results for Individual testsfrom unfiltered data.)

*** Percent of maximum applied.

Table 2. Calibration results—UMTRI 5th-Wheel Load Cell #2

Calibration of May, 1998

Test Conditions*

Peak values of applied loads

Test	Fx	Fy	Fz	Mx	My	Mz
	[kilo lb]			[kilo in-lb]		
1			-20.9			
2			-20.8			
3			-20.8	-41.6		
4			-20.7	-41.3		
5			-20.5	-41.0		
6			-20.4	-40.9		
7			-20.4			
8			-20.5			
9			-20.2	40.5		
10			-20.3	40.7		
11			20.5	-41.0		
12			20.4	-40.8		
13			20.4	40.9		
14			20.5	41.0		
15			20.5			
16			22.4			
17			13.6		27.2	
18			19.3		38.7	
20			20.4		-40.7	
21		21.2				
22		21.3				
23		21.0		-42.0		
24		20.7		-41.4		
25		20.8		41.7		
26		20.9		41.8		
27		20.7				41.5
28		21.3				42.5
29		20.6				-41.2
30		20.5				-41.1
31		-20.5				
32		-20.7				
33		-20.6		-41.2		
34		-20.8		-41.5		
35		-20.4		40.8		
36		-20.6		41.2		
37		-20.6				41.2
38		-20.5				41.0
39		-20.5				-41.0
40		-20.5				-41.1
41	-20.6					
42	-20.7					
43	-20.6					41.2
44	-20.6					41.3
45	-20.6					-41.2
46	-20.5					-41.1
47	20.7					41.5
48	20.7					41.3
49	20.6					
50	20.7					
51	20.5					-41.1
52	20.5					-41.1

Load Cell Evaluation**

Correlation coefficients (r^2)								
Test	Fx		Fy		Fz		Mx	
All	0.999994		0.999989		0.999874		0.999895	
Errors in measured loads								
Test	Fx [lb]		Fy [lb]		Fz [lb]		Mx [in-lb]	
	Peak to peak	RMS	Peak to peak	RMS	Peak to peak	RMS	Peak to peak	RMS
All	101	14	139	25	522	86	729	150
	0.5%	0.1%	0.7%	0.1%	2.3%	0.4%	1.7%	0.4%
1	12	86	86	195	67	36	195	115
2	12	83	83	184	70	41	184	87
3	14	19	19	462	108	7	462	237
4	13	18	18	482	117	8	482	260
5	13	19	19	391	166	8	391	204
6	11	19	19	367	142	9	367	179
7	10	76	76	423	97	32	423	201
8	10	78	78	411	95	34	411	246
9	13	139	139	611	115	62	611	270
10	14	138	138	633	104	65	633	195
11	18	108	108	512	152	20	512	102
12	17	79	79	481	167	16	481	100
13	16	124	124	662	155	59	662	184
14	15	127	127	683	163	61	683	204
15	12	81	81	295	105	38	295	123
16	13	91	91	360	138	49	360	171
17	5	37	37	73	64	16	73	20
18	11	68	68	165	95	30	165	45
20	27	86	86	620	112	43	620	328
21	6	50	50	179	295	19	179	50
22	6	54	54	184	286	14	184	63
23	5	61	61	430	166	14	430	254
24	4	55	55	418	159	12	418	192
25	6	52	52	646	500	12	646	247
26	8	60	60	729	503	16	729	296
27	11	55	55	206	284	13	206	85
28	13	51	51	181	296	13	181	71
29	15	51	51	143	305	13	143	58
30	13	43	43	182	305	10	182	54
31	4	65	65	147	287	40	147	50
32	5	47	47	214	291	11	214	67
33	5	52	52	288	196	21	288	107
34	5	33	33	253	200	9	253	119
35	6	58	58	473	490	17	473	178
36	6	43	43	540	522	8	540	216
37	8	41	41	343	290	13	343	166
38	8	50	50	355	292	14	355	205
39	9	43	43	522	270	9	522	258
40	9	39	39	504	274	9	504	259
41	90	20	20	93	130	12	93	50
42	82	15	15	101	126	7	101	52
43	75	10	10	43	134	5	43	25
44	101	6	6	35	145	2	35	18
45	71	7	7	144	129	3	144	67
46	68	7	7	148	124	2	148	76
47	84	2	2	100	111	0	100	54
48	64	6	6	96	106	3	96	48
49	59	11	11	94	113	5	94	45
50	61	11	11	97	112	5	97	43
51	54	13	13	269	180	8	269	144
52	55	15	15	258	167	9	258	132

*Loads smoothly applied from zero to maximum to zero over approximately 30 seconds.

**Evaluations performed following digital filtering at 5 hz.

*** Percent of maximum applied.

Table 3. Base-deformation tests of the UMTRI fifth-wheel load cells —May, 1998—

Load Cell #1

Test	Loads applied to base			False Load Cell Signals F_x, lb	F_y, lb	F_z, lb	M_x, in-lb
49	F_z, lb	609	Max	32	7	21	293
	M_x, in-lb	50,522	Min	-6	-18	-125	-56
	M_y, in-lb	8,522	Range	37	25	146	349
50	F_z, lb	612	Max	31	8	21	253
	M_x, in-lb	50,834	Min	-9	-17	-126	-62
	M_y, in-lb	8,574	Range	40	25	147	315
51	F_z, lb	593	Max	5	6	12	155
	M_x, in-lb	1,779	Min	-39	-56	-109	-31
	M_y, in-lb	55,155	Range	44	62	120	185
52,53	F_z, lb	618	Max	14	14	33	188
	M_x, in-lb	1,853	Min	-42	-67	-127	-56
	M_y, in-lb	57,457	Range	56	82	160	244

Load Cell #2

Test	Loads applied to base			False Load Cell Signals F_x, lb	F_y, lb	F_z, lb	M_x, in-lb
53	F_z, lb	588	Max	-24	-29	11	526
	M_x, in-lb	48,816	Min	-141	-52	-112	47
	M_y, in-lb	8,234	Range	99	40	123	479
54	F_z, lb	663	Max	-22	-28	5	568
	M_x, in-lb	55,047	Min	-142	-51	-114	52
	M_y, in-lb	9,285	Range	85	42	119	516
55	F_z, lb	616	Max	-12	-29	-66	147
	M_x, in-lb	1,849	Min	-38	-53	-353	-836
	M_y, in-lb	57,305	Range	26	45	288	983
56	F_z, lb	666	Max	-13	-36	-33	144
	M_x, in-lb	1,999	Min	-38	-59	-366	-772
	M_y, in-lb	61,970	Range	26	49	333	916

CONNECTORS, CIRCUITS, AND PIN-OUT

Each of the two transducers is wired for four individual channels: X, Y, ZR, and ZL. Two of these channels are each composed of four, 4-arm strain gauge bridges in parallel. The other two channels each have two bridges.

The associated circuits are shown in figure 5. Each circuit has six external connections: +signal, -signal, +sense, -sense, +excitation, -excitation. These connections are

accomplished via a single, 24-pin connector (Amphenol PT02E-16-26P). Pin-outs for this connector are also indicated in the figure.

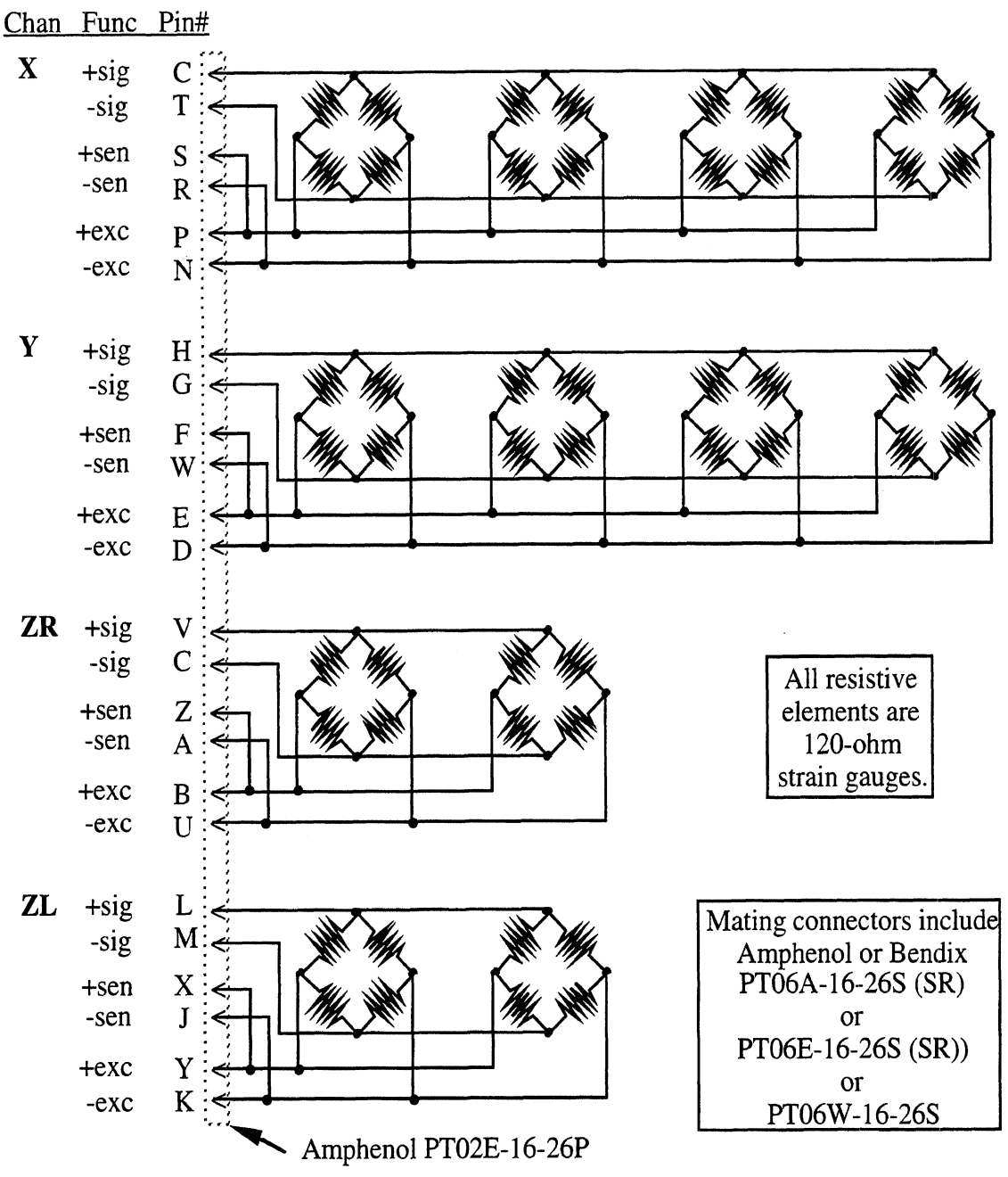

Figure 5. Circuits and pin-outs

EXCITATION

Recommended excitation is a precision regulated 2.5 volts. At this voltage, channels X and Y require 0.083 amperes and channels ZR and ZL require 0.042 amperes.

Higher excitation voltages (not exceeding 10 volts) may be used to increase signal strength, but the cells sensitivity to temperature may also increase as a result.

CALIBRATIONS FACTORS AND DATA REDUCTION

The following information is based on calibrations conducted in May, 1998. Calibration factors are in reference to the use of precision resistors of the indicated values applied as shunt-calibration resistors across the +sig, +sen terminals of the indicated strain-gauge bridge channels. (See figure 5.)

Note that the reference center of each individual transducer, which identifies the height of the longitudinal axis about which overturning moments (M_X) are defined, is located on the centerline of the bushing for the fifth-wheel-plate retaining pin. (See figure 3.)

In all of the following, polarities are such that the resulting values represent forces applied by the trailer to the fifth wheel according to the polarities of the SAE vehicle-dynamics axis systems (SAE J670,e). (Also see figures 1 and 3.)

Channel calibrations for right-side transducer

Channel	*Shunt cal resistance, ohms*	*Equivalent pounds*
XR	10,000	9,216
YR	10,000	9,125
ZLR	16,000	19,271
ZRR	16,000	19,331

Channel calibrations for left-side transducer

Channel	*Shunt cal resistance, ohms*	*Equivalent ponds*
XL	10,000	9,200
YL	10,000	8,999
ZLL	16,000	19,363
ZRL	16,000	19,388

The load-cell signals, in engineering units (pounds), are used in the following matrix calculations to determine the loads on the individual transducers.

Reduction matrix calculation for right-side transducer

$$\begin{bmatrix} F_{XR} \\ F_{YR} \\ F_{ZR} \\ M_{XR} \end{bmatrix} = \begin{bmatrix} 1 & -.0002 & -.0042 & -.0012 \\ -.0005 & 1 & .0083 & -.0167 \\ -.0044 & .0185 & 1 & 1 \\ .0071 & -2.0490 & -1.5237 & 1.5479 \end{bmatrix} \begin{bmatrix} XR \\ YR \\ ZLR \\ ZRR \end{bmatrix}$$

where XR, YR, ZLR, ZRR, F_{XR}, F_{YR}, and F_{ZR} are in pounds and M_{XR} is in inch-pounds.

Reduction matrix calculation for left-side transducer

$$\begin{bmatrix} F_{XL} \\ F_{YL} \\ F_{ZL} \\ M_{XL} \end{bmatrix} = \begin{bmatrix} 1 & -.0008 & .0005 & -.0008 \\ -.0018 & 1 & .0111 & -.0137 \\ .0176 & .0159 & 1 & 1 \\ .0239 & -2.0313 & -1.4709 & 1.5980 \end{bmatrix} \begin{bmatrix} XL \\ YL \\ ZLL \\ ZRL \end{bmatrix}$$

where XL, YL, ZLL, ZRL, F_{XL}, F_{YL}, and F_{ZL} are in pounds and M_{XL} is in inch-pounds.

Finally, the loads determined for the two individual cells are used in the following calculations to determine fifth-wheel loads.

$$F_X = F_{XR} + F_{XL}$$

$$F_Y = F_{YR} + F_{YL}$$

$$F_Z = F_{ZR} + F_{ZL}$$

$$M_X = S/2\,(F_{ZR} - F_{ZL}) + M_{XR} + M_{XL}$$

where F_X, F_Y, and F_Z are in pounds, M_X is in inch-pounds, and S is the lateral spacing of the two transducers, centerline-to-centerline, in inches. S is nominally 29.5 inches, but should be determined for each installation. See the following section on physical installation.

INSTALLATION

In order to insure fairly balanced sharing of lateral loading, the UMTRI fifth-wheel chair transducers are design to fit more closely in the bushing pockets of the fifth-wheel plate than are typical chairs. To insure that the chairs can be properly mounted on most truck frames, the transducers are mounted on their angle-iron bases such that the inner vertical surfaces of those angle irons will have lateral spacing slightly in excess of the typical 34-inch width of truck frame rails. Thus, it is expected that some shimming between the frame rail and the angle iron base of at least one chair will be required.

Accordingly, to install the fifth-wheel load transducer assembly, the entire assembly, including fifth-wheel plate should first be placed on the truck frame at the desired fore/aft position, and one side only should be firmly bolted to its frame rail. Then, with a feeler gauge, the width of the lateral gap between the other chair base and its frame rail should be determined. Shims of the appropriate size to fill this gap should be prepared and installed. (Shims may be installed on only one side, or they may be split and installed on both sides to put the fifth-wheel accurately on the centerline of the frame.) The entire assembly should then be bolted in place in accordance with normal practice for mounting fifth wheels.

DESIGN LOADS

Since little is known about the dynamic loads which can be expected at the fifth wheel coupling (either in conventional use or under conditions of proving grounds testing) it is difficult to clearly specify the maximum allowable trailer weights and/or static fifth-wheel loads which can be used with the UMTRI fifth-wheel load transducer. The following are provided as guidelines.

For on-highway use or for handling and braking tests on nominally smooth surfaces at proving-grounds, the UMTRI fifth-wheel load transducer should be limited to use with trailers whose static vertical fifth-wheel load does not exceed 30,000 pounds. By way of example, with such a nominal load, maximum stresses in the most heavily stressed sections can reach or exceed 50% of yield under either of the following load conditions: (1) simultaneous loads equivalent to 3 g vertical (90,000 lb) and 1 g longitudinal and lateral (30,000 pounds each); (2) a vertical load only of 8 g (240,000 pounds).

For use on uneven surfaces, trailer load should be significantly less than 30,000 pounds. Users should proceed cautiously, examining data closely during testing.

For operational safety, two 1-1/4 inch grade-8 bolts back up the heavily stressed, sensitive sections of each transducer chair. In normal use, these bolts carry no load. But in the case of failure of the highly stressed, sensitive sections of the transducer, these bolts would come into play to secure the upper and lower sections of the transducers to one another. (Note these bolts are not overload protectors which would prevent damage to the transducer; they are fail-safe devices only.)